SIMULATION OF ODOUR DISPERSION AROUND NATURAL WINDBREAKS

by
Xing Jun Lin

A thesis submitted to McGill University in partial fulfillment of the requirements for the degree of
Doctor of Philosophy

Department of Bioresource Engineering
Macdonald Campus of McGill University
Ste-Anne-de-Bellevue, Quebec, Canada
August 2006

Your file Votre référence
ISBN: 978-0-494-32208-6
Our file Notre référence
ISBN: 978-0-494-32208-6

ABSTRACT

The research objective was to calibrate a model to simulate odour dispersion downwind from natural windbreaks and then, use this model to observe the effect of windbreak characteristics and climatic conditions on the size of the odour dispersion plume. Computational fluid dynamic (CFD) models were used for the simulations because of their capability in reproducing turbulent wind conditions. The model was initially calibrated to ensure the proper velocity recovery ratio (VRR), and then to reproduce odour plumes measured in the field by three groups of four panellists.

The visual and statistical analysis of the field panellist observations indicated that a windbreak with an optical porosity of 0.35 could reduce by 21% the length of the odour dispersion plume, as compared to a site without a windbreak. Also, these analyses indicated that the site with a windbreak offering an optical porosity of 0.55 had no significant impact on the length of the odour plume, as compared to the site without a windbreak.

The models selected for the simulations were the Fluent 6.2 standard k-ε and SST k-ω models. Their odour dispersion calibration indicated that both models can accurately reproduce the field measured odour hedonic tone and odour concentration by transforming the odour mass fraction computed by the models into the hedonic tone with a power function, and then into the odour concentration with an exponential function. The correlations between the simulated and measured absolute HT and between the simulated and measured odour concentrations were statistically significant ($P < 0.01$). However, the SST k-ω was preferred over the standard k-ε because it could physically better reproduce the high turbulence conditions created by the windbreak.

The SST k-ω model simulations indicated that odour plume length was mostly affected by windbreak porosity and height, as well as distance from the source. In terms of climatic conditions, odour plume size was mostly affected for atmospheric stability conditions which generally established ambient wind speed

and rate of change of temperature. Wind direction has an impact on the length of the odour plume and the formation of a fin intensifying odour concentration near the windbreak, where an angle of 45 ° produces the shortest odour plume and the largest fin.

Key words: Simulation; odour; dispersion; natural Windbreak; CFD.

RÉSUMÉ

L'objectif principal de la présente recherche était de calibrer un modèle pour la simulation de la dispersion des odeurs par brise-vent naturels et ensuite, de déterminer l'effet des caractéristiques du brise-vent et des conditions climatiques sur la longueur du panache de dispersion des odeurs. Étant capable de reproduire des conditions de haute turbulence de vents, des modèles de computation de dynamique des fluides (CFD) furent utilisés pour les simulations. Les modèles furent calibrés pour assurer leur reproduction du ratio de récupération de la vélocité du vent (VRR) et de la dispersion des odeurs telle que mesurée par des groupes de panélistes au champ.

Des panaches de dispersion d'odeur furent observés au champ par trois groupes de quatre panélistes dûment formés pour cette tache. L'observation visuelle et l'analyse statistique de ces données de champ ont permis de conclure que, comparativement à un site sans brise-vent, un site avec brise-vent, dont la porosité visuelle est de 0,35 peut réduire de 21 % la longueur du panache de dispersion des odeurs. De plus, l'analyse statistique de ces données a permis de conclure qu'un brise-vent avec une porosité visuelle de 0.55 n'a aucun effet sur la longueur du panache de dispersion des odeurs, comparativement à un site sans brise-vent.

Les modèles Fluent 6.2 k-ε standard and SST k-ω furent choisis pour effectuer les simulations. Ces modèles furent calibrés pour bien reproduire les observations au champ de ton hédonique. Pour cette calibration, il a fallu transformer la valeur calculée de dispersion des gaz odorant en valeur de caractère hédonique, en utilisant une équation exponentielle obtenue suite à une analyse de corrélation, qui fut statistiquement significative ($P < 0,01$). Par contre, le modèle SST k-ω fut plus performant que le modèle k-ε standard, parce qu'il pouvait mieux reproduire physiquement, les conditions de haute turbulence de vent près des brise-vent.

RÉSUMÉ SUITE

Les simulations obtenues avec le modèle SST k-ω ont démontré que la longueur du panache de dispersion des odeurs était principalement établie par la porosité et la hauteur du brise-vent. Pour différentes conditions climatiques, la longueur du panache de dispersion d'odeur était affectée surtout par les conditions de stabilité atmosphérique, qui gouvernent la vitesse du vent et le taux de changement de la température de l'air en hauteur. La direction du vent avait aussi un impact sur la longueur du panache de dispersion des odeurs et la formation d'une aile prêt du brise-vent. Un angle de 45 ° maximisait cet effet.

Mots clefs: Simulation; odeur; dispersion ; Coupe-vent naturel; CFD.

ACKNOWLEDGEMENT

I would like to express my sincere gratitude to Dr. Suzelle Barrington, my thesis supervisor for her intellect, guidance, advice, encouragement, kindness and financial support throughout this research. I particularly appreciate her helping revise the methods of the analysis and the content of the thesis from the first to the last chapter with her depth of knowledge.

I would like to express my gratitude to Dr. Shiv O. Prasher, Dr. James A. Nicell, of McGill University and Mr. Denis Choinière of Comsumaj Inc., and Dr. Guangcai Gong of Hunan University in China for their cooperation and advice.

I am grateful to Dr. Robert Kok, Dr. Vijaya Raghavan, Dr. Ning Wang, Mr. Peter Enright, Dr. Ian B. Strachan, Dr. Roger I. Cue, and Dr. Gérard Szejwach for their excellent lectures, help and friendliness.

I wish to acknowledge the Department of the Bioresource Engineering staff, Susan Gregus, Trish Singleton, and Abida Subhan for all the administrative and secretarial help.

I gratefully acknowledge the financial contribution of Consumaj inc., CDAQ, the Livestock Initiative Program, Agriculture and Agro-Food Canada and the Natural Sciences and Engineering Research Council of Canada.

A heartfelt gratefulness is extended to my beloved parents and mother in-law for their love and constant encouragement.

This thesis is dedicated to my wife, Shumei Jiang, and my daughter, Shuang Lin, for their understanding, encouragement and support.

TABLE OF CONTENTS

LIST OF TABLES

LIST OF FIGURES

NOMENCLATURE

$(\tau_{ij})_{eff}$	The effective deviatoric stress tensor
AHT	Absolute value of hedonic tone
a_s	Constant
C_1 and C_2	Constants equal to 1.458×10^{-6} kg $m^{-1}s^{-1}$ $K^{-1/2}$ and 110.1K
$C_{1\varepsilon}$, $C_{2\varepsilon}$, and $C_{3\varepsilon}$	Constants
C_{ir}	Inertial resistance coefficient
C_{ir0}	Constant
C_p	Specific heat of air
C_μ	Constant
D_1 and D_2	Tree diameters
$D_{1,2}$	Mass diffusion coefficient of clear air into hydrogen sulphide
$D_{2,1}$	Mass diffusion coefficient of hydrogen sulphide into clean air
$D_{i,m}$	Diffusion coefficient for species i in the gaseous mixture
D_{MAX}	Maximum of the diameters of a tree
$D_{T,i}$	Thermal diffusion coefficient for species i in the gaseous mixture
E	Total energy (internal and kinetic energy expressed by formula (6.4)
F_i	Resistance body force exerted by a windbreak in *i*th direction
g	Acceleration of gravity
g_i	Component of the gravitational vector in the *i*th direction
H	Total height of the windbreak
h_1, h_2 and h_3	Windbreak height at which the porosity changes with a value between 0 and H
h_{ABL}	Height of the atmospheric boundary layer
H_F	Vertical heat flux
h_j	Sensible enthalpy of *j*th species
HT	hedonic tone from -10 to 0

J_i	Diffusion flux of species i
k	Turbulence kinetic energy
k_{eff}	Effective thermal conductivity
k_{tc}	Thermal conductivity
l	Turbulence length scale
L_{MO}	Monin Obukhov length
LOP	Length of odour plume
LR_1, LR_2 and LR_3	Lapse rate, defined as the decrease of temperature with the increase in height, measured from the ground to height z_1, z_1 to z_2 and above z_2
M or M_1	Molecular weight of dry air (0.028966 kg mol^{-1})
M_2	Molecular weight of hydrogen sulphide
MAHT	Measured absolute hedonic tone
m_{H2S}	Mass of hydrogen sulphide in one odour unit
MOC	Measured odour concentration (OU m^{-3})
MODD	Maximum odour dispersion distance
OC	Odour concentration, in OU m^{-3}
OC_g	The odour concentration at the odour generator, in OU m^{-3}
OMF	odour mass fraction, dimensionless
p	Wind profile exponent
p	Static pressure
P_a	Atmospheric pressure (101325 Pa at sea level)
R	Universal gas constant (8.31432J mol^{-1} K^{-1})
SAHT	Simulated absolute hedonic tone
Sc_t	The turbulent Schmidt number, generally equal to 0.7
S_h	Heat of chemical reaction and other volumetric heart sources
S_k and S_ε	Source terms
SOC	Simulated odour concentration in OU m^{-3}
SOMC	Simulated odour mass concentration in μg m^{-3}
SST	Shear stress transport
$S_T(z)$	Horizontal section area of an element or tree at height z
T	Temperature
t	Time

T_0	Temperature at the ground surface
T_3	Air temperature is at a height z = 7.62 m
T_s	Temperature at the z_s
T_{WC}	Factor to control the convective energy varied with height
T_{WN}	Factor to control the TKE decreases with height in the atmospheric boundary layer
u_*	Friction velocity
u_i' (i=1, 2, 3)	fluctuating component of the instantaneous velocity in *i*th direction, indicating in x, y, z direction in Cartesian coordinate system, respectively
u	Instantaneous velocity
u and u'	Mean and fluctuating component of instantaneous velocity
u_1	Open wind velocity at height z_1 = 7.62 m, height at which wind speed was measured
u_i (i=1, 2, 3)	Scalar component of the mean velocity in *i*th direction, indicating in x, y, z direction in Cartesian coordinate system, respectively
u_{mag}	Magnitude of mean velocity
V_1 and V_2	Molar volumes for the air and hydrogen sulphide fractions, respectively
w_*	Mixing layer velocity scale
w_1, w_2, and w_3	Three constants corresponding to the thickness of the real windbreak
WOP	Width of odour plume
$w_T(z)$	Thickness of the windbreak at the height z
Y_2	Odour mass fraction at odour generator
Y_j	Mass fraction of the species j in a mixture of gases
z	Coordinate in the vertical direction
z_0	Roughness length
z_1 and z_2	Heights in the domain, where $0 < z_1 < z_2$
z_s	Height of 1.35 m above surface
α	Aerodynamic porosity, or permeability
β	Optical porosity
γ_d	Dry adiabatic lapse rate, 0.01 K m^{-1}

ω	Specific dissipation rate
δ_{ij}	Unit tensor
ε	Turbulence dissipation rate
κ_a	Von Karman constant, ranged from 0.35 to 0.43, $\kappa_a \approx 0.4$
μ	Viscosity of mixture of the air and odorous gases
μ_{eff}	Effective viscosity
μ_t	Turbulence kinetic viscosity
ρ	Fluid density
σ_u, $\sigma_v$and σ_w	Turbulence components in x, y, z coordinates

Chapter 1
Introduction

1.1. Problem statement

1.1.1. Odour nuisances

Adequate ventilation is a necessary prerequisite to the environmental well-being of livestock housed in shelters. Livestock produce manure which is stored in open storage tanks and spread on land as a soil amendment. Odours are emitted from the livestock building, the manure storage and the land during manure application. The emission of such odours is unavoidable and causes a nuisance to surrounding residents and passersby.

There are two main factors which contribute to the increase in odour concentration. First is the industrialisation or concentration of the livestock production into units of larger capacity. This has led to large amounts of animal waste concentrated into relatively small geographic areas. The larger quantity of manure produced per farm has increased the intensity and duration of odour events. The second is urban expansion. This phenomenon has reduced the distance between suburban communities and larger livestock facilities. As a result, the separation distance between facilities and neighbours is shrinking (Tyndall and Collettii, 2000).

When common law was first developed, an overriding principle was that a landowner had the right to use and enjoy his/her land as he/she wished. An unreasonable interference with a person's right to enjoy their property is now legally a nuisance (Brant and Elliott, 2002).

Adverse effects caused by odours are mental and physical health concerns for human and animals, a decrease in real estate value and some stressed relationships developed between facility owners, neighbours and communities (Tyndall and Collettii, 2000). The affected citizen may resort to common-law nuisance litigation. Sometimes in extreme cases, the livestock facilities are shut down by

law. Thus, for social and legal reasons, livestock producers must deal with the odours emanating from their facilities

1.1.2. Odour control with windbreaks

There are three strategic categories of odour control management technologies. The first is to reduce odour generation (examples as manure and feed additives). The second is to capture and destroy the odours before they enter the atmosphere (such as bio-filters). The last uses innovations that disperse and dilute odours before they accumulate and become a nuisance and involve manipulating air movement such as with windbreaks.

A windbreak is a barrier used to reduce and redirect wind. A living windbreak consists of plantings of single or multiple rows of trees or shrubs. Windbreaks provide many benefits such as snow and sand drifting control and wildlife habitat, enhanced farmstead value, and generally give a more pleasant environment. Most importantly, windbreaks have the potential to dilute odours in the air, deposit and intercept large odorous particles and absorb odorous compounds (Bottcher et al., 2001; Leuty, 2003; Leuty, 2004; Tyndall and Collettii, 2000).

1.1.3. Limited data and models to describe odour dispersion over windbreaks

Little research pertains to the ability of a windbreak to reduce odours. Nevertheless, it seems evident that windbreaks should have the ability to control odour dispersion.

Currently, there are no models associated with windbreaks and odour dispersion. The models often used to predict the odour dispersion have no interface to input information about windbreaks, which means they do not consider odour dispersion by porous barriers such as windbreaks. The present models used to simulate windbreak action simply focus on wind dynamics, emphasizing velocity and pressure changes around windbreaks. Odour transport and dispersion are rarely analysed.

1.2. Objective

1. Theoretical and empirical mathematical models simulating windbreak odour dilution

The first objective of this project was to build a model to simulate odour dispersion around natural windbreaks. The model includes mass, momentum, energy and species equations to describe the odour dispersion. These equations were solved by Fluent software with inputs of windbreak characteristics, weather conditions and strength of the odour source.

2. Calibrating the models

The second objective of the project was to collect odour dispersion data in the field downwind from windbreaks and to use these data to calibrate the theoretical models for odour dispersion.

3. Odour dispersion simulation

The third objective of the project was to use the calibrated models to simulate the effects of the windbreak characteristics and the weather conditions on odour dispersion.

1.3. Hypothesis

The project was developed on the basis of the following hypotheses:

i) Windbreak structure determines air pressure loss across the windbreak.

ii) Windbreak porosity, height and width have an impact on odour dispersion.

iii) Odour source distance from the windbreak has an impact on odour dispersion.

iv) Atmospheric stability and wind velocity and direction influence the odour dispersion.

1.4. Scope

Odours were simulated using a single gas (H_2S) and those odours carried by dust were not considered. The project focused on odour dispersion from a single

source as affected by windbreaks and did not consider the impact of windbreak's other possible functions as a sink, deposition, or interception. Windbreaks consisted of a single row of trees and excluded the effect of artificial windbreaks such as fences.

1.5. Organization of thesis

The thesis consists of 10 chapters, including the introduction, general literature review, six scientific articles, conclusions and references. After the introduction in Chapter 1, Chapter 2 reviews the impact of livestock odour dispersion on the ambient environment, and the impact of livestock production practices on the basic concepts of livestock odours and emissions. Chapter 2 also reviews the odour dispersion potential of windbreaks and the existing models which can simulate odour dispersion around windbreaks.

Chapter 3 describes the materials and methodology used to measure odours in the field about four natural windbreaks and on a site without a windbreak. The odour concentration and wind direction were normalised and the parts of the odour plumes derived from 39 measurements were visualized to demonstrate the effects on the odour dispersion of windbreak porosity, odour source position, tree species, air temperature, and wind speed and direction.

Chapter 4 uses regression and classification methods to calculate the maximum odour dispersion distance (MODD) under standardised odour concentrations. The effects of the windbreak and weather conditions on odour dispersion are compared by means of MODDs.

Chapter 5 uses a statistical classification method to compare the effect of various parameters observed in the field, on the size of the resulting odour dispersion plume. This chapter also produces a relationship between field odour hedonic tone and laboratory odour concentration using the measured data. Then, the length and width of the odour plumes observed in the field are compared to conclude on the effects of various factors.

Chapter 6 uses the theory of computational fluid dynamics (CDF) to express odour dispersion around natural windbreaks. The standard k-ε model is calibrated to reproduce 2-dimensional wind velocity recovery rate (VRR) and 3-dimensional field odour dispersion measurements. The calibrated model is used to explain how a windbreak can help disperse odours.

Chapter 7 calibrates the Fluent 6.2 SST k-ω model and then uses this model to evaluate the effects of the windbreak porosity, height, tree structure and orientation on the odour dispersion.

Chapter 8 uses the calibrated SST k-ω model to analyse the effects of the weather conditions, such as wind velocity, direction, temperature and atmospheric stability on the odour dispersion around the natural windbreaks.

Chapter 9 gives the general conclusions on the research work.

Chapter 10 lists all references cited in the thesis.

1.6. References

Bottcher, R.W., Munilla, R.D., Keener, K.M. and Gates, R.S., 2001. Dispersion of livestock building ventilation using windbreaks and ducts. 2001 ASAE Annual International Meeting.: 01-4071. 2950 Niles road, St. Joseph, Mi. USA.

Brant, R.C. and Elliott, H.A., 2002. Pennsylvania odor management manual, Pennsylvania State University, University Park, PA. USA.

Leuty, T., 2003. Using shelterbelt to reduce odours associated with livestock production barns. Ministry of Agriculture and Food, Ontario, http://www.gov.on.ca/OMAFRA/english/crops/facts/info_odours.htm, visited in 2004.

Leuty, T., 2004. Wind management can reduce offensive farm odours. Ministry of Agriculture and food, Ontario, http://www.gov.on.ca/OMAFRA/english/crops/facts/info_windmanagement.htm, visited February, 2005.

Tyndall, J. and Collettii, J., 2000. Air quality and shelterbelts: Odour mitigation and livestock production - A literature review. Final project report to USDA National Agroforestry Center, Lincoln, NB. Project Number 4124-4521-48-3209. Forestry Department, Iowa State University, Ames, IA. http://www.forestry.iastate.edu/res/Shelterbelts_and_Odor_Final_Report.pdf (2007/01/17).

Chapter 2
Literature Review

This literature review focuses on the dispersion of odours emitted from livestock operations by windbreaks. The main topics are: (i) the necessity to study and determine odour dispersion; (ii) basic concepts of livestock odour emissions; (iii) the odour dispersion potential of windbreaks and (iv) the existing models, which can simulate odour dispersion from windbreaks.

2.1. Odour nuisances affect livestock production

Several factors have contributed to the increasing problem of odour emissions from livestock facilities. Modern livestock facilities house a large number of animals such as swine, cattle, dairy and poultry, and these facilities must be ventilated. The waste air generally contains smelly and unpleasant gases, called odours. Odour dispersion into the atmosphere is unavoidable as the livestock facilities must be vented and all excess heat, humidity and gases must be removed to maintain animal comfort and hygiene.

The industrialization of livestock facilities has led to higher levels of odour emissions from single source. From 1978 to 1992, the average number of animal units per operation increased by 56% for cattle, 93% for dairy cows, 134% for hogs, 176% for laying hens, 148% for broilers, and 129% for turkeys (Tyndall and Collettii, 2000). Also, with the increased size of the facilities, the total manure output per operation has increased. In the U.S. alone, about 130 times more animal waste is produced than human waste. The estimated solid animal manure production in the U.S. in 1997 was 1.37 Pg (Tyndall and Collettii, 2000). This trend of industrialisation has led to an increase in intensity of odours emanating from livestock operations.

The urban expansion phenomenon has also brought people closer to livestock facilities. For example, a 1998 survey of Iowa farmers conducted by Iowa State

University showed that in the 2312 survey respondents, 20% live 400 m or less from a livestock facility, 26% live between 400 and 800 m, 25% live between 800 and 1600 m and 29% live over 1600 m away (Tyndall and Collettii, 2000).

Odours can be transported to nearby residents under some weather conditions. The value of property owned by neighbours likely decreases. As a result, property owners have been appealing to the courts to prohibit nearby livestock operations.

Since 1976, several animal feeding operations (AFO) have been confirmed as odour nuisances by the Nebraska Supreme Court. In one case, the AFO was allowed to continue operating after relocating its lagoons. In other cases, two AFOs had to pay damages and were under court order to improve their operations or shut down. In 1985, another AFO was closed by the court: it housed 800 sows and 6,000 to 7,000 grower hogs, which produced an odour nuisance as far away as 800 m while the farm residence and the plaintiff's home were located at less than 400 m from one of the manure holding ponds (Aiken, 2001).

Odour nuisance is regulated by common law, the law on the "right-to-farm" and state provisions in the U.S. According to Common law, no one can interfere with another's enjoyment of their property (Brant and Elliott, 2002; Chapin et al., 1998). As a public nuisance, the local or state agency will lodge actions seeking abatement of the odour, administrative penalties, or injunctive relief. However, a private nuisance action consists of a lawsuit between private parties and a court order is sought to get the AFO to abate the odour, to close the operation, to get compensation for actual damages, or to get some combination of these (Brant and Elliott, 2002; Miner, 1997).

All 50 states and some communities in U.S. have passed "right-to-farm" legislation and AFOs are protected from odour nuisance court orders, as long as their practices respect some norms or industrial standards. A typical right-to-farm law, such as exists in North Carolina, declares that an agricultural operation which has existed for a year without being a nuisance is presumed not to be a nuisance even when new neighbours move adjacent to it (Telega, 2003; Tyndall and Collettii, 2000).

There are some state or provincial laws directly regulating odours. For example, in the province of Quebec, the guideline establishing a setback distance is effectively applied (Quebec Regulation, 2006).

Europe has been more active than the United States in addressing air quality and odour problems from large-scale swine facilities. The Netherlands' Nuisance Act defines the maximum number of animals allowed in a facility, given the distance between the operation and its neighbours. A producer may, however, increase that number of animals if the total ammonia and odour emissions do not increase. However, even if a farm abides by all these rules, neighbours can still bring legal action if there is a significant odour problem (Chapin et al., 1998).

In light of above discussion, livestock facilities must comply with the regulations of odour control. Therefore, measures to manage the odour dispersion are very important. There are three existing strategies used to control odours.

- The first strategy is to reduce the odour production. This can be achieved through the use of feed additives which can improve nutrient digestion and decrease manure nutrient content and odour emission rate.
- The second strategy is to employ a system treating the odorous air, such as a bio-filter to filter the air vented out of livestock shelters or a cover over the manure storage facility to reduce the odour emission.
- The last strategy is to disperse the odours to below their detection threshold before they reach the neighbours. For example, large separation distances between the livestock facility and the near neighbours allow the odours to fully dilute (Tyndall and Collettii, 2000).

Windbreaks have the potential to further disperse odorous air and reduce separation distances protecting neighbours. There is a limited literature proving the ability for windbreaks to dilute odours with air. However, the traditional Gaussian type of odour dispersion models are only suitable for flat surfaces and do not apply to porous windbreaks. Therefore, new models are needed to predict the distribution of odour concentrations resulting from windbreaks.

2.2. Livestock odours

The word "odour" represents any smell, pleasant or unpleasant, fragrant or offensive. Odour is a kind of substance that may be detected if its molecules collide on the olfactory organ when being sniffed (CEN, 2001; EPA, 2001). The term "livestock odour" refers to the complex combination of gases, vapours and dust that are generated by livestock facilities and offend people. Livestock odours are generated from confinement buildings, manure and feed storage facilities and manure during land application (Kempen and Heugten, 2003; Tyndall and Collettii, 2000). Odours consist of 168 odorous compounds which arise from the incomplete anaerobic degradation of carbohydrates, fatty acids and protein. Sulphur is a key element in odours (O'Neill and Phillips, 1992).

Odour sensation has four attributes: detection threshold, intensity, character and hedonic tone (ASHRAE, 2001). Detection threshold (for a reference material) is the odorant concentration which has a probability of 0.5 of being detected under the conditions of the test (CEN, 2001). For ammonia, the detection threshold is 33 mg/m^3 (ASHRAE, 1997) or 17 parts per million by volume (ppmv) (ASHRAE, 2001).

The intensity of odour is the strength of the perceived magnitude of the odour. Odour intensity can be expressed by various scales and standard references. One of the scale is 0-7: 0, 1, 2, 3, 4, 5, 6 and 7 representing none, threshold, very slight, slight, slight-moderate, moderate, moderate-strong and strong, respectively.

The relation between the intensity and the concentration of odour conforms to a power function, namely the Psychophysical Power Law (ASHRAE, 2001):

$$S = kC^n \tag{2.1}$$

Where

S is perceived intensity (magnitude) of sensation,
k is characteristic constant,
C is odorant concentration and
n is exponent of psychophysical function.

The odour character is defined as a familiar smell, e.g. fishy, sour and flowery, etc. (ASHRAE, 2001). The hedonic tone of an odour is the degree to which an odour is perceived as pleasant or unpleasant (ASHRAE, 2001). The hedonic tone of an odour is often evaluated and ranked using a scale ranging from +10 to 0 to -10. At +10 an odour is classified as very pleasant, neutral at 0 and very unpleasant at -10.

Odour concentration is the amount of odour per unit volume. In absolute values, it is expressed as mg/m^3 or volumetric parts per million (ppmv). The odour concentration measured by olfactometry is expressed as "odour units" (OU) (mostly in North America) or "odour units per cubic meter" (OU/m^3) (in Europe) (Zhang et al., 2002). In the first case, the odour concentration can be expressed as the number of unit volumes that a unit volume of odorous sample occupies when diluted to the odour threshold with non-odorous air. In the second case, according to the draft standard prEN13725 "Air quality — Determination of odour concentration by dynamic olfactometry" (2001), odour concentration is defined as the number of European odour units in a cubic meter of gas at standard conditions. One European odour unit is equivalent to 123 μg n-butanol, evaporated in 1.0 m^3 of neutral gas at standard conditions (CEN, 2001; Schauberger et al., 2002).

There are two methods used to measure odour concentration. The first is an olfactometer which can dilute an odour sample presented to a panel. The panellists sniff the sample and decide the detection threshold of the odour. The second method uses an electronic nose (e-nose), a technology which has the potential of measuring both quality and quantity of odour (Edeogn et al., 2001). The Human nose is still the most sensitive odour measurement instrument, as long as bias is eliminated (ASHRAE 2001).

Odour emission rate is the production of a given odour concentration at a specific flow rate. Odour emission rates vary widely among different facilities and even in the same facility at different times. For example, the mean odour emission rate is from 8.4 to 13.2 $OU/s/m^2$ over different cycles of a swine operation (Zhang et al., 2002). Mean emission rates from earthen manure storages are 10.9 $OU/s/m^2$ of manure surface area, with a range of 0.1 to 51.3 $OU/s/m^2$ (Zhang et al., 2002).

Odour emission rate is influenced by diet, age and type of animal, activity or time of the day and manure storage type. Feed wastage, digestibility, fibre, protein and sulphur content also influence odour emission rates, which increase in parallel with the amount of fibre and sulphur in the diet but decrease with feed digestibility (Kempen and Heugten, 2003).

2.3. Odour dispersion

Odour dispersion is the process of widely distributing odorants into the atmosphere. These odorants travel downwind and dilute with air, leading to the odour concentration decreasing downwind. It has been observed that odours can travel over longer and wider distances when the atmosphere is stable with lower wind velocity (Guo et al., 2001a). Weather stability can be classified into 6 different classes (from A to F): class A is strongly unstable while class F is strongly stable. The stable weather is not favourable to odour dispersion (Guo et al., 2001a). Further studies show that odour dispersion is influenced by the prevailing wind direction (Schauberger et al., 2002).

Dispersion models are basic tools used to analyse distribution of odour concentration during dispersion. These models are FPM (Mussio et al., 2001), AODM (Schauberger et al., 2000), Inpuff-2 (Guo et al., 2001a; Zhu et al., 2000), ISCST3(Sheridan et al., 2003) , Screen3 and AERMOD (Choinière, 2003). Most dispersion models are Gaussian and assume odour concentrations across the plume in the vertical and horizontal directions to exhibit a normal distribution. These models cannot be used to predict porous windbreak odour dispersion. For example, the Industrial Source Complex - Short Term (ISCST3) dispersion model from the U. S. Environmental Protection Agency (EPA) is a steady-state Gaussian plume model. It can assess pollutant concentrations and/or deposition fluxes from a wide variety of complex industrial sources. The ISCST3 can handle plume buoyancy, multiple sources, varied pollutant emission rate, building downwash, large particle deposition, precipitation scavenging for gases, grid receptors, complex terrain and real time meteorological data. The result outputs are concentration and deposition fluxes (Lakes Environmental Software, 2002; Thé et

al., 2002). However, the model does not consider porous obstacles in the vicinity of the source (CEN, 2001; Sheridan et al., 2003).

2.4. Setback distance

If there is enough distance between the odour source and its receptor, such as neighbours, the odour nuisance may be avoided (Zhang et al., 2002). Statistical analysis has shown that if a swine facility was located 800 m away from a neighbour, the probability of it not causing an odour complaint was 0.99 (VanDevender, 2000).

Different setback models have been developed in the world. The Minnesota OFFSET model gives the occurrence frequency of faint odours at various distances away from a source and produces different setback distances according to odour annoyance-free frequencies varying from 91% to 99% (Guo et al., 2001).

In 1996, Illinois adopted the Livestock Management Facilities Act which requires facilities to develop a waste management plan and provides for varying setback distances. For an operation with 125 to 2,500 finishing pigs, a setback distance of 400m is required from a non-farm residence and of 800 m from a populated area. The distance increases by 70 m to 140 m for every increase of 2,500 hogs, to a maximum setback of 800 m and 1600 m, respectively. Again, citizens in this state find this regulation too weak and want a greater control (Chapin et al., 1998).

In the province of Quebec, the setback distance is calculated as (Quebec Regulation, 2006):

$$\text{Setback distance} = B \times C \times D \times E \times F \times G \qquad (2.2)$$

Where

B is the basic distance based on animal units;

C is the odour load per animal according to the animal category;

D is the type of manure,

E is the project type (new operation or expansion of existing operation);

F is an attenuation factor reflecting the effect of attenuating technology used; and

G is a usage factor based on the type of neighbouring units in question.

2.5. Windbreaks

Windbreak research started in the 1930s and focused on the reduction of wind velocity, to control snow and sand accumulation and pesticide drift. Windbreaks have also been observed to increase crop yield and protect animals and buildings, reduce soil erosion and noise, and improve aesthetics. Aerodynamically, windbreaks are wind momentum sinks as they can protect surrounding zones from wind damage. They are also presumed to mitigate odours by mixing them with clean air, although the process is still not fully understood. To further understand this mechanism, windbreak dynamics, research methods and simulation models are reviewed.

2.5.1. Basic concept about windbreaks

Windbreaks are barriers used to reduce and redirect wind. Living windbreaks are plantings of single or multiple rows of trees or shrubs. Several words are synonymous with living windbreaks: shelter, shelterbelt and fence (Eimern et al., 1964). The basic functions of windbreaks are to reduce wind velocity and change its direction around windbreaks. The functions depend on the height (H), width or thickness, porosity and orientation of the windbreaks.

Windbreak porosity can be described by optical porosity β and aerodynamic porosity α. The optical porosity is the ratio of the open surface to the total surface of the windbreak. The aerodynamic porosity α is defined as the ratio of mean wind speed (bleed wind speed) immediately leeward from the bottom to the top of the windbreak to that upwind before windbreak interference. Guan et al. (2003) suggested the following relationship between the optical and aerodynamic porosities.

$$\alpha = \beta^{0.4} \tag{2.3}$$

Thus, the aerodynamic porosity is larger than or equal to the optical porosity. Windbreaks normally have the shape of a rectangle and usually the higher the

windbreak, the larger the protected zone. For the most efficient results, the best windbreak orientation is perpendicular to prevailing winds during the odour nuisance season (Dierickx et al., 2003; Dierickx et al., 2002).

Horizontal distances and wind speed are usually expressed in terms of height of the windbreak (H) and approach wind speed ($U_{approach}$), respectively. Windbreak influence extends from approximately -5 H (windward) to 30-35 H (leeward). Minimum wind speed is achieved in the near lee, at distances of 4-6 H. Further leeward, at about 20 H, wind speed recovers to 80% of the approaching wind speed. For very dense windbreaks, the wind profile shows a lower minimum wind speed but a faster wind speed recovery near the lee (between 0 H and 10 H), compared to a porous windbreak (Eimern et al., 1964; Heisler and Dewalle, 1988; Plate, 1971; Ucar and Hall, 2001; Vigiak et al., 2003).

2.5.2. Windbreaks mitigate odours

Windbreaks are supposed to dilute, deposit, intercept, and sink odours (Tyndall and Collettii, 2000) and improve aesthetic appearance (Leuty, 2003; Leuty, 2004). The use of windbreak walls in the control of odour dispersion has been reported (Bottcher et al., 2000; Bottcher et al., 2001). The function of dilution and dispersion will be fully discussed according to the scope of this research. The dilution caused by the windbreak depends on the bleed, displaced and equilibration flows, and quiet and mixing zones created by windbreaks.

There are two flows and two zones associated with windbreaks as shown in Fig. 2.1. First, some air flows through the porous windbreak creating a *bleed flow* immediately to the lee and its velocity is reduced because of the drag exerted by the windbreak vegetation. Secondly, another part of the air called *displaced flow* with a high wind speed actually flows over the top of the windbreak. The displaced flow with high wind speed is a result of mass conservation and extends at least 1.5 H above the windbreak (Plate, 1971; Cleugh, 1998; McNaughton, 1988).

A ***quiet zone*** is formed in the lee of the windbreak. It has a roughly triangular shape where the boundaries are formed by the windbreak itself, the ground

surface and a line sloping downwards and downwind from the top of the windbreak intersecting the ground between 3 and 8 H. The minimum wind speed (U_{min}) occurs in the quiet zone and its downwind position moves closer to the windbreak with decreasing porosity. If the windbreak is very dense (porosity < 0.3), the flow in the quiet zone can reverse direction to form a re-circulating eddy (Cleugh, 1998; McNaughton, 1988; Lee and Kim, 1999; Schwartz et al., 1995).

A ***mixing zone*** is constructed by windbreaks above and downwind of the quiet zone which eventually ($X >> 10H$) merges into an equilibration zone where the upwind profile is re-established. The mixing layer grows vertically and downwards from a thin layer initiated at the top of the windbreak and extends to intersect the ground surface downwind, marking the limit of the quiet zone. This mixing zone is typically referred to as the wake zone (Cleugh, 1998).

The high turbulence at the top of the windbreak results from the variance in the horizontal wind speed. Recent studies have shown that the mixing zone is created by the merging of the displaced flow and the bleed flow with strong wind shears. By contrast, the turbulence in the quiet zone is typically smaller and less energetic than in the mixing zone.

When designed properly, windbreaks force a part of the airflow upwards over the top of the windbreak, enter the mixing zone and therefore enhance odorous gas mixing. Furthermore, the reduced wind speed in the quiet zone can deposit the odorous particles. Meanwhile, the reduced wind speed around the livestock facility can reduce the quantity of exhausted odours away from the site. It has been shown that solid windbreak walls near exhaust fans can divert fan airflow and enhance mixing with wind (Bottcher et al., 2001).

Regarding the other three ways to reduce odours, "deposition" means windbreaks can deposit dust being carried in odorous air in the quiet zone. "Interception" implies trees are highly effective at physically collecting small dust particles that are carried in the wind and pass through the windbreak. "Sink" is that odorous gases, chemicals and dust particles can stick to living windbreak surfaces and enter into the plant tissue.

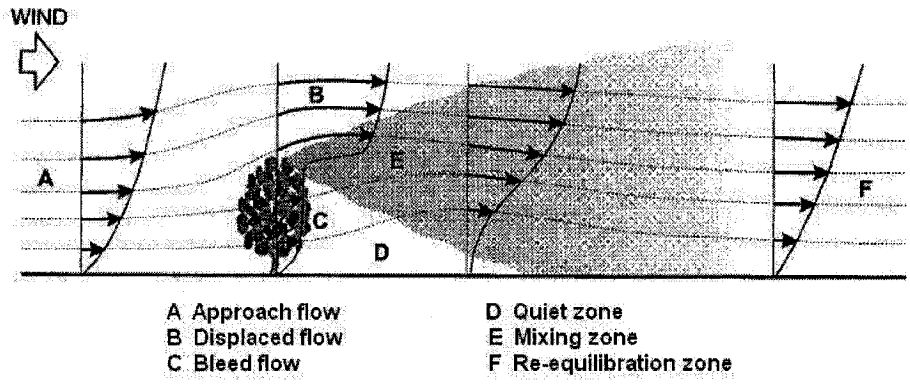

Fig. 2.1. Schematic of airflows and zones around a single windbreak, oriented normal to the flow in neutral atmospheric conditions. Shown are hypothetical vertical profiles of mean horizontal wind speed and streamlines (Cleugh, 1998).

As to aesthetic appearance, tree windbreaks create a visual barrier to livestock barns and make cropped fields and pastures more visibly pleasant. They also send an 'environmental statement' to neighbours telling everybody that the producer is making every effort to resolve odour problems in as many ways as possible. Finally, they hide the livestock shelter from sight.

2.6. Methods to simulate the odour dispersion over windbreaks

Windbreaks have mainly been studied through field tests, wind tunnel experiments and computational fluid dynamic (CFD) simulations. Early studies consisting of field measurements and wind tunnel experiments have led to considerable progress in understanding wind flow and turbulence characteristics (Boldes et al., 2001). But a full understanding of the aerodynamics of windbreaks is not easy because natural barriers are irregular and difficult to characterize structurally. Besides variable topographical settings, wind speed and direction change constantly in natural settings along with conditions of atmospheric stability (Heisler and Dewalle, 1988).

CFD models such as the k–ε, and a large-eddy simulation (LES) were reported to simulate windbreaks in 2 and 3 dimensions, with a good prediction of the mean wind field (Packwood, 2000; Patton et al., 1998; Schwartz et al., 1995; Wang and Takle, 1995; Wilson, 1985; Wilson and Yee, 2003). Windbreaks as porous barriers were treated as a momentum sink, namely, the pressure loss, which results from the viscous and inertial resistance and can be measured using a wind tunnel and simulated by the CFD model (Guan et al., 2003). The pressure loss coefficient is defined as the difference of air pressure before and after the windbreak divided by $1/2\rho U^2_H$ where U_H is approaching wind speed at the height of the windbreak (Heisler and Dewalle, 1988; Schwartz et al., 1995). For the same porosity, windbreak pressure losses can differ because of a different structure of the solid and empty portions of the windbreak (Gan and Riffat, 1997).

The CFD software, Fluent, is considered to be a valuable tool in simulating pesticide drift (Ucar and Hall, 2001). The model was coupled with conservation equations for heat and moisture. These factors were estimated from the simulated

momentum, temperature and humidity fields which were adequately simulated by the model (Hipsey et al., 2004).

So far, there is no simulated and measured data which describes odour dispersion around windbreaks. However, CFD models have the potential to do windbreak odour dispersion simulation. CFD can simulate windbreaks as discussed above. CFD was successfully used to simulate 2 and 3-dimensional airflow patterns and ammonia distribution throughout the air space within an experimental High-Rise Hog Building (HRHB) (Sun et al., 2001; Sun et al., 2002a; Sun et al., 2002b). CFD was also used to simulate the disturbed flow through and over a two dimensional array of rectangular buildings (Lien et al., 2004). Therefore, it is likely that the mass and momentum conservation equations along with the odour transport equation could solve the problem of estimation of odour dispersion over windbreaks.

2.7. Conclusions

This survey of literature has reviewed nuisance odour generation, dispersion and dispersion modeling as well as the aerodynamic effects of windbreaks along with methods of simulating odour dispersion with windbreaks. In keeping with the objective of the project, this literature review identifies the steps needed to model windbreak odour dispersion.

Livestock operations emit significant amounts of odours, which are recognized as a major source of nuisance. These odours are jeopardizing the expansion and even the operation of livestock production units, especially in North America and Europe, where facilities can be legally forced to shut down. Thus, methods of dispersing odour are urgently needed.

Odour dispersion is largely influenced by the atmospheric and surface conditions. Odour nuisances often result from stable weather conditions which lead to limited air dispersion. The setback distance between the odour sources and neighbours is a buffer zone which allows odours to fully disperse. There are many ways to calculate the setback distance depending on which odour nuisance standard is being used. The planting of windbreaks is one of several strategies which can

help disperse odour between livestock facilities and surrounding residences. This is a new concept which needs further study.

So far, windbreaks have been studied and simulated aerodynamically to estimate their capability of redirecting and reducing wind speed and of controlling snow and sand/soil drifting. Created by windbreaks, the mixing zone with higher turbulence helps air dispersion and the quiet zone helps trap odours. To properly simulate the effects of windbreaks, the momentum sink or air pressure loss coefficient must be used and correctly estimated. Field measurements, wind tunnel tests and CFD simulations are appropriate methods to study windbreaks. The proper windbreak simulation also requires solving the mass and momentum equations as well as the transport equations for odorous gases.

Because of their capability in redirecting and changing the characteristics of winds, windbreaks should also be able to disperse odours. Furthermore, it is believed that windbreaks can intercept, adsorb and deposit odorous gases. Because available odour dispersion models do not offer a momentum sink function to simulate odour dispersion through the porous medium, they cannot be used to simulate the effect of windbreaks. The present project proposes a new approach to study the potential of windbreaks on odour dispersion. It proposes the construction of a model using both CDF principles and dispersion concepts to model windbreak odour dispersion.

2.8. References

Aiken, J.D., 2001. Manure matters archive files Nebraska livestock nuisance law. http://manure.unl.edu/adobe/v7n7_01.pdf, visited, 200607.

ASHRAE, 1997. ASHRAE fundamentals handbook. American Society of Heating, Refrigeration and Air Conditioning, Atlanta, Georgia, USA, 13.1-13.6 pp.

ASHRAE, 2001. ASHRAE fundamentals handbook. American Society of Heating, Refrigeration and Air Conditioning, Atlanta, Georgia, USA, 13.1-13.8 pp.

Boldes, U., Colman, J. and Leo, J.M.D., 2001. Field study of the flow behind single and double row herbaceous windbreaks. Journal of Wind Engineering and Industrial Aerodynamics, 89: 665-687.

Bottcher, R.W., Munilla, R.D., Baughman, G.R. and Keener, K.M., 2000. Designs for windbreak walls for mitigating dust and odor emissions from tunnel ventilated swine buildings. pp. 174-181 in: Swine Housing, Proc. of the 1st International Conference, Oct. 9-11, 2000, Des Moines, Iowa. American Society of Agricultural Engineers, 2950 Niles road, St. Joseph, Mi. USA.

Bottcher, R.W., Munilla, R.D., Keener, K.M. and Gates, R.S., 2001. Dispersion of livestock building ventilation using windbreaks and ducts. 2001 ASAE Annual International Meeting.: Paper No. 01-4071. 2950 Niles road, St. Joseph, Mi. USA.

Brant, R.C. and Elliott, H.A., 2002. Pennsylvania odor management manual, Pennsylvania State University, University Park, PA. USA.

CEN, 2001. Air quality - determination of odor concentration by dynamic olfactometry. prEN13725, European Committee for Standardization, 36 rue de Stassart, B-1050 Brussels. <http://www.aerox.nl/images/eurstandard.pdf>, visited August, 2004.

Chapin, A., Boulind, C. and Moore, A., 1998.Controlling odor and gaseous emission problems from Industrial swine facilities. Yale Environmental Protection Clinic Handbook. <http://www.kerrcenter.com/publications/Controlling_Odor.pdf#search='Controlling%20Odor%20and%20Gaseous%20Emission%20Problems%20from'>.

Choinière, D., 2003. Validation of a dispersion model for agricultural odors in Quebec, The CSAE Odor dispersion annd regulation workshop, The Canadian society for engineering in agricultural, food and biological systems, Saskatoon, Canada.

Cleugh, H.A., 1998. Effects of windbreaks on airflow, microclimates and crop yields. Agroforestry Systems, 41: 5-84.

Dierickx, W., Cornelis, W.M. and Gabriels, D., 2003. Wind tunnel study on rough and smooth surface turbulent approach flow and on inclined windscreens. Biosystems Engineering, 86(2): 151-166.

Dierickx, W., Gabriels, D. and Cornelis, W.M., 2002. Wind tunnel study on oblique windscreens. Biosystems Engineering, 82(1): 87-95.

Edeogn, I., Feddes, J.J.R., Qu, G., Coleman, R. and Leonard, J., 2001. Odour measurement and emissions from pig manure treatment/storage systems. Final report to Canada Pork Council. Project Number CPC-01. University of Alberta, Edmonton, AB. http://www.cpc-ccp.com/HEMS/CPC-01_Feddes.PDF (2007/01/17)..

Eimern, J.v., Karschon, R., Razumova, L.A. and Robertson, G.W., 1964. Windbreaks and shelterbelts. Report of a working group of the Commission for Agricultural Meteorology, World Meteorological Organization, Technical Note No. 59. Secretariat of the World Meteorological Organization, Geneva, 188 pp.

EPA, 2001. Odor impacts and odor emission control measurement for intensive agriculture, <http://www.epa.ie/pubs/docs/Odour%20Impacts%20Final.pdf>,visited on July, 2006.

Gan, G. and Riffat, S.B., 1997. Pressure loss characteristics of orifice and perforated plates. Experimental Thermal and Fluid Science, 14: 160-165.

Guan, D., Zhang, Y. and Zhu, T., 2003. A wind-tunnel study of windbreak drag. Agri. Ecosystem & Environment, 118: 75-84.

Guo, H., Jacobson, L.D., Schmidt, D.R. and Janni, K.A., 2001a. Simulation of odor dispersion as impacted by weather conditions. ASAE Publication Number 701P0201, 2950 Niles road, St. Joseph, Mi. USA.

Guo, H., Jacobson, L.D., Schmidt, D.R. and Nicolai, R.E., 2001b. Calibrating inpuff-2 model by resident-panelists for long-distance odor dispersion from animal production sites. American Society of Agricultural Engineers, 17(6): 859-868.

Guo, H., Jacobson, L.D., Schmidt, D.R., Nicollai, R.E. and Janni, K.A., 2001c. Comparison of five models for setback distance determination. ASAE Meeting Presentation Paper Number 01-4045, ST Joseph, Michigan, USA.

Heisler, G.M. and Dewalle, D.R., 1988. Effects of windbreak structure on wind flow. Agriculture, Ecosystems and Environment, 22-23: 41-69.

Hipsey, M.R., Sivapalan, M. and Clement, T.P., 2004. A numerical and field investigation of surface heat fluxes from small wind-sheltered waterbodies in semi-arid western austrilia. Environmental Fluid mechanics, 4: 79-106.

Kempen, T.v. and Heugten, E.v., 2003. Impact of diet on odor. http://mark.asci.ncsu.edu/SwineReports/2003/vankempen2.htm.

Lakes Environmental Software, 2002. ISCST3 tech guide. <http://www.weblakes.com/ISCVOL2/Contents.htm>, Waterloo, Ontario, Canada.

Lee, S.-J. and Kim, H.-B., 1999. Laboratory measurements of velocity and turbulence field behind porous fences. Journal of Wind Engineering and Industrial Aerodynamics, 80: 311-326.

Leuty, T., 2003. Using shelterbelt to reduce odors associated with livestock production barns. Ministry of Agriculture and Food, Ontario, http://www.gov.on.ca/OMAFRA/english/crops/facts/info_odours.htm, visited in 2004.

Leuty, T., 2004. Wind management can reduce offensive farm odours. Ministry of Agriculture and food, Ontario, http://www.gov.on.ca/OMAFRA/english/crops/facts/info_windmanagement.htm, visited February, 2005.

Lien, F.S., Yee, E. and Cheng, Y., 2004. Simulation of mean flow and turbulence over a 2D building array using high-resolution CFD and a distributed drag force approach. Journal of Wind Engineering and Industrial Aerodynamics, 92: 117-158.

McNaughton, K.G., 1988. Effects of windbreaks on turbulent transport and microclimate. Agri. Ecosystem & Environment, 22-23: 17-39.

Miner, J.R., 1997. Nuisance concerns and odor control. J Dairy Sci, 80: 2667-2672.

Mussio, P., Gnyp, A.W. and Henshaw, P.F., 2001. A Fluctuating plume dispersion model for the prediction of odor-impact frequencies from continuous stationary sources. Atmospheric Environment, 35: 2955-2962.

O'Neill, D.H. and Phillips, V.R., 1992. A review of the control of odour nuisance from livestock buildings: Part 3, properties of the odorous substances which have been identified in livestock wastes or in the air around them. Journal of Agricultural Engineering Research, 53: 23-50.

Packwood, A.R., 2000. Flow through porous fence in thick boundary layers: comparisons between laboratory and numerical experiments. Journal of Wind Engineering and Industrial Aerodynamics, 88: 75-90.

Patton, E.G., Shaw, R.H., Judd, M.J. and Raaupach, M.R., 1998. Large-eddy simulation of windbreak flow. Boundary-Layer Meteorology, 87: 275-306.

Plate, E.J., 1971. The aerodynamics of shelter belts. Agric. Meteorol, 8, 203.

Quebec Regulation, 2006. Guidelines for determining minimum distance to ensure odour management in rural areas, R.Q. c. P-41.1, r.1.1. Quebec Ministry of Environment, Quebec, Canada. http://www.canlii.org/qc/laws/regu/p-41.1r.1.1/20060614/whole.html.

Schauberger, G., Piringer, M. and Petz, E., 2002. Calculating direction-dependent separation distance by a dispersion model to avoid livestock odor annoyance. Biosystems Engineering, 82(1): 25-37.

Schauberger, G., Pringer, M. and Petz, E., 2000. Diurnal and annual variation of the sensation distance of odor emitted by livestock building calculated by the Austrian odor dispersion model(AODM). Atmospheric Environment, 34: 4839-4851.

Schwartz, R.C., Fryrear, D.W., Harris, B.L., Billbro, J.D. and Juo, A.S.R., 1995. Mean flow and shear stress distributions as influenced by vegetative windbreak structure. Agricultural and forest meteorology, 75: 1-22.

Sheridan, B.A., Hayes, E.T., Curran, T.P. and Dodd, V.A., 2003. A dispersion modeling approach to determining the odor impact of intensive pig production units and Ireland. Bioresource Technology, 91: 145-152.

Sun, H., Keener, H., Stowell, R.R. and Michel, F.C., 2001. Three-dimensional numerical simulation of mechanical ventilation in a high-riseTM hog building (HRHB), 2001 ASAE International Meeting, Sacramento, CA, Paper No. 014040.

Sun, H., Keener, H., Stowell, R.R. and Michel, F.C., 2002a. Two-dimensional computational fluid dynamics (CFD) modeling of air velocity and ammonia distribution in a high-riseTM hog building, 2002 ASAE Annual International Meeting/CIGR International Congress. ASAE, Chicago, USA, Paper No. 024117.

Sun, H., Stowell, R.R., Keener, H.M. and Michel, F.C., 2002b. Comparison of predicted and measured ammonia distribution in a high-riseTM hog building (HRHB) for summer conditions. Transactions of the ASAE, Vol. 45(5): 1559-1568.

Telega, L., 2003. Legal primer for farms and their neighbors. http://www.dairybusiness.com/northeast/June03/F2%20p22,23%20Legal%20primer.pdf.

Thé, J.L., Thé, C.L. and Johnson, M.A., 2002. ISC-AERMOD View User's Guide. Lakes Environmental Software. Lakes Environmental Software, 419 Phillip Street, Unit 3, Waterloo, Ontario N2L 3X2.

Tyndall, J. and Collettii, J., 2000. Air quality and shelterbelts: Odour mitigation and livestock production - A literature review. Final project report to USDA National Agroforestry Center, Lincoln, NB. Project Number 4124-4521-48-3209. Forestry Department, Iowa State University, Ames, IA. http://www.forestry.iastate.edu/res/Shelterbelts_and_Odor_Final_Report.pdf (2007/01/17).

Ucar, T. and Hall, F.R., 2001. Review windbreaks as a pesticide drift mitigation strategy: a review. Pest Management Science, 57: 663-675.

VanDevender, K., 2000. Arkansas swine odor survey. http://www.uaex.edu/Other_Areas/publications/PDF/FSA-1030.pdfodorsurvey.pdf, visited 200408.

Vigiak, O., Sterk, G., Warren, A. and Hagen, L.J., 2003. Spatial modeling of wind speed around windbreaks. Catena, 52: 273-288.

Wang, H. and Takle, E.S., 1995. A numerical simulation of boundary-layer flows near shelterbelts. Boundary-Layer Meteorology, 75(1 - 2): 141-173.

Wilson, J.D., 1985. Numerical study of flow through a windbreak. Journal of Wind Engineering and Industrial Aerodynamics, 21: 119-154.

Wilson, J.D. and Yee, E., 2003. Calculation of winds distribution by an array of fences. Agricultural and forest meteorology, 115: 31-50.

Zhang, Q. et al., 2002. Odor production, evaluation and control. http://www.manure.mb.ca/projects/completed/pdf/02-hers-03.pdf, visited August, 2004., Manitoba Livestock manure Management Initiative Inc.

Zhu, J., Jacobson, L.D., Schmidt, D.R. and Nicolai, R., 2000. Evaluation of inpuff-2 model for predicting downwind odors from animal production facilities. American Society of Agricultural Engineers, 16(2): 159-164.

Connecting statement

Chapter 3 presents visualisation of odour plumes measured on five field sites, where four offered different natural windbreaks and one was without windbreak. All odour plumes were standardised by normalising odour concentrations and wind directions for the purpose of visual comparison. Then the effects of windbreak presence, porosity, odour source position, tree species, air temperature, wind speed and direction on the odour dispersion were observed.

This paper was published in the Agriculture, Ecosystems & Environment, 116 (3-4): 263-272. Authors are Lin, X.J., Barrington, S., Nicell, J., Choiniere, D. and Vezina. A.. The contributions of the authors are i) First author carried out a part of field measurements, the whole data analysis and wrote the manuscript; ii) Second author supervised and helped revise the methods of analysis and the content of the paper; iii) Third author advised the method of analysis; iv) Fourth author organized and managed the collection of the field data; and v) The last author measured the optical porosity of the windbreaks.

Chapter 3
Influence of windbreaks on livestock odour dispersion plume in the field

3.1. Abstract

Windbreaks are believed to help disperse odours emitted by livestock facilities. The objective of the project was to measure the effect of windbreaks on the size and hedonic tone of odour dispersion plumes developed in the field when subjected to a point odour source. Comparisons were made for odour plumes observed with and without windbreaks, and with windbreaks exposed to different conditions. Besides a control site without windbreak, four windbreak sites were selected, two of which had one row of deciduous trees while the other two had one row of coniferous trees. Odour dispersion plumes were measured 6 times on the control site and 33 times on the windbreak sites. Each time, an odour generator was used to produce a controllable level of odour emission. Three groups of four trained panellists measured the size and hedonic tone of the odour plume developing in the field downwind from the odour generator. Using a forced choice dynamic olfactometer, all 12 panellists were calibrated every test day and the group's field odour hedonic tone perception was correlated to odour concentrations. Windbreaks were found to have an effect on odour dispersion. This effect was more pronounced when the windbreak was dense (lower optical porosity) and consisted of coniferous trees. Moreover, odour dispersion was improved when the source was located 15 m upwind from the windbreak, rather than 60 m. When temperatures were above 15 °C, odours were dispersed over a shorter distance, likely because of added convective effects. Wind speed was found to have a limited effect on the size and hedonic tone of the odour plume while wind direction perpendicular to the windbreak reduced the size of the odour plume but not the trapping of odours on the leeward side of the windbreak. In

general, windbreaks can improve odour dispersion, but a better study of their performance is required through modeling.

Keywords: Windbreak; Odour dispersion and concentration; Porosity; Wind direction and speed; Tree type.

3.2. Introduction

Odours released from livestock facilities are disperse into the atmosphere while being transported to nearby dwellings and communities. Insufficient dispersion of odours leads to nuisance and law suits (Brant and Elliott, 2002; Tyndall and Collettii, 2000). To prevent such nuisance, a common practice is to leave sufficient setback distance between the livestock facilities and the neighbours, thus increasing the probability of atmospheric dilution. To further increase this probably, natural windbreaks have been recommended around livestock facilities (Leuty, 2003; Leuty, 2004; Tyndall and Collettii, 2000).

Windbreaks are well known to act as barriers reducing and redirecting the wind, and thus theoretically have been presumed to help dilute odours. However, the odour dispersion capability of windbreaks and the ideal design of the windbreak shelter (size, location, and distance from the livestock facility) still need investigation. In the past, windbreak research has focused on the reduction of wind velocity and turbulence, the control of snow and sand accumulation and the reduction in pesticide drifting. Windbreaks have also been observed to increase crop yield and protect animals and buildings, reduce wind erosion and noise and improve aesthetics (Dierickx et al., 2002; Eimern et al., 1964; Guan et al., 2003; Heisler and Dewalle, 1988; Plate, 1971; Ucar and Hall, 2001; Vigiak et al., 2003; Wang and Takle, 1997; Wilson and Yee, 2003).

Field measurement, wind tunnel test and computational fluid dynamic (CFD) simulation are the three main methods used to study windbreaks (Boldes et al., 2001; Lee and Kim, 1999; Patton et al., 1998). Research pertaining to livestock odour dispersion has focused on the measurement of odours emitted from barns, manure storage facilities and fields used for manure spreading

(Edeogn et al., 2001; Guo et al., 2003; Zhu et al., 2000). However, field odour dispersion around windbreaks is less commonly reported.

Livestock and poultry producers in North America have installed windbreak walls near the outlets of the fans venting their livestock shelters to help reduce dust and odours emissions. The effect of such walls was studied by means of smoke emitters and simulated using a Gaussian model (Bottcher et al., 2000; Bottcher et al., 2001). The windbreak walls were found to vertically divert the odours and dust from the exhaust fans and promote mixing of the odorous dusty air with the wind flowing over the building, but not to be as effective as tall stacks. However, field measurements are still needed to determine the effectiveness of porous windbreaks for odour dispersion.

The objective of this project was to conduct a preliminary investigation to observe the effect of windbreaks on odour dispersion produced from a point source. Thus, the project investigated the size and hedonic tone of odour dispersion plumes created in the absence and presence of windbreaks in the field. An odour generator was used to produce a controlled point odour source to conduct the experiment away from any interfering sources. Three teams of four trained panellists measured the odour plumes. The size of the measured plumes was visually compared to evaluate the windbreak effect.

3.3. Materials and methods

3.3.1. *Sites and windbreaks*

For this field experiment, four uniform single row windbreaks were selected and these were located at least 5 km from any livestock operation to eliminate interferences (Fig. 3.1). The porosity of each windbreak was optically evaluated by measuring the percentage of open surface visible through the windbreak (Guan et al., 2003; Heisler and Dewalle, 1988).

The four windbreaks were selected in such a way as to offer different conditions. The optical porosity of the windbreaks on sites 1 and 3 was 55% compared to that of 35% for that on sites 2 and 4 (Table 4.3.1). Deciduous tress constituted the windbreaks on sites 1 and 2 while conifers constituted those of

sites 3 and 4. All sites were located on farm land with a relatively flat and consistent slope of 0.1%. Tree height varied among windbreaks, sites 1 and 4 offering windbreaks with a height exceeding 15 m compared to sites 2 and 3 offering windbreaks with a height under 10 m.

A control site (site 5) without windbreak was selected to also observe odour dispersion. This site consisted of relatively flat (0.1% uniform slope) land without trees or fences, where a cereal crop had been freshly harvested.

3.3.2. *Odour generator*

A mobile odour generator (Fig. 3.2) was used to control the emission of odours during the test, and to carry out the test away from any infrastructure capable of interfering with the results. During the tests, the odour generator was positioned upwind from the windbreak, at a distance of 15, 30 or 60 m.

The odour generator consisted of a 500 L tank filled with swine manure. A pump dropped the manure at the top of a vertical porous filter through which air was blown. The odour generator was found to produce 76.8 m^2 of air/liquid contact surface (Choinière, 2004). The contaminated air was released at a mean rate of 1.65 m^3 s^{-1}. At every 30 minutes during the test, an air sample was collected at the outlet of the odour generator using Alinfan® bags. Using a forced choice dynamic olfactometer, the threshold dilution value of each air samples was determined in the laboratory by the same 12 trained panellists who observed the field odour plume dispersion.

The odour concentration was expressed as "odour units per cubic meter" (OU m^{-3}) as used in Europe (CEN, 2001; Schauberger et al., 2002; Zhang et al., 2002), rather than as "odour units" (OU) as mostly used in North America. Thus, the rate of odour production, OU s^{-1}, could be computed from the air flow of the odour generator.

3.3.3. *Weather station*

During each test, a 7.6 m high weather station tower was installed 200 m upwind from the windbreak, to avoid disturbance. A computer recorded the temperature,

wind direction and wind speed every minute during the field test. The measured wind direction was used before hand to determine the range of the field odour plume and to direct panellists into the odour plume zone.

3.3.4. *Panellists*

Three groups of four (3 x 4 = 12) trained panellists were used to establish the size of odour plumes in the field. The panellists were selected by requiring them to detect n-butanol at concentrations of 20 to 80 ppb and to show consistency in their individual measurements (Choinière and Barrington, 1998; Edeogn et al., 2001). In the laboratory, the olfactory ability of each group of panellists was calibrated using a dynamic forced choice olfactometer. Odour hedonic tone was established using a scale of 0 to -10, where 0 to -2 is tolerable, -2 to -4 is unpleasant, -4 to -6 is very unpleasant, -6 to -8 is terrible and -8 to -10 is intolerable. Using the odorous air samples collected from the odour generator during the field tests at full strengths, each panellists was asked to rate the odour hedonic tone using this scale of 0 to -10. Then, each panellist was used to determine the odour threshold level of each odorous sample. A relationship was thus obtained between odour hedonic tone and odour concentration (Fig. 3.3b), for each group of four panellists. Thus, the odour hedonic tone reading (0 to -10) of each group of panellists in the field could be translated into an odour concentration in terms of OU m^{-3}.

3.3.5. Olfactometer

The laboratory forced choice dynamic olfactometer used in this experiment was fully automated and capable of analyzing 4 contaminated air samples in 20 minutes, using 12 panellists. The olfactometer is unique because of its level of automation and speed suitable to evaluate air samples (Choinière and Barrington, 1998).

3.3.6. *Test procedure*

Before each test, the odour generator and weather station tower were installed upwind from the windbreak and checked to be effectively working. Then, the three groups of four panellists were given a GPS to keep track of their field position and a planned route with specific measurement points. The odour

generator would be turned on 15 minutes before the panellists would start covering their specified path to measure the odour plume (Fig. 3.3a). At each measurement point, the group would stop walking, removed their face masks and evaluated the odour hedonic tone during one minute, using a scale of 0 to -10. The odour hedonic tone observed by each panellist was recorded along with their GPS position and the actual time of reading. An odour point was defined as a point in the field where at least 50% (2 out of 4) of the panellists detected an odour. The odour hedonic tone at an odour reading point was the average of the four panellist evaluation.

Following each field test, the same panellists were used to determine the odour concentration of the odour samples collected at the outlet of the odour generator. The relationship between field odour hedonic tone readings and actual odour concentrations (OU m^{-3}) was also determined at the same time, to translate the field readings into concentration (OU m^{-3}) values (Choinière, 2004).

On 18 different days, 39 different tests were conducted on the four windbreak sites and the single control site (Table 3.2). A test consisted in the measurement of the odour plume by the panellists on a given site with the odour generator located at a specific distance upwind from the plume area or the windbreak. On the control site, six repeated tests were conducted on 4 different days. Then, 33 tests were conducted on the windbreak sites. A total of 12, 11 and 9 tests were conducted with the odour generator located 15, 30 and 60 m upwind from the windbreak, respectively. One test was conducted with the odour generator located 49m from the windbreak, on site 3. Tests on sites 1, 2, 3 and on the control site were conducted in late August and early September 2003 while tests on site 4 were conducted in December 2003, because of delays in finding a suitable windbreak site.

3.3.7. *Standardising the resulting odour plumes*

During each test, the odour generator emitted a different odour concentration (OU m^{-3}) because of variations in temperature and in the source of manure used to generate the odour. Also, the odour level emitted was always high initially, and

dropped with time to reach a steady level (Fig. 3.3b). Thus, all odour measurements were normalised as follows to be able to compare the results. A curve of odour emission level with time was obtained from the analysis of the odorous air samples collected from the odour generator every 30 minutes. For each test, the odour concentration reported at a point by each group of panellists, at a given period in time, was divided by the odour concentration released by the generator at that time and then multiplied by average odour concentration calculated for all 39 tests. The average odour concentration measured at the odour generator was 471.6 OU m^{-3}.

Also, the wind direction changed with respect to the windbreak, during the test and from one test and site to the other, which changed the shape of the odour dispersion plume. For the purpose of relating all measured odour plumes, the position of each measured point was standardised as follows. For each 10 minute period during which the wind direction and speed was averaged, the windbreak was assumed to stand perpendicular to the wind direction and new x and y coordinates were computed for each odour point observed. The x and y coordinates were defined perpendicular and parallel to the windbreak, respectively, with the odour generator standing at the origin (Choinière, 2004). Using these newly computed coordinates for each point along with the normalised odour concentration measured, a standardised odour plume was constructed.

3.4. Results and Discussion

The measured odour plumes, illustrated in Figs 4 to 10, demonstrated several peaks separated by areas with no measurable odour concentration, reflecting the variability of odour dispersion in the field. Nevertheless, if these peak values are plotted against distance, there is a drop in odour concentration with distance downwind from the source. This distance is most likely affected by the windbreak, its porosity and tree type and height, by the location of the odour generator and the ambient climatic conditions. The following is a general discussion on the impact of each of these factors. For each parameter, the cases or case used for the comparison are as similar as possible, considering the limitations in the variability

of the tests, despite the 39 cases measured. The only factor which could not be tested is that of tree height. The size of each plume is limited by a 2 OU m^{-3} contour line.

3.4.1. Effects of the presence of a windbreak

Fig. 3.4 illustrates the average odour plume observed without (tests 37, 38 and 39 on site 5) and with (tests 5, 8, 12 and 16, on site 2) a windbreak where the odour generator was located 30 m upwind. The average air temperature was 26.4 and 22.6 °C, respectively, for the odour plume without and with a windbreak. On site 2, the wind direction ranged between 20 to 90° with respect to the windbreak, 90° being perpendicular. Both odour plumes were observed in late August and early September under similar environmental conditions.

By contrast, the plumes developed without the windbreak reached a much longer standardised distance downwind, compared to that developed with the windbreak. With the windbreak, a normalised peak odour concentration of 3.0 OU m^{-3} was measured at x = 477m and y = -98m, compared to that of 3.7 OU m^{-3} measured without a windbreak at x = 520 m (Table 3.3). In the absence of the windbreak, a maximum odour peak of 16 OU m^{-3} occurred at x = 69 m while that of the windbreak measured 50 OU m^{-3} at x = 117 m (Table 3.3). Comparing Figs 4a and b, the windbreak is observed to concentrate or trap the odours on its leeward position before dispersing them further on.

3.4.2. Effect of windbreak optical porosity

Fig. 3.5 illustrates the odour plume observed using a windbreak with an optical porosity of 55% (test 2 on site 1) and 35% (test 16 on site 2). In both cases, the odour generator was located 30 m upwind from the windbreaks, the wind direction was mostly perpendicular to the windbreaks, and the air temperature was 20 and 23°C, respectively.

Despite the greater height of its trees, the more open windbreak (55% optical porosity) was found to produce a longer odour plume covering 150 m in width by 600 m in length, compared to that of the 35% porosity windbreak covering also 150 m in width but only 300m in length. The furthest standardised

odour peak concentrations for the 55 and 35% optical porosity windbreaks had values of 3.2 and 4.0 OU m^{-3} at x = 601 and 281 m, respectively. However, the 55% optical porosity windbreak produced a maximum odour peak of 22 OU m^{-3} at x = 138 m while that with a 35% optical porosity produced a much higher maximum odour peak of 50 OU m^{-3} at x = 117 m (Table 3.3). Again, the smaller odour plume corresponded to a more intense odour trapping in the leeward position of the windbreak.

The more open windbreak was found to produce an odour plume which was similar to that obtained without a windbreak, likely because a porous windbreak produces less turbulent energy and therefore less odour mixing and odour dilution, compared to a denser windbreak. Therefore, a denser windbreak will more effectively disperse odours.

3.4.3. Effect of odour generator position upwind from the windbreak

Fig. 3.6 compares the odour plume observed with the odour generator located 15 and 60 m upwind from the site 2 windbreak (tests 13 and 14). An average wind direction of 50 and 40° and an air temperature of 23 and 26°C were measured for each respective test.

For the 15 and 60 m position, the maximum peak odour concentrations were 15 and 14 OU m^{-3} at x = 19 and 65 m, respectively (Table 3.3). Also downwind from the windbreak, the 60 m position seemed to produce a set of secondary odour peaks of higher intensity, compared to the 15 m position. Thus, the closer the windbreak is positioned with respect to the source, the better the odour is trapped and dispersed. With the odour source at 60m from the windbreak, the odour is likely dispersed to a certain extent before reaching the windbreak and peaks of lower intensities are therefore trapped on the leeward side. It is therefore preferable to locate the windbreak closer to the source, for better entrapment and dispersion.

3.4.4. Effect of tree species

Fig. 3.7 illustrates the odour plume observed in the presence of poplars (test 1 on site 1) with a height of 18 m and conifers (test 20 on site 3) with a height of 7.6 m,

where both windbreaks had a porosity of 55%. In both cases, the odour generator was located 15 m upwind from the windbreak and the temperature averaged 19 and 13 °C, respectively with wind directions at 90 and 80°. Conditions of wind speed were nevertheless different, averaging 6.4 and 1.8 m s^{-1}, respectively.

The conifer windbreak trapped more odours on its leeward side, compared to the poplar windbreak, despite the lower wind speed likely to induce less mixing. The peak odour concentrations were 30 and 47 OU m^{-3} at x = 78 and 52 m, for the poplar and conifer windbreaks, respectively (Table 3.3). The contour line of 2 OU m^{-3} also showed a shorter odour plume of 450 m for the coniferous windbreak compared to 500 m for the poplar windbreak.

Despite its shorter height and conditions of lower wind speed, the conifer windbreak produced a shorter odour plume compared to the poplar windbreak. Likely, conifers offer more air flow resistance, because of their stronger and less flexible branches. Thus, conifers would have a lower aerodynamic porosity, compared to poplars, for the same measured optical porosity.

3.4.5. Effect of air temperature

Air temperature impacts the odour plume development as a result of convection created by the different air and ground temperatures. Fig. 3.8 compares the odour plume observed in early September (tests 6, 10, 18 and 19, on site 2) with a deciduous windbreak, to that observed in December (tests 29 and 30, on site 4) with a coniferous windbreak. In both cases, the odour generator was located 60m from the windbreak, the windbreak optical porosity was 35%, and the wind velocity averaged 2.3 and 2.0 m s^{-1} for the summer and winter conditions, respectively, while the average temperature at 22.5 and -7.5 °C, respectively.

The odour plume measured in September was much shorter (350 m) compared to that measured in December (over 500 m), despite the greater height of the coniferous windbreak and the fact that its tree type may better trap odours, as observed earlier. The standardised maximum peak odour concentrations were 68 and 31 OU m^{-3} at x = 52 and 91 m, respectively (Table 3.3), indicating better odour trapping under warmer temperatures. Therefore, the warmer environmental

conditions likely resulted in more air turbulence because of the lower air viscosity, and in better odour dispersion as a result of greater convective forces, compared to cooler winter conditions where the odour source seemed to remain at ground level.

3.4.6. Effect of wind speed

Fig. 3.9 illustrates the odour plume observed with an average wind speed of 1.2 m s^{-1} (tests 9, 11, 13 and 17, on site 2) compared to 4.9 m s^{-1} (tests 7 and 15, on site 2). In both cases, the odour generator was located 15m upwind from the windbreak, the wind directions were 45 and 65°, respectively, and the air temperature was 23°C. Although the maximum peak odour concentrations were 34 and 22 OU m^{-3} at x = 116 and 27 m, respectively (Table3.3), wind speed had limited effects on the size of the odour plume. The lower wind speed resulted in an odour concentration of 6.8 OU m^{-3} at x = 499 m downwind from the windbreak, compared to an odour plume reaching 4.0 OU m^{-3} at x = 530 and y = -43 m for the higher wind speed. The only difference observed, among odour plumes, is the smaller more sporadic odour zones obtained with the higher wind speed, compared to more extensive odour zones obtained with the lower wind speed.

Higher wind speeds through a windbreak were observed to create stronger turbulence (Cleugh, 1998), which is believed to further dilute and mix odours. In the present work, a limited effect was observed, likely influenced by the atmospheric stability. During conditions of high wind speed, an atmospheric class stability of B and C was observed, while for the lower wind speed, an atmospheric class stability of D was observed, where the less stable atmospheric conditions under class D could have induced more air mixing.

3.4.7. Effect of wind direction

The observed odour plumes were not standardised for wind direction, in this comparison, for the purpose of observing wind direction effect. Fig. 3.10 compares the odour plume observed with a 90° (test 15 on site 2) and a 40° wind (test 17 on site 2), using positive x and y coordinates pointing East and North, respectively. In both cases, the odour generator was located 15 m away from the

windbreak and the air temperature was 28 and 24 °C, respectively. The respective average wind speeds of 5.1 and 1.5 m s^{-1} definitely had an impact on odour dispersion, along with wind direction.

A higher wind direction perpendicular to the windbreak was observed to produce a shorter odour plume, reaching 300m, compare to over 500m for a lower wind speed at 40° to the windbreak. The odour concentrations were 3.1 and 6.8 OU m^{-3} at 318 and 499 m downwind from the odour generator, for the 90 and 40° wind directions, respectively. Interestingly enough, the 40° wind direction created an odour plume of higher intensity and width, on the leeward side of the windbreak. The higher wind speed could have masked the effect of wind direction, as the non perpendicular wind direction was expected to provide a deeper windbreak layer against the wind and therefore a less porous windbreak. Because of the interference of wind speed, the effect of wind direction could not be properly investigated.

3.5. *Conclusion*

Field tests were conducted to observe the size and hedonic tone of odour plumes developing in the presence and absence of windbreaks with different properties and under different climatic conditions. From a visual comparison of the plumes, the following conclusions were drawn:

1) Windbreaks were observed to be effective in reducing the size of the odour plume when of low optical porosity and when located close (15m) from the source;

2) Conifers were found to offer more wind resistance and produce more odour dispersion, as compared to deciduous trees;

3) Higher temperatures favour odour dispersion, likely because of less viscous air and greater convective effects at the ground level;

The effect of wind speed and direction could not be properly evaluated because of variable conditions among tests compared. Effectively, despite the 39 field tests conducted, the comparisons were not perfect, as other factors varied, besides that

being evaluated, such as climatic conditions and tree properties. Also, the optical porosity of some windbreaks was not constant with height. The effectiveness of windbreaks could most likely be better compared through modeling, where all parameters can be controlled.

3.6. *Acknowledgements*

The authors wish to acknowledge the financial contribution of Consumaj inc., CDAQ, The Livestock Initiative Program, Agriculture and Agro-Food Canada and the Natural Sciences and Engineering Research Council of Canada.

3.7. *References*

Boldes, U., Colman, J. and Leo, J.M.D., 2001. Field study of the flow behind single and double row herbaceous windbreaks. Journal of Wind Engineering and Industrial Aerodynamics, 89: 665-687.

Bottcher, R.W., Munilla, R.D., Baughman, G.R. and Keener, K.M., 2000. Designs for windbreak walls for mitigating dust and odor emissions from tunnel ventilated swine buildings. pp. 174-181 in: Swine Housing, Proc. of the 1st International Conference, Oct. 9-11, 2000, Des Moines, Iowa. American Society of Agricultural Engineers, 2950 Niles road, St. Joseph, Mi. USA.

Bottcher, R.W., Munilla, R.D., Keener, K.M. and Gates, R.S., 2001. Dispersion of livestock building ventilation using windbreaks and ducts. 2001 ASAE Annual International Meeting.: 01-4071. 2950 Niles road, St. Joseph, Mi. USA.

Brant, R.C. and Elliott, H.A., 2002. Pennsylvania odor management manual, Pennsylvania State University, University Park, PA. USA.

CEN, 2001. Air quality - determination of odor concentration by dynamic olfactometry. prEN13725, European Committee for Standardization, 36 rue de Stassart, B-1050 Brussels. <http://www.aerox.nl/images/eurstandard.pdf>, visited August, 2004.

Choinière, D., 2004. L'influence des haies brise-vent naturelles sur les odeur, Division Environnement Consumajing, Saint-Hyacinthe (Québec).

Choinière, D. and Barrington, S., 1998. The conception of an automated dynamic olfactometer, CSAE/SCGR Paper No.98-208.

Dierickx, W., Gabriels, D. and Cornelis, W.M., 2002. Wind tunnel study on oblique windscreens. Biosystems Engineering, 82(1): 87-95.

Edeogn, I., Feddes, J.J.R., Qu, G., Coleman, R. and Leonard, J., 2001. Odor measurement and emissions from pig manure treatment/storage systems. Final report, University of Alberta, Edmonton, Canada.

Eimern, J.v., Karschon, R., Razumova, L.A. and Robertson, G.W., 1964. Windbreaks and shelterbelts. Report of a working group of the Commission for Agricultural Meteorology, World Meterologocal Organization, Technical Note No. 59. Secretariat of the World Meteorological Organization, Geneva, 188 pp.

Guan, D., Zhang, Y. and Zhu, T., 2003. A wind-tunnel study of windbreak drag. Agri. Ecosystem & Environment, 118: 75-84.

Guo, H., Jacobson, L.d., SChmidt, D.R. and Nicodai, R.E., 2003. Evaluation of influence of atmospheric condition on odor dispersion from animal production sites. American Society of Agricultural Engineers, 46(2): 461-466.

Heisler, G.M. and Dewalle, D.R., 1988. Effects of windbreak structure on wind flow. Agriculture, Ecosystems and Environment, 22-23: 41-69.

Lee, S. and Kim, H., 1999. Laboratory measurements of velocity and turbulence field behind porous fences. Journal of Wind Engineering and Industrial Aerodynamics, 80(3): 311-326.

Leuty, T., 2003. Using shelterbelt to reduce odors associated with livestock production barns. Ministry of Agriculture and Food, Ontario, http://www.gov.on.ca/OMAFRA/english/crops/facts/info_odours.htm, visited in 2004.

Leuty, T., 2004. Wind management can reduce offensive farm odours. Ministry of Agriculture and food, Ontario, http://www.gov.on.ca/OMAFRA/english/crops/facts/info_windmanagement.htm, visited February, 2005.

Patton, E.G., Shaw, R.H., Judd, M.J. and Raaupach, M.R., 1998. Large-eddy simulation of windbreak flow. Boundary-Layer Meteorology, 87: 275-306.

Plate, E.J., 1971. The aerodynamics of shelter belts. Agric. Meteorol, 8, 203.

Schauberger, G., Piringer, M. and Petz, E., 2002. Calculating direction-dependent separation distance by a dispersion model to avoid livestock odor annoyance. Biosystems Engineering, 82(1): 25-37.

Tyndall, J. and Collettii, J., 2000. Air quality and shelterbelts: odour mitigation and livestock production a literature review. Final project report, Forestry Department, Iowa State University, Ames, Iowa, U.S.A.

Ucar, T. and Hall, F.R., 2001. Review windbreaks as a pesticide drift mitigation strategy: a review. Pest Management Science, 57: 663-675.

Vigiak, O., Sterk, G., Warren, A. and Hagen, L.J., 2003. Spatial modeling of wind speed around windbreaks. Catena, 52: 273-288.

Wang, H. and Takle, E.S., 1997. Momentum budget and shelter mechanism of boundary-layer flow near a shelterbelt. Boundary-Layer Meteorology, 82: 417-435.

Wilson, J.D. and Yee, E., 2003. Calculation of winds distribution by an array of fences. Agricultural and forest meteorology, 115: 31-50.

Zhang, Q., Feddes, J., Edeogu, I., Nyachoti, M., House, J., Small, D., Liu, C., Mann, D. and Clark, G., 2002. Odor production, evaluation and control. http://www.manure.mb.ca/projects/completed/pdf/02-hers-03.pdf, visited August, 2004., Manitoba Livestock manure Management Initiative Inc.

Zhu, J., Jacobson, L.D., Schmidt, D.R. and Nicolai, R., 2000. Evaluation of inpuff-2 model for predicting downwind odors from animal production facilities. American Society of Agricultural Engineers, 16(2): 159-164.

Tables and Figures

Table 3.1 Experimental windbreak found on each site.

Description	Site			
	1	2	3	4
Tree type	poplar	mixed mature deciduous	conifers	conifers
Windbreak				
- length (m)	2100	1050	405	380
- height (m)	18.3	9.2	7.6	15.2
- depth (m)		7		6
- optical porosity (%)	55	35	55	35
- porosity at the base (%)	70	30	70	40
Location	Sherrington	St Chrysostome	St Amable	St Charles

Note : all locations are located within 50 km of the Island of Montreal, Canada, in the South West direction.

Table 3.2 Test conditions

Test	Site	Date (2003)	OG (m)	OE (OU s^{-1})	WS (m s^{-1})	Angle (°)	*T* (°C)	AS
1	1	Aug-29	15	621	6.4	90	19	B
2	1	Aug-29	30	760	6	90	20	D
3	1	Sep-02	30	859	2.5	50	17	C
4	1	Sep-02	60	551	2.5	50	20	C
5	2	Sep-03	30	1373	3	90	21	B
6	2	Sep-03	60	492	4.4	90	23	C
7	2	Sep-05	15	578	4.7	40	18	D
8	2	Sep-05	30	585	4.2	40	19	D
9	2	Sep-08	15	214	1	60	22	B
10	2	Sep-08	60	218	1.1	70	20	B
11	2	Sep-10	15	5360	1.2	30	22	C
12	2	Sep-10	30	1096	2.7	20	27	D
13	2	Sep-12	15	559	1.2	50	23	B
14	2	Sep-12	60	294	1	40	26	B
15	2	Sep-15	15	744	5.1	90	28	D
16	2	Sep-15	30	745	1.5	90	23	D
17	2	Sep-18	15	1879	1.5	40	24	C
18	2	Sep-18	60	13052	1.4	50	21	B
19	2	Sep-18	60	846	2.2	60	26	B
20	3	Sep-29	15	318	1.8	80	13	C
21	3	Sep-29	49	368	1.7	70	14	B
22	4	Dec-03	15	1339	4.1	60	-2	D
23	4	Dec-03	30	690	3.5	60	-4	D
24	4	Dec-03	60	208	2.6	50	-4	D
25	4	Dec-10	15	166	1.3	70	-2	D
26	4	Dec-10	15	148	1.9	70	-2	D
27	4	Dec-10	30	101	1.7	60	-2	D
28	4	Dec-13	30	111	0	60	-8	D
29	4	Dec-13	60	175	2.1	50	-6	D
30	4	Dec-13	60	79	1.4	50	-9	D
31	4	Dec-14	15	205	3.1	70	-8	D
32	4	Dec-14	30	394	3.3	60	-8	D
33	4	Dec-14	30	350	3	80	-8	D
34	2	Sep-09	197	166	1.2	0	18	C
35	4	Dec-09	191	102	0.3	57	-2	B
36	4	Dec-09	318	99	0.4	0	-3	C
37	5	Aug-21	NW	766	4.1	NW	28	C
38	5	Aug-21	NW	480	3.6	NW	26	C
39	5	Aug-22	NW	310	6.1	NW	26	D

* NW- no windbreak; OG – odour generator distance upwind from the windbreak; OE – average odour emission during a test; WS- average wind speed; Angle – angle between the windbreak and the wind, 90° being perpendicular; T – average temperature measured during the test; AS – Pasquill-Gifford atmospheric stability condition, where B and C are unstable classes and D is a neutral class.

Table 3.3 Tests selected to compare windbreak performance.

Comparison	Fig.	Condition	Test No.	MOP			FOP		
				x (m)	y (m)	OU m^{-3}	x (m)	y (m)	OU m^{-3}
Windbreak	3.4	without	37,38,39	69	19	16	520	0	3.7
presence		with	5,8,12,16	117	-49	50	477	-98	3.0
Windbreak	3.5	55%	2	138	8	22	601	30	3.2
porosity		35%	16	117	- 49	50	281	-64	4.0
Odour generator distance	3.6	15m	13	19	32	15	326	0	3.7
		60m	14	65	22	14	394	0	6.1
Tree type	3.7	deciduous	1	78	15	30	547	0	2.5
		conifer	20	52	5	47	345	76	6.6
Temperature	3.8	22.5°C	6,10,18,19	52	63	68	336	-69	2.1
		-6.1°C	29,30	91	-43	31	519	-39	6.8
Wind speed	3.9	1.5m s^{-1}	9,11,13,17	116	-97	34	499	0	6.8
		4.9m s^{-1}	7,15	27	45	22	530	-43	4.0
Wind direction	3.10	90° angle	15	-54	64	11	-115	297	3.1
		40° angle	17	-112	102	34	-499	-20	6.8

Note: MOP – maximum odour peak; FOP – odour peak measured further away from the source.

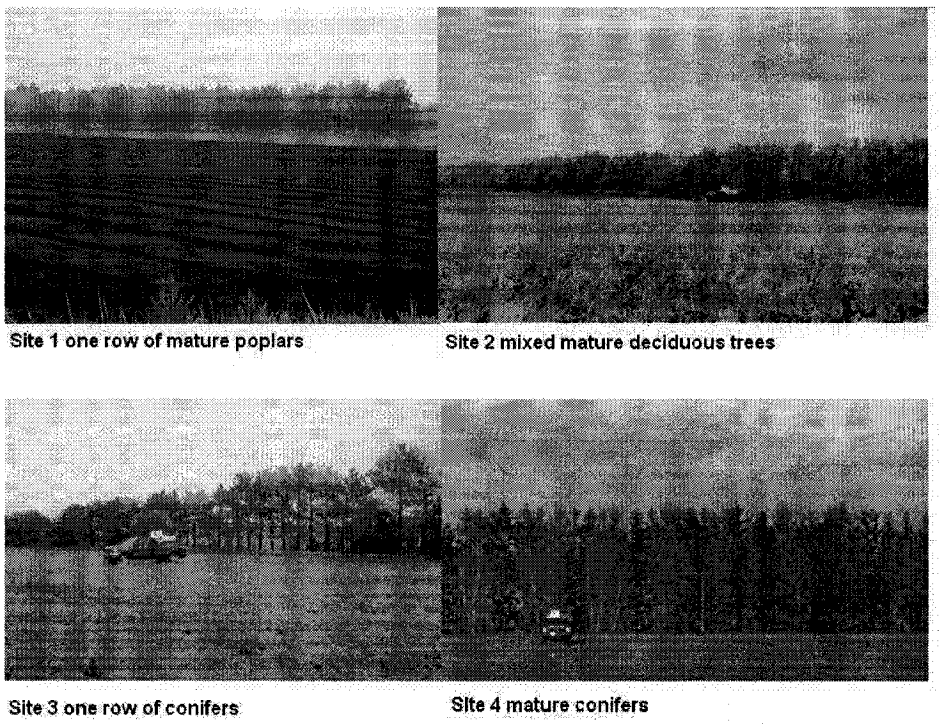

Fig. 3.1. Experimental windbreaks on all four sites, also illustrating the odour generator mounted in the box of a pick up truck.

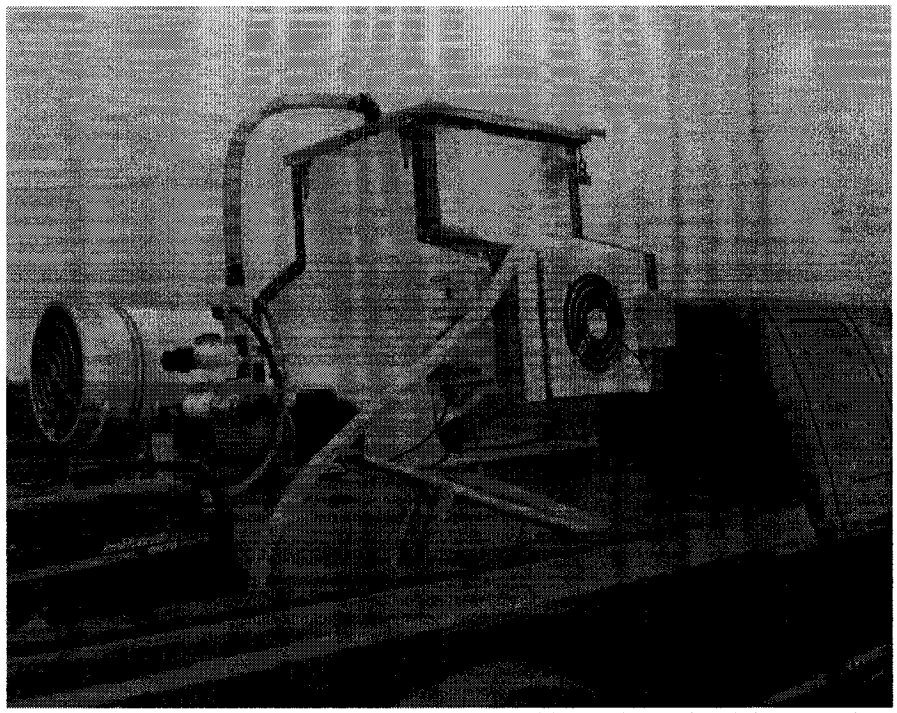

Fig. 3.2. The mobile odour generator mounted in the box of a pick up truck

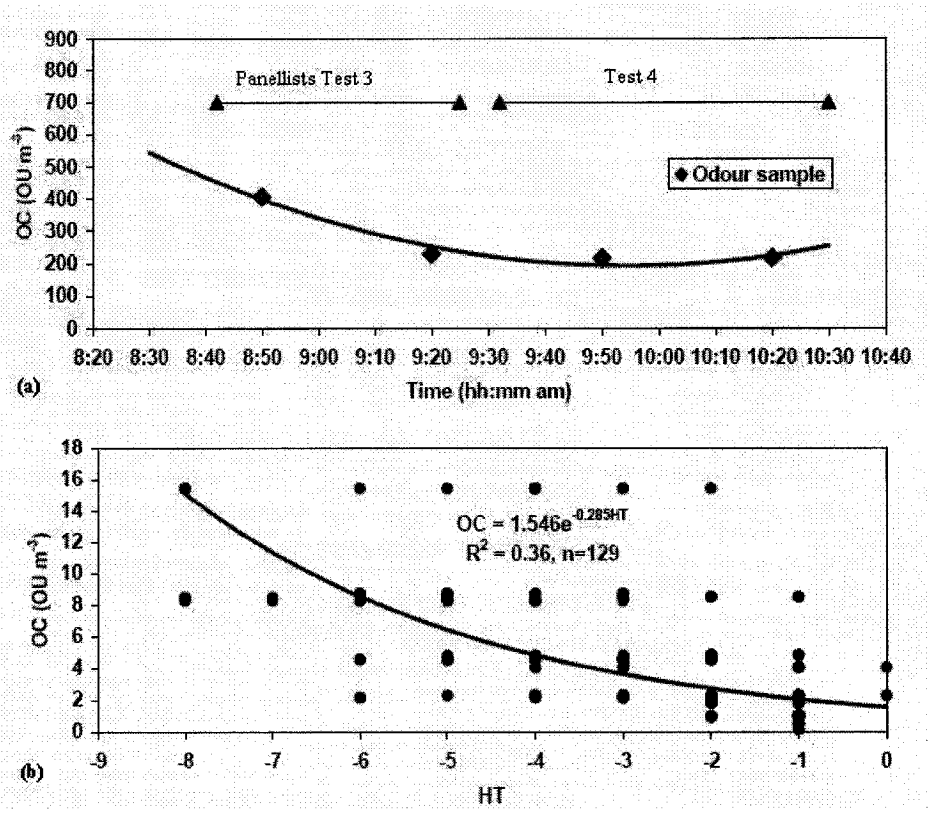

Fig. 3.3. (a) Typical odour concentration (Odour) produced by the generator during a test day (tests 3 and 4) started at 8:30 am; the panellists started to evaluate the odour plume at 8:42 am and finished evaluating the second plume at 10:30 am, while odour samples were taken at the generator at 8:50, 9:20, 9:50 and 10:20 am, and the odour generator flow rate was 1.65 m^3 s^{-1}. (b) Typical relationship between the hedonic tone of the odour (HT) and odour concentration (OC) for a group of four panellists (tests 3 and 4).

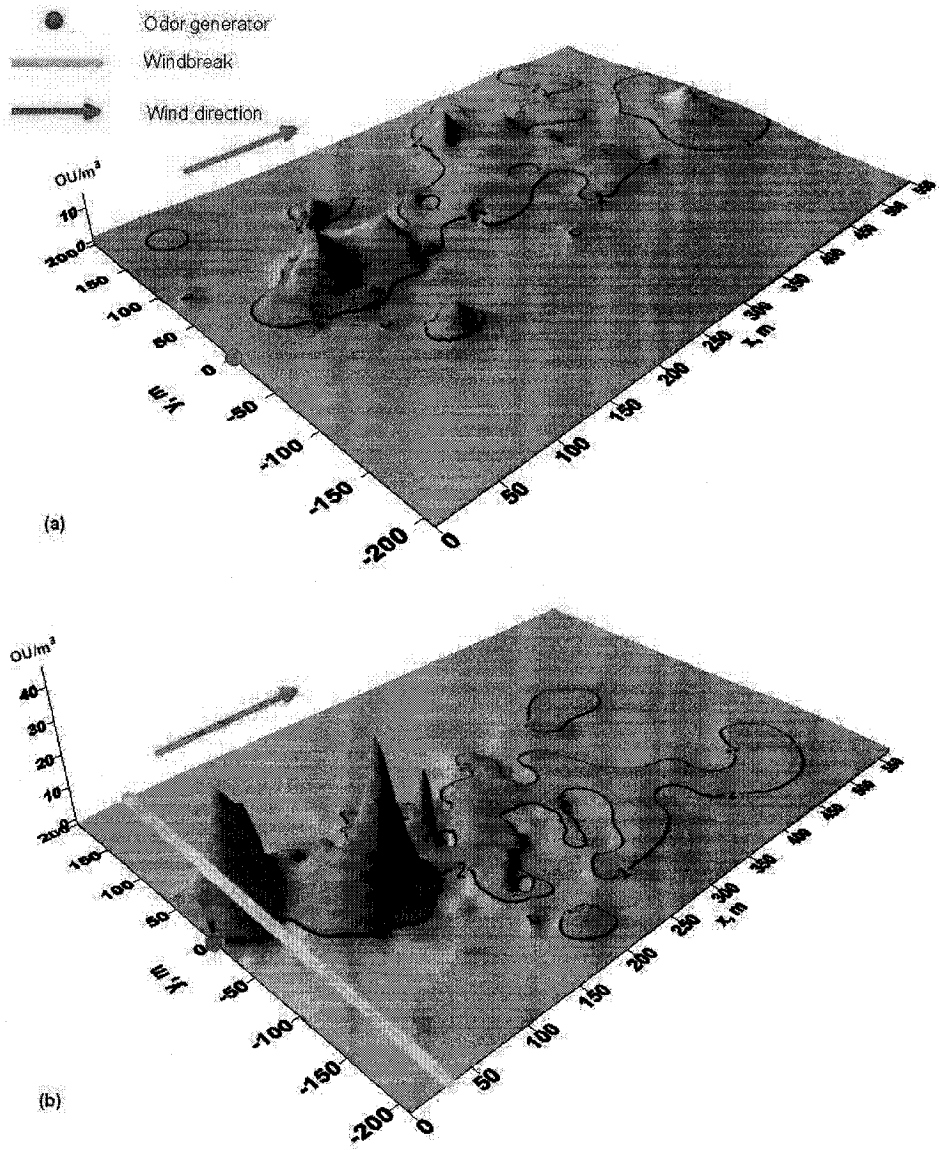

Fig. 3.4. Odour plumes on sites 2 and 5 with and without a windbreak. (a) without windbreak (tests 37, 38 and 39); (b) with windbreak on the site 2 (tests 5, 8, 12 and 16). An odour concentration of 2 OU m^{-3} is used to draw the final contour of the odorous zones.

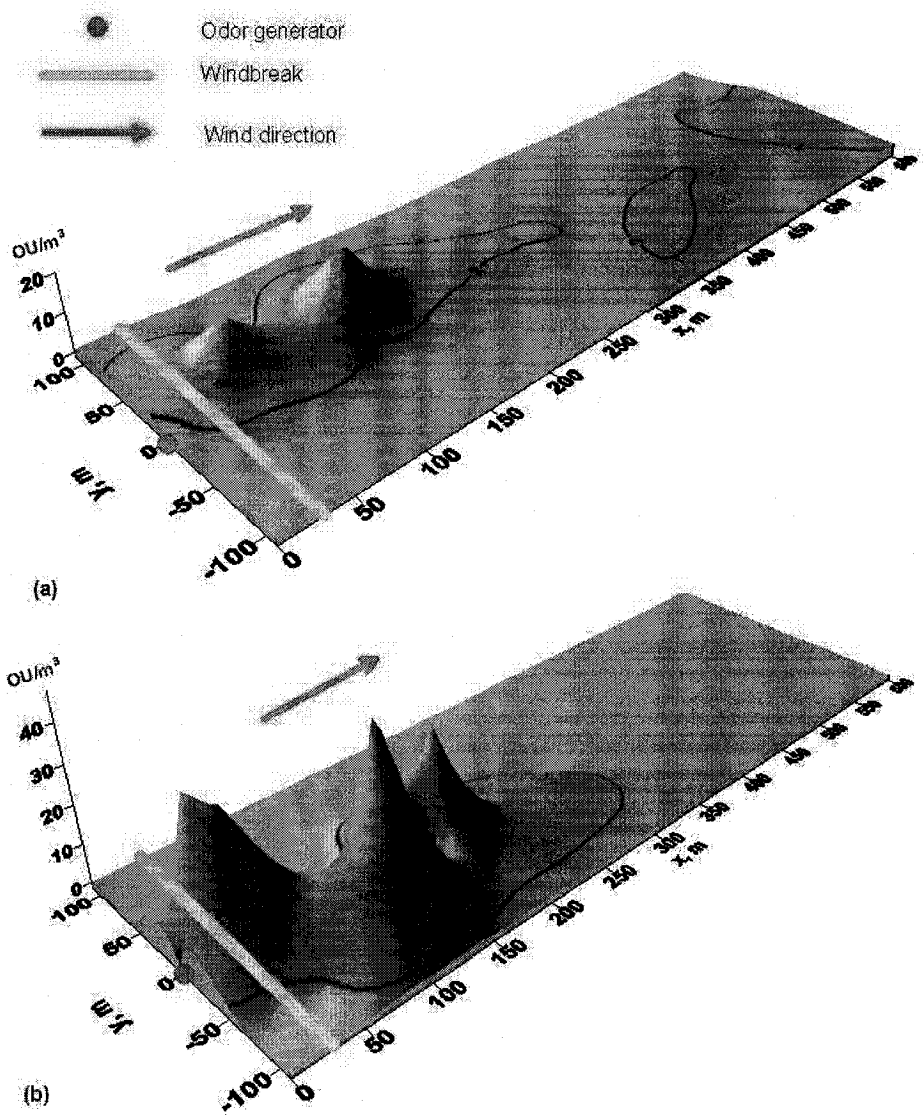

Fig. 3.5. Effect of windbreak optical porosity on odour plume: (a) windbreak porosity of 55% on site 1 (test 2); (b) windbreak porosity of 35% on site 2 (test 16). The odour generator is 30 m away from the windbreak. An odour concentration of 2 OU m^{-3} is used to draw the final contour of the odorous zone.

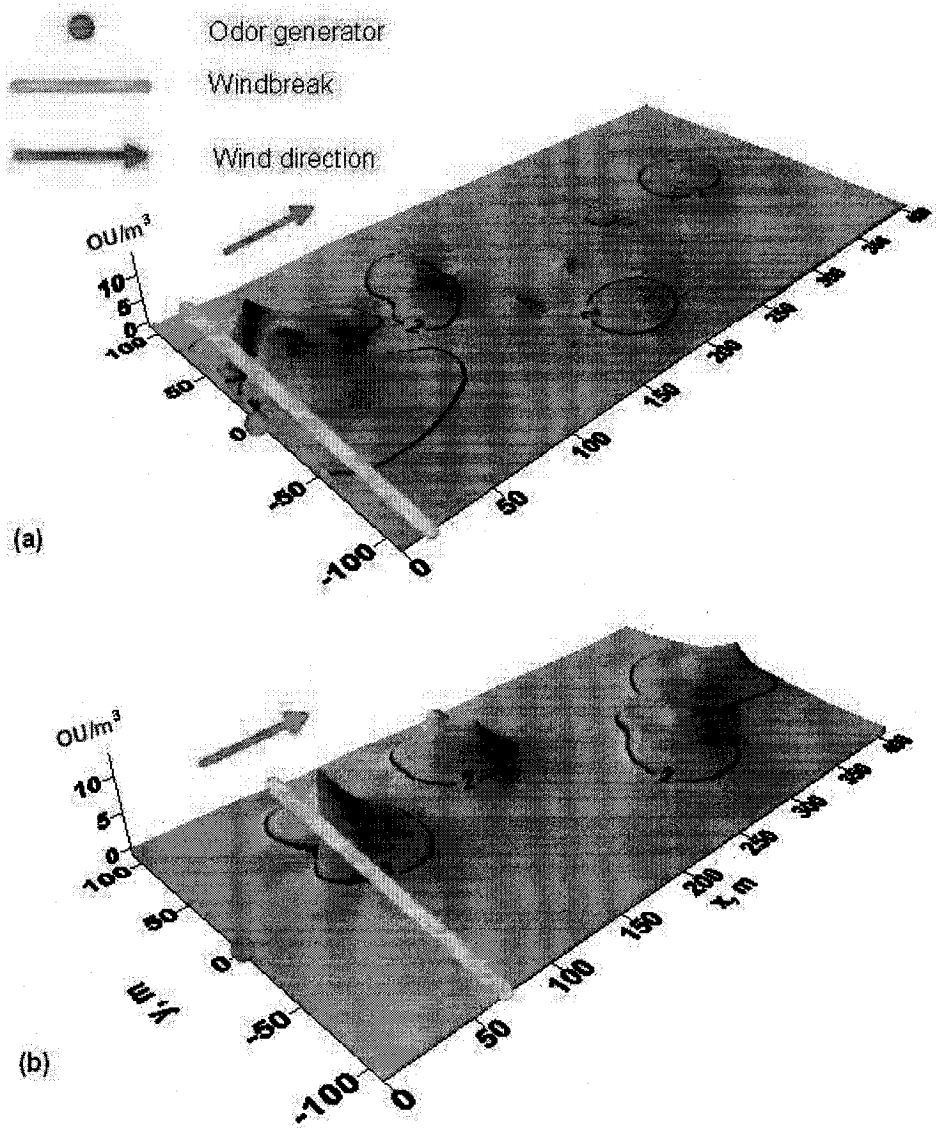

Fig. 3.6. Effect on odour plume of odour generator distance from the windbreak for site 2: (a) odour generator 15 m away (test 13); (b) odour generator 60 m away (test 14). An odour concentration of 2 OU m^{-3} is used to draw the final contour of the odorous zone.

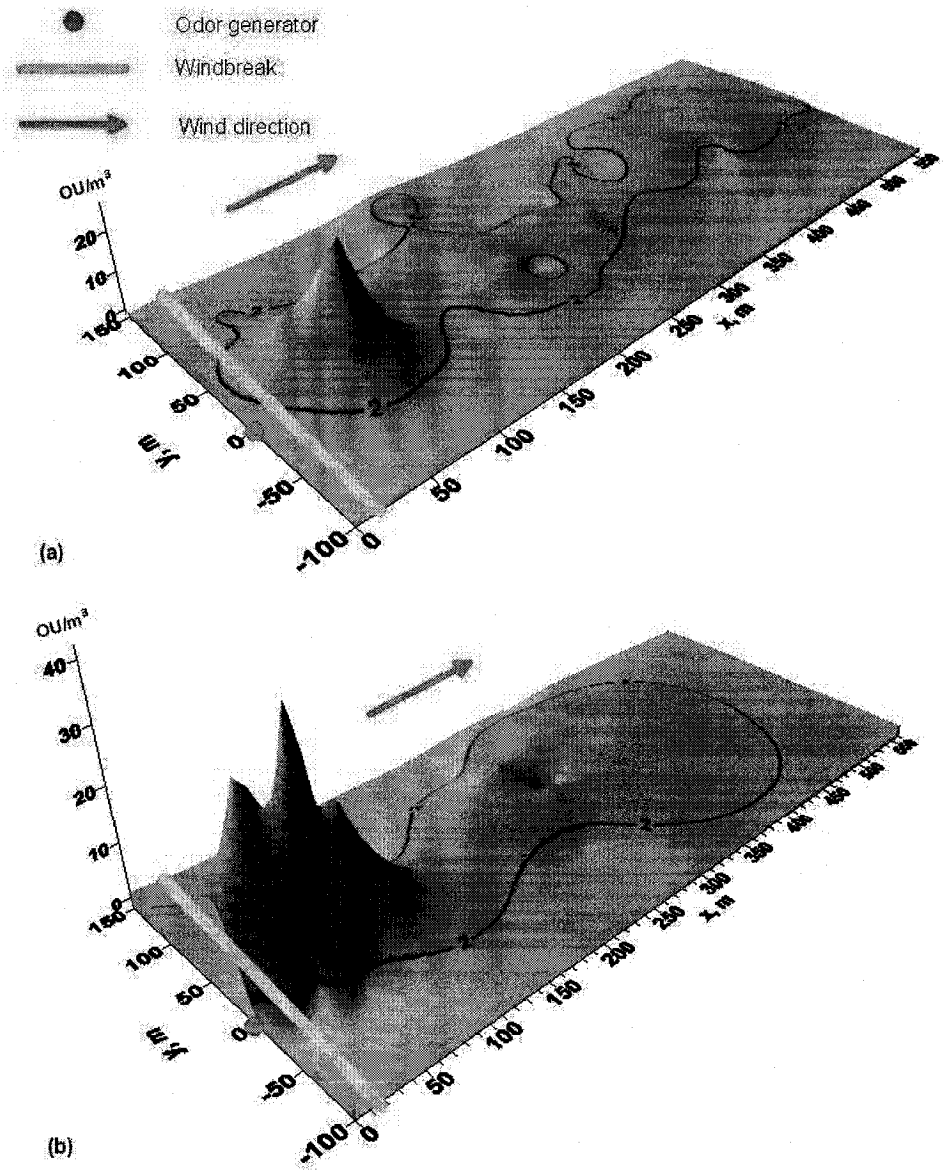

Fig. 3.7. Effect of tree type on odour plume: (a) site 1 with deciduous trees (test 1); (b) site 3 with coniferous trees (test 20). The odour generator is 15 m away from the windbreak. An odour concentration of 2 OU m^{-3} is used to draw the final contour of the odorous zone.

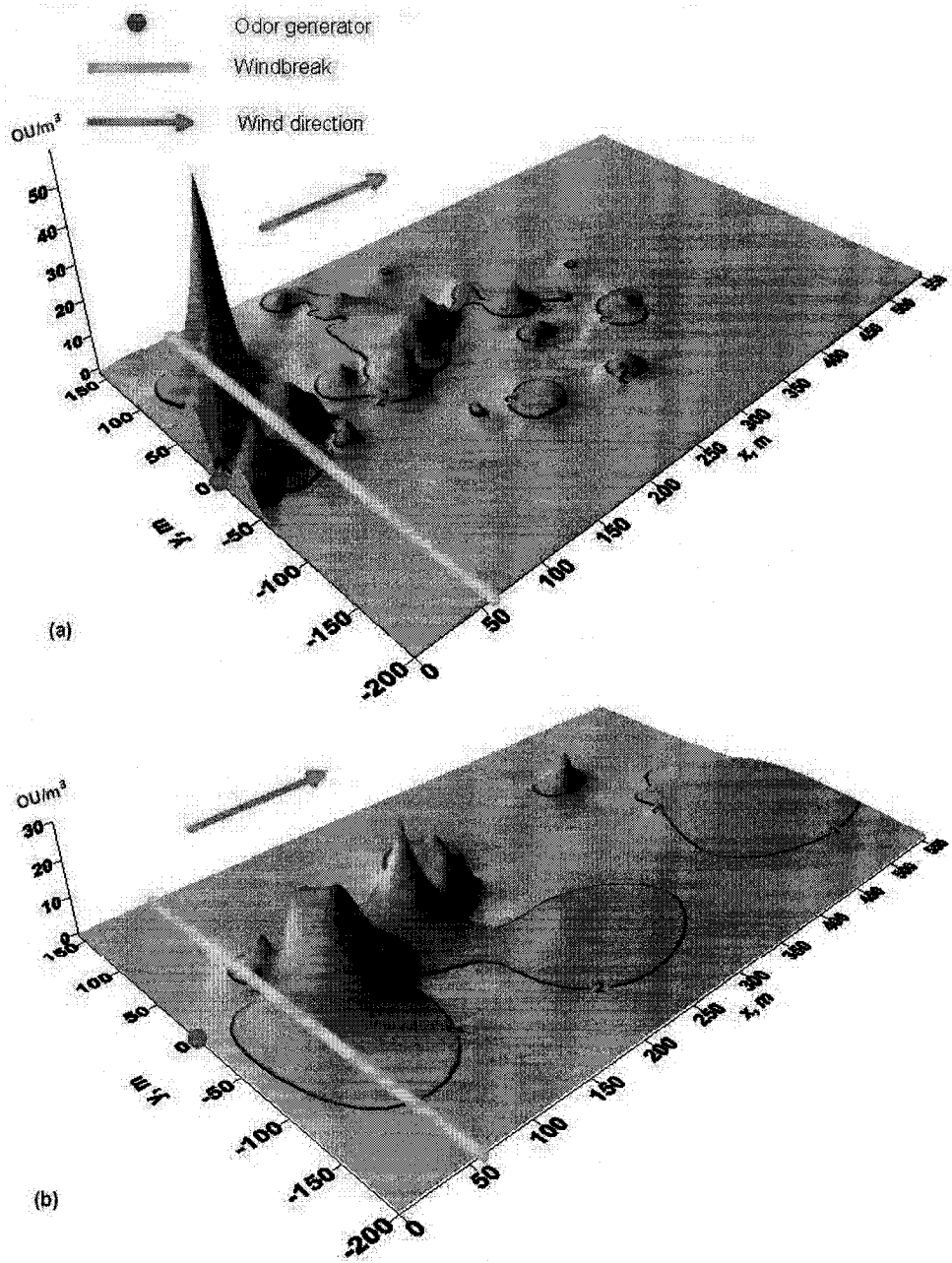

Fig. 3.8. Effect of air temperature on odour plume: (a) air temperature above 20°C for site 2 (test 6, 10, 18 and 19); (b) air temperature below 0°C for site 4 (test 29 and 30). The odour generator is 60 m away from the windbreak. An odour concentration of 2 OU m^{-3} is used to draw the final contour of the odorous zone.

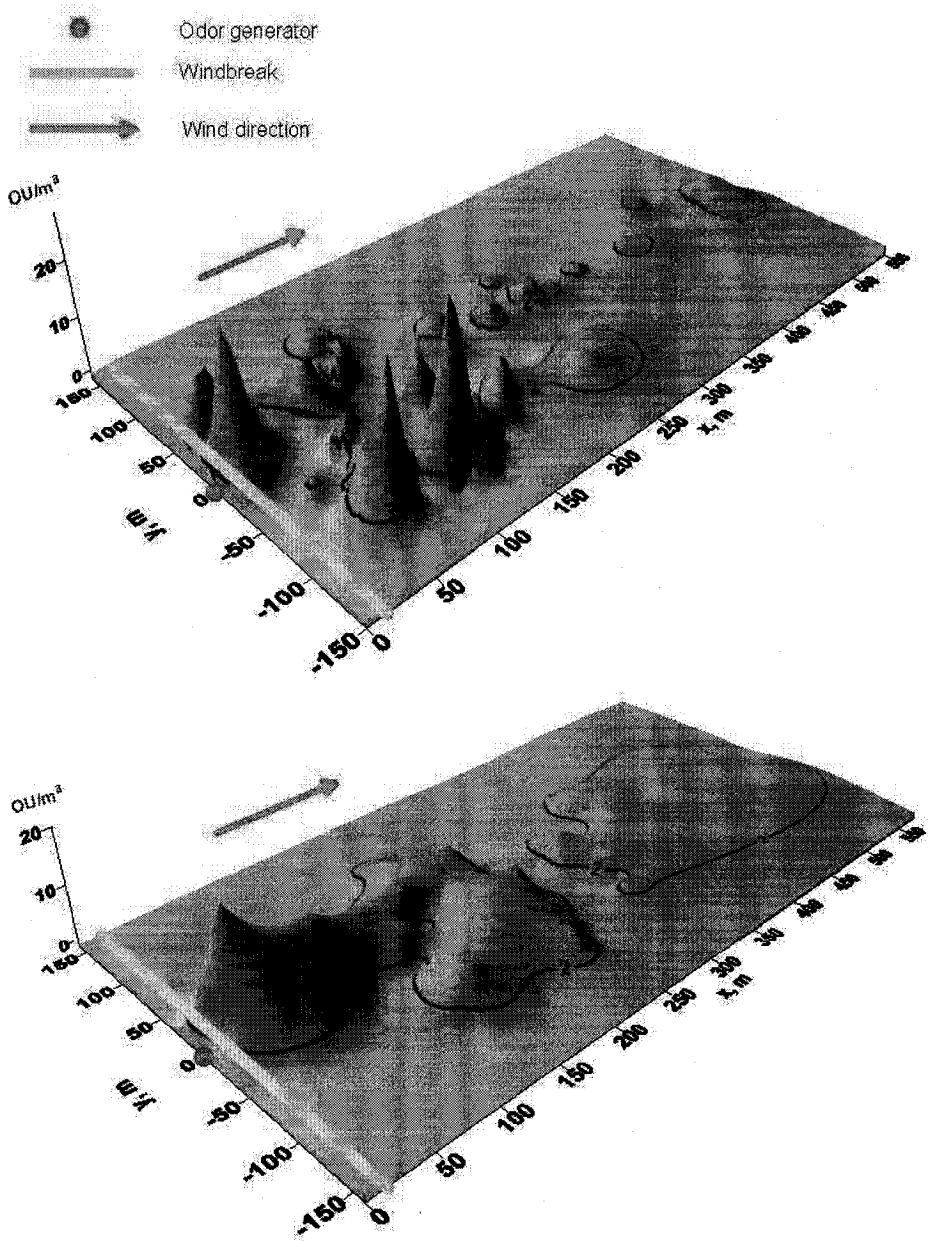

Fig. 3.9. Effect of wind speed on the odour plume for site 2: (a) wind speed of 1.2 m s^{-1} (test 9, 11, 13 and 17); (b) wind speed of 4.9 m s^{-1} (test 7 and 15). The odour generator is 15 m away from the windbreak. An odour concentration of 2 OU m^{-3} is used to draw the final contour of the odorous zone.

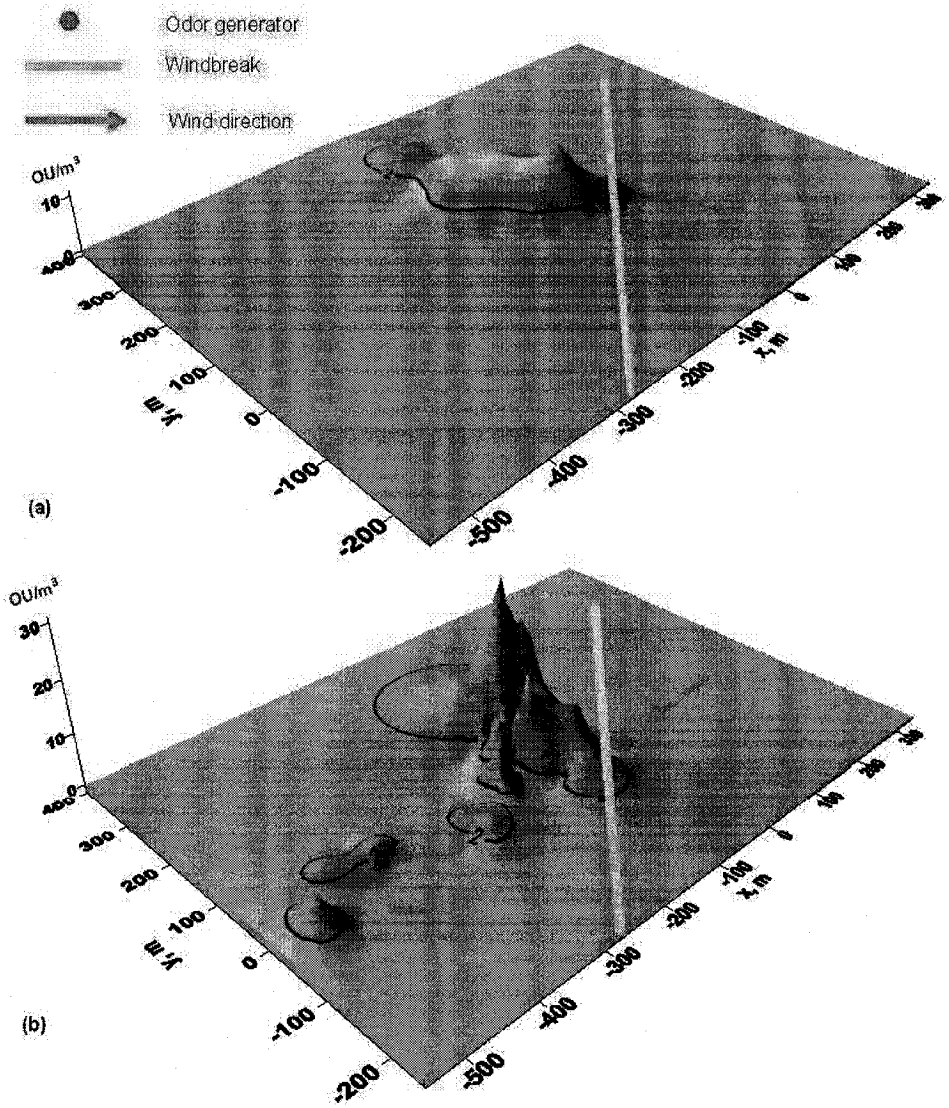

Fig. 3.10. Effect of wind direction on odour plume: (a) wind direction at 90° to the windbreak (test 15); (b) wind direction at 40° to the windbreak (test 17). In this coordinate system, positive x and y axes point to east and north, respectively and wind direction has not been normalised. The odour generator is 15 m away from the windbreak, and the respective wind velocities are 5.1 and 1.5 m s^{-1}. An odour concentration of 2 OU m^{-3} is used to draw the final contour of the odorous zone.

Connecting statement

In chapter 3, the data associated with field odour plume measurement was visualised to demonstrate the effects of the windbreak on odour dispersion. Chapter 4 was a statistical analysis of this data to test whether or not windbreak presence, windbreak characteristics and weather conditions have an impact on odour plume length. In this chapter, the odour plume length was defined as MODD, namely, the maximum odour dispersion distance.

Chapter 4 used regression and classification methods to calculate the MODD obtained after standardising the field measurements as described in chapter 3. The effects on MODD of the windbreak, its tree species and porosity, the odour source position, the air temperature, and wind speed and direction were compared.

This paper was published in Canadian Biosystems Engineering, 2007, vol. 49, 6.21 – 6.32. Authors are Lin, X.J., Barrington, S., Nicell, J. and Choinière, D. The contributions of the authors are i) First author carried out a part of field measurements, the whole data analysis and wrote the manuscript; ii) Second author supervised and helped revise the method of analysis and the content of the paper; iii) Third author advised the method of analysis; iv) Last author organized and managed the collection of the field data.

Chapter 4
Effect of natural windbreaks on maximum odour dispersion distance (MODD)

4.1. ABSTRACT

Because of their frequency and intensity, livestock odour emissions are considered a nuisance often affecting the rural population. Although not extensively studied, windbreaks are said to improve odour dispersion. This paper therefore evaluates in the field, the effect of four natural windbreaks on maximum odour dispersion distance (MODD) and as compared to a control site without a windbreak. Odour plumes were measured in the field by three groups of four trained panellists during the release of odours by a generator located 15, 30 and 60 m upwind from the windbreak. In the laboratory, the trained panellists were characterized by asking them to evaluate the hedonic tone (HT) of various n-butanol concentrations. Also in the laboratory, the trained panellists were asked to translate into odour concentration (OC), the HT of various odour samples, to produce a regression equation converting field HT observations into OC. The panellists' translation of HT into OC for 72 odour samples, produced a statistically significant exponential relationship (P=0.05). Using all and only the maximum OC points observed in the field, MODD for 1 and 2 OU/m^3 were obtained from regression and classification equations. The odour dispersion analyses show that the windbreaks with an optical porosity of 35% reduced MODD by 21 to 40%, compared to the site without windbreak (P = 0.05). The best MODD reduction was obtained with a windbreak located 15 m downwind from the odour source, rather than 30 and 60 m, and offering an optical porosity of 35% rather than 55%. Conifers were better at reducing MODD than poplars. Finally, higher temperatures and wind speeds favoured shorter MODD in the presence of a windbreak.

Keywords: windbreak, odour dispersion, optical porosity, wind direction and speed, tree type, separation distance, MODD.

4.2. INTRODUCTION

Air quality in rural communities could be greatly improved if practical methods were introduced to attenuate odour emissions from confinement livestock operations. These odours are mainly produced during the handling of manures, from building ventilation, from storages and during land spreading. Since there are no technologies which can completely eliminate these odours, livestock operations and environmental authorities use air dilution as a remediation measure. The concept consists in distancing the livestock operation from neighbouring sites, such that ambient climatic conditions can dilute the emitted odours to an acceptable level before reaching critical points. Such distances separating the livestock building from neighbouring sites, are called "set back" or "separation" distances. Most Canadian provinces, U.S. states and European countries have adopted a method of calculating setback distances based on climatic conditions, topography and practices used by local livestock operations. Among other options, this method allows for the introduction of correction factors accounting for the use of odour controlling technologies.

Known to affect air currents and improve air mixing, natural windbreaks can reduce separation or setback distances between livestock operations and their neighbours. Natural windbreaks are plantings of single or multiple rows of trees or shrubs, used to reduce and redirect wind (Eimern et al., 1964). While diverting an approaching air mass upwards, windbreaks form a zone of lower air speed on their downwind side (Heisler and Dewalle, 1988; McNaughton, 1988). This function is widely used to provide many benefits such as snow control, sand drifting control, better wildlife habitat, and an enhanced farmstead environment. Most importantly, windbreaks have the potential to dilute odours (Bottcher et al., 2001; Leuty, 2003, 2004; Tyndall and Collettii, 2000). When planted around livestock facilities, a windbreak can dilute odours entering its leeward mixing

zone where strong wind shearing forces are developed. Therefore, windbreaks can potentially reduce the setback or separation distance required to reduce odours to an acceptable level. The distance required to dilute odours below their threshold level is often referred to as the "maximum odour dispersion distance" (MODD).
The objective of this paper was to compare the MODD required for sites with and without natural windbreak, and to measure the effect of various windbreak properties and climatic conditions on MODD. In calculating setback distances, the resulting analysis provides information pertaining to the value of the reduction factor applicable in the presence of windbreaks. .

4.3. MATERIALS AND METHODS

4.3.1. Sites and windbreak

Four uniform single row windbreaks were selected at least 5 km from any livestock operation and free from the interference of odour sources. The four windbreaks offered different properties (Table 4.1): on sites 1 and 3, the windbreaks offered an optical porosity of 55%, and; on sites 2 and 4, the windbreaks offered an optical porosity of 35%. The porosity of each windbreak was optically evaluated by measuring the percentage of open surface visible through the windbreak (Guan et al., 2003; Heisler and Dewalle, 1988).

Also, the four windbreaks consisted of different types of trees: poplars and mixed mature deciduous trees on sites 1 and 2, and; evergreens on sites 3 and 4. Tree height varied among windbreaks, sites 1 and 4 offering windbreaks with a height exceeding 15 m, compared to sites 2 and 3 offering windbreaks with a height under 10 m. A control site without windbreak was selected to also observe odour dispersion.
All sites were located on farm land South West of Montreal, with a relatively flat and consistent slope of 0.1% and without trees or fences, where a cereal crop had been freshly harvested.

4.3.2. Experimental equipment

A mobile odour generator (Fig. 4.1) was used as a point odour source to carry out the tests away from any infrastructure capable of interfering with the results.

During the tests, the odour generator was positioned upwind from the windbreak, at a distance of 15, 30 and 60 m (Fig. 4.2). Fully described by Lin et al. (2006), this odour generator used swine manure to generate the odorous air. At the start of each new day of testing, the odour generator tank was filled with fresh swine manure and therefore, the level of odour generation changed with test day. Because the odour emission dropped with time, morning testing never exceeded 2 h to limit to 30% the drop in odour emission. At 30-min intervals during each test, an air sample was collected from the outlet of the odour generator using Alinfan® sampling bags. The threshold dilution value of each air sample was determined in the laboratory, using a forced choice dynamic olfactometer and the same 12 panellists who observed the field odour plume distribution. Odour threshold was defined as the largest number of dilutions causing half of the panellists to detect or recognize an odour (ASHRAE, 2003). Odour concentration was expressed according to the European practices, as "odour units per cubic meter" (OU/m3) (CEN, 2001; Schauberger et al., 2002; Zhang et al., 2002).

To measure wind speed and direction and air temperature without disturbance during each test, a weather station (Davis Weather Wizard III) equipped with a portable PC as data log was installed on a tower, 7.6m in height, and some 200 m upwind from the windbreak. During the entire span of all tests, the temperature and wind direction and speed were recorded at one minute intervals. The air stability conditions were obtained from the closest weather station, that of the Pierre Elliot Trudeau airport, in Dorval, Canada.

The McGill University triangular forced-choice dynamic olfactometer used in this experiment was fully automated and capable of analyzing 4 contaminated air samples in 20 minutes, using two sets of 6 panellists (Choinière and Barrington, 1998)

4.3.3. Panellists

Panellists were selected and trained for this field and laboratory olfactory work according to the European Odour Standard (CEN, 2001). Before starting the experiment, a group of 20 panellists was selected by requiring them to detect n-butanol within a concentration of 20 to 80 ppb. Using the dynamic olfactometer,

these panellists were then further selected by requiring them to correlate statistically (P=0.05) the hedonic tone and odour concentration of four odorous air samples, presented at different concentrations (Fig. 4.3). The selection and training of 20 panellists when only 12 were used during the field measurements, provided replacements to conduct the test during the experimental days.

For each test day, all 12 panellists were calibrated once more by measuring their individual n-butanol detection threshold, which had to respect 20 to 80 ppb (CEN, 2001; Choinière and Barrington, 1998; Edeogn et al., 2001). For the n-butanol calibration, a clean air sample with 32 905 ppb of n-butanol at 293 K, was prepared as follows: 5 µL of n-butanol was injected into an Alinfan® bag previously filled with 40 L of air cleaned using an active carbon filter. Panellists were required to detect the n-butanol sample within a dilution factor of 411 to 1645 (80 to 20 ppb).

For the panellist field observations, hedonic tone (HT) was selected as odour sensation attribute because it refers to the degree of pleasant or unpleasant odour perception. The HT scale used in this project ranged from -10 to 0, where 0 to -2 was tolerable, -2 to -4 was unpleasant, -4 to -6 was very unpleasant, -6 to -8 was terrible and -8 to -10 was intolerable (Lim et al., 2001; Nimmermark, 2006; Parker et al., 2005). In the laboratory and using the olfactometer, the selected panellists were further rated by being asked to subjectively assess HT of an n-butanol air sample (32 905 ppb of n-butanol at 293 K) presented at various dilution levels. Each level of n-butanol was randomly presented three times to each panellist (Table 4.2).

4.3.4. Test procedure

Odour plume evaluation was initiated some 15 min after starting the odour generator and the weather station recordings. Three groups of four (3×4=12) trained panellists detected the odour plume developing downwind from a windbreak by moving about a random path predetermined from the wind direction and covering the odour plume zone. At each randomly designated observation station along this path, the group would stop walking, remove their carbon filter air masks, face the odour generator, and evaluate the odour hedonic tone during

60 s, using the previously described scale of -10 to 0. Each field odour hedonic tone observation by individual panellists was recorded along with their GPS position and the actual time of reading. The odour hedonic tone observed at an odour reading station was the average of the four panellists reading. The groups of panellists moved from one station to the next while wearing their face masks.

At 30-min intervals and while the panellists were observing each odour plume, a vacuum lung box was used to fill Alinfan® bags with 40L of odorous air at the outlet of the odour generator, within a 3-min period. During each test day, the air velocity and therefore flow, was also verified at 8 points over the surface of the generator outlet using an Alnor anemometer (Alnor 8570, TSI Inc., Shoreview, Minnesota, USA).

After observing two field odour plumes during the morning of each test day, the 12 panellists went to the olfactometry laboratory in the afternoon to assess the odour concentration of each generator air sample, according to the ASTM E679-91 Standard (1997) and the CEN prEN13725 Standard (2000). The threshold dilution value of each odour sample was established by the 12 panellists exposed to a decreasing number of dilutions. The odour concentration of each air sample was calculated using the principle of geometric mean (ASTM, 1990, 1997, 1998; CEN, 1995a, 1995b, 2001).

Some 39 odour plumes were observed, generally 2 per mornings, to evaluate the performance of the four windbreaks and the control site (without a windbreak). Some 2 to 3 tests were conducted for each of the three odour generator positions (15, 30 and 60 m upwind from the windbreak) and five windbreak sites including the control. These tests offered variable climatic conditions with high and low temperatures and wind speeds, and with wind angles varying from 0 to 90° with respect to the windbreak (Table 4.3).

4.3.5. Standardising the resulting odour plumes and computing MODD

During each test, the odour generator emitted a slowly decreasing odour level and, from one test to others, the odour level varied. Each odour plume was therefore standardised for purposes of comparison. Thus, the odour concentration measured at every station by each group of panellists, at a given period in time,

was divided by the odour concentration of the generator at that time, and multiplied by the average odour level of 472 OU/m^3 calculated from all 39 tests. The maximum odour dispersion distance (MODD) is impacted by criteria such as odour concentration, where a lower odour criterion will result in the longer MODD. The criteria are generally determined by government regulations and, in the present paper, were set at 1 and $2OU/m^3$, where 1 OU/m^3 implies that half of the population can detect the odour.

4.3.6. Statistical analysis

Before conducting the statistical tests, a series of regression analyses were conducted to establish that the exponential function best described the relationship between the radial distance from the source and OC. This regression equation produced MODDs corresponding to 1 and 2 OU/m^3.

During all tests, the odour plume observed presented zones of high OC separated by zones of lower and sometimes no OC, rather than a uniform zone with a continuously descending OC with distance downwind from the source (Lin et al., 2006). Nevertheless, the OC of these maximum zones decreased with radial distance from the source. Therefore and for each odour plume, two regression equations and MODD values were produced: that obtained from all the data points, representing an MODD computed from an average OC regression, and; that obtained from peak values representing an MODD computed from the maximum OC regression.

Based on the data available, two statistical tests were conducted: the first tested whether or not the windbreaks had a significant effect on MODD, as compared to the control site without a windbreak; the second verified the effect of the windbreak and climatic parameter on odour concentration (OC) with radial distance from the source, namely, the odour generator.

To determine the effect of windbreak on MODD, sites 2 and 5 with a windbreak, were compared to the control site without a windbreak. For each treatment, OC measured and its radial distance from the source were considered the two main factors. The following covariance model was used to combine the regression and classification models (Cue, 2006; SAS Institute Inc., 2001):

$$\ln OC_{ij} = \mu + site_i + b_1 x_{ij} + e_{ij} \quad (4.1)$$

where:

$\ln OC_{ij}$ = the natural logarithm of the OC at the j^{th} odour point for the i^{th} site, i = 1 for the site without a windbreak and i = 2 for the site with a windbreak;

μ = the effect of the overall mean;

$site_i$ = the fixed effect of the i^{th} site on OC;

b_1 = the regression effect of the OC;

x_{ij} = the odour dispersion distance on the j^{th} odour point in the i^{th} site;

e_{ij} = random residual error of OC associated with the j^{th} odour point on the i^{th} site.

To measure the effect of windbreak properties (porosity and tree type) and climate (temperature, wind speed and velocity) on OC, case comparisons were conducted because of the difficulty in collecting, in the field, data related to specifically one factor. Therefore, similar tests were selected and all measured odour points were used to produce a regression equation comparing one factor. The sets of field conditions compared did not always provide conditions for an ideal comparison, but represented the best comparison possible, given all 39 field tests. For example, between sites compared, wind speed may be different, while all other parameters (temperature, wind direction, windbreak species and porosity) were similar but not equal.

4.4. RESULTS

The panellists used to conduct the experiment are described in Fig. 4.3 presenting a relationship between hedonic tone (HT) and odour concentration (OC), and in Table 4.2 presenting a relationship between n-butanol rating and HT.

Odour dispersion distance reflected by MODD is most likely affected by the presence of a windbreak, its porosity and tree species, by the location of the odour generator and ambient climatic conditions. These effects on MODDs are compared in Figs. 4.4 to 4.10 illustrating OC as a function of radial distance downwind from the source. In all cases, two regression equations are presented,

both for all the data points, and for the maximum data points for MODD criteria of 1 and 2 OU/m^3 (Table 4.4). In Figs. 4.4 to 4.10 and despite low R^2 values especially for the average OC regression, both the average and maximum regression lines are presented because the equations are statistically significant (P = 0.05). For example, the R^2 of the average regression line in Fig. 4.9 is 0.14 (48 pairs of data), but the F-test interpreting OC drop with distance is statistically significant (P = 0.01).

4.4.1. Characterization of the panellists

The typical relationship between HT and OC for an odorous air sample, as perceived by one group of four panellists (tests 3 and 4) is shown in Fig. 4.3 (a). A certain degree of variation was obtained despite the training and selection of the panellists.

For 129 comparisons conducted by all groups of panellists, the relationship obtained between HT and OC was:

$$OC = 1.546\, e^{-0.285HT} \qquad (4.2)$$

where OC is the odour concentration in OU/m^3 and HT ranges from 0 to -10. Equation (4.2) was found to be statistically significant (P = 0.01) meaning that HT can explain variation in OC.

The assessment of the 72 odour samples collected at the odour generator on the 18 different test days produced 54 regression lines in the form of Equation (4.2). Each line represents the average assessment of a group of four panellists on a given test day. Out of 54, 51 lines produced a statistically significant regression equation (P=0.05); one group associated with tests 22, 23, and 24 did not produce a statistically significant regression equation at the P=0.05 level. Fig. 4.3 (b) shows the range of the 51 lines, where the low, high and average values are, respectively:

$$OC=0.885e^{-0.150HT} \quad \text{Low} \qquad (4.3)$$

$$OC=2.008e^{-0.470HT} \quad \text{High} \qquad (4.4)$$

$$OC=1.445e^{-0.266HT} \quad \text{Mean} \quad (4.5)$$

In Fig. 4.3 (b), the relationship between HT and OC, obtained in this project, is compared to that of other projects:

$$HT = -0.33\ OC^{0.523} \quad \text{(Lim et al. 2001)} \quad (4.6)$$

$$HT = 2.5 \times (0.373 - 1.165\ \text{Log}_{10}(OC)) \quad \text{(Nimmermark 2006)} \quad (4.7)$$

Because the lines obtained by Lim et al. (2001) and Nimmermark (2006) stand above those of the present work (Fig. 4.3), the panellists selected for the present field and laboratory work were found to be more sensitive to odours. In fact, Lim et al. (2001) report a panellist n-butanol detection threshold of 865 ppb which is 22 times higher than the CEN standard of 40 ppb. Nimmermark (2006) reports a panellist n-butanol detection threshold identical to that used in this project (20 to 80 ppb detection threshold) but for OC above the threshold, the panellists used on the present experiment were more sensitive reporting a higher HT as compared to the panellists used by Nimmermark (2006). This increased sensitivity to odours may result from a more rigorous training method or the exposure of the panellists to a different every day cultural context.

4.4.2. Effect of the windbreak

The data measured on site 5 (tests 37, 38, and 39 - Table 4.3) with 84 odour points and on site 2 (tests 5, 6, 8, 9, 10, 11, 13, 14, 15, 16, 17 and 19 - Table 4.3) with 189 odour points were used in Equation (4.1) to conduct an analysis of variance (Table 4.5). The F-test results for the model, the mean, the model over and above the mean, the sites and b_1 (Equation 4.1) are significant at the 5% probability level. Therefore, the model does explain OC as a function of site (with and without windbreak) and distance. The F-test results also imply that the windbreaks (sites 2 and 5) had a significant impact on MODD, as compared to the control site without a windbreak.

For the windbreak and control sites (Fig. 4.4 and Table 4.4), the MODD obtained for 2 OU/m^3, were 564 and 717m, respectively when using the maximum values. When the OC criterion was set at 1 OU/m^3, the MODD were

676 and 871 m, respectively. In comparison and for the criterion of 2 OU/m^3, the windbreak on site 2 with an optical porosity of 35%, produced MODD of 355 and 564 m for the average and maximum OC regressions; for 1 OU/m^3, the MODDs were 493 and 676 m, respectively.

When considering all events measured in September 2003, for both the windbreak and control sites, the MODD produced by the windbreak were at least 21% shorter. Thus, windbreaks can effectively improve odour dispersion and this capability can likely be improved by selecting better performing windbreak parameters.

4.4.3. Effect of windbreak porosity

The impact on odour dispersion of windbreak porosity is illustrated in Fig. 4.5 for site 1 (tests 2 and 3) with an optical porosity of 55%, compared to that on site 2 (test 16) with an optical porosity of 35%. In both cases, the odour generator was located 30 m upwind from the windbreak, the wind speed was 4.2 and 1.5m/s and the air temperature was 19 and 23 °C, respectively. The wind direction was 50 to 90° for tests 2 and 3 and 90° for test 16.

For 2 OU/m^3 and the maximum regression line, MODD reached 391 m for the denser windbreak, as compared to 642 m for the more porous windbreak, despite its greater height and exposure to higher wind velocities. For the same criterion but with the average OC regression, the predicted MODD was 353 m for the denser windbreak, compared to 538 m for the more porous windbreak. Using the criterion of 1 OU/m^3, the denser windbreak produced MODD of 463 and 427 m for the maximum and average regressions, respectively, compared to the more porous windbreak which produced MODD of 852 and 815m under the same conditions. On the average, the denser windbreak reduced MODD by 42%, as compared to the more porous windbreak.

Improved odour dispersion indicates that a dense windbreak produced stronger turbulence and greater atmospheric mixing as compared to the porous windbreak. Therefore, conditions required to dilute odours are quite different

from those of high porosity required to lower wind velocity downwind from the windbreak.

4.4.4. Effect of odour generator location

Effect of odour generator location on MODD was measured using the data from 12 tests measured on site 2 (Fig. 4.6). For the odour generator located 15 m upwind from the windbreak, the average wind speed and direction, and the air temperature were 2 m/s, 58°, 22°C; for that at 30 m, the average wind speed and direction, and the air temperature of 3.2 m/s, 73°, 21°C, and; for that at 60 m, the average wind speed and direction, and the air temperature of 2.2 m/s, 56°, 24°C, respectively.

For the criterion of 2 OU/m^3 and the maximum OC regression, the odour generator produced MODD of 511, 533 and 569 m when positioning at 15, 30 and 60 m upwind from the windbreak, respectively. For the criterion of 1 OU/m^3 and the maximum OC regression, MODD of 619, 648 and 700 m were produced, for the same respective locations. Thus, reducing the distance between the odour source and the windbreak had a significant effect on MODD. The 15m position reduced MODD by 10 to 34% compared to the 60 m position.

A windbreak positioned closer to the odour source is therefore better able to trap odours on its downwind side, to disperse them thereafter. With the odour source located 60 m upwind from the windbreak, the odour is somewhat dispersed before reaching the windbreak, the odour trapping process is less effective and the downwind dispersion is not as complete.

4.4.5. Effect of tree species

Odour dispersion was influenced by windbreak tree species (Figs. 4.7). The poplar windbreak (test 1 on site 1) with a height of 18 m was compared to that of conifers (test 20 on site 3) with a height of 7.6 m. Both windbreaks had an optical porosity of 55%. In both cases, the odour generator was located 15 m upwind from the windbreak, the air temperature was 19 and 13°C, and the wind direction was 90 and 80°, respectively. Wind speed was nevertheless different, averaging 6.4 and 1.8 m/s, respectively.

For the criterion of 2 OU/m^3 and maximum and average OC regression for the conifer windbreak produced MODD of 588 and 575 m compared to MODD of 698 and 631 m for the taller poplar windbreak, despite higher wind velocities. Furthermore, for the criterion of 1 OU/m^3 and the maximum as well as average OC regressions, conifers produced MODD of 724 and 723 m compared to 987 and 1064 m for the poplar windbreak.

As compared to poplars, coniferous trees reduced MODD by 9 to 32%, likely because their stronger branches offered greater wind resistance for a more effective odour dispersion.

4.4.6. Effect of air temperature

The effect of air temperatures was compared under conditions of similar atmospheric stability (Figs. 4.8). Odour points from 3 tests (tests 5, 8 and 16) observed in September on site 2 with a deciduous windbreak were compared to those of tests 28, 32 and 33 conducted in December on site 4, with an coniferous windbreak. In both cases, the odour generator was located 30 m upwind from the windbreak, the optical porosity of both windbreaks was 35%, the wind velocity and direction averaged 3.2 and 2.4 m/s and 73° and 67°, and the average temperature was at 21 and -7°C, respectively. For both summer and winter conditions, the Pasquill-Gifford atmospheric stability condition was mostly D.

Warmer temperatures lead to shorter MODD compared to colder temperatures. For the criterion of 2 OU/m^3 and the maximum and average OC regressions, warm air temperatures produced MODD of 533 and 398 m compared to 623 and 401 m for cold air temperatures, despite the fact that conifers may be better at dispersing odours. For the criterion of 1 OU/m^3 and maximum and average OC regression, warm air temperatures produced MODD of 648 and 555 m compared to 777 and 524 m for the cold air temperatures.

Air viscosity increases with temperature and therefore produces more mixing on the downwind side of the windbreak. Therefore, odours will be transported over longer distance during the winter, for the same OU production at the source.

4.4.7. Effect of wind speed and direction

Fig. 4.9 compares the results of tests 9, 11, 13 and 17 (site 2 and wind direction ranging from 30 to 60°) with an averaged wind speed of 1.2 m/s, to those of test 15 (site 2 and wind direction of 90°) with an average wind speed of 5.1 m/s. In both cases, the odour generator was located 15 m upwind from the windbreak and the air temperature was 23 and 28°C, respectively.

For the criterion of 2 OU/m^3 and the maximum and average OC regressions, respectively, higher wind speeds produced MODD of 426 and 327 m as compared to 607 and 498 m for the lower wind speed. For the criterion of 1 OU/m^3 and the maximum and average OC regressions, respectively, higher wind speeds reduced MODD by 27% as compared to lower wind speed.

The greater dispersion associated with stronger wind speeds is consistent with the Gaussian odour dispersion model (Schnelle and Dey, 2000) and the results of the Inpuff-2 model (Guo et al., 2001).

For site 2, Fig. 4.10 illustrates the effect of the wind direction where test 15 (average wind direction of 90°) is compared to test 17 (average wind direction of 40°). In both cases, the odour generator was located 15m upwind from the windbreak, the wind speed was 5.1 and 1.5 m/s and the air temperature was 28 and 24°C, respectively.

For the criterion of 2 OU/m^3 and the maximum and average OC regressions, the 90° wind angle produced MODD of 426 and 397 m, compared to 626 and 462 m obtained with a smaller wind angle. For the criterion of 1 OU/m^3 and the maximum and average OC regressions, respectively, the 90° wind angle produced MODD of 564 and 539 m as compared to 777 and 627 m for the 40° wind angle.

Wind direction perpendicular to the wind windbreak can therefore reduce MODD by 15 to 30%, compared to a wind angle of 40°. This observation needs

further verification as the wind speed for the 90° wind direction was quite different from that of the other case and may have interfered with the results.

4.5. SUMMARY and CONCLUSIONS

Through field data regression and classification analysis, functions were obtained to relate odour concentration (OC) with radial distance from the source in the presence and absence of windbreak, and for windbreaks of different types exposed to various climatic conditions. These functions also provided some basis for the statistical comparison of odour dispersion under different conditions. The analysis conducted in this project lead to the following conclusions:

1) The OC and hedonic tone (HT) of odorous air samples observed by trained panellists were found to be exponentially related (P=0.05);
2) Under variable climatic conditions, windbreaks can improve odour dispersion and reduce MODD by at least 21%, especially when offering an optical porosity of 35%, and as compared to a site without a windbreak;
3) For the same optical porosity, conifers were better at dispersing odours than poplars;
4) Odour dispersion was optimized with a windbreak of limited optical porosity (35% as compared to 55%); therefore, a porous windbreak designed to reduce wind speed over a long distance on its downwind side, is not designed to disperse odour;
5) Windbreaks are more effective in dispersing odours when close to the source; as compared to a distance of 15m, a distance of 30 and 60m increased MODD by 6 and 12%, respectively; for livestock shelters using natural ventilation, a 30 m distance is preferred to allow for some air movement about the inlets and outlets;
6) Climatic conditions such as air temperature and wind speed and direction impact the odour dispersion efficiency of windbreaks; higher temperatures and wind speeds improve odours trapping on the downwind side for a more extensive dispersion.

Despite the fact that these conclusions were based on 39 field tests, each comparison was not perfect as all factors could not be controlled. For an effective comparison, the air mixing performance of windbreaks should be reproduced by modelling.

4.6. ACKNOWLEDGEMENT

The authors wish to acknowledge the financial contribution of Consumaj inc., CDAQ, The Livestock Initiative Program, Agriculture and Agro-Food Canada and the Natural Sciences and Engineering Research Council of Canada.

4.7. REFERENCES

ASHRAE, 2003. Handbook of fundamentals. American Society of Heating Refrigeration and Air Conditioning Engineering. Atlanta, USA. Chapter 12.

ASTM, 1990. Standard method for defining and calculating sensory thresholds from intermediate size. AWMA E 18.04.25. American Society for the Testing of Materials, Washington, DC, USA.

ASTM, 1997. Standard Practice for Determination of Odor and Taste Thresholds By a Forced-Choice Ascending Concentration Series Method of Limits, American Society for the Testing of Materials, Washington, DC, USA.

ASTM, 1998. Standard Practices for referencing supra-threshold odour intensity. American Society for the Testing of Materials, Washington, DC, USA.

Bottcher, R.W., Munilla, R.D., Keener, K.M. and Gates, R.S., 2001. Dispersion of livestock building ventilation using windbreaks and ducts. 2001 ASAE Annual International Meeting.: Paper No. 01-4071. 2950 Niles road, St. Joseph, Mi. USA.

CEN, 1995a. Document 064/e, Odour concentration measurement by dynamic olfactometry. CEN TC 264/WG2. Comité Européen de Normalisation. Dusseldorf, Germany.

CEN, 1995b. Odour Standards. CEN/TC 264N 134. Comité Européen de Normalisation, Dusseldorf, Germany.

CEN, 2001. Air quality - determination of odor concentration by dynamic olfactometry. prEN13725, European Committee for Standardization, 36 rue de Stassart, B-1050 Brussels. <http://www.aerox.nl/images/eurstandard.pdf>, visited August, 2004.

Choinière, D. and Barrington, S., 1998. The conception of an automated dynamic olfactometer. CSAE/SCGR Paper No.98-208.

Cue, R.I., 2006. Statistical methods AEMA-610. http://animsci.agrenv.mcgill.ca/servers/anbreed/statisticsII/stats2e.pdf (visited 200606).

Edeogn, I., Feddes, J.J.R., Qu, G., Coleman, R. and Leonard, J., 2001. Odour measurement and emissions from pig manure treatment/storage systems. Final report to Canada Pork Council. Project Number CPC-01. University of Alberta, Edmonton, AB. http://www.cpc-ccp.com/HEMS/CPC-01_Feddes.PDF (2007/01/17).

Eimern, J.v., Karschon, R., Razumova, L.A. and Robertson, G.W., 1964. Windbreaks and shelterbelts. Report of a working group of the Commission for Agricultural Meteorology, World Meteorological Organization, Technical Note No. 59. Secretariat of the World Meteorological Organization, Geneva, 188 pp.

Guan, D., Zhang, Y. and Zhu, T., 2003. A wind-tunnel study of windbreak drag. Agri. Ecosystem & Environment, 118: 75-84.

Guo, H., Jacobson, L.D., Schmidt, D.R. and Nicolai, R.E., 2001. Calibrating inpuff-2 model by resident-panelists for long-distance odor dispersion from animal production sites. American Society of Agricultural Engineers, 17(6): 859-868.

Heisler, G.M. and Dewalle, D.R., 1988. Effects of windbreak structure on wind flow. Agriculture, Ecosystems and Environment, 22-23: 41-69.

Leuty, T., 2003. Using shelterbelt to reduce odors associated with livestock production barns. Ministry of Agriculture and Food, Ontario, http://www.gov.on.ca/OMAFRA/english/crops/facts/info_odours.htm, visited in 2004.

Leuty, T., 2004. Wind management can reduce offensive farm odours. Ministry of Agriculture and food, Ontario, http://www.omafra.gov.on.ca/english/crops/facts/info_odours.htm (2007/01/24).

Lim, T.T., Heber, A.J., Ni, J.Q., Sutton, A.L. and Kelly, D.T., 2001. Characteristics and Emission Rates of Odor from Commercial Swine Nurseries. Trnsaction of the ASAE, 44(5)(0001-2351): 1275-1282.

Lin, X.J., Barrington, S., Nicell, J., Choiniere, D. and Vezina, A., 2006. Influence of windbreaks on livestock odour dispersion plume in the field. Agriculture, Ecosystems & Environment, 116(3-4): 263-272.

McNaughton, K.G., 1988. Effects of windbreaks on turbulent transport and microclimate. Agri. Ecosystem & Environment, 22-23: 17-39.

Nimmermark, S., 2006. Characterization of odor from livestock and poultry operation by the hedonic tone. Paper number 064157. In: ASABE (Editor), 2006 American Society of Agricultural and Biological Engineering Annual International Meeting, Oregon Convention Center, Portland, Oregon, 9 - 12 July 2006.

Parker, D.B., Rhoades, M.B., Schuster, G.L., Koziel, I.A. and Perschbacher-Buser, Z.L., 2005. Odor characterization at open-lot beef cattle feedyards using triangular forced-choice olfactometry. Transactions of the ASAE, 48(4): 1527-1535.

SAS Institute Inc., 2001. SAS (r) Proprietary Software Release 8.2, Cary, NC, USA.

Schauberger, G., Piringer, M. and Petz, E., 2002. Calculating direction-dependent separation distance by a dispersion model to avoid livestock odor annoyance. Biosystems Engineering, 82(1): 25-37.

Schnelle, K.B. and Dey, P.R., 2000. Atmospheric dispersion modeling compliance guide. McGraw-Hill, New York, USA.

Tyndall, J. and Collettii, J., 2000. Air quality and shelterbelts: Odour mitigation and livestock production - A literature review. Final project report to USDA National Agroforestry Center, Lincoln, NB. Project Number 4124-4521-48-3209. Forestry Department, Iowa State University, Ames, IA. http://www.forestry.iastate.edu/res/Shelterbelts_and_Odor_Final_Report.pdf (2007/01/17).

Zhang, Q. et al., 2002. Odor production, evaluation and control. http://www.manure.mb.ca/projects/completed/pdf/02-hers-03.pdf, visited August, 2004., Manitoba Livestock manure Management Initiative Inc.

Tables and Figures

Table 4.1 Experimental windbreak found on each site.

Description	Site			
	1	2	3	4
Tree type	poplar	mixed mature deciduous	conifers	conifers
Windbreak				
length (m)	2100	1050	405	380
height (m)	18.3	9.2	7.6	15.2
depth (m)		7		6
optical porosity (%)	55	35	55	35
porosity at the base (%)	70	30	70	40
Location*	Sherrington	St Chrysostome	St Amable	St Charles

* all locations are located within 50 km of the Island of Montreal, Canada, in the southwest direction.

Table 4.2 Panellist evaluation of hedonic tone versus n-butanol concentration

Hedonic tone	Average n-butanol level (ppb)	Range of n-butanol level (ppb)
0	59	0-69
-1	80	69-93
-2	109	93-127
-3	149	127-174
-4	204	174-238
-5	278	238-325
-6	380	325-444
-7	519	444-607
-8	709	607-828
-9	968	828-1131
-10	1322	>1131

Table 4.3 Test conditions

Test number	Site	Date (2003)	Test conditions*					AS
			OG	OE	WS	Angle	T	
			(m)	OU/s)	(m/s)	(°)	(°C)	
1	1	Aug 29	15	621	6.4	90	19	B
2	1	Aug 29	30	760	6	90	20	D
3	1	Sep 02	30	859	2.5	50	17	C
4	1	Sep 02	60	551	2.5	50	20	C
5	2	Sep 03	30	1373	3	90	21	B
6	2	Sep 03	60	492	4.4	90	23	C
7	2	Sep 05	15	578	4.7	40	18	D
8	2	Sep 05	30	585	4.2	40	19	D
9	2	Sep 08	15	214	1	60	22	B
10	2	Sep 08	60	218	1.1	70	20	B
11	2	Sep 10	15	5360	1.2	30	22	C
12	2	Sep 10	30	1096	2.7	20	27	D
13	2	Sep 12	15	559	1.2	50	23	B
14	2	Sep 12	60	294	1	40	26	B
15	2	Sep 15	15	744	5.1	90	28	D
16	2	Sep 15	30	745	1.5	90	23	D
17	2	Sep 18	15	1879	1.5	40	24	C
18	2	Sep 18	60	13052	1.4	50	21	B
19	2	Sep 18	60	846	2.2	60	26	B
20	3	Sep 29	15	318	1.8	80	13	C
21	3	Sep 29	49	368	1.7	70	14	B
22	4	Dec 03	15	1339	4.1	60	-2	D
23	4	Dec 03	30	690	3.5	60	-4	D
24	4	Dec 03	60	208	2.6	50	-4	D
25	4	Dec 10	15	166	1.3	70	-2	D
26	4	Dec 10	15	148	1.9	70	-2	D
27	4	Dec 10	30	101	1.7	60	-2	D
28	4	Dec 13	30	111	0	60	-8	D
29	4	Dec 13	60	175	2.1	50	-6	D
30	4	Dec 13	60	79	1.4	50	-9	D
31	4	Dec 14	15	205	3.1	70	-8	D
32	4	Dec 14	30	394	3.3	60	-8	D
33	4	Dec 14	30	350	3	80	-8	D
34	2	Sep 09	197	166	1.2	0	18	C
35	4	Dec 09	191	102	0.3	57	-2	B
36	4	Dec 09	318	99	0.4	0	-3	C
37	5	Aug 21	NW	766	4.1	NW	28	C
38	5	Aug 21	NW	480	3.6	NW	26	C
39	5	Aug 22	NW	310	6.1	NW	26	D

Note: NW- no windbreak; OG – odour generator distance upwind from the windbreak; OE – average odour emission during a test; WS- average wind speed; Angle – angle between the windbreak and the wind, 90° being perpendicular; T – average temperature measured during the test; AS – Pasquill-Gifford atmospheric stability condition, where B and C are unstable classes and D is a neutral class.

Table 4.4 MODD values for the windbreak comparisons illustrated in Figs. 4.4 to 4.10.

Comparison	Figure	Condition	Test No.	MODD criterion			
				2 OU/m^3		1 OU/m^3	
				Max	Ave	Max	Ave
Windbreak presence	4	without	37,38,39	717	562	871	818
		with	5, 6, 8, 9, 10, 11, 13, 14, 15, 16, 17,19	564	355	676	493
		reduction		21%	37%	22%	40%
Windbreak porosity	5	55%	2, 3	642	538	852	815
		35%	16	391	353	463	427
		reduction		39%	34%	46%	48%
Odour generator distance	6	15m	9,11,13,15,17	511	285	619	427
		30m	5, 8, 16	533	398	648	555
		60m	6, 10, 14, 19	569	430	700	558
		Reduction 1*		4%	28%	4%	23%
		Reduction 2		10%	34%	12%	24%
		Reduction 3		6%	7%	7%	1%
Tree type	7	deciduous	1	698	631	987	1064
		conifer	20	588	575	724	723
		reduction		16%	9%	27%	32%
Temperature	8	21°C	5, 8, 16	533	398	648	555
		-7°C	28, 32, 33	623	401	777	524
		reduction		14%	1%	17%	-6%
Wind speed	9	1.2m/s	9,11,13,17	607	498	758	745
		5.1m/s	15	426	397	564	539
		reduction		30%	20%	26%	28%
Wind direction	10	90° angle	15	426	397	564	539
		40° angle	17	626	462	777	627
		reduction		32%	14%	27%	14%

* reduction 1: 15m versus 30m; reduction 2: 15m versus 60m; reduction 3: 30m versus 60m

Table 4.5 ANOVA for sites with and without windbreaks

Source	Degrees of freedom	Sum of Squares	Mean of the squares	F-ratio	F-tab at 5%	Test result
Total sum of squares	273	877.92				
Reduction sum of squares for model	3	647.81	215.94	253.38	2.638	Significant
Correction factor for the mean	1	589.44	589.44	691.64	3.876	Significant
Reduction sum of squares for model over and above the mean	2	58.37	29.19	34.25	3.029	Significant
Reduction sum of squares for the site over the μ and b_1	1	4.24	4.24	4.97	3.876	Significant
Reduction sum of squares for b_1 over μ and site	1	57.93	57.93	67.97	3.876	Significant
Sum of squares of residual	270	230.10	0.852			

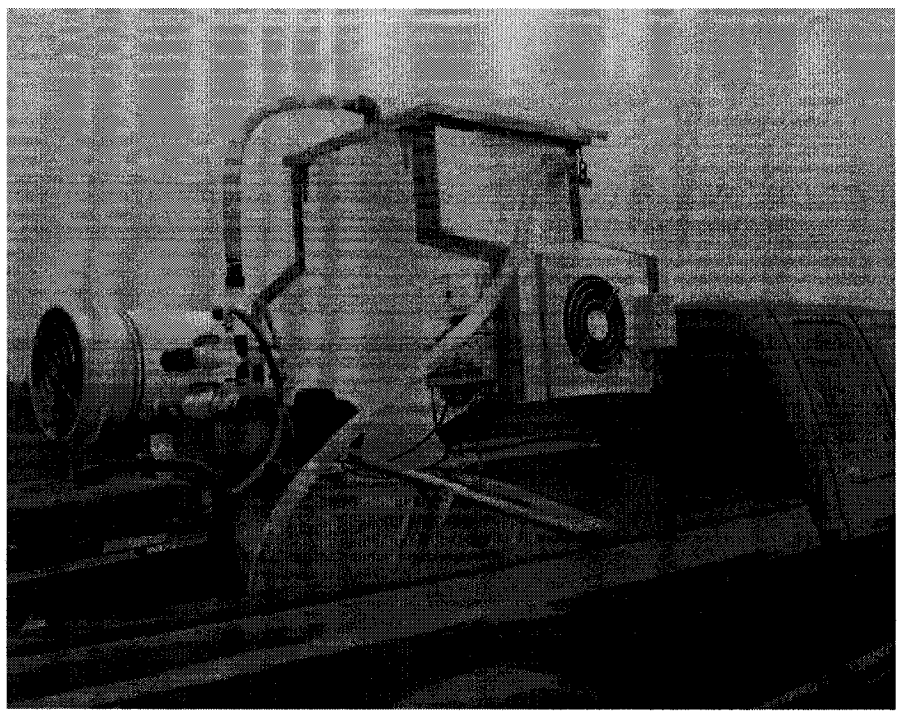

Fig. 4.1. The experimental odour generator.

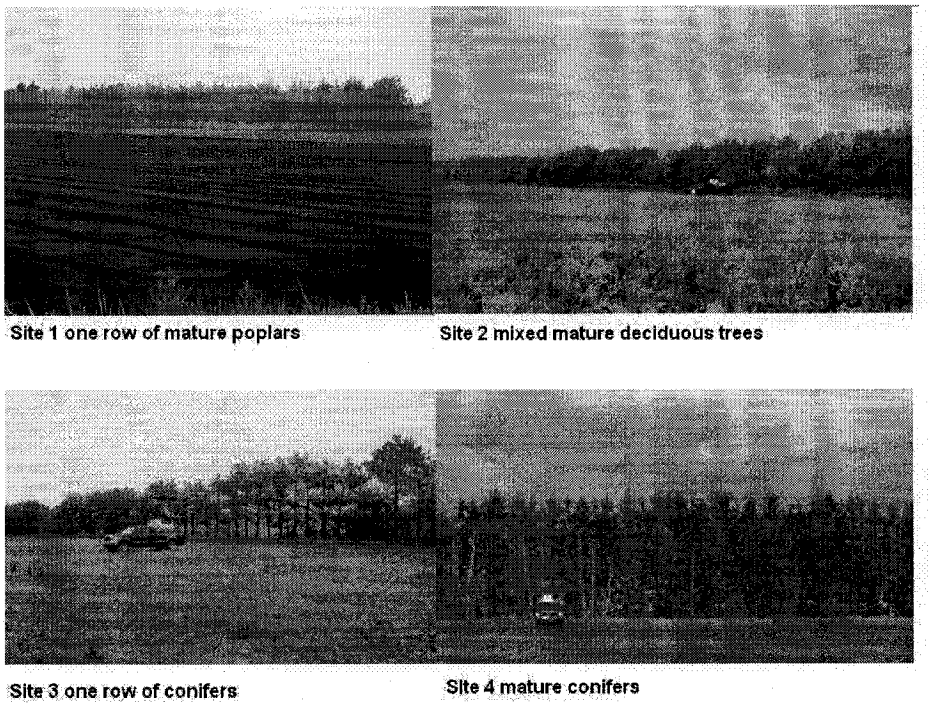

Fig. 4.2. The experimental windbreaks with the odour generator in position to run the tests.

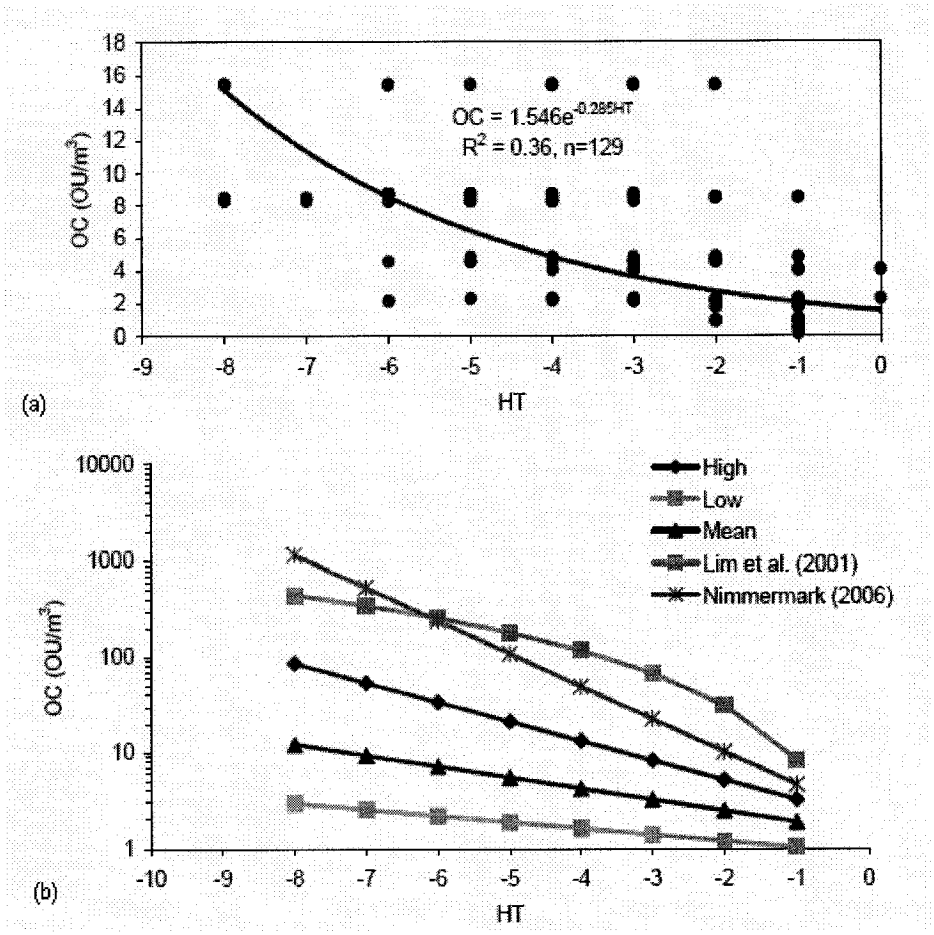

Fig. 4.3. Typical relationship between hedonic tone (HT) and odour concentration (OC) of an odorous air sample: (a) for a group of four panellists (tests 3 and 4); (b) data collected by Lim et al. (2001) and Nimmermark (2006) compared to that of the present project for the low, mean and high curves.

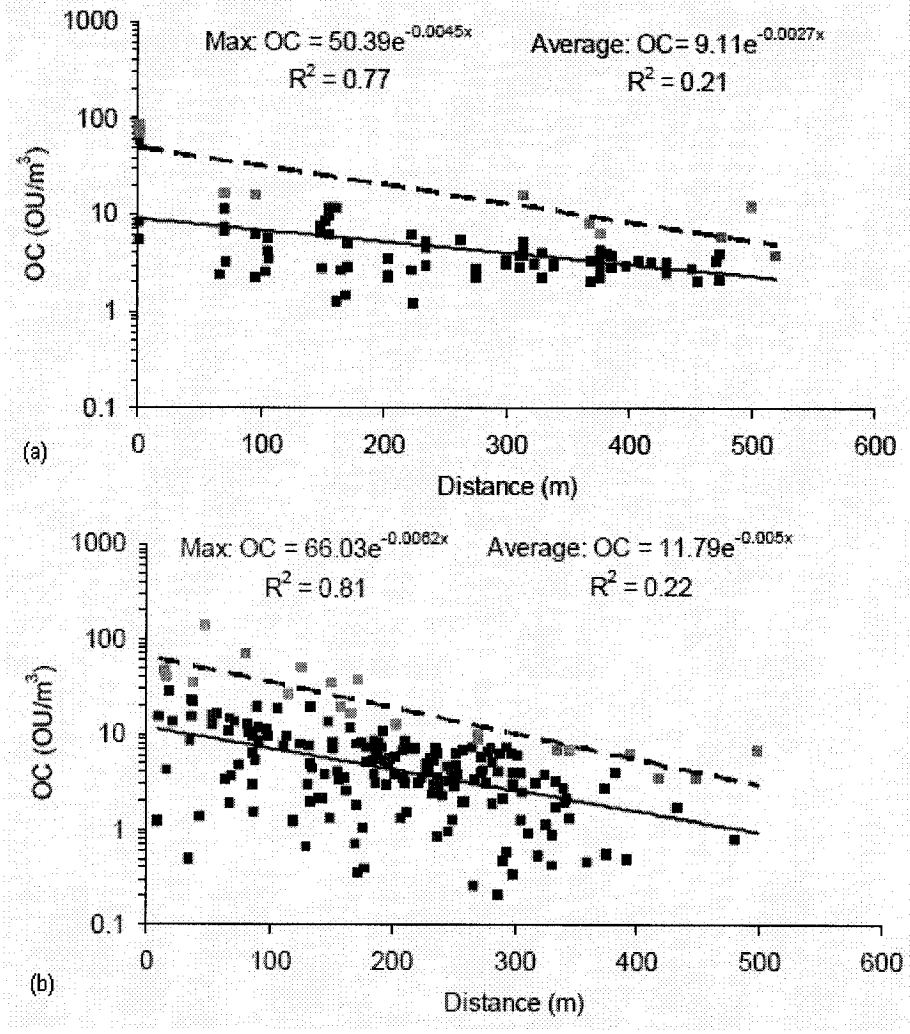

Fig. 4.4. Odour concentration with distance from the source, for sites: (a) without a windbreak (tests 37, 38 and 39); (b) with a windbreak (tests 5, 6, 8, 9, 10, 11, 13, 14, 15, 16, 17 and 19). The odour generator was located 15, 30 and 60 m upwind from the windbreak. The dotted line is the correlation for the maximum data (peak values are illustrated by pink squares), while the solid line is the correlation for all the data.

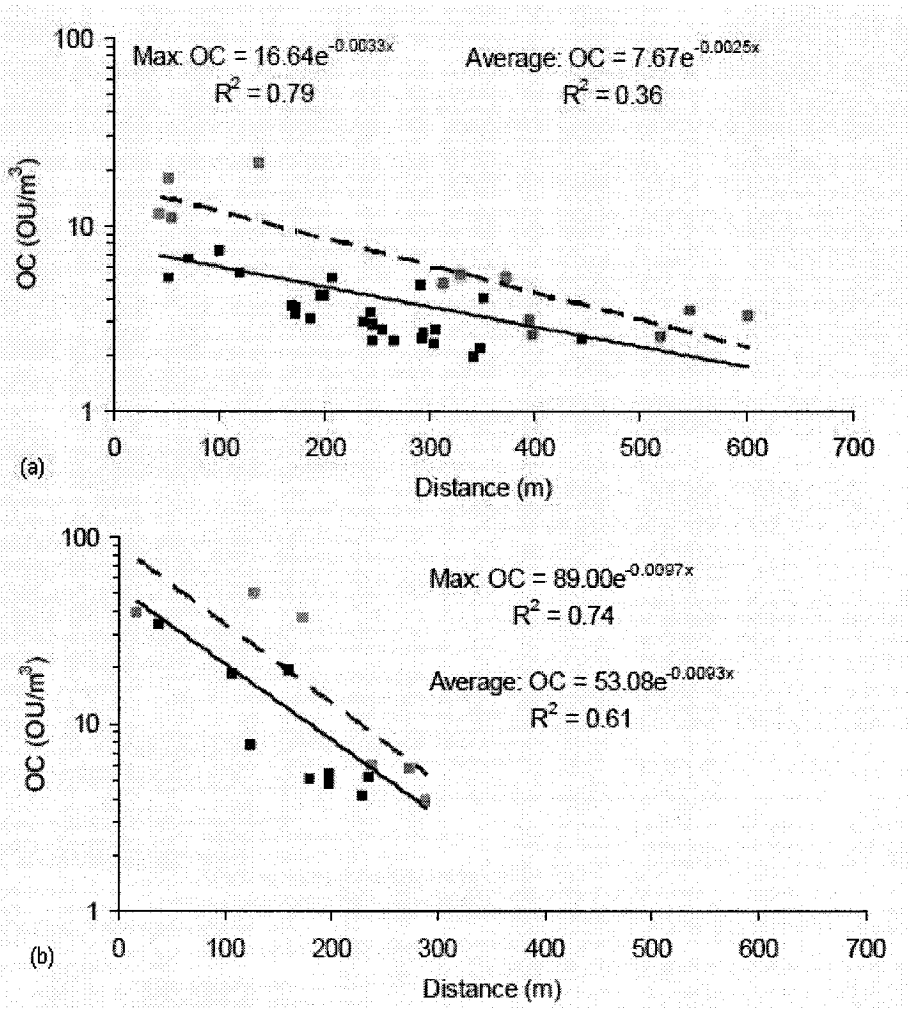

Fig. 4.5. Effect of windbreak porosity on odour dispersion with distance, for windbreak porosity of: (a) 55% (test 2 and 3); (b) 35% (test 16). In both cases, the odour generator is 30 m away from the windbreak. The dotted line is the correlation for the maximum data (the peak values are illustrated by pink squares), while the solid line is the correlation for all the data.

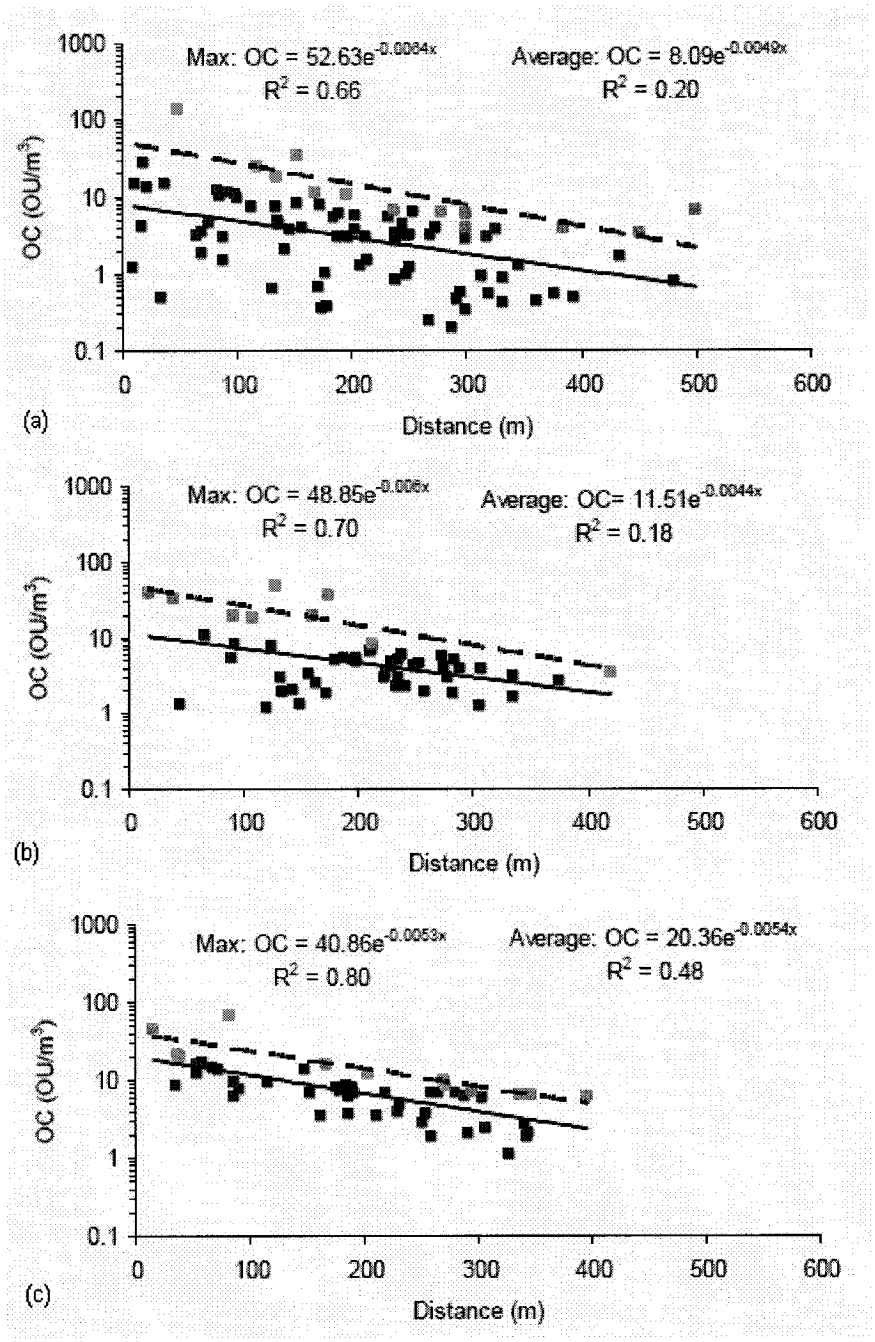

Fig. 4.6. Effect of odour generator location upwind from a windbreak: (a) 15 m (test 9, 11, 13, 15, and 17); (b) 30 m (test 5, 8, and 16), and; (c) 60 m (tests 6, 10, 14 and 19). The dotted line is the correlation for the maximum data (the peak values are illustrated by pink squares), while the solid line is the correlation for all the data.

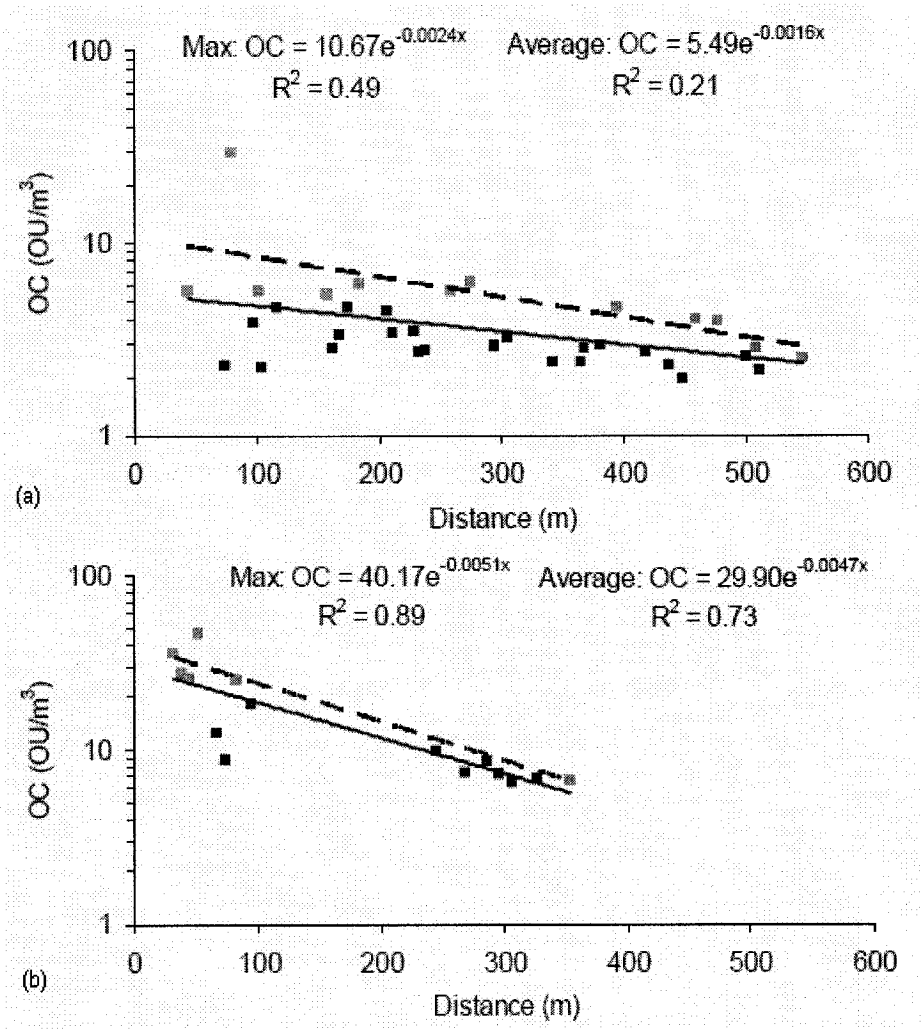

Fig. 4.7. Effect of tree species on odour dispersion: (a) site 1 with poplars (test 1); (b) site 3 with conifers (test 20). The odour generator is 15 m away from windbreak. The dotted line is the correlation for the maximum data (the peak values are illustrated by pink squares), while the solid line is the correlation for all the data.

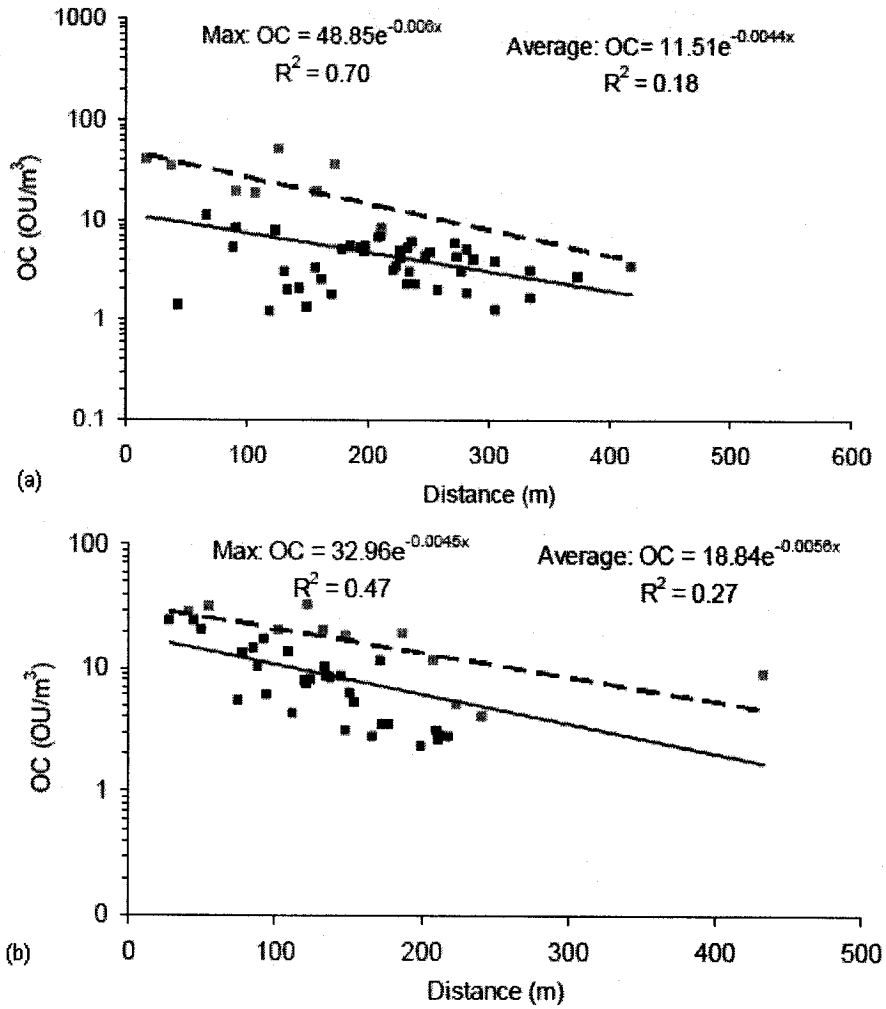

Fig. 4.8. Effect of air temperature on odour dispersion: (a) above 20°C for site 2 (test 5, 8 and 16); (b) below 0°C for site 4 (test 28, 32 and 33). The odour generator is located 30 m away from the windbreak. The dotted line is the correlation for the maximum data (the peak values are illustrated by pink squares), while the solid line is the correlation for all the data.

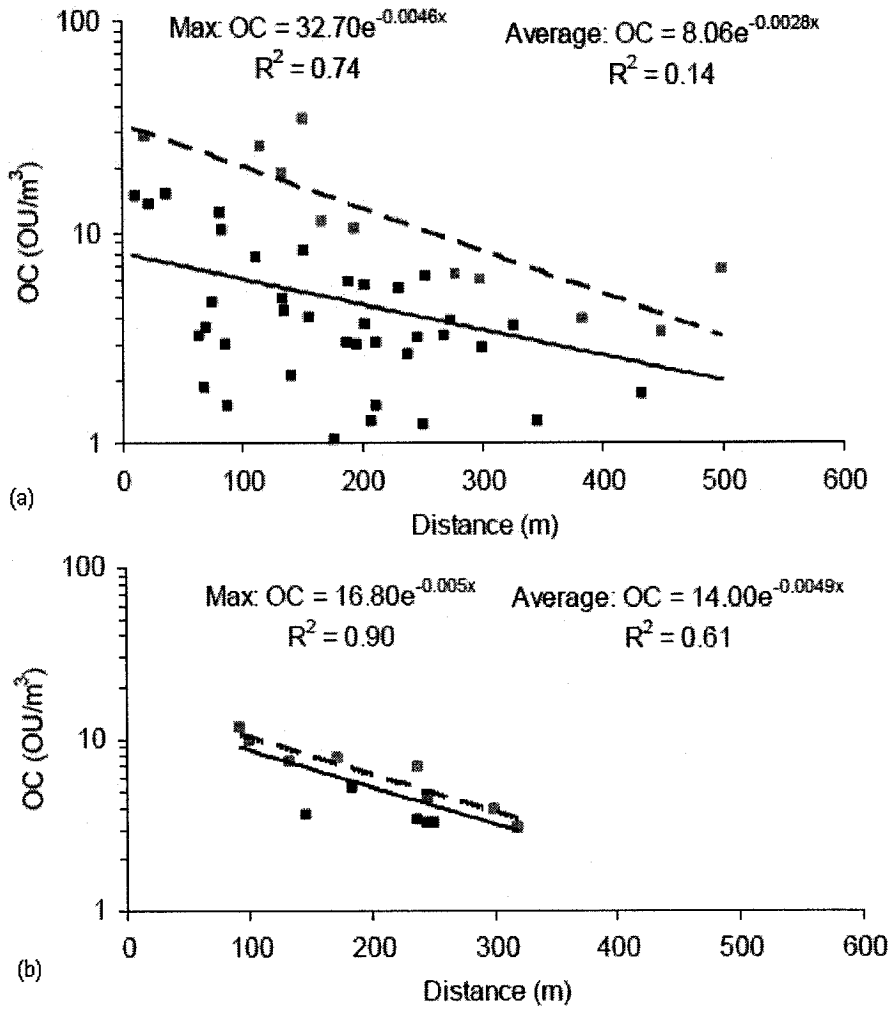

Fig. 4.9. Effect of wind speed on odour dispersion: (a) 1.2 m/s (tests 9, 11, 13 and 17): (b) 5.1 m/s (test 15). The odour generator is located 15 m away from windbreak. The dotted line is the correlation for the maximum data (the peak values are illustrated by pink squares), while the solid line is the correlation for all the data.

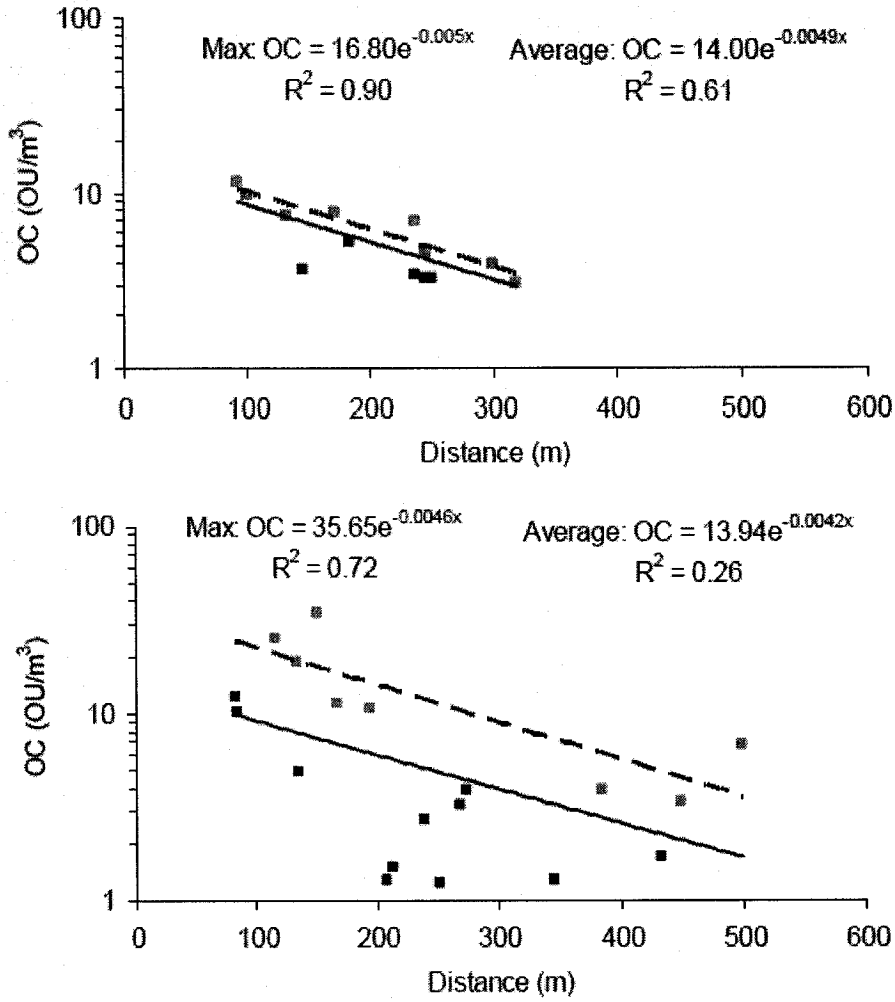

Fig. 4.10. Effect of wind direction on odour dispersion: (a) 90° (test 15); (b) 40° (test 17). The odour generator is located 15 m away from the windbreak. The dotted line is the correlation for the maximum data (the peak values are illustrated by pink squares), while the solid line is the correlation for all the data.

Connecting statement

In chapter 4, the odour dispersion data measured around natural windbreaks was normalised and mainly analysed with the regression and case comparison to demonstrate the effects of windbreaks on odour dispersion. In chapter 5, the measured odour plumes were evaluated in terms of length of odour plume (LOP) and width of odour plume (WOP) without any standardisation. The statistical classification and covariance models were used to analyse effects of windbreak on LOP and WOP.

This chapter firstly correlated odour hedonic tone and odour concentration evaluated by the panellists. Secondly, LOPs and WOPs from the 39 field measurements were plotted and measured. Finally, the effects on odour dispersion, of the windbreak, porosity, odour emission rate, odour source position, air temperature, wind speed and direction were statistically analysed.

This paper was published in Water, Air and Soil Pollution, 2007 (in press). Authors are Lin, X.J., Barrington, S., Nicell, J., Choiniere, D. and King, S. The contributions of the authors are i) First author carried out a part of field measurements, the whole data analysis and wrote the manuscript; ii) Second author supervised and helped revise the method of analysis and the content of the paper; iii) Third author advised the method of analysis; iv) Fourth author organized and managed the collection of the field data; and v) Last author reviewed the paper.

Chapter 5
Livestock odour dispersion as affected by natural windbreaks

5.1. Abstract

Natural windbreaks have been planted around livestock shelters to improve odour dispersion without substantial knowledge of their best implementation practices. Using three groups of four trained panellists and an odour generator, the objective of the present research was to measure and compare the length of odour plumes (LOP) produced in the field in the absence of, and in the presence of four natural windbreaks exposed to various climatic conditions. During 39 mornings in August, September and December 2003, panellists observed the resulting odour plumes using hedonic tone (HT) as scale and in the afternoon, evaluated the odour concentration (OC) of the odorous air sampled at the generator. By correlating HT with to their corresponding OC, filed HT values were converted into OC units, and 2 OU m^{-3} contours were used to establish LOP. A multiple factor analysis verified the effect significance on LOP of the presence of a windbreak, of windbreak properties and of climatic conditions. While being diluted, OC decreased exponentially with HT as observed by panellists ($P<0.05$). Secondly, the windbreaks significantly reduced LOP by 22% as compared to the site without a windbreak. Thirdly, the denser windbreaks had a greater impact on reducing LOP. The LOP of windbreaks with an optical porosity of 0.55 was not significantly different compared to that created in the absence of a windbreak. The wind speed, direction and ambient temperature had a strong influence on LOP while atmospheric stability, windbreak position downwind from the odour source within 60 m and odour emission rate had little impact, based on the analysis of 36 field tests in the presence of a windbreak.

Keywords: windbreak, porosity, odour dispersion, hedonic tone, climatic conditions.

5.2. Introduction

In rural areas, odour emissions from livestock operations constitute a major social issue (Agriculture and Agro-Food Canada, 1998). In the Province of Quebec, Canada, a three year moratorium was imposed on the swine industry to examine possible solutions to environmental problems caused by manure management, such as odour emissions and water contamination. In the US, agricultural odours constitute an annoyance of increasing importance especially because of the size of farms and the concentration of livestock wastes (Lammers *et al.*, 2001). In the US and the Province of Ontario, Canada, an important number of large livestock operations, and particularly owners of poultry barns, feedlots and piggeries, have faced a law suite as a result of odour nuisances (Tyndall and Collettii, 2000; Brant and Elliott, 2002; Leuty, 2003).

In Asia, solid walls have been used around livestock barns to precipitate dust released by the ventilation system (Bottcher *et al.*, 2000). Dust has been shown to carry odours (Das *et al.*, 2004). Such application requires a windbreak with a high porosity capable of reducing wind velocity and turbulence. The same principle has been applied to control snow and sand accumulation, reduce pesticide drift, increase crop yield and reduce heat losses from animals and buildings (Plate, 1971; Heisler and Dewalle, 1988; Wang and Takle, 1997; Ucar and Hall, 2001; Guan *et al.*, 2003; Vigiak *et al.*, 2003; Wilson and Yee, 2003).

Based on the successful precipitation of dust in Asia, North American livestock producers have used natural and artificial windbreaks on the fan side of livestock shelters to reduce odour emissions. The effect of a windbreak wall was studied by means of smoke emitters and simulated using a Gaussian model (Bottcher *et al.*, 2000; Bottcher *et al.*, 2001). The windbreak wall was found to vertically divert the odours from the exhaust fans and promote mixing with the wind flowing over the building, but not to be as effective as tall stacks.

Nevertheless and as opposed to precipitating dust, limited research has pertained to the use of natural windbreaks to disperse odorous gases. Although all over North America, an important number of operations are planting natural windbreaks around livestock buildings, little is know about their best implementation practices. First and foremost, field measurements are needed to observe the odour dispersion effect of natural windbreaks and acquire some data to simulate their performance and recommend best implementation practices.

Using five different field sites and three groups of four trained panellists, the first objective of this project was to observe the effect of the presence of a windbreak on the size of the resulting dispersion plume initiated by a point odour source produced by an odour generator. The second objective was to statistically identify the windbreak factors and climatic conditions which significantly affect the length of the resulting odour plumes.

5.3. Materials and methods

5.3.1. SITES AND WINDBREAKS

This experiment was conducted using four uniform single row natural windbreaks located at least 5 km away from any livestock operation to eliminate interferences (Table 5.1). The porosity of each windbreak was optically evaluated by measuring the percentage of open surface visible through the windbreak (Heisler and Dewalle, 1988; Guan *et al.*, 2003).

Each natural windbreak was different in terms of porosity, tree type and height (Lin *et al.*, 2006). The optical porosity of the windbreaks on sites 1 and 3 was 0.55 as compared to 0.35 for those on sites 2 and 4 (Table 5.1). The windbreaks on sites 1 and 2 were of deciduous trees as compared to conifers for those on sites 3 and 4. All sites were located on farm land with a relatively flat and consistent slope of 0.1 % and where the vegetation did not exceed a height of 0.7 m. The windbreaks on sites 1 and 4 had a height exceeding 15 m while that on sites 2 and 3 was less than 10 m. A control site (site 5) without a windbreak was selected to also observe odour dispersion. This site consisted of relatively flat (0.1

% uniform slope) land without trees or fences, where a cereal crop had been freshly harvested.

5.3.2. FIELD INSTRUMENTATION

To produce a controllable level of odour emission during the experiment, a mobile odour generator was used as described by Lin *et al.* (2006). The odour generator consisted of a 500 L tank filled with swine manure. A pump provided a consistent flow of manure over a vertical porous filter through which air was blown at a rate of 1.65 $m^3 s^{-1}$. The odour generator offered 76.8 m^2 of air/liquid contact surface. The odorous air released was sampled at regular 30 minute intervals during each test, using Alinfan® bags.

Odour concentration (OC) was expressed as "odour units per cubic meter" (OU m^{-3}) (CEN, 2001; Schauberger *et al.*, 2002; Zhang *et al.*, 2002). The rate of odour production, OU s^{-1}, was computed using the air flow rate of the odour generator.

During each field test, a 7.6 m high weather station tower was installed 200 m upwind from the windbreak, to avoid disturbance. At one minute intervals, a computer recorded the temperature, wind direction and wind speed. The wind direction was measured before hand to estimate the range of the field odour plume and to direct panellists into the odour plume zone.

Atmospheric stability values were obtained from the weather station at the Pierre Elliott Trudeau Airport (Montreal, Canada) located 50 km north of the field sites. This weather station was the nearest measuring Pasquill-Gifford atmospheric stability conditions.

5.3.3. THE PANELLISTS AND THE OLFACTOMETER

For the field tests and laboratory olfactory work, three groups of four panellists were trained by requiring them to detect n-butanol at concentrations of 20 to 80 ppb and to show consistency in their individual measurements according to European Odour Standards (CEN 2001, Choinière and Barrington, 1998;

Edeogn *et al.*, 2001). For the n-butanol calibration, a clean air sample with 32 905 ppb of n-butanol at 293 K was prepared as follows: 5 μL of n-butanol was injected into an Alinfan® bag previously filled with 40 L of air cleaned using an active carbon filter. Panellists were required to detect the n-butanol sample within a dilution factor of 411 to 1645 (80 to 20 ppb).

For the panellist field observations, hedonic tone (HT) was selected as odour sensation attribute because it directly indicates the degree of pleasant or unpleasant odour perception. The HT scale used in this project ranged from -10 to 0, where 0 to -2 was tolerable, -2 to -4 was unpleasant, -4 to -6 was very unpleasant, -6 to -8 was terrible and -8 to -10 was intolerable (Nimmermark 2006; Parker et al. 2005; Lim et al. 2001).

The panellists used in this field experiment where characterized by asking them to evaluate the HT of various concentrations of n-butanol (Table 5.2). This evaluation was conducted in the laboratory, using the olfactometer and an n-butanol air sample (32 905 ppb of n-butanol at 293 K) presented at various dilution levels. Each level of n-butanol was randomly presented three times.

The McGill University triangular forced-choice dynamic olfactometer used in this experiment was fully automated and capable of analyzing 4 contaminated air samples in 20 minutes, using 12 panellists (Choinière and Barrington, 1998).

5.3.4. TEST PROCEDURE

Before each field test, the odour generator and weather station tower were checked and installed upwind from the windbreak. Three groups of four panellists detected HT over part of a 25 ha area (500m × 500m downwind from the windbreak or odour generator) and given a GPS to keep track of their exact field position. After operating the odour generator for 15 minutes, the three groups of panellists would start walking downwind from the windbreak, covering an overlapping path predetermined from the wind direction, and with specific observation stations (Fig. 5.1). At each observation station, the group would stop walking, remove their carbon filter air masks and evaluate for one minute, the HT

of the ambient air using the scale of -10 to 0. An odour point was defined as a point in the field where at least 50 % (2 out of 4) of the panellists detected an odour. The HT of the ambient air at an odour point was averaged from the four panellist evaluations.

At 30-min intervals and while the panellists were observing each odour plume, a vacuum lung box was used to fill Alinfan® bags with 40L of odorous air obtained from the outlet of the odour generator, within a 3-min period. During each test day, the air velocity and therefore flow, was also verified at 8 points over the surface of the generator outlet using an Alnor anemometer (Alnor 8570, TSI Inc., Shoreview, Minnesota, USA).

After observing two field odour plumes during the morning of each test day, the 12 panellists went to the olfactometry laboratory in the afternoon to assess the odour concentration (OC) of each generator air sample, according to the ASTM E679-91 Standard (1997) and the CEN prEN13725 Standards (2001). The threshold dilution value of each odour sample was established by the 12 panellists exposed to a decreasing number of dilutions. The odour concentration of each air sample was calculated using the principle of geometric mean (ASTM, 1997; CEN, 2001).

For each day of field testing, HT evaluations were translated into OC (OU m^{-3}) by asking the panellists in the laboratory, to evaluate the HT of various dilutions of the odorous air samples collected at the generator. The observations of four panellists within a group were averaged and used to convert their field HT observations into OC values, as described by section on statistical analysis.

During 18 days between the end of August and the beginning of December 2003, 39 different tests were conducted on the four windbreak sites and the single control site (Table 5.3). A test consisted in having the panellists measure HT at various stations, thus locating the odour plume while the odour generator was located at a specific distance upwind from the natural windbreak. On the control site, six repeated tests were conducted on 4 different days. A total of 12, 11, 1 and 9 tests were conducted with the odour generator located 15, 30, 49 and 60 m

upwind from the windbreak, respectively. Tests on site 4 were conducted in December 2003, because of delays in finding a suitable windbreak site.

5.3.5. STATISTICAL ANALYSIS

In the laboratory, the panellists' perception of HT and OC evaluations were correlated using a forced choice dynamic olfactometer. During the 39 tests conducted over 18 days, the odorous air released by the odour generator was sampled 72 times (4 samples per day). Fig. 5.2 (a) shows a typical OC curve produced over time by the odour generator during tests 3 and 4 which started at 8:30am. During that emission period, the panellists evaluated the first odour plume from 8:42 to 9:26 am and the second one from 9:32 to 10:30am while odorous air was sampled at the generator at 8:50, 9:20, 9:50 and 10:20 am. During that same afternoon but in the laboratory, each one of the 12 panellists evaluated the 4 odorous air samples for threshold concentration (OC) and then, at various dilutions to correlated HT and OC. Hence, each group of 4 panellists observed on the average, 95 sets of HT and corresponding OC. Based on this data set, a regression equation was produced to correlate OC with HT using SAS (SAS Institute Inc., 2001).

Before statistically analyzing the effect of various factors associated with windbreak odour dispersion, the measured odour plumes were evaluated in terms of length (LOP) and width (WOP), based on OC contours of 2 OU m^{-3}, because most of the furthest odour points measured in the field had an OC of 2 OU m^{-3}. These odour contours were determined from OC trends and interpolations. Fig. 5.1 shows the 2 OU m^{-3} contour and odour plume definition for test 5 where 22 odour points were observed from 69 stations. During test 5, the wind directions varied by ±25° about the mean direction perpendicular to the windbreak. The odour plume rectangle enclosing the 2 OU m^{-3} contour measured 338 and 278 m in length and width, respectively, defining LOP and WOP, parallel and perpendicular to the average wind direction, respectively.

A statistical classification model was used to analyse effects on LOP of the sites with and without windbreak:

$$LOP_{ij} = \mu + site_i + e_{ij} \tag{5.1}$$

where LOP_{ij} is length of the odour dispersion plume measured during the *j*th test on the *i*th site; μ is the overall mean; $site_i$ is the effect for the *i*th site where $site_1$ was the site without a windbreak and $site_2$ was any of the four sites with a windbreak, and; e_{ij} is the random residuals for *i*th site and *j*th test.

The statistical classification model was used to analyse the effect on LOP of windbreak sites with different porosities, and as compared to the site without a windbreak:

$$LOP_{ij} = \mu + site_i + e_{ij} \tag{5.2}$$

where $site_i$ is site i = 1, 2, 3, corresponding respectively to a windbreak with an optical porosity of 0.35, 0.55 and 1.00 (no windbreak).

Finally, the covariance model (Cue, 2006; SAS Institute Inc., 2001) was selected to analyse the effect of various factors on windbreak LOP:

$$LOP = \mu + porosity + DWO + AS + b_1 u + b_2 \alpha + b_3 T + b_4 OER + e \tag{5.3}$$

where *LOP* is defined previously; μ is the overall mean; *porosity* is the optical porosity of the windbreak or 0.35 for sites 2 and 4 and 0.55 for sites 1 and 3; *DWO* is the distance between the windbreak and the odour generator of either 15, 30, 49 or 60 m; *AS* is the atmospheric stability class of either B, C or D; u is the wind speed; α is the angle between the wind direction and the windbreak (90° being perpendicular); T is the ambient air temperature; *OER* is the generator odour emission rate; b_1, b_2, b_3 and b_4 are effects for u, α, T and *OER*, and; e is the random residual. Tree height could not be compared, because of the variability in values between sites.

Because statistical model (5.3) demonstrated a lack of significant effect for DWO, AS and OER, these were dropped and consequently, statistical model (5.4) was formulated and tested:

$$LOP = \mu + porosity + b_1 u + b_2 \alpha + b_3 T + e \tag{5.4}$$

A factor was considered to have a significant effect when $P < 0.10$.

5.4. Results and Discussion

5.4.1. Relationship between hedonic tone and odour concentration

The emission of odours by the generator dropped slightly over time during the same test period and also varied from one test day to the next as a different manure source was used. Fig. 5.2 (a) shows a typical OC production curve over time for the odour generator during tests 3 and 4 which started at 8:30am. Fig. 5.2 (b) shows a typical relationship between HT and OC measured by one group of four panellists (tests 3 and 4) based on 129 observations, some of which were superposed. The OC was found to exponentially decrease with HT and the relationship was statistically significant ($P < 0.05$).

During 18 test days, the 72 odorous air samples collected at the generator offered a wide range of HT which produced the following regression with OC:

$$OC = ae^{bHT} \tag{5.5}$$

where OC is odour concentration, OU m^{-3}; HT is the hedonic tone of the odour using a scale -10 to 0, and; a and b are constants.

Since each test day was not necessarily conducted using the same 12 trained panellists, a regression similar to equation (5.5) was formulated for each one of the 54 different groups of 4 panellists. Out of 54, 51 groups respectively produced 54 statistically significant regression equations ($P < 0.05$) while one group associated with tests 22, 23, and 24 did not ($P > 0.10$). Fig. 5.3 shows the relationships between OC and HT for the 51 groups of 4 panellists. The means of constants a and b were 1.445 and -0.266, and their standard error was 0.481 and 0.09, respectively while their respective coefficient of variation (CV) were 0.338 and -0.333. The OC was enclosed by a minimum and maximum black curve which ranged from 1 to 4 OU m^{-3}, for an HT of -1, and from 4 to 222 OU m^{-3} for an HT of -10. Therefore, more variability in translating OC from HT was observed for more offensive odour levels.

The OC values which determined the size of the odour plumes were derived from the regression equations converting HT values observed in the field by the groups of panellists. Because of the lack of significant correlation between HT and OC, tests 22, 23 and 24 were excluded from the statistical analyses.

5.4.2. Effect of windbreak presence on odour plume length

All tests were considered to have a windbreak except for tests 37, 38 and 39 conducted on the site without a windbreak and those of 34, 35 and 36 with a windbreak but conducted under a wind direction parallel to the windbreak. The measured LOP and WOP are listed in the Table 5.4.

According to statistical model (1), the windbreak presence had a statistically significant effect ($P < 0.06$) on LOP. The means of LOP for the sites without and with a windbreak were 453 and 352 m respectively, resulting in a difference of 101 m. Therefore, the windbreaks did significantly reduce LOP by 22% on the average.

According to statistical model (2) testing the effect of porosity, the multiple comparisons and the results of the least square means (LSM) analysis showed that the three sites produced LOP measuring 333, 428, and 453 m (Fig. 5.4), for a porosity of 0.35, 0.55 and 1.0 (no windbreak). There was a significant difference in LOP of 120 m between the windbreaks with an optical porosity of 0.35 and that without a windbreak ($P < 0.08$). However, there was no statistical difference in LOP between the windbreak sites with and optical porosity of 0.55 and 1.0, and between the windbreak sits with an optical porosity of 0.35 and 0.55.

Thus, the two dense windbreaks with an optical porosity of 0.35 reduced the LOP on the average by 26.5%, and as compared to the site without a windbreak. Nevertheless, this analysis does not consider the effect many other factors which varied simultaneously during the field tests.

5.4.3. Effect of various windbreak parameters

Several windbreak factors can influence LOP, such as distance between the odour generator and the windbreak (DWO), windbreak optical porosity, atmospheric

stability (AS), wind speed and angle with respect to the windbreak, generator odour emission rate (OER) and temperature (T).

Statistical model (5.3) applied to all tests (1 to 33 except for 22, 23 and 24) using SAS (SAS Institute Inc., 2001) showed that the effects of DWO, AS and OER were not significant. Comparing DWO of 15, 30, 49 and 60 m, their respective LOP-LSMs were 397, 361, 300 and 382 m, respectively and multiple comparisons showed no significant difference among them ($P > 0.10$). This conclusion may not be realistic because a limited number of defined odour plumes were available to conduct the comparison. As for AS of B, C and D (Pasquill stablility category), their respective LOP-LSMs were 340, 348, and 392 m, but the difference was not significant ($P > 0.10$). This conclusion is likely reached because atmospheric stability is a systematic factor, defining specific conditions of wind speed, temperature and turbulent kinetic energy profiles. Finally, OER was not a significant factor affecting LOP ($P > 0.10$), likely because higher HT values lead to a greater uncertainty in OC translation.

The statistical model (5.4) indicated that porosity was significant ($P < 0.10$) along with wind speed and angle, and temperature ($P < 0.01$). Using the parameters estimated by the covariance model (5.4), regression equations (5.6) and (5.7) were produced for the two levels of porosity:

$$LOP = 406.4 + 36.3u - 3.3\alpha + 3.4T \qquad for \quad porosity = 0.35 \qquad (5.6)$$

$$LOP = 476.7 + 36.3u - 3.3\alpha + 3.4T \qquad for \quad porosity = 0.55 \qquad (5.7)$$

where wind speed ranged from 0 to 6.4 m s^{-1}, wind direction (α) from 20 to 90°, and temperature (T) from -9 to 28°C.

Wind speed was found to directly affect LOP, according to equations (5.6) and (5.7), implying that greater wind speeds carry the odour further away from the windbreak. This conclusion was not expected as theoretically, higher wind speeds should induce stronger turbulence around the windbreak and increase the atmospheric mixing of odours to shorten the LOP. This effect requires further

analysis considering the effect of tree height and type, and associated atmospheric stability.

Considering the effect of wind angle with respect to windbreak, using equations (5.6) and (5.7), a negative slope was obtained indicating that LOP decreases with wind angle. Therefore, a smaller wind angle leads to the longer LOP. When the wind direction is almost parallel to the windbreak, no effect on odour dispersion should be expected and odours can travel without obstruction.

Temperature was also found to significantly affect LOP ($P < 0.03$) according to equations (5.6) and (5.7). The LOP was found to be proportional to temperature with the odours travelling over a longer distance with higher temperatures.

5.4.4. EFFECT OF VARIOUS FACTORS ON WIDTH OF ODOUR PLUME

The average WOP for the site without a windbreak was 290 m, or 80 m wider than that of the windbreak sites. Nevertheless, these widths were not statistically different. Also for all windbreak sites, factors such as windbreak porosity, DWO, AS, wind speed and direction, T and OER did not significantly influence WOP. In fact, odours were dispersed along the wind direction and hence the variation in wind direction during each test was more likely to determine the width of the odour dispersion plume. Thus, variations in wind direction may have masked any effect pertaining to WOP.

5.5. Conclusion

Based on the statistical analysis of the odorous air samples collected at the field generator and the size of the odour plumes observed on the sites with and without a windbreak, the following conclusions can be reached:

1. The odour concentration and hedonic tone of the odorous air samples, as perceived by 51 out of 54 groups of four trained panellists, were found to be exponentially related ($P < 0.05$);
2. The presence of a windbreak significantly reduced by 22% the length of the odour plume as observed on the five experimental sites. When only the

windbreaks with an optical porosity of 0.35 were compared to the site without a windbreak, the length of the odour plume was further and significantly reduced by 26.5% ($P < 0.08$). Nevertheless, there was no significant difference observed between the effect of the site without a windbreak and that with a windbreak offering an optical porosity of 0.55.

3. Factors such as odour source position downwind from the windbreak within 60 m, atmospheric stability for the unstable and neutral classes, and odour emission rate, have little impact on the length of the odour plume, and hence on odour dispersion. Wind speed, wind angle with respect to wind direction and temperature were found to have a significant influence on the length of the odour plume.

The statistical analysis conducted on the effect of windbreaks and their optical porosity, as compared to a site without a windbreak, was conducted with a satisfactory number of data points. Nevertheless, for the statistical analysis of the windbreak and climatic factors, the number of data points was rather limited and the conclusions reached require further verifications.

5.6. Acknowledgements

The authors wish to acknowledge the financial contribution of Consumaj inc., CDAQ, The Livestock Initiative Program, Agriculture and Agro-Food Canada and the Natural Sciences and Engineering Research Council of Canada.

5.7. References

Agriculture and Agro-Food Canada, 1998. Research strategy for hog manure management in Canada. Supply & Services Canada, No. A42-77/1998F, Ottawa, Canada.

ASTM, 1997. Standard Practice for Determination of Odor and Taste Thresholds By a Forced-Choice Ascending Concentration Series Method of Limits, American Society for the Testing of Materials, Washington, DC, USA.

Bottcher, R.W., Munilla, R.D., Baughman, G.R. and Keener, K.M., 2000. Designs for windbreak walls for mitigating dust and odor emissions from tunnel

ventilated swine buildings. pp. 174-181 in: Swine Housing, Proc. of the 1st International Conference, Oct. 9-11, 2000, Des Moines, Iowa. American Society of Agricultural Engineers, 2950 Niles road, St. Joseph, Mi. USA.

Bottcher, R.W., Munilla, R.D., Keener, K.M. and Gates, R.S., 2001. Dispersion of livestock building ventilation using windbreaks and ducts. 2001 ASAE Annual International Meeting.: Paper No. 01-4071. 2950 Niles road, St. Joseph, Mi. USA.

Brant, R.C. and Elliott, H.A., 2002. Pennsylvania odor management manual, Pennsylvania State University, University Park, PA. USA.

CEN, 2001. Air quality - determination of odor concentration by dynamic olfactometry. prEN13725, European Committee for Standardization, 36 rue de Stassart, B-1050 Brussels. <http://www.aerox.nl/images/eurstandard.pdf>, visited August, 2004.

Choinière, D. and Barrington, S., 1998. The conception of an automated dynamic olfactometer, CSAE/SCGR Paper No. 98-208. The Canadian society for engineering in agricultural, food and biological systems, Saskatoon, Canada.

Cue, R.I., 2006. Statistical methods AEMA-610. http://animsci.agrenv.mcgill.ca/servers/anbreed/statisticsII/stats2e.pdf (visited 200606).

Das, K.C., Kastner, J.R. and Hassan, S.M., 2004. Potential of particulate matter as a pathway for odor dispersion. ASAE paper number 04-4125. American Society of Agricultural Engineering, St Joseph, Michigan, USA.

Edeogn, I., Feddes, J.J.R., Qu, G., Coleman, R. and Leonard, J., 2001. Odour measurement and emissions from pig manure treatment/storage systems. Final report to Canada Pork Council. Project Number CPC-01. University of Alberta, Edmonton, AB. http://www.cpc-ccp.com/HEMS/CPC-01_Feddes.PDF (2007/01/17).

Guan, D., Zhang, Y. and Zhu, T., 2003. A wind-tunnel study of windbreak drag. Agri. Ecosystem & Environment, 118: 75-84.

Heisler, G.M. and Dewalle, D.R., 1988. Effects of windbreak structure on wind flow. Agriculture, Ecosystems and Environment, 22-23: 41-69.

Lammers, P., S., Wallenfang, O. and Boeker, P., 2001. Computer modelling for assessing means to reduce odour emissions. Paper number 01-4042. American Society of Agricultural Engineering, St Joseph, Michigan, USA.

Leuty, T., 2003. Using shelterbelt to reduce odors associated with livestock production barns. Ministry of Agriculture and Food, Ontario, http://www.gov.on.ca/OMAFRA/english/crops/facts/info_odours.htm, visited in 2004.

Lim, T.T., Heber, A.J., Ni, J.Q., Sutton, A.L. and Kelly, D.T., 2001. Characteristics and Emission Rates of Odor from Commercial Swine Nurseries. Trnsaction of the ASAE, 44(5)(0001-2351): 1275-1282.

Lin, X.J., Barrington, S., Nicell, J., Choiniere, D. and Vezina, A., 2006. Influence of windbreaks on livestock odour dispersion plume in the field. Agriculture, Ecosystems & Environment, 116(3-4): 263-272.

Nimmermark, S., 2006. Characterization of odor from livestock and poultry operation by the hedonic tone. Paper number 064157. In: ASABE (Editor), 2006 American Society of Agricultural and Biological Engineering Annual International Meeting, Oregon Convention Center, Portland, Oregon, 9 - 12 July 2006.

Parker, D.B., Rhoades, M.B., Schuster, G.L., Koziel, I.A. and Perschbacher-Buser, Z.L., 2005. Odor characterization at open-lot beef cattle feedyards using triangular forced-choice olfactometry. Transactions of the ASAE, 48(4): 1527-1535.

Plate, E.J., 1971. The aerodynamics of shelter belts. Agric. Meteorol, 8, 203.

SAS Institute Inc., 2001. SAS (r) Proprietary Software Release 8.2, Cary, NC, USA.

Schauberger, G., Piringer, M. and Petz, E., 2002. Calculating direction-dependent separation distance by a dispersion model to avoid livestock odor annoyance. Biosystems Engineering, 82(1): 25-37.

Tyndall, J. and Collettii, J., 2000. Air quality and shelterbelts: Odour mitigation and livestock production - A literature review. Final project report to USDA National Agroforestry Center, Lincoln, NB. Project Number 4124-4521-48-3209. Forestry Department, Iowa State University, Ames, IA. http://www.forestry.iastate.edu/res/Shelterbelts_and_Odor_Final_Report.pdf (2007/01/17).

Ucar, T. and Hall, F.R., 2001. Review windbreaks as a pesticide drift mitigation strategy: a review. Pest Management Science, 57: 663-675.

Vigiak, O., Sterk, G., Warren, A. and Hagen, L.J., 2003. Spatial modeling of wind speed around windbreaks. Catena, 52: 273-288.

Wang, H. and Takle, E.S., 1997. Momentum budget and shelter mechanism of boundary-layer flow near a shelterbelt. Boundary-Layer Meteorology, 82: 417-435.

Wilson, J.D. and Yee, E., 2003. Calculation of winds distribution by an array of fences. Agricultural and forest meteorology, 115: 31-50.

Zhang, Q. et al., 2002. Odor production, evaluation and control. http://www.manure.mb.ca/projects/completed/pdf/02-hers-03.pdf, visited August, 2004., Manitoba Livestock manure Management Initiative Inc.

Tables and Figures

Table 5.1 Experimental windbreak found on each site.

Description	Site			
	1	2	3	4
Tree type	poplar	mixed mature deciduous	conifers	conifers
Windbreak				
length (m)	2100	1050	405	380
height (m)	18.3	9.2	7.6	15.2
depth (m)		7		6
optical porosity (%)	55	35	55	35
porosity at the base (%)	70	30	70	40
Location	Sherrington	St Chrysostome	St Amable	St Charles

Note: all sites are located 50 km Southwest of the Island of Montreal, Canada.

Table 5.2 Panellist evaluation of hedonic tone versus n-butanol concentration.

Hedonic tone	Average n-butanol level (ppb)	Range of n-butanol level (ppb)
0	59	0-69
-1	80	69-93
-2	109	93-127
-3	149	127-174
-4	204	174-238
-5	278	238-325
-6	380	325-444
-7	519	444-607
-8	709	607-828
-9	968	828-1131
-10	1322	>1131

Table 5.3 Test conditions

Test	Site	Date (2003)	OG (m)	OE (OU s^{-1})	WS (m s^{-1})	Angle (°)	T (°C)	AS
1	1	Aug-29	15	621	6.4	90	19	B
2	1	Aug-29	30	760	6	90	20	D
3	1	Sep-02	30	859	2.5	50	17	C
4	1	Sep-02	60	551	2.5	50	20	C
5	2	Sep-03	30	1373	3	90	21	B
6	2	Sep-03	60	492	4.4	90	23	C
7	2	Sep-05	15	578	4.7	40	18	D
8	2	Sep-05	30	585	4.2	40	19	D
9	2	Sep-08	15	214	1	60	22	B
10	2	Sep-08	60	218	1.1	70	20	B
11	2	Sep-10	15	5360	1.2	30	22	C
12	2	Sep-10	30	1096	2.7	20	27	D
13	2	Sep-12	15	559	1.2	50	23	B
14	2	Sep-12	60	294	1	40	26	B
15	2	Sep-15	15	744	5.1	90	28	D
16	2	Sep-15	30	745	1.5	90	23	D
17	2	Sep-18	15	1879	1.5	40	24	C
18	2	Sep-18	60	13052	1.4	50	21	B
19	2	Sep-18	60	846	2.2	60	26	B
20	3	Sep-29	15	318	1.8	80	13	C
21	3	Sep-29	49	368	1.7	70	14	B
22	4	Dec-03	15	1339	4.1	60	-2	D
23	4	Dec-03	30	690	3.5	60	-4	D
24	4	Dec-03	60	208	2.6	50	-4	D
25	4	Dec-10	15	166	1.3	70	-2	D
26	4	Dec-10	15	148	1.9	70	-2	D
27	4	Dec-10	30	101	1.7	60	-2	D
28	4	Dec-13	30	111	0	60	-8	D
29	4	Dec-13	60	175	2.1	50	-6	D
30	4	Dec-13	60	79	1.4	50	-9	D
31	4	Dec-14	15	205	3.1	70	-8	D
32	4	Dec-14	30	394	3.3	60	-8	D
33	4	Dec-14	30	350	3	80	-8	D
34	2	Sep-09	197	166	1.2	0	18	C
35	4	Dec-09	191	102	0.3	57	-2	B
36	4	Dec-09	318	99	0.4	0	-3	C
37	5	Aug-21	NW	766	4.1	NW	28	C
38	5	Aug-21	NW	480	3.6	NW	26	C
39	5	Aug-22	NW	310	6.1	NW	26	D

Note: NW- no windbreak; OG – odour generator distance upwind from the windbreak; OE – average odour emission during a test; WS- average wind speed; Angle – angle between the windbreak and the wind, 90° being perpendicular; T – average temperature measured during the test; AS – Pasquill-Gifford atmospheric stability condition, where B and C are unstable classes and D is a neutral class.

Table 5.4 Length and width of the odour plumes for a contour of 2 OU m^{-3}.

Test No.	Odour plume		Test No.	Odour plume	
	Length (m)	Width (m)		Length (m)	Width (m)
1	545	369	21	285	141
2	538	406	22	502	233
3	386	222	23	408	173
4	429	219	24	468	172
5	338	278	25	208	337
6	233	167	26	227	234
7	529	236	27	255	342
8	420	194	28	141	69
9	159	83	29	481	158
10	329	119	30	218	65
11	504	201	31	255	257
12	525	347	32	254	197
13	312	336	33	220	170
14	390	143	34	395	193
15	370	167	35	400	191
16	328	146	36	523	177
17	566	236	37	424	479
18	344	248	38	429	427
19	392	298	39	548	275
20	385	202			

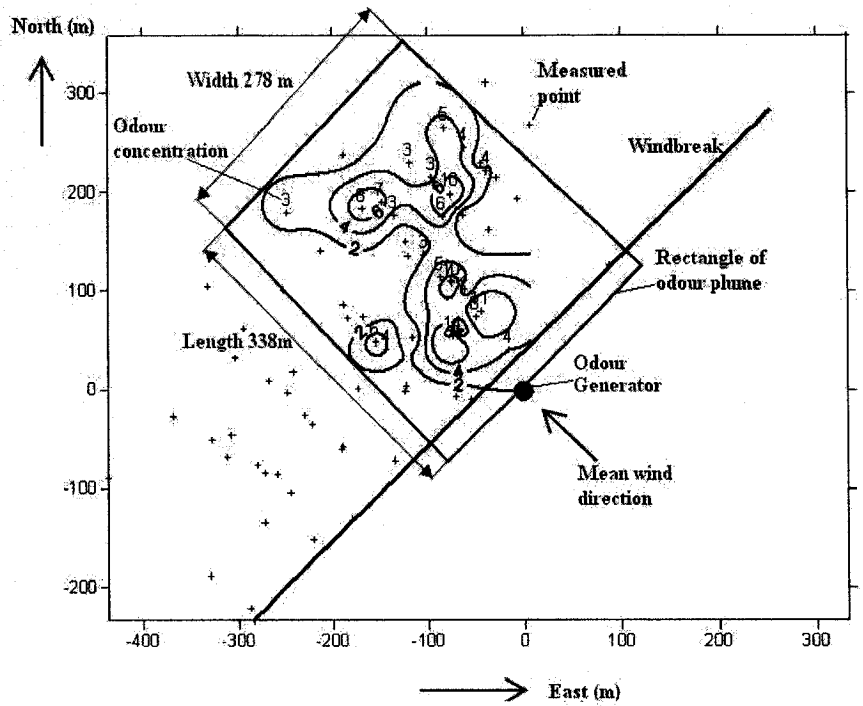

Fig. 5.1. Odour plume definition for test 5. The 69 measured points produced 22 odour points forming a rectangle enclosing the 2 OU m^{-3} contour. Wind direction changed by ± 25° around the mean direction. The length and width of the odour plume (LOP and WOP), measured parallel and perpendicular to the mean wind direction, were 338 and 278 m, respectively.

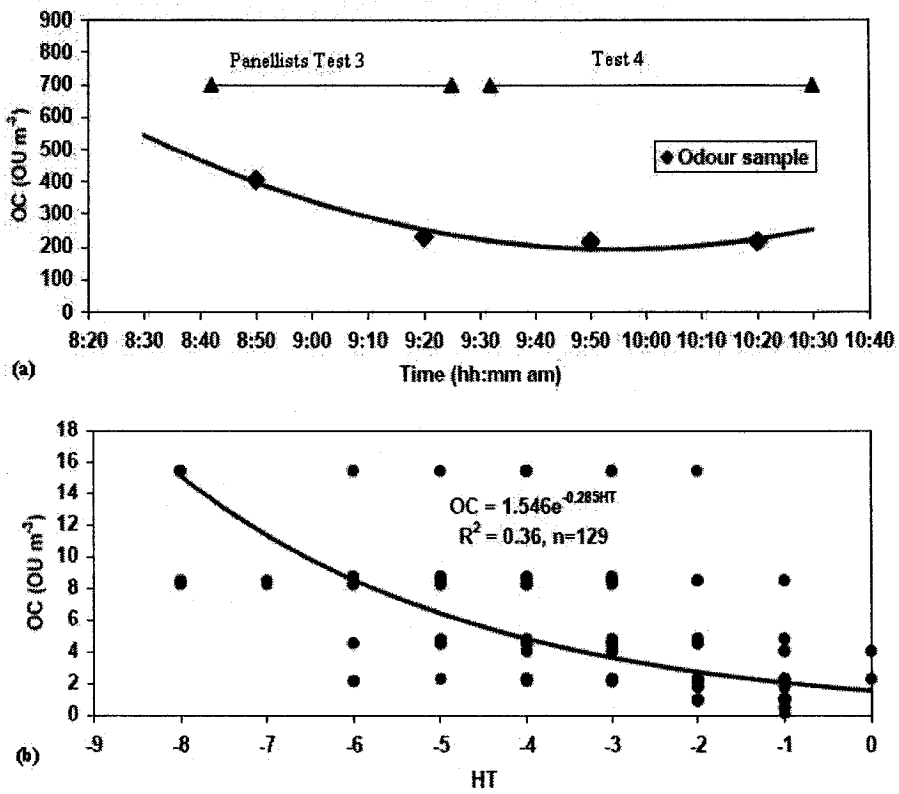

Fig. 5.2. (a) Typical odour concentration (OC) produced by the generator during a test day (tests 3 and 4) started at 8:30 am; the panellists started to evaluate the odour plume at 8:42 am and finished evaluating the second plume at 10:30 am, while odour samples were taken at the generator at 8:50, 9:20, 9:50 and 10:20 am, and the odour generator flow rate was 1.65 m^3 s^{-1}; (b) Typical relationship between the odour hedonic tone (HT) and OC for a group of four panellists (tests 3 and 4).

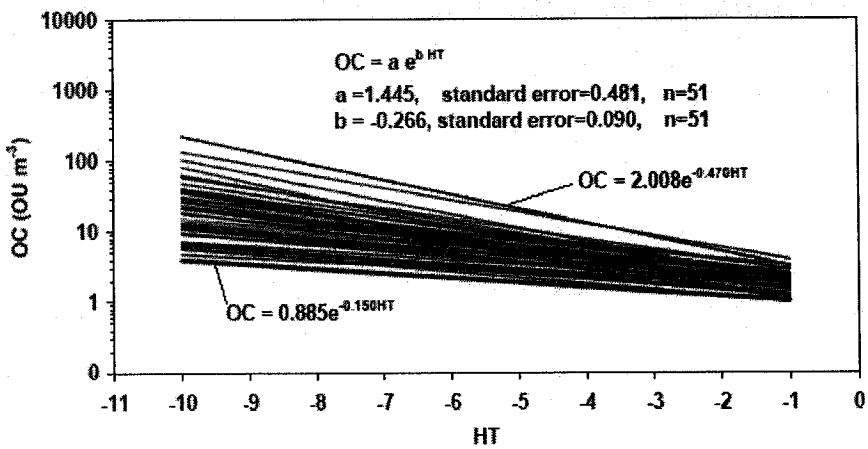

Fig. 5.3. Relationship between odour concentration (OC) and hedonic tone (HT) for the 51 groups of 4 trained panellists evaluating odorous air samples collected during 17 test days.

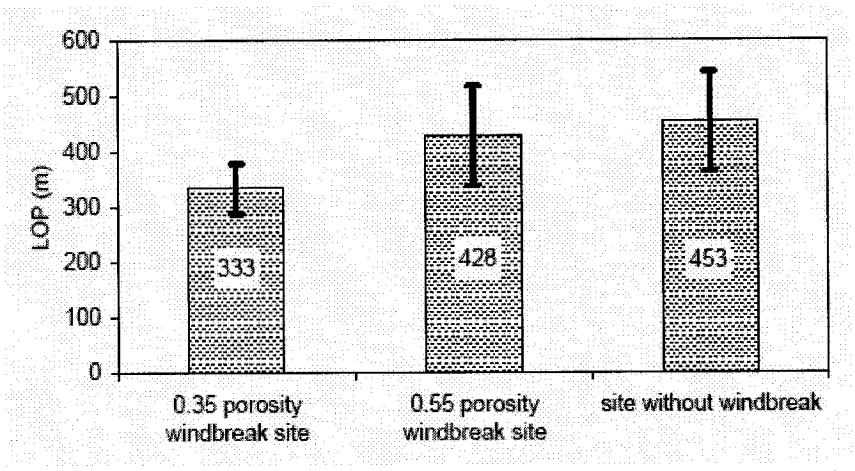

Fig. 5.4. The prediction of the mean length of the odour plume (LOP) for the sites with and without a windbreak; the error bars illustrates the standard error of ± 1.96 meter.

Connecting statement

Chapter 3, 4 and 5 demonstrated the effects of the natural windbreaks on the odour dispersion using the data measured in the field. Chapter 6 produces an odour dispersion model calibrated using the field data presented in the previous three chapters. The model modified for this purpose was the Fluent standard k-ε model.

Chapter 6 used the theory of the computational fluid dynamics to simulate odour dispersion around natural windbreaks. Using a 2-dimensional system, the standard k-ε model was calibrated for wind velocity recovery rate, and using a 3-dimensional system as well as the data from 11 field tests, the model was calibrated for odour dispersion. The model was found to require a power function to transform the simulated odour mass concentration into odour hedonic tone. Then the hedonic tone was transformed into odour concentration with an exponential function. The correlations between the simulated and field measured hedonic tone and between the simulated and measured odour concentration were statistically significant ($P < 0.01$). The model was then used to simulate the odour dispersion around natural windbreaks and demonstrate the mechanism of a windbreak on odour dispersion.

This paper was submitted to Transactions of the ASAE for publication. Authors are Lin, X. J., Barrington, S., Gong, G. and Choinière, D.. The contributions of the authors are i) First author carried out a part of field measurements, CFD simulation and wrote the manuscript; ii) Second author supervised and helped revise the method of analysis and the content of the paper; iii) Third author advised the method of CFD computation; and iv) Last author organized and managed the collection of the field data.

Chapter 6
Simulation of odour dispersion downwind from natural windbreaks using the CFD standard k-ε model

6.1. ABSTRACT

By enhancing air turbulence, windbreaks have been said to help disperse odour emissions from livestock operations, which are presently a major environmental and social issue. However, the effect of windbreaks on odour dispersion has not been extensively researched. To properly evaluate the odour dispersion effect of windbreaks, this paper introduces a model based on air flow theory. After calibrating and testing this model with field data, the present project simulated odour dispersion around windbreaks. Odour dispersion was modelled by mass, momentum, energy and species conservation equations, solved using the standard k-ε model of the Fluent software requiring as input: climatic conditions, wind velocity (magnitude, direction and profile), turbulence intensity, temperature profile, windbreak structure and odour emission rate. The model was calibrated for three main factors: wind velocity recovery; odour mass dispersion to reproduce field measured odour hedonic tone (HT) and odour concentration (OC) values, where HT was the criteria used in the field to observe the odour plumes; and the inertial resistance parameter of the windbreaks as a function of porosity. Once calibrated, the model was found to properly and accurately reproduce the odour plume developing downwind from the windbreaks expressed in both HT and OC. The correlation between HT and OC observed during 11 field trials and that simulated by the model were statistically significant ($P < 0.01$), indicating that the model was accurate. The model demonstrated that a windbreak did alter the magnitude and direction of the wind velocity, thus creating a pressure jump

across its width. This pressure jump produces a strong downwind turbulence which forms a mixing layer capable of enhancing odour dispersion.

Keywords: Windbreak, odour dispersion, hedonic tone, k-ε model, simulation, porosity.

6.2. INTRODUCTION

The venting of livestock facilities and the management of their manure produce odours leading to neighbourhood nuisance and interference with the right to enjoy one's property. Measures to properly dilute odours emitted from livestock operations consists mainly in distancing (separation distance) the livestock facility far enough away from the nearest neighbours for odours to disperse in the atmosphere below their threshold level (Tyndall and Collettii, 2000). Empirically determined, these separation distances are often not large enough to be effective, but are costly to the operator who must build facilities far away from public roads and neighbours.

Positioned in the vicinity of livestock facilities, windbreaks can potentially help dilute odours because of the turbulence created (Bottcher et al., 2001; Leuty, 2004; Tyndall and Collettii, 2000), and reduce separation distances. A natural windbreak is a barrier consisting of plantings of single or multiple rows of trees or shrubs, capable of reducing and redirecting wind. By measuring odour plumes in the field, the odour dispersion effect of natural windbreaks was demonstrated by Lin et al. (2006). Despite the 39 field odour plumes observed under various climatic conditions, and about four different windbreaks, the effect of specific parameters could not be properly evaluated because of the lack of control on all factors. Nevertheless, this field data can be used to calibrate models to simulate conditions where only one parameter is varied.

Gaussian-based models have been used in the past to simulate odour dispersion from livestock facilities. Examples of such models are AODM, Inpuff II and Aermod (Gorgy, 2003; Guo et al., 2001; Guo et al., 2005; Jacobson et al.,

2005; Schauberger et al., 2000; Sheridan et al., 2002; Zhu et al., 2000). Models based on computational fluid dynamic (CFD) perform better than Gaussian models, because they are better designed to account for conditions of high turbulence in the vicinity of the natural windbreaks.

The Reynolds Average Navier Stokes (RANS) and the Large-Eddy Simulation (LES) are CFD models which were successfully used to simulate windbreaks in 2 and 3 dimensional systems (Lien and Yee, 2005; Lien et al., 2005; Lien et al., 2004; Packwood, 2000; Patton et al., 1998; Schwartz et al., 1995; Wang and Takle, 1995; Wilson, 2004; Wilson, 1985; Wilson and Yee, 2003). Accurately simulating wind velocity profiles, the RANS model is not capable of properly modelling conditions of turbulence (Wilson, 1985), but of prediction accuracy is considered sufficient for some purposes (Gosman, 1999). The Fluent software offers CFD models which have successfully simulated heat exchange under natural convection (Dirkse et al., 2006), odour dispersion on sites without windbreaks (Riddle et al., 2004), ammonia distribution in barns (Sun et al., 2002) and the transport of spray droplets in the field (Ucar and Hall, 2001).

Compared to other contaminants, the monitoring of odours is challenging because it can only be measured through human perception. Not yet replaced by any instrument, the human nose is capable of detecting numerous odorous compounds produced by livestock manures (O'Neill and Phillips, 1992) at concentrations as low as 0.0005 mg m-3 (ASHRAE, 1997). In the field, the generally low odour levels can only be observed by panellists (Jacobson et al., 2005; Zhang et al., 2003) using either a hedonic tone (HT) scale or an n-butanol reference. Lin et al. (2006) used panellists to observe HT at specific locations in the field, downwind from an odour source intercepted by a windbreak. HT expresses the degree of pleasantness or unpleasantness of an odorous air sample; HT scales generally range from 10 to -10, where 10 is highly pleasant, 0 is neutral and -10 is highly unpleasant. As opposed to HT, odour concentration (OC) is defined as the number of dilutions required for an odour to no longer be detected by half of the trained panellists forming a group of at least six. Lin et al. (2006)

found that HT was highly correlated to OC and hence, field HT observations can be translated into OC values.

The objective of the present paper was therefore to adapt, calibrate and use the standard k-ε model to simulate odour HT and OC downwind from a windbreak, using the results of 11 field tests performed on three sites each with a different windbreak. The model parameters were initially adjusted to obtain the correct velocity recovery rate, windbreak porosity and correspondence between observed and simulated HT and OC values.

6.3. METHODOLOGY AND MATERIALS

6.3.1. DISPERSION EQUATIONS AND NUMERICAL SOLVER

For a cell of fixed volume through which odorous air is flowing, the governing equations expressing the average air flow are those of mass, momentum, energy and species conservation (Hinze, 1975; Saatdjian, 2000). Besides the first three equations, the odour species equations are:

$$\frac{\partial}{\partial t}(\rho Y_i)+\nabla\bullet(\rho u Y_i)=-\nabla\bullet J_i \tag{6.1}$$

where

$$J_i=-(\rho D_{i,m}+\frac{\mu_t}{Sc_t})\nabla Y_i-D_{T,i}\frac{\nabla T}{T} \tag{6.2}$$

where ρ is fluid density; t is time; u is the mean instantaneous velocity; J_i is the diffusion flux of the species i; Y_i is the mass fraction of the species i; $D_{i,m}$ is the diffusion coefficient of species i in the mixture; $D_{T,i}$ is the thermal diffusion coefficient; Sc_t is the turbulence Schmidt number generally equal to 0.7, and; μ_t is the turbulence viscosity (Bird et al., 2002; Saatdjian, 2000). Odour dispersion is dependent on the species gradient, the rate of temperature gradient, the turbulence viscosity and the diffusion coefficients.

The odour species dispersion equations were solved using the standard k-ε model of the Fluent 6.2 software (Fluent Inc., 2005) with a steady 3-dimension segregated solver. Within each cell, the solver converts the governing equations to algebraic equations for the discrete dependent variables, such as velocity, pressure, temperature, and odour mass fraction. Discretization is a technique yielding a discrete equation that conserves each quantity on the basis of a control-volume and for the integration of the governing equations. The computed result of any scalar variable, Φ, is stored in the cell center, and is interpolated from its center value by means of an upwind scheme. The upwind scheme derives the face value Φ_f from quantities in the cell upstream.

There are several upwind schemes, such as the first-order upwind, the second-order upwind, the power law and the QUICK scheme. For the first-order upwind scheme, Φ_f is set equal to the cell center value of the upstream cell. For the second-order upwind scheme, Φ_f is calculated using the center value of the two upstream cells. For hexahedral cells, the QUICK scheme calculates Φ_f using the value of two upwind cells and the downwind cell. Because of its higher accuracy, the second-order scheme was applied to compute pressure and the dispersion of the odorous gas, while the QUICK scheme was applied to compute momentum, turbulence kinetic energy, turbulence dissipation rate and energy (Fluent inc., 2005).

SIMPLE (Semi-Implicit Method for Pressure-Linked Equations) was used to introduce pressure into the continuity equation. The SIMPLE algorithm computes the pressure field and enforces mass conservation by relating velocity and pressure corrections (Fluent inc., 2005).

6.3.2. FIELD ODOUR OBSERVATIONS AND MODEL DISPERSION SYSTEM

Odour dispersion plumes around natural windbreaks were measured in August, September and December 2003, as described by Lin el al. (2006). Tables 1 and 2 describe the three windbreak sites and the conditions pertaining to the 11 field odour tests performed on these sites. These test results were used to calibrate the standard k-ε model. Before conducting the field tests, 24 panellists were selected

by requiring them to detect n-butanol at a threshold of 20 to 80 ppb (ASTM, 1990, 1997, 1998; CEN, 2001) and then trained to be consistent in their response when exposed to the same odour concentration. These panellists were characterized by having them rate the HT of an n-butanol sample presented at different concentrations, and comparing this performance to that of panellists used by other researchers (Fig. 6.1). Likely because of culture and social context, the panellists used for the present field tests were more sensitive than those used by Lim et al. (2001) and Nimmermark (2006), although they respected the n-butanol standard selection criteria mentioned above.

The field observations by panellists were conducted using a HT scale of 0 to -10, and then, in the laboratory, these HT readings were translated into OC values, by asking each group of panellists to rate the HT of odorous samples at a known OC.

Windbreak odour dispersion was simulated using a rectangular volume of space enclosing the odour generator and the windbreak. Since field tests offered different conditions, such as windbreak porosity, odour source location upwind from the windbreak and strength of the odour source, their simulation required the definition of an odour dispersion system (ODS). Table 6.3 defines seven ODSs grouping field tests offering similar conditions to provide more data points to compare the measured and simulated values.

For all ODSs, the left and right faces of the simulated space were designed as the wind inlet and outlet, respectively, while the front, back and top faces of the volume were boundaries with an open or undisturbed wind velocity. Blowing odorous air into this computational volume, the odour generator was presumed to measure 3 m x 0.376 m x 1.75 m in x, y, z directions. Odours were introduced into the computational volume through an odour inlet, a rectangle (the red zone in Fig. 6.2) measuring 0.376 m x 0.376 m. The centre of the odour inlet positioned at $x = y = 0$ and $z = 1.562$ m. Odour dispersion within the computational volume was assumed to start as soon as generated.

Each ODS was designed to reproduce specific site conditions. For example, ODS 1 covered a space with a length of 690 m (75 H where H is the height of the windbreak of 9.2 m) a width of 276 m (30 H) and a height of 73.6 m (8 H) (Fig. 6.2). The ODS 1 was divided into discrete control volumes or cells, using a computational grid, which had 177, 96, and 46 segments in the x, y and z coordinates, respectively. The cells, with a rectangular hexahedral shape, gradually increased in size away from the odour generator and towards the outward faces of the system. At the odour inlet, 64 rectangles were meshed to effectively transfer the odour mass fraction to other cells. Similar mesh schemes were used to model the other ODSs.

6.3.3. WINDBREAK SIMULATION

A windbreak is a porous medium resisting wind or air flow and therefore defined as a momentum sink. This resistance can be introduced in the momentum equation in terms of viscous and inertial resistance:

$$F_i = -\frac{\mu}{\alpha} u_i - \frac{1}{2} C_{ir} \rho u_{mag} u_i \tag{6.3}$$

where F_i is a resistance; μ is fluid viscosity; α is the aerodynamic dynamic porosity or permeability of the windbreak; α^{-1} is the viscous resistance coefficient; C_{ir} is the inertial resistance coefficient caused by the windbreak; u_{mag} is the magnitude of the average velocity, and; u_i (i=1, 2, 3, indicating x, y, and z direction) is the mean velocity u in ith direction.

In Equation 3, the term $\mu\, u_i / \alpha$ is Darcy's law for porous medium which calculates the resistance exerted by the windbreak due to fluid viscosity (Bird et al., 2002). The term $C_{ir} \rho u_{mag} u_i / 2$ computes the inertial loss of the fluid flowing through the windbreak, which varies over the height of the tree depending on its shape (Wang and Takle, 1995; Wilson, 2004; Wilson, 1985). Poplars offer dense foliage at their top compared to conifers which offer more foliage at their base. Accordingly, a valid simulation uses an inertial resistance coefficient which varies over tree height.

In Fig. 6.2, the simulated windbreak (green zone) was designed as a cubic volume measuring 7 m in width, 9.2 m in height and 276 m in length, and offering an optical porosity of 0.35. The windbreak was positioned at x =30 m (distance between the odour generator and the windbreak). The optical porosity was used to compute the aerodynamic porosity representing the exact amount of air flowing through the foliage of the windbreak. The aerodynamic porosity, or permeability, is defined as the ratio of wind speed perpendicular to the windbreak, immediately downwind and averaged over the full height of the windbreak, to that upwind from the windbreak (Guan et al., 2003; Wang and Takle, 1995):

$$\alpha = \frac{\int_{0@windbreak}^{H} u_1 dz}{\int_{0@inlet}^{H} u_1 dz} \tag{6.5}$$

The relationship between optical and aerodynamic porosity is defined according to the wind tunnel measurements of Guan et al. (2003):

$$\alpha = \beta^{0.4} \tag{6.6}$$

where α is the aerodynamic porosity and β is the optical porosity. Accordingly, an optical porosity of 0.35 results in an aerodynamic porosity of 0.66, implying that 66% and 34% of the air flow through and over the windbreak, respectively.

On site 1, the windbreak offered an averaged optical porosity of 0.35 but the optical porosity at its base was 0.30 while that over the rest of its profile was 0.40. Therefore, the inertial resistance C_{ir} was defined as proportional to the density (1.0 minus its porosity) of the windbreak:

$$C_{ir} = \begin{cases} w_1 - \dfrac{w_1 - w_2}{h_1} z & z \le h_1 \\ w_2 - \dfrac{w_2 - w_3}{H - h_1}(z - h_1) & h_1 < z \le H \end{cases} \tag{6.7}$$

where z is the coordinate value in the vertical direction; H is the height of the windbreak; h_1 is the height at which the porosity of the windbreak changes ($0 < h_1$

< H), and; w_1, w_2, and w_3 are three constants corresponding to the thickness of the real windbreak, set in the simulation to allow 66% of the air to pass through.

For the windbreak on site 2, the averaged optical porosity was 0.35: the optical porosity at the base was 0.40; that between heights of 3 to 14 m was 0.3, and; above 14 m, the porosity was gradually increased from 0.3 to 1.0. Therefore C_{ir} was:

$$C_{ir} = \begin{cases} w_1 - \dfrac{w_1 - w_2}{h_1} z & z \le h_1 \\ w_2 & h_1 < z \le h_2 \\ w_2 - \dfrac{w_2 - w_3}{H - h_2}(z - h_2) & h_2 < z \le H \end{cases} \tag{6.8}$$

where w_1, w_2, and w_3 were set at 0.27, 0.39 and 0.05, and; h_1, h_2 and H were set at 3, 14 and 15 m, respectively. Again, such conditions allowed 66% of the air to pass through the windbreak.

The windbreak on site 3 offered an average optical porosity of 0.55. Its porosity was assumed to be 0.7 at a height of 1.0 m, to linearly decrease to 0.47 at a height of 3 m, to remain constant between heights of 3 to 15 m, and; then, to increase to 1.0 at the tree top. These conditions produced an average air permeability of 0.79 and a C_{ir} calculated as:

$$C_{ir} = \begin{cases} w_1 & z \le h_1 \\ w_1 + \dfrac{w_2 - w_1}{h_2 - h_1}(z - h_1) & h_1 < z \le h_2 \\ w_2 & h_2 < z \le h_3 \\ w_2 - \dfrac{w_2}{H - h_3}(z - h_3) & h_3 < z \le H \end{cases} \tag{6.9}$$

where w_1 and w_2 were set at 0.1 and 0.205, and; h_1, h_2, h_3 and H were set at 1, 3, 15 and 18 m, respectively.

6.3.4. PROPERTIES OF THE ODOROUS GAS

Livestock manures emit more than 168 odorous gases, where six of the ten compounds with the lowest detection thresholds contained sulphur (O'Neill and Phillips, 1992). Therefore, hydrogen sulphide (H_2S) was selected as the odorous gas presumed to be mix into and flow along with odourless or clean air. Hence, the fluid used for the present simulation was defined as a mixture of clean air and H_2S. For both individual species, the following fluid properties were introduced in the model: density, specific heat capacity, thermal conductivity, viscosity, mass fraction and thermal diffusion coefficient. Because the Mach number was under 10%, the mixture was presumed to be an incompressible ideal gas where its density varied with temperature but not with pressure.

The mixture's specific heat capacity was calculated as a function of temperature (T) using the mixing-law (Fluent inc., 2005) for the respective mass fractions of both clean air and H_2S. For summer and winter conditions, two specific heat values were selected based on temperature ranges of 283 to 313 K and 258 to 273 K, respectively: for clean air, 1005.4 J kg^{-1} K^{-1} and 1004.7 J kg^{-1} K^{-1} (Ierardi, 2000), and; for H_2S, 1005.3 J kg^{-1} K^{-1} and 995.7 J kg^{-1} K^{-1}, respectively (Yaws, 2001).

The thermal conductivity of the air mixture was calculated based on the mass-weighted-mixing-law for the respective fractions of clean air and H_2S, respectively: 0.0260 and 0.0137 W $m^{-1}K^{-1}$ for temperatures ranging from 283 to 313 K and 0.0235 and 0.0114 W $m^{-1}K^{-1}$ for temperatures ranging from 258 to 273 K (Ierardi, 2000; Yaws, 2001).

The viscosity of the air mixture was presumed to vary with T and was calculated based on the mass-weighted-mixing-law for the respective mass fractions of clean air and H_2S (Sutherland law):

$$\mu = \frac{C_1 T^{\frac{3}{2}}}{T + C_2} \tag{6.10}$$

where μ is the air viscosity; T is temperature, and; C_1 and C_2 are 1.458×10^{-6} kg m^{-1}s^{-1} K$^{-1/2}$ and 110.1 K, respectively (Fluent inc., 2005). The viscosity of H_2S was calculated according to Yaws (2001):

$$\mu = -1.4839 \times 10^{-6} + 5.1 \times 10^{-8} T - 1.26 \times 10^{-11} T^2 \tag{6.11}$$

For the diffusion of H_2S into clean air, the mass diffusion coefficient $D_{2,1}$ was calculated using the FSG method (Lyman et al., 1990):

$$D_{2,1} = \frac{10^{-7} T^{1.75} \sqrt{\frac{1}{M_1} + \frac{1}{M_2}}}{P_a (V_1^{1/3} + V_2^{1/3})^2} \tag{6.12}$$

where $D_{2,1}$ is the mass diffusion coefficient of H_2S into clean air in m^2 s^{-1}; M_1 and M_2 are the molecular weight of clean air and H_2S, respectively; T is temperature in K; P_a is atmospheric pressure in atmospheres, and; V_1 and V_2 are molar volumes for the clean air and H_2S fractions, respectively. In the present case, M_1 = 28.966g mol^{-1}; V_1 = 20.1 cm^3 mol^{-1}; M_2 = 34.07994 g mol^{-1}; V_2 = 20.96 cm^3 mol^{-1}, and; P_a = 1 atm method (Lyman et al., 1990). For T ranging from 283 to 313 K, $D_{2,1}$ was:

$$D_{2,1} = -1.34970 \times 10^{-5} + 1.05772 \times 10^{-7} T \tag{6.13}$$

and for T ranging from 258 to 273 K:

$$D_{2,1} = -1.10340 \times 10^{-5} + 9.69997 \times 10^{-8} T \tag{6.14}$$

Equations 13 and 14 show that the diffusion coefficient of clean air and H_2S are equivalent ($D_{1,2} \sim D_{2,1}$). Finally, the thermal diffusion coefficient was calculated according to the kinetic-theory (Fluent inc., 2005).

6.3.5. MODEL BOUNDARY CONDITIONS

To simulate odour dispersion in the field downwind from a windbreak, the model requires the values of wind velocity, temperature and odour emission rate. Case 2 (Table 6.4) was used to calibrate the model for odour dispersion: the magnitude of wind velocity was defined by the power law where it increases with

height as follows (Fang and Wang, 1997; Lakes Environmental Software, 2002; Lee and Lim, 2001; Schnelle and Dey, 2000; Thé et al., 2002):

$$u_{mag} = u_1 \left(\frac{z}{z_1} \right)^p \tag{6.15}$$

where z is height; u_1 is the open wind velocity at height z_1 = 7.62 m, where wind speed was measured, and; p is the wind profile exponent based on weather stability. For rural areas, and a Pasquill-Gifford weather stability indexes of B, C, D, p = 0.07, 0.10, 0.15, respectively (Schnelle and Dey, 2000). The velocity on the left, front, back and top faces of the dispersion system was defined by Equation (6.15).

Wind velocity turbulence at the inlet, represented the turbulence of the surface layer of the atmosphere, and was expressed by the turbulence intensity and turbulence length scale. Turbulence intensity is the ratio of the root-mean-square of the fluctuation in wind velocity to the mean air flow velocity. Statistically, the turbulence intensity is the coefficient of variance (CV) of wind velocity, and is calculated using the wind velocity data collected in the field on each test.

The turbulence length scale is a physical quantity related to the size of the large eddies that contain the energy of the turbulent flow and is determined by the surface roughness length (Schnelle and Dey, 2000). For the present study conducted over farmland with an open appearance, the roughness length was taken as 0.13 m for the fall, according to (WASP, 2006) where the roughness height for a crop surface is 0.095, 0.15, 0.265 and 0.13 m for winter, spring, summer and fall, respectively.

In the CFD model, odour mass fraction and flow velocity were inputs characterizing the odour inlet produced by the odour generator. Odour mass fraction at the generator was calculated as:

$$Y_2 = \frac{OC_g \bullet m_{H_2S}}{\frac{P_a M_1}{RT} + OC_g \bullet m_{H_2S}} \tag{6.16}$$

where Y_2 is the odour mass fraction at the generator, dimensionless; P_a is the atmospheric pressure (101325 Pa at sea level); T is temperature in K; M_1 is the molecular weight of dry air or 0.028966 kg mol^{-1}; R is the universal gas constant or 8.31432 J mol^{-1} K^{-1} (Jacobson, 1999); OC_g is the odour concentration at the generator in OU m^{-3}; m_{H_2S} is the mass of hydrogen sulphide required to produce 1.0 OU m^{-3} in kg OU^{-1}.

The detection threshold (1.0 OU m^{-3}) of H_2S occurs at a concentration of 7 μg m^{-3} (ASHRAE, 1997). Hence $m_{H_2S} = 7.0\times10^{-9}$ kg OU^{-1}, where odour units represents the number of dilutions required to obtain a mass fraction equivalent to the odour threshold of H_2S. For case 2 (Table 6.4), the temperature and odour concentration were 294 K and 830 OU m^{-3}, respectively, representing a mass fraction for H_2S of 4.84 x 10^{-6} at odour generator.

The ambient air vertical temperature profile was defined as:

$$T = \begin{cases} T_0 - LR_1 z & 0 \le z \le z_1 \\ T_0 - LR_1 z_1 - LR_2 (z - z_1) & z_1 < z \le z_2 \\ T_0 - LR_1 z_1 - LR_2 z_2 - LR_3 (z - z_2) & z > z_2 \end{cases} \quad (6.17)$$

where z is a height in the domain; z_1 and z_2 are heights such that $0<z_1<z_2$; T is the air temperature at height z; T_0 is the ground temperature and LR_1, LR_2 and LR_3 are the Lapse rate, defined as the drop in temperature with height, measured from the ground to heights z_1, z_1 to z_2 and above z_2, respectively.

Since the field air temperature was measured at a height of 7.62 m, T_0 was calculated as:

$$T_0 = T_3 + LR_3(7.62 - z_2) + LR_2(z_2 - z_1) + LR_1 z_1 \quad (6.18)$$

where T_3 is the air temperature at height z = 7.62 m.

In the present paper, z_1 = 0.3 m and z_2 = 1.2 m, and LR_1 and LR_2 respected the values defined by Geiger (2003). For example, in case 2 (Table 6.4), the values assigned to LR_1 and LR_2 were 3.21 and 0.36 K m^{-1} (Geiger et al., 2003), respectively, as the test was conducted from 8:00 to 10:00am, in September, 2003.

The value LR_3 was based on the level of atmospheric stability. For the Pasquill-Gifford atmospheric stability coefficients of B, C, and D, the Lapse rate LR_3 was 0.0180, 0.0160 and 0.010 K m^{-1}, respectively (Beychok, 1994).

The outlet was designed as an outflow boundary condition. Outflow boundary conditions in the Fluent 6.2 software are used to model flow exits where the details of the flow velocity and pressure are not known prior to solving the flow problem and do not need definition (Fluent inc., 2005). The bottom face of the computational volume was assumed to be solid, to exert resistance and friction on the air flow, to be no-slip and of uniform roughness.

6.3.6. CALIBRATION FOR AERODYNAMIC PERFORMANCE

The standard k-ε model uses standard default parameters C_μ, $C_{1\varepsilon}$ and $C_{2\varepsilon}$ which require calibration to properly simulate wind velocity changes and odour dispersion around a windbreak. This paper calibrated the parameters for wind speed recovery rate, defined as the ratio of wind speed at a height of 0.5 H and at a windbreak downwind distance of 30 H, to that undisturbed at the same height, upwind from the windbreak. The parameters C_μ, $C_{1\varepsilon}$ and $C_{2\varepsilon}$ were calibrated using values measured in the field by Naegeli in 1953 (Eimern et al., 1964), about a windbreak of reed measuring 2.2 m in height and 0.44 m in width, and with an aerodynamic porosity ranging between 0.45 and 0.55.

The windbreak effect on wind recovery was simulated using a two-dimensional domain measuring 60 H in length by 12 H in height, where the x coordinates ranged from -10 H to 50 H, the y coordinates ranged from 0 to 12 H and the right side of the windbreak was at x = 0 m. Mesh sizes in both the x and y directions measured 0.1 H. The wind speed and its turbulence intensity were set to 4 m s^{-1} and 10%, and the ambient air and ground temperatures were set at 294 and 297 K, respectively. An aerodynamic porosity of 0.54 was used to define the windbreak (case 1 in Table 6.4). The viscous resistance, defined as the inverse of the aerodynamic porosity, was set at 1.85 and the inertial resistance was adjusted to allow 54% of the air mass to flow through the windbreak.

6.3.7. *CALIBRATION FOR ODOUR DISPERSION*

The standard k-ε model was calibrated to reproduce HT values measured in the field. Firstly, the odour (H_2S) mass fraction (OMF) computed by the standard k-ε model was transformed into the simulated odour (H_2S) mass concentrations (SOMC) as follows:

$$SOMC = \frac{OMF}{\frac{Y_2}{OC_g}} m_{H_2S} \times 10^9 \qquad (6.19)$$

where SOMC is simulated odour (H_2S) mass concentration in μg m^{-3}; OMF is odour (H_2S) mass fraction computed by the model, dimensionless; Y_2 and OC_g are the odour mass fraction and odour concentration at the odour generator defined by Equation (6.16), respectively, and; m_{H_2S} is the mass of H_2S required to produce 1.0 OU m^{-3} in kg OU^{-1} in (6.16).

The SOMC could not be converted directly into OC, using m_{H_2S}, because OC is exponentially related to HT (ASHRAE, 1997). To obtain such an exponential relationship, the measured absolute HT (MAHT) observations were correlated to SOMC values for each 11 field tests (Table 6.2) and tested for significance (F-tests confidence level of 99%). The resulting correlation defined simulated absolute HT (SAHT) as a function of SOMC.

The standard k-ε model was also calibrated to reproduce OC values which are easier to measure by olfactometry, as compared to HT. To convert the HT into OC, the 56 odour samples collected at the odour generator were used to establish relationship between the HT into OC. These odour samples were diluted to various levels and randomly presented to the 17 groups of 12 different panellists to produce 5527 pairs of HT and OC values (Fig. 6.1). One pair of data represents the HT detected by a panellist at one level of odour concentration. Found to be significant ($P < 0.01$), the following regression equations give an average OC

correlation with HT, and upper and lower lines corresponding to the 95 % confidence interval, respectively:

$$OC = 0.92e^{-0.45HT} \tag{6.20}$$

$$OC = 6.73e^{-0.45HT} \tag{6.21}$$

$$OC = 0.13e^{-0.45HT} \tag{6.22}$$

where OC is odour concentration in OU m^{-3}; HT is odour hedonic tone from -10 to -1, and; OC was defined as zero for HT = 0.

In the present paper, equation (6.20) was used to transform MAHT into measured OC (MOC) and SAHT into simulated OC (SOC) for each 11 tests, respectively. The accuracy of the model in reproducing MOC as a function of distance from the odour source was observed by plotting MOC and SOC against distance from the source. The model was expected to be accurate if the SOC line fell within the MOC values and the correlation between the MOC and SOC is significant.

6.4. RESULTS

6.4.1. CALIBRATING THE MODEL FOR WIND VELOCITY RECOVERY RATE

The standard k-ε model was calibrated to reproduce the proper wind recovery coefficient using a two-dimensional simulation and the inputs from case 1 (Table 6.4). The model parameter C_{μ}, and $C_{2\varepsilon}$ were adjusted from the default of 0.09 and 1.92, to 0.12 and 2.2, respectively. Also, the inertial resistance parameter of the windbreak was set at 10.3 m^{-1}. These adjustments allowed the model to properly reproduce the measured wind recovery rate.

The simulated and measured wind speeds around a windbreak at its height of 0.5 H show that (Fig. 6.3): between the distances 0 to -10 H, the computed velocity recovery rate corresponds to that measured; at a distance of 2 H, both curves reach their lowest values; from 2 H to 16 H, the simulated values are slightly greater than that measured, while from 16 H to 30 H, they are slightly lower, and; at 30 H, an 88% velocity recovery rate was computed and found to be

off by 4.8% of that measured. An R^2 value of 0.97 was obtained between the measured and simulated velocity values.

To respect a ratio of turbulence viscosity to molecular viscosity lower than 10^5 in the 3-D system built to solve case 2 (Table 6.4), while still aiming for a correct velocity recovery rate, only $C_{1\varepsilon}$ could be adjusted from the 1.44 to 1.4. This issue reflects the limitations of the standard k-ε model.

6.4.2. EVALUATING THE MODEL FOR ODOUR DISPERSION

The performance of the standard k-ε model in reproducing field HT observations was tested using the data from all 11 field tests. The computed relationship between SOMC and MAHT for field test 2 is illustrated in Fig. 6.4a, where SOMC is expressed in μg m^{-3} and plotted against MAHT using an absolute scale of 1 to 10. The regression equation in Fig. 6.4a obtained was found to be statistically significant ($P < 0.01$) and was used as transform function of SOMC into simulated absolute hedonic tone (SAHT) in form:

$$SAHT = aSOMC^b \tag{6.23}$$

where SAHT is the simulated absolute hedonic tone, and; $a = 0.975$ and $b = 0.366$ for field test 2.

For the 11 simulations, correlations between MAHT and SOMC were found to be statistically significant ($P < 0.01$) and the value of their parameters a and b in form (6.23) are listed in Table 6.5. The 11 curves expressing the transform functions are shown in Fig. 6.4b and are all found to be within close range of each other, indicating that the model is adequately reproducing odour dispersion. Curves 2 and 3 were measured on the same day but with the odour generator producing a different odour level and located at a different distance from the windbreak, and under a different atmospheric stability condition; therefore their SOMC versus SAHT curves are similar but offer a different slope. Curves 6 and 7 were also measured on the same day, and exhibit the same slope, but are separated by a small gap because they were measured under different environmental conditions: wind speeds of 5.1 and 1.5 m s^{-1} and temperatures 28 and 23 °C,

respectively. Curves 8 and 9 are almost superposed; their data was measured on the same day, under very similar weather conditions.

Slight differences in the functions illustrated in Fig. 6.4b also result from the variability in the human perception of HT and the fact that a different source of swine manure was used for each test day (Fig. 6.1). Panellists exposed to the same odour, produced a slightly different response or HT evaluation based on their past memory and cultural experience. Because odorous gases exert a synergetic effect, the use of a different source of swine manure for each test day may have produced a different HT versus OC function. Accordingly, a variation is expected among all 11 different curves which are contained by that of tests 8 and 9 (on the right) and that of test 10 (on the left), and intercepted by that of tests 4 and 11 measured under a high rate of odour production by the odour generator.

The correlations between MAHT and SAHT for the 11 tests, as a function of distance from the source, were found to be statistically significant ($P = 0.01$) in Table 6.5, implying that the standard k-ε model can accurately predicts odour HT downwind from windbreaks. As illustrated in Fig. 6.5 a, c, e, and g for tests 2, 5, 7, and 8, the simulated lines are found in the centre of the range of MAHT, which is a good indication that the model can reproduce the observations. Depending on the test, the R^2 value ranged between 0.49 and 0.90.

Fig. 6.1 and Equations (6.20, 6.21, 6.22) indicate that one HT value corresponds to a range of OC. For example, when HT = -2, OC varies from 0.3 to 16.6 OU m^{-3} with a geometric mean of 2.3 OU m^{-3}. This implies that an OC of 16.6 OU m^{-3} is translated into an HT of -2 by a less sensitive panellist whereas an average and very sensitive panellist needs an OC for 2.3 and 0.3 OU m^{-3} to observe the same HT of -2.

Using equation (6.20), the MAHT was transformed into MOC, and SAHT was transformed into SOC, respectively. The correlations between MOC and SOC for the 11 tests were found to be statistically significant ($P < 0.01$) in Table 6.5 and, depending on the tests, the R^2 value ranged between 0.49 and 0.96. As illustrated in Fig. 6.5 b, d, f, and h for tests 2, 5, 7, and 8, the simulated lines were also found

in the centre of the range of MOC, indicating that the standard k-ε model can produce OC plumes from HT observations. Translation of odorous gas mass dispersion by the model is likely more useful if converted in OC, rather than HT, because OC is measurable by olfactometry.

6.4.3. SIMULATED ODOUR PLUME

Fig. 6.6a illustrates the simulated odour dispersion plume for test 2 (Table 6.5) on the horizontal and vertical plane, respectively, using 4 contours of hedonic tone varying from 1 to 3. The red zone representing the highest odour level is concentrated near the windbreak where odorous air is trapped. In this case, an absolute hedonic tone (AHT) of 3 is reached at a distance of 182 m downwind from the odour generator or 145 m downwind from the windbreak. For the AHT of 2 and 1.5, the odour plume reaches a distance of 303 and 508 m downwind from the odour source, respectively.

Fig. 6.6b illustrates the odour dispersion plume in terms of odour units (OU) instead of AHT, for the purpose of demonstrating that the standard k-ε model can also model odour dispersion on such basis. In Fig. 6.1, panellists rated HT against OC, and this relationship was used to create Fig. 6.6b.

6.4.4. WINDBREAK EFFECT ON WIND VELOCITY AND TURBULENCE

Figs. 6.7 and 6.8 demonstrate that a windbreak enhances odour dispersion by changing wind velocity, air pressure and turbulence (Lin et al., 2006). The x and z components of the wind velocity is illustrated in Fig. 6.7. The velocity at the left edge of the simulation volume varies with height from 0 to 4.63 m s^{-1}. The velocity (x component) increases immediately upwind and decreases downwind from the windbreak. The contour density also decreases with height implying that the air flow closer to the ground has a greater velocity gradient than that of the upper levels. The zone between the contours of 2.3 and 4.5 m s^{-1}, called the mixing zone (Cleugh, 1998), shows a greater velocity gradient implying that momentum is transported upwards.

Fig. 6.7b illustrates the z-component of the wind velocity contours in the plane y = 0 m. A positive upward z-velocity component is observed at a height reaching 100 m (11 H) downwind from the windbreak. The upward component of the velocity reaches a maximum value of 0.7 m s^{-1} (red zone) between a height of 8 and 13 m (0.9 to 1.4 H), at the windbreak. Furthermore, wind velocity changes direction beyond a distance of 100 m (11 H) along the x axis, and the downward velocity reaches a minimum (-0.05 m s^{-1}) beyond a distance of 150 m (16 H).

The magnitude of the velocity is illustrated in Fig. 6.8a at a height of 0.5 H or 4.6 m and at y = 0 m. The velocity decreases near and even more so through the windbreak, to reach its lowest value at x = 14 m (1.5 H), and then to slowly recover 76 % and 87 % of its full value at distances of 276 m (30 H) and 515 m (56 H), respectively, downwind from the windbreak. Fig. 6.8a also demonstrates the static pressure jump which occurs across the windbreak at a height of 0.5 H. The windbreak builds a positive pressure on its immediate windward side and then sharply drops this pressure on its downwind position. The highest pressure difference across the windbreak was found to be 5.6 Pa.

The turbulence kinetic energy contours on the plane y = -20 m expresses the extent of wind turbulence (Fig. 6.8b). While the quiet zone is located immediately upwind from the windbreak, the strongest turbulence zone appears between 125 to 179 m (13.5 to 19.5 H) downwind from the windbreak. The mixing zone with the strongest turbulence energy created by the windbreak is located above the quiet zone. High turbulence kinetic energy means a greater degree of wind velocity fluctuation and a more intensive mixing of the clean air and odorous gases. The distance required to reach the dilution threshold for an odour source is mainly influenced by the level of turbulence kinetic energy.

6.5. CONCLUSION

An odour dispersion model for air flowing over and through a windbreak was formulated using computational fluid dynamics (CFD). The development of such model leads to the following conclusions:

1. The standard k-ε model was able to accurately reproduce the odour hedonic tone (HT) and odour concentration (OC) measured by the panellists in the field around three different windbreaks. The correlations between the simulated and measured absolute HT and between the simulated and measured OC were statistically significant ($P < 0.01$);

2. The odour mass concentration calculated by the standard k-ε model was successfully transformed into HT and odour concentration values. Although HT is subjected to the variable sensitivity of panellists, all curves simulated from 11 different tests fell within a close range of each other;

3. By simulating air flow dynamics, windbreaks were observed to alter the wind velocity magnitude and direction, and to create a pressure jump across their width, hence produce a strong turbulent field downwind from their position along with a mixing layer capable of enhancing odour dispersion.

6.6. ACKNOWLEDGEMENT

The authors wish to acknowledge the financial contribution of Consumaj inc., CDAQ, the Livestock Initiative Program, Agriculture and Agro-Food Canada and the Natural Sciences and Engineering Research Council of Canada.

6.7. REFERENCES

ASHRAE, 1997. ASHRAE fundamentals handbook. American Society of Heating, Refrigeration and Air Conditioning, Atlanta, Georgia, USA, 13.1-13.6 pp.

ASTM, 1990. Standard method for defining and calculating sensory thresholds from intermediate size. AWMA E 18.04.25. American Society for the Testing of Materials, Washington, DC, USA.

ASTM, 1997. Standard Practice for Determination of Odor and Taste Thresholds By a Forced-Choice Ascending Concentration Series Method of Limits, American Society for the Testing of Materials, Washington, DC, USA.

ASTM, 1998. Standard Practices for referencing supra-threshold odour intensity. American Society for the Testing of Materials, Washington, DC, USA.

Beychok, M.R., 1994. Fundamentals of stack gas dispersion. Beychok, Milton R., Irvine, California, USA, 193 pp.

Bird, R.B., Stewart, W.E. and Lightfoot, E.N., 2002. Transport phenomena. J. Wiley, New York, 895 pp.

Bottcher, R.W., Munilla, R.D., Keener, K.M. and Gates, R.S., 2001. Dispersion of livestock building ventilation using windbreaks and ducts. 2001 ASAE Annual International Meeting.: Paper No. 01-4071. 2950 Niles road, St. Joseph, Mi. USA.

CEN, 2001. Air quality - determination of odor concentration by dynamic olfactometry. prEN13725, European Committee for Standardization, 36 rue de Stassart, B-1050 Brussels. <http://www.aerox.nl/images/eurstandard.pdf>, visited August, 2004.

Cleugh, H.A., 1998. Effects of windbreaks on airflow, microclimates and crop yields. Agroforestry Systems, 41: 5-84.

Dirkse, M.H., van Loon, W.K.P., van der Walle, T., Speetjens, S.L. and Bot, G.P.A., 2006. A Computational Fluid Dynamics Model for Designing Heat Exchangers based on Natural Convection. Biosystems Engineering, 94(3): 443.

Fang, F.M. and Wang, D.Y., 1997. On the flow around a vertical porous fence. Journal of Wind Engineering and Industrial Aerodynamics, 67 & 68: 415-424.

Fluent inc., 2005. Fluent 6.2 user's guide, Fluent Inc., Centerra Resource Park, 10 Cavendish Court, Lebanon, NH 03766, USA.

Geiger, R., Aron, R.H. and Todhunter, P., 2003. The climate near the ground. Rowman & Littlefield, Lanham, Md., 584 pp.

Gorgy, T.G.A., 2003. Validation of an air dispersion model for odour impact assessment. M Eng, McGill Unversity, Montreal, Canada. Thesis, 69 [50] leaves pp.

Gosman, A.D., 1999. Developments in CFD for industrial and environmental applications in wind engineering. Journal of Wind Engineering and Industrial Aerodynamics, 81(1-3): 21-39.

Guan, D., Zhang, Y. and Zhu, T., 2003. A wind-tunnel study of windbreak drag. Agri. Ecosystem & Environment, 118: 75-84.

Guo, H., Jacobson, L.D., Schmidt, D.R. and Nicolai, R.E., 2001. Calibrating inpuff-2 model by resident-panelists for long-distance odor dispersion from animal production sites. American Society of Agricultural Engineers, 17(6): 859-868.

Guo, H. et al., 2005. Development of the OFFSET model for determination of odor-annoyance-free setback distances from animal production sites: part II. model development and evaluations. Transaction of the ASAE, 48(6): 2269-2276.

Hinze, J.O., 1975. Turbulence. McGraw-Hill, New York; USA, 790 pp.

Ierardi, J.A., 2000. Air property calculator. http://users.wpi.edu/~ierardi/FireTools/air_prop.html.

Jacobson, L.D. et al., 2005. Development of the OFFSET model for determination of odor-annoyance-free setback distances from animal production sites: part I. review and experiment. Transaction of the ASAE, 48(6): 2259-2268.

Jacobson, M.Z., 1999. Fundamentals of atmospheric modeling. Cambridge University Press, Cambridge, UK, 656 pp.

Lakes Environmental Software, 2002. ISCST3 tech guide. <http://www.weblakes.com/ISCVOL2/Contents.htm>, Waterloo, Ontario, Canada.

Lee, S. and Lim, H., 2001. A numerical study on flow around a triangular prism located behind a porous fence. FLUID DYNAMICS RESEARCH, 28(3): 209-221.

Leuty, T., 2004. Wind management can reduce offensive farm odours. Ministry of Agriculture and food, Ontario, http://www.omafra.gov.on.ca/english/crops/facts/info_odours.htm (2007/01/24).

Lien, F.-s. and Yee, E., 2005. Numerical modelling of the turbulent flow developing within and over a 3-d building array, part iii: a distributed drag force approach, its implementation and application. Boundary-Layer Meteorology, 114(2): 287-313.

Lien, F.-s., Yee, E. and Wilson, J.D., 2005. Numerical modelling of the turbulent flow developing within and over a 3-d building array, part ii: a mathematical foundation for a distributed drag force approach. Boundary-Layer Meteorology, 114(2): 245.

Lien, F.S., Yee, E. and Cheng, Y., 2004. Simulation of mean flow and turbulence over a 2D building array using high-resolution CFD and a distributed drag force approach. Journal of Wind Engineering and Industrial Aerodynamics, 92: 117-158.

Lim, T.T., Heber, A.J., Ni, J.Q., Sutton, A.L. and Kelly, D.T., 2001. Characteristics and Emission Rates of Odor from Commercial Swine Nurseries. Trnsaction of the ASAE, 44(5)(0001-2351): 1275-1282.

Lin, X.J., Barrington, S., Nicell, J., Choiniere, D. and Vezina, A., 2006. Influence of windbreaks on livestock odour dispersion plume in the field. Agriculture, Ecosystems & Environment, 116(3-4): 263-272.

Lyman, W.J., Reehl, W.F. and Rosenblatt, D.H., 1990. Handbook of chemical property estimation methods: environmental behavior of organic compounds. American Chemical Society, Washington, DC, USA, 1000 pp.

Nimmermark, S., 2006. Characterization of odor from livestock and poultry operation by the hedonic tone. Paper number 064157. In: ASABE (Editor), 2006 American Society of Agricultural and Biological Engineering

Annual International Meeting, Oregon Convention Center, Portland, Oregon, 9 - 12 July 2006.

O'Neill, D.H. and Phillips, V.R., 1992. A review of the control of odour nuisance from livestock buildings: Part 3, properties of the odorous substances which have been identified in livestock wastes or in the air around them. JOURNAL OF AGRICULTURAL ENGINEERING RESEARCH, 53: 23-50.

Packwood, A.R., 2000. Flow through porous fence in thick boundary layers: comparisons between laboratory and numerical experiments. Journal of Wind Engineering and Industrial Aerodynamics, 88: 75-90.

Patton, E.G., Shaw, R.H., Judd, M.J. and Raaupach, M.R., 1998. Large-eddy simulation of windbreak flow. Boundary-Layer Meteorology, 87: 275-306.

Riddle, A., Carruthers, D., Sharpe, A., McHugh, C. and Stocker, J., 2004. Comparisons between FLUENT and ADMS for atmospheric dispersion modelling. Atmospheric Environment, 38(7): 1029-1038.

Saatdjian, E.b., 2000. Transport phenomena: equations and numerical solutions. John Wiley, New York, USA, 414 pp.

Schauberger, G., Pringer, M. and Petz, E., 2000. Diurnal and annual variation of the sensation distance of odor emitted by livestock building calculated by the Austrian odor dispersion model(AODM). Atmospheric Environment, 34: 4839-4851.

Schnelle, K.B. and Dey, P.R., 2000. Atmospheric dispersion modeling compliance guide. McGraw-Hill, New York, USA.

Schwartz, R.C., Fryrear, D.W., Harris, B.L., Billbro, J.D. and Juo, A.S.R., 1995. Mean flow and shear stress distributions as influenced by vegetative windbreak structure. Agricultural and forest meteorology, 75: 1-22.

Sheridan, B.A., Curran, T.P. and Dodd, V.A., 2002. Assessment of the influence of media particle size on the biofiltration of odorous exhaust ventilation air from a piggery facility. Bioresource Technology, 84: 129-143.

Sun, H., Stowell, R.R., Keener, H.M. and Michel, F.C., 2002. Comparison of predicted and measured ammonia distribution in a high-riseTM hog building (HRHB) for summer conditions. Transactions of the ASAE, Vol. 45(5): 1559-1568.

Thé, J.L., Thé, C.L. and Johnson, M.A., 2002. ISC-AERMOD View User's Guide. Lakes Environmental Software. Lakes Environmental Software, 419 Phillip Street, Unit 3, Waterloo, Ontario N2L 3X2.

Tyndall, J. and Collettii, J., 2000. Air quality and shelterbelts: Odour mitigation and livestock production - A literature review. Final project report to USDA National Agroforestry Center, Lincoln, NB. Project Number 4124-4521-48-3209. Forestry Department, Iowa State University, Ames, IA. http://www.forestry.iastate.edu/res/Shelterbelts_and_Odor_Final_Report.pdf (2007/01/17).

Ucar, T. and Hall, F.R., 2001. Review windbreaks as a pesticide drift mitigation strategy: a review. Pest Management Science, 57: 663-675.

Wang, H. and Takle, E.S., 1995. A numerical simulation of boundary-layer flows near shelterbelts. Boundary-Layer Meteorology, 75(1 - 2): 141-173.

WASP, 2006. Table of roughness lengths. http://www.risoe.dk/vea/projects/nimo/WAsPHelp/TableofRoughnessLengths.htm.

Wilson, J., 2004. Oblique, stratified winds about a shelter fence. part II: Comparison of measurements with numerical models. JOURNAL OF APPLIED METEOROLOGY, 43(10): 1392-1409.

Wilson, J.D., 1985. Numerical study of flow through a windbreak. Journal of Wind Engineering and Industrial Aerodynamics, 21: 119-154.

Wilson, J.D. and Yee, E., 2003. Calculation of winds distribution by an array of fences. Agricultural and forest meteorology, 115: 31-50.

Yaws, C.L., 2001. Chemical properties handbook -physical, thermodynamic, environmental, transport, safety, and health related properties for organic and inorganic chemicals. McGraw-Hill, New York. USA.

Zhang, Q., Feddes, J.J.R., Edeogu, I.K. and Zhou, X.J., 2003. Correlation between odor intensity assessed by human assessors and odor concentration measured with olfactometers. CANADIAN BIOSYSTEMS ENGINEERING, 44 (6): 27-32.

Zhu, J., Jacobson, L.D., Schmidt, D.R. and Nicolai, R., 2000. Evaluation of inpuff-2 model for predicting downwind odors from animal production facilities. American Society of Agricultural Engineers, 16(2): 159-164.

Nomenclature

AHT is absolute hedonic tone

$C_{1\varepsilon}$, $C_{2\varepsilon}$, and $C_{3\varepsilon}$ are constants

C_1 and C_2 are constants equal to 1.458×10^{-6} kg $m^{-1}s^{-1}$ $K^{-1/2}$ and 110.1 K

C_{ir} is the inertial resistance coefficient

C_μ is a constant

$D_{i,m}$ is the diffusion coefficient for species i in the gaseous mixture

$D_{T,i}$.is the thermal diffusion coefficient for species i in the gaseous mixture

$D_{1,2}$ is the mass diffusion coefficient of clean air into hydrogen sulphide

$D_{2,1}$ is the mass diffusion coefficient of hydrogen sulphide into clean air

F_i is the resistance body force exerted by a windbreak in ith direction

H is the total height of the windbreak

HT is hedonic tone from -10 to 0

h_1, h_2 and h_3 are the windbreak height at which the porosity changes, with a value between 0 and H

J_i is the diffusion flux of species i

LR_1, LR_2 and LR_3 are the Lapse rate, defined as the decrease of temperature with the increase in height, measured from the ground to height z_1, z_1 to z_2 and above z_2

M_1 is the molecular weight of dry air (0.028966kg mol^{-1})

M_2 are the molecular weight of hydrogen sulphide

MAHT is measured absolute hedonic tone

MOC is measured odour concentration (OU m^{-3})

m_{H_2S} is the mass of hydrogen sulphide representing one odour unit

OC_g is the odour concentration at the odour generator, in OU m^{-3}

OC is the odour concentration downwind from the odour generator, in OU m^{-3}

OMF is odour (H_2S) mass fraction

P_a is the atmospheric pressure (101325 Pa at sea level)

p is the wind profile exponent

R is the universal gas constant (8.31432J mol^{-1} K^{-1})

Sc_t is the turbulent Schmidt number generally equal to 0.7

SAHT is simulated absolute hedonic tone

SOC is simulated odour concentration (OU m^{-3})

SOMC is simulated odour mass concentration (μg m^{-3})

T is temperature

T_0 is temperature at the ground surface

T_3 is the air temperature is at a height z = 7.62m

t is time

u and u' are mean and fluctuating component of instantaneous velocity

u_i (i=1, 2, 3) is scalar component of the mean velocity in *i*th direction, indicating in x, y, z direction in Cartesian coordinate system, respectively

u_{mag} is magnitude of mean velocity

u_1 is the open wind velocity at height z_1 = 7.62m, height at which wind speed was measured

V_1 and V_2 are molar volumes for the air and hydrogen sulphide fractions, respectively

w_1, w_2, and w_3 are three constants corresponding to the thickness of the real windbreak

Y_i is the mass fraction of the species *i* in a mixture of gases

Y_2 is the odour mass fraction at the generator

z is a coordinate in the vertical direction

z_1 and z_2 are heights in the domain, where $0<z_1<z_2$,

α is the aerodynamic porosity, or permeability

β is the optical porosity

ε is turbulence dissipation rate

μ is viscosity of mixture of the air and odorous gases

μ_t is the turbulence kinetic viscosity

ρ is fluid density

Tables and Figures

Table 6.1 Description of experimental windbreak sites.

Parameter	**Site**		
	1	2	3
	Mixed mature deciduous [a]	Conifers [a]	Poplars [a]
Length(m)	1050	380	2100
Height(m)	9.2	15.2	18.3
Width(m)	7	6	6
Average porosity	0.35	0.35	0.55
Porosity at the base	0.30	0.40	0.70
Location	St Chrysostome	St Charles	Sherrington

Note: All locations are located within 50km of the Island of Montreal, Canada, in the south west direction. [a] Tree type.

Table 6.2 Field test conditions evaluating model performance.

Test number	Site	Date -2003	Test condition					
			OG (m)	OE (OU s^{-1})	WS (m s^{-1})	WD (°)	T (°C)	AS
1	3	Sep-02	30	859	2.5	40	17	C
2	1	Sep-03	30	1373	3.9	0	21	B
3	1	Sep-03	60	492	4.4	0	23	C
4	1	Sep-05	30	585	4.2	50	19	D
5	1	Sep-10	30	1096	2.7	70	27	D
6	1	Sep-15	15	744	5.1	0	28	D
7	1	Sep-15	30	745	1.5	0	23	D
8	1	Sep-18	15	1879	1.5	50	24	C
9	1	Sep-18	60	846	2.2	30	26	B
10	2	Dec-03	30	690	3.5	30	-4	D
11	2	Dec-14	30	394	3.3	30	-8	D

Note: NW- no windbreak; OG – odour generator distance downwind from the windbreak; OE – average odour emission during the test; WS- average wind speed; WD - wind direction with respect to the x-axis, 0° being perpendicular to the windbreak; T – average temperature measured during the test; AS – Pasquill-Gifford atmospheric stability condition, where B and C are unstable classes and D is a neutral class.

Table 6.3 Dimensions of field odour dispersion systems.

ODS	Test	OG	Windbreak	ODS dimensions (m)				
number	number	(m)	Height (m)	x_L	x_R	y_F	y_B	z_H
1	2, 7	30	9.2	-138	552	-184	92	73.6
2	4, 5	30	9.2	-138	552	-368	46	73.6
3	6	15	9.2	-138	552	-184	92	73.6
4	8	15	9.2	-138	552	-368	92	73.6
5	3, 9	60	9.2	-138	552	-368	46	73.6
6	10, 11	30	15	-150	450	-240	150	120
7	1	30	18	-180	594	-396	144	144

Note: ODS - odour dispersion systems; OG – odour generator distance downwind from the windbreak; x_L and x_R are the x-coordinates of left and right faces of the ODS, respectively; y_B and y_F are the y-coordinates for the back and front faces, respectively; and z_H is the height from the bottom to the top faces

Table 6.4 Model and boundary conditions.

Main parameters	unit	Case 1	Case 2
Computed domain	H	60 x 12	75 x 30 x 8
Model parameters			
C_μ		0.12	0.09
$C_{1\varepsilon}$		1.44	1.4
$C_{2\varepsilon}$		2.20	1.92
Left, top, front and back faces in the block			
Weather stability			**B**
Velocity magnitude	m s^{-1}	$4.0(z/9.2)^{0.1}$	$3.95(z/7.62)^{0.07}$
Wind direction in x-axis	°	0	0
Temperature	°K	294	294
Turbulence intensity	%	10	17
Turbulence length scale	m	0.4	0.13
Odour inlet			
Velocity magnitude	m s^{-1}		11.89
Wind direction in x-axis	°	0	0
Temperature	K		294
Odour concentration	OU m^{-3}		830
Odour mass fraction			4.839E-06
Turbulence intensity	%		17
Turbulence length scale	m		0.13
Windbreak			
Windbreak height	m	2.2	9.2
Windbreak thickness	m	0.44	7
Optical porosity (β)		0.54	0.35
Aerodynamic porosity (α)		0.54	0.66
Viscous resistance (1/α)	m^{-2}	1.85	1.515
Inertial resistance (C_{ir})	m^{-1}	10.25	0.305
Bottom face			
Temperature	K	297	295.4

Note: z is height in m; H is the windbreak height.

Table 6.5 Coefficients of transformation function and R^2-values.

Simu-lation	Correlation between MAHT and SOMC				SAHT = a $SOMC^b$ in equation (6.23)			R^2-value	
	R^2 - value	F Value	F Value (p=0.01)	F test (p=0.01)	a	b	n	MAHT and SAHT	MOC and SOC
1	0.64	14.27	11.26	SG	0.678	0.445	10	0.59	0.59
2	0.63	29.14	8.40	SG	0.957	0.366	19	0.59	0.49
3	0.65	16.45	10.56	SG	0.574	0.551	11	0.84	0.73
4	0.53	13.34	9.33	SG	0.831	0.680	14	0.69	0.81
5	0.50	26.59	7.68	SG	0.281	0.774	29	0.68	0.96
6	0.69	24.92	9.65	SG	0.971	0.461	13	0.71	0.58
7	0.85	58.01	10.04	SG	0.761	0.475	12	0.90	0.90
8	0.48	15.89	8.40	SG	0.433	0.498	19	0.49	0.52
9	0.76	35.53	9.65	SG	0.470	0.482	13	0.89	0.88
10	0.83	46.43	10.04	SG	1.257	0.410	12	0.79	0.77
11	0.81	51.52	9.33	SG	0.588	0.736	14	0.83	0.60

Note: n - number of odour points; SG – significant; SOMC – simulated odour (H_2S) mass concentration; SAHT – simulated absolute hedonic tone; MAHT – measured absolute hedonic tone. The R^2-values for MAHT and SAHT and for MOC and SOC in all 11 simulations are significant ($P < 0.01$).

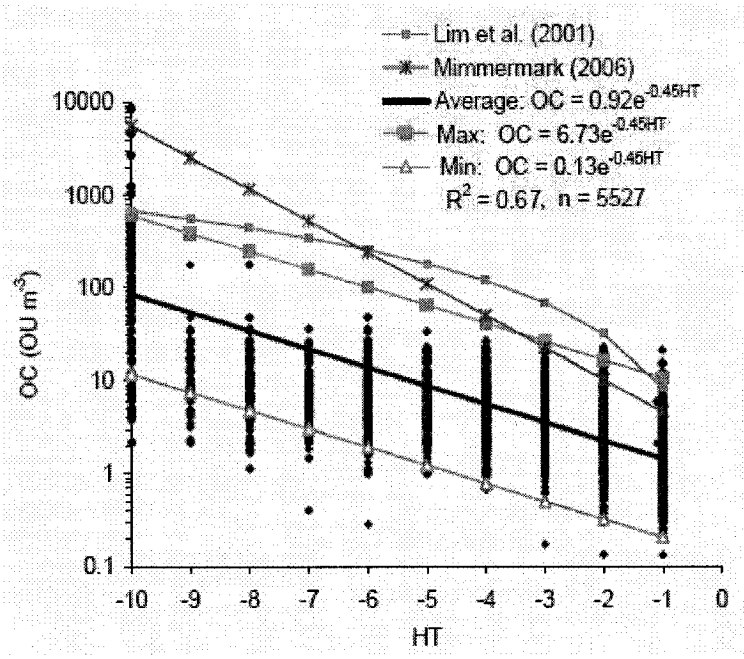

Fig. 6.1. Relationship among 5527 pairs of odour hedonic tone (HT) and odour concentration (OC) observations from the 65 odour samples measured by 17 groups of 12 panellists compared to those of Lim et al. (2001) and Nimmermark (2006). The solid black line represents the exponential regression of all the data, while the maximum and minimum represent the 95 % confidence interval. R^2 is the correlation coefficient between the HT and OC and *n* is total pairs of data.

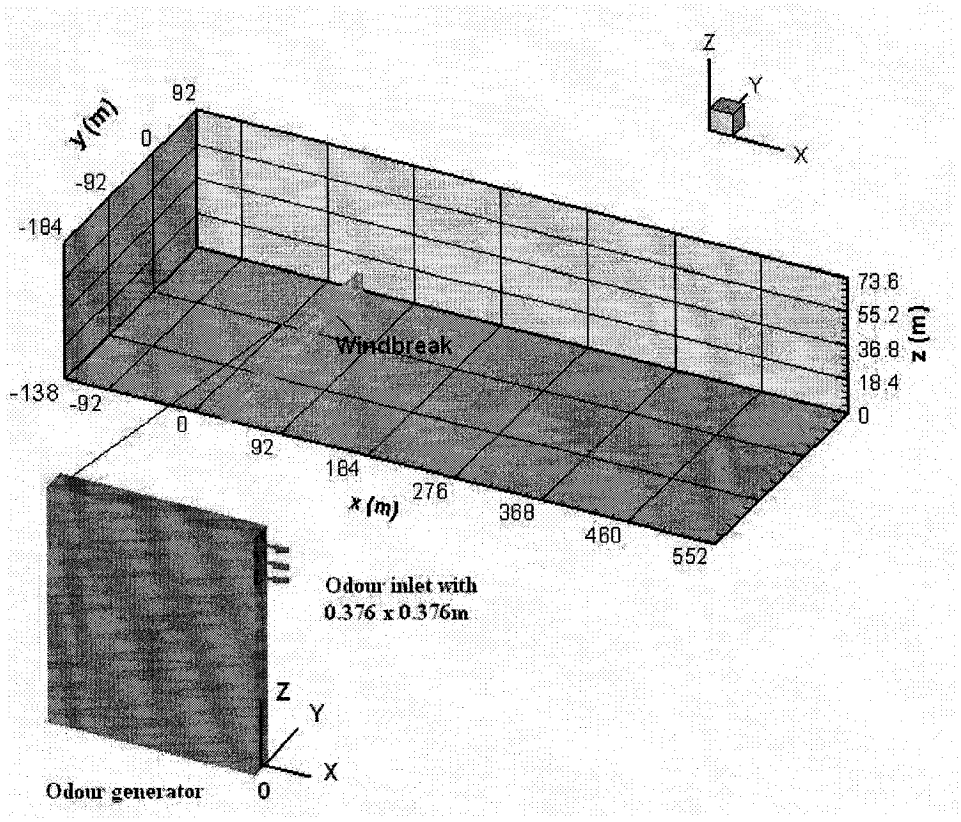

Fig. 6.2. Schematic of the computational volume used to predict odour dispersion. The z coordinate is magnified 2-fold and the windbreak optical porosity is 0.35. The green bar represents the windbreak. The centre of the odour emission surface of the odour generator stands at x = 0, y = 0 and z = 1.562m.

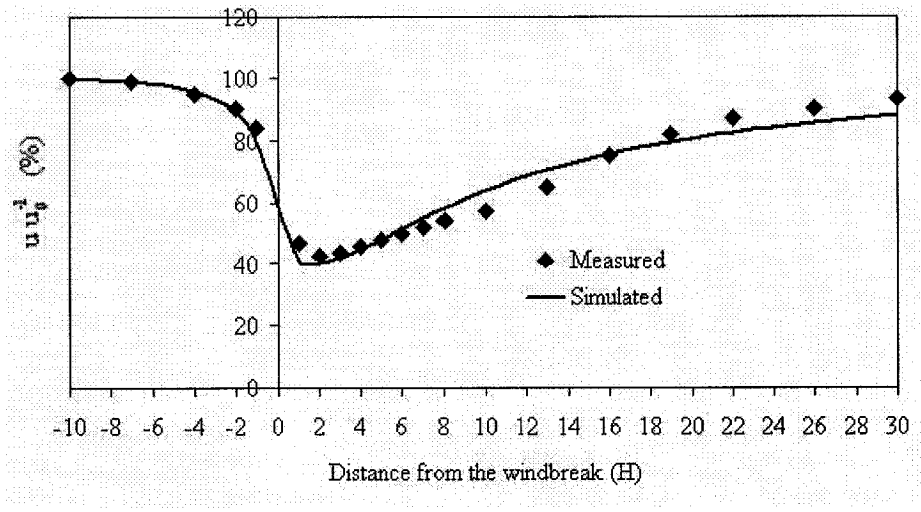

Fig. 6.3. Simulated and measured wind speeds at windbreak half height where u is the wind speed, u_0 is the undisturbed wind speed and H is the height of the windbreak. The measured wind speed is taken from Naegeli, 1953 (Eimern et al, 1964).

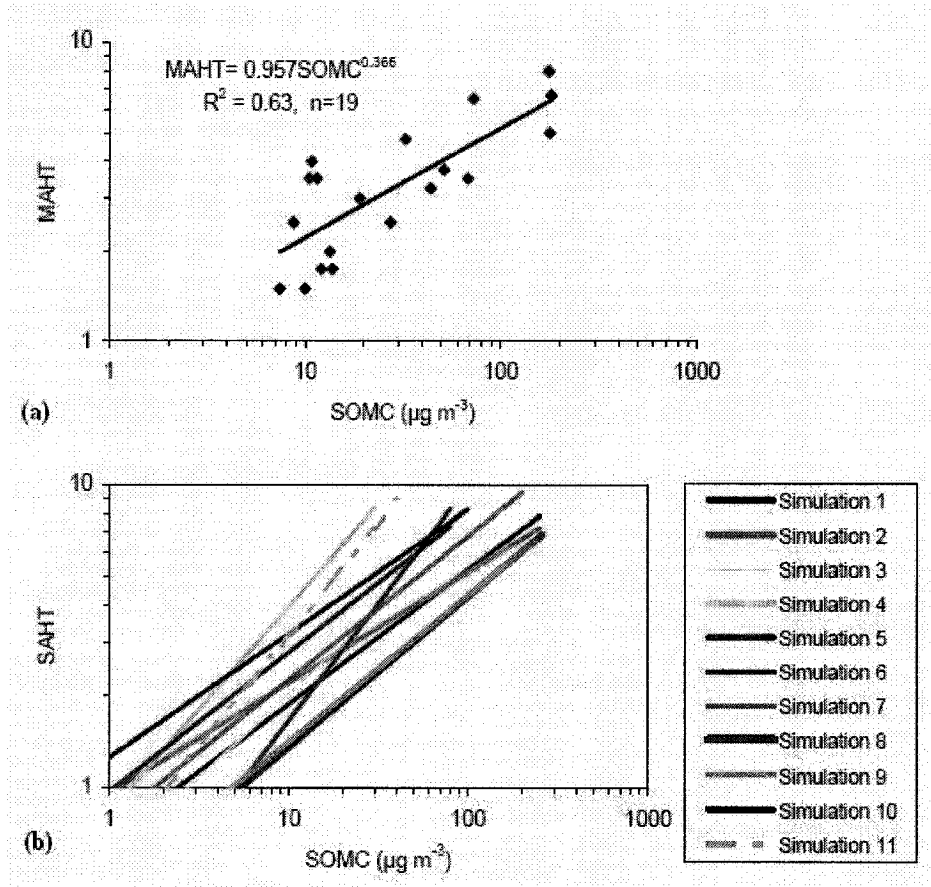

Fig. 6.4. (a) For test 2, correlation between the simulated odour (H_2S) mass concentration (SOMC) and the field-measured absolute hedonic tone (MAHT). This correlation produced an equation defining the simulated absolute hedonic tone (SAHT); (b) transformation of SOMC into simulated absolute hedonic tone (SAHT), for 11 simulation tests.

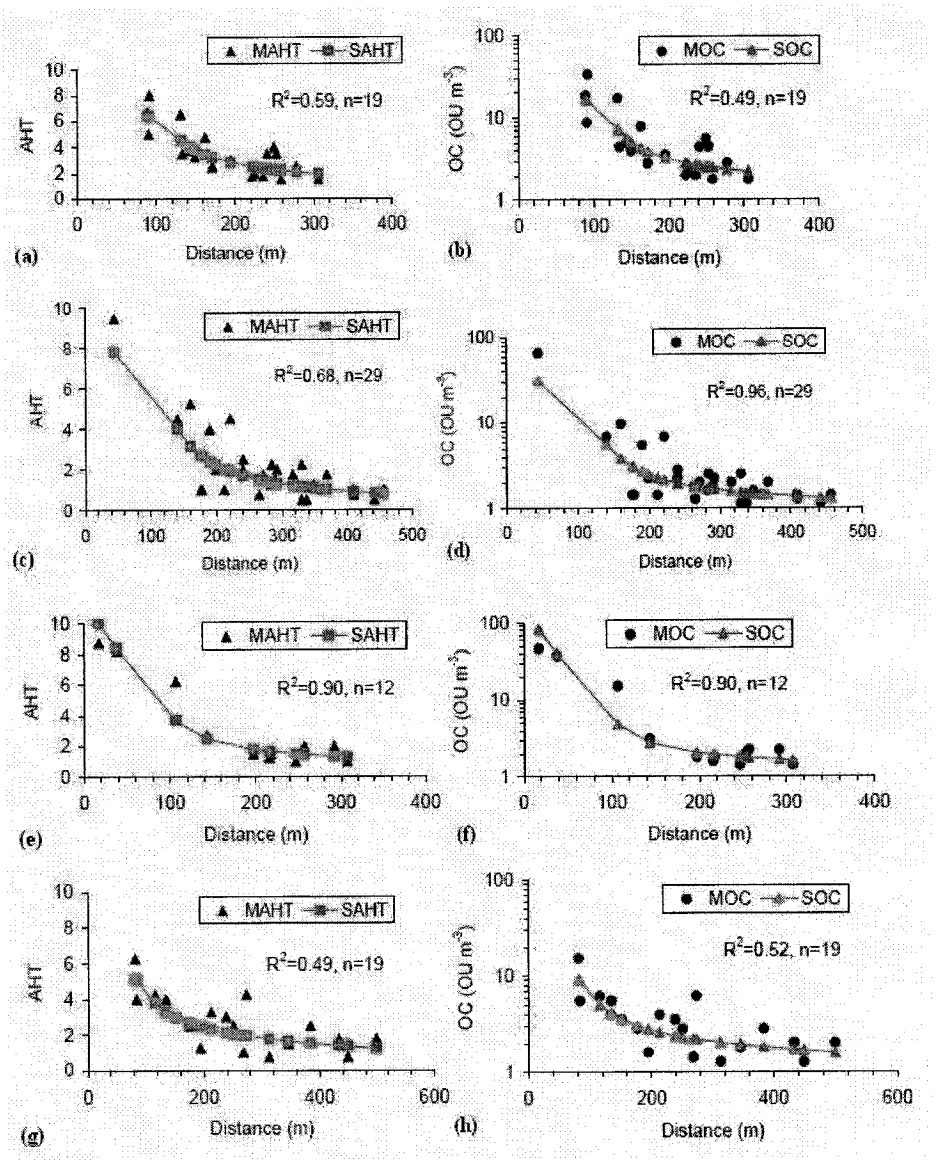

Fig. 6.5. (a), (c), (e) and (g) Measured and simulated absolute hedonic tone for tests 2, 5, 7 and 8 respectively, where AHT is the absolute hedonic tone, MAHT and SAHT are the measured and simulated hedonic tone, respectively, R^2 is the correlation coefficient between the MAHT and SAHT and n is odour points measured; (b), (d), (f) and (h) Measured and simulated odour concentration for tests 2, 5, 7 and 8, respectively, where OC is odour concentration, MOC and SOC are respective measured and simulated OC, and R^2 is the correlation coefficient between MOC and SOC. The x axis indicates the distance from the odour source.

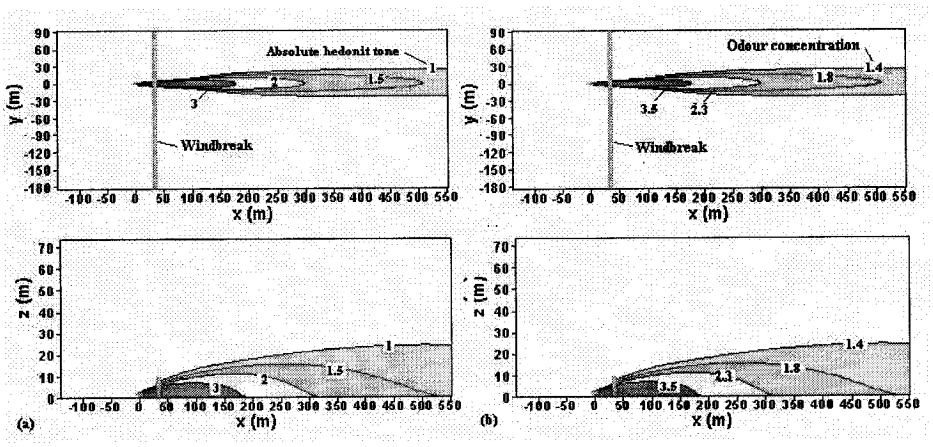

Fig. 6.6. Simulated odour dispersion plume in the horizontally z = 1.5 m and vertically y = 0 m planes: (a) hedonic tone contours, and; (b) odour concentration contours in OU m^{-3}.

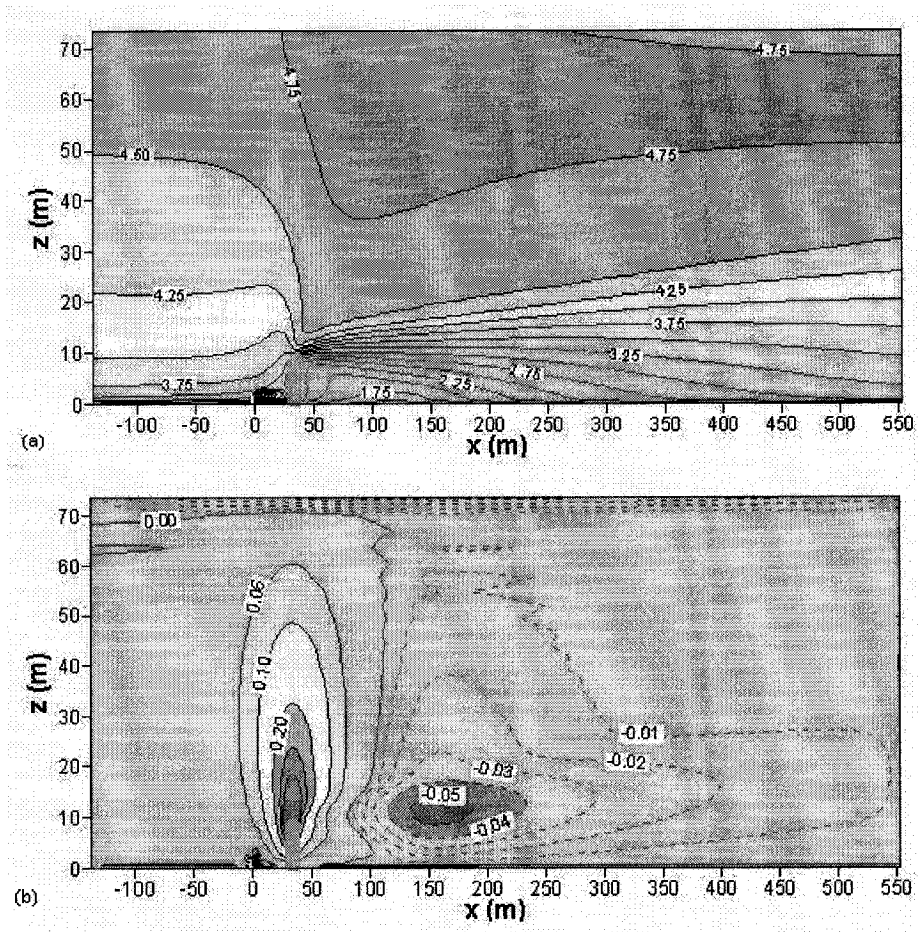

Fig. 6.7. Wind velocity (m s^{-1}) contours in the plane y = 0 m; (a) velocity in the x-component; (b) velocity in the z-component.

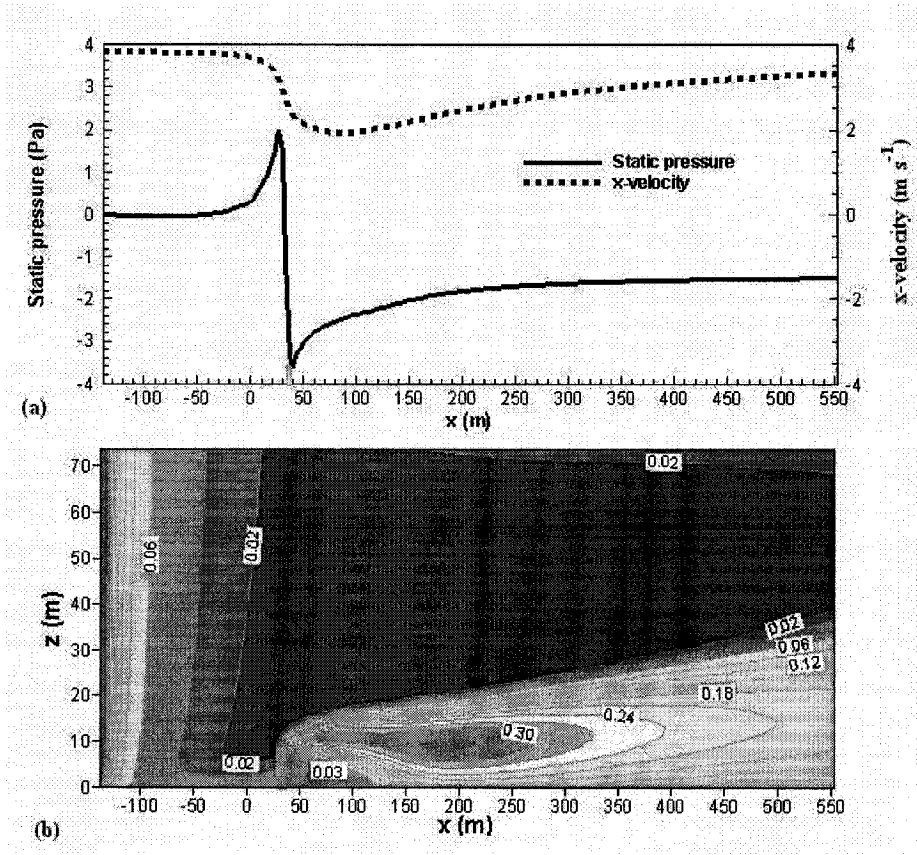

Fig. 6.8 (a) Static pressure and velocity distribution around a windbreak at y = 0 and z = 4.6 m. The windbreak creates a pressure differential of 5.6 Pa, and; (b) contours of turbulent kinetic energy ($m^2 s^{-2}$) on the plane y = -20 m.

Connecting statement

In chapter 6, the standard k-ε model was successfully calibrated with the field data to simulate odour dispersion around the natural windbreak. However, this model offered limitations because many generated cells had a ratio of turbulent viscosity to molecular viscosity exceeding the physical limit, especially when simulating denser windbreaks. Hence the SST k-ω was tested in chapter 7.

Chapter 7 calibrated the SST k-ω model for velocity recovery rate using a 2-dimensional system and for odour dispersion in a 3-dimensional system using 5 field measurements. The Monin Obukhov similarity theory was applied to formulate vertical profiles of horizontal wind velocity, temperature and turbulence energy. After successfully calibrated, the SST k-ω model was used to evaluate the effects of porosity, height, tree structure and orientation on the odour dispersion.

This paper was submitted to Biosystems Engineering. The authors are Lin, X.J., Barrington, S., Choinière, D. and Prasher, S. The contributions of the authors are i) First author carried out a part of field measurements, the CFD simulation and wrote the manuscript; ii) Second author supervised and helped revise the method of analysis and the content of the paper; iii) Third author organized and managed the collection of the field data; iv) The last author helped review the modelling process.

Chapter 7

Simulation of the effect of windbreaks on odour dispersion using CFD SST k-ω model

7.1. Abstract

Computational fluid dynamic (CFD) simulation is a technique capable of defining best management practices associated with the wide use of natural windbreaks to help disperse livestock odours and reduce setback distances. The objective of the project was therefore to use the Fluent Shear Stress Transport (SST) k-ω model to simulate odour dispersion downwind from natural windbreaks and to test the effect of tree characteristics (tree porosity, structure and height, and windbreak distance from the odour source). The air flow inertial resistance of windbreaks was defined as proportional to the square of the tree diameter. The SST k-ω model was initially calibrated for air velocity recovery rate (VRR) on the downwind side of the windbreak, using a two dimensional simulation. Once further calibrated with field odour measurement data, the model was used to compare the size and length of odour plumes developing downwind from windbreaks with different tree characteristics. With the VRR calibration, the SST k-ω model predicted the wind velocity profile with an acceptable error of 4.5%. When calibrated for odour dispersion, the SST k-ω model requires a function to transform the simulated odour mass concentration (SOMC) into simulated absolute hedonic tone (SAHT), which was significantly ($P < 0.01$) correlated with the measured absolute hedonic tone (MAHT). Furthermore, the simulated odour concentration (SOC) transformed from the SAHT was found significantly ($P < 0.01$) correlated with field measured odour concentration (MOC). Once calibrated, the SST k-ω model was able to accurately predict odour concentration downwind from the windbreak. By comparison, the SST k-ω simulations indicated that a dense (aerodynamic porosity of 0.2) and tall (9.2 m) natural windbreak produces a shorter but more intense odour plume as compared to a porous (aerodynamic porosity of 0.66) and

short (4.6 m) windbreak. For the same aerodynamic porosity, tree structure changed the air velocity profile through the windbreak: with more foliage at the top, a poplar windbreak produced a slightly shorter odour plume as compared to a conifer windbreak with more foliage at the bottom. As compared to a source located further away (60 m), an odour source located close (15 m) to the windbreak produced a shorter plume because less dilution occurred upwind from the windbreak for a more intense trapping of odours downwind. Thus, odour dispersion is enhanced when the natural windbreak is tall, dense and located no more than 15 m downwind from the odour source.

Keywords: SST k-ω model simulation; Windbreak; Odour dispersion; Concentration, Hedonic tone, Tree porosity, type and height.

7.2. Introduction

Manure odour nuisance created by livestock operations can be reduced using setback distances favouring atmospheric dispersion. When built around livestock shelters, windbreaks were found to improve odour dispersion and help reduce setback distances (Lin et al., 2006). A natural windbreak with an optical porosity of 35 % reduced on the average, the maximum odour dispersion distance (MODD) by 21 % compared to a site without windbreak (Lin et al., 2007b).

Before planting costly natural windbreaks to enhance odour dispersion, the air mixing mechanism must be defined as a function of tree characteristics such as type, height and porosity, and distance from the odour source. For example, the tree foliage density needs optimization because of its effect on air flow resistance and the resulting turbulence. Field comparison of the effect of tree characteristics is difficult to achieve because of the lack of control on all other parameters, such as air temperature gradient, stability, and wind velocity and direction. For this purpose, simulations are preferred as long as the model is capable of accurately representing all conditions.

In the past, odour dispersion from livestock facilities was simulated using Gaussian-based models, such as AODM, INPUFF II and AERMOD developed for flat terrain (Gorgy, 2003; Guo et al., 2001; Schauberger et al., 2000; Sheridan et

al., 2002; Zhu et al., 2000). Limited to conditions of low turbulence, these models are not suited for the simulation of the microclimate in the vicinity of the natural windbreaks.

Computational fluid dynamic (CFD) models, such as the Reynolds Average Navier Stokes (RANS) model and the Large-Eddy Simulation (LES), were used to simulate windbreaks in 2 and 3 dimensional systems (Lien and Yee, 2005; Lien et al., 2005; Lien et al., 2004; Packwood, 2000; Patton et al., 1998; Schwartz et al., 1995; Wang and Takle, 1995; Wilson, 2004; Wilson, 1985; Wilson and Yee, 2003). The RANS can accurately simulate wind velocity profiles, except under conditions of high turbulence (Gosman, 1999; Wilson, 1985). The CFD models of the Fluent software successfully simulated conditions of high turbulence such as heat exchanges under natural convection (Dirkse et al., 2006), odour dispersion on sites without windbreaks (Li and Guo, 2006; Riddle et al., 2004), ammonia distribution in barns (Sun et al., 2002) and spray droplet transport (Ucar and Hall, 2001). When simulating odour dispersion around dense windbreaks, the Fluent standard k-ε model generated in the computational domain, a high number of cells whose ratio of turbulence viscosity to molecular viscosity exceeded the physical limit of 10^5 (Lin et al., 2007a).

Besides high turbulence, the simulation of odour dispersion requires the conversion of odorous mass concentration (OMC) into a parameter expressing human sensation, expressed either as odour concentration (OC) in OU m^{-3} or hedonic tone (HT). Measured in the laboratory, odour concentration is the dilution factor at which 50% of panellists can detect odours and is directly related to OMC. But, OC is not easy to measure in the field because the very low concentrations encountered are too close to their dilution threshold (Zhang et al., 2003). Odour hedonic tone (HT) is therefore preferred for field tests because panellists can evaluate odour sensation even at levels close to the detection threshold (Guo et al., 2001; Jacobson et al., 2005; Lin et al., 2006; Zhu et al., 2000). However, an exponential relationship exists between HT and OC or OMC, and this function must be initially defined by correlating odorous mass

concentrations (OMC) as computed by the CFD model, with measured field HT (CEN, 2001; EPA, 2001).

The objective of the present paper was therefore to calibrate the SST k-ω model for wind velocity recovery rate (VRR) downwind from windbreaks and to validate this model for odour dispersion with HT and OC measured in the field by trained panellists in field. The SST k-ω model was then used to analyse the effect on odour dispersion of windbreak tree characteristics, such as aerodynamic porosity, tree type or structure and height, and distance from the source.

7.3. Model

7.3.1. Odour species equation

For a fixed volume cell through which odorous air is flowing, the governing equations expressing the average air flow are mass, momentum, energy and species conservation (Hinze, 1975; Saatdjian, 2000). Besides the first three equations, the odour species equation is:

$$\frac{\partial}{\partial t}(\rho Y_i)+\nabla\bullet(\rho u Y_i)=-\nabla\bullet J_i \tag{7.1}$$

where

$$J_i=-(\rho D_{i,m}+\frac{\mu_t}{Sc_t})\nabla Y_i-D_{T,i}\frac{\nabla T}{T} \tag{7.2}$$

where ρ is fluid density; t is time; J_i is the diffusion flux of the species i; Y_i is the mass fraction of the species i; $D_{i,m}$ is the diffusion coefficient for species i in the mixture; $D_{T,i}$ is the thermal diffusion coefficient; Sc_t is the turbulent Schmidt number generally equal to 0.7, and; μ_t is the turbulent viscosity (Bird et al., 2002; Saatdjian, 2000). The odour dispersion is dependent on the species gradient, rate of the temperature gradient, turbulent viscosity and diffusion coefficients.

7.3.2. *Windbreak simulation*

A windbreak is a porous medium resisting wind or air flow and therefore constituting a momentum sink. This resistance can be introduced in the momentum equation in terms of viscous and inertial resistance:

$$F_i = -\frac{\mu}{\alpha} u_i - \frac{1}{2} C_{ir} \rho u_{mag} u_i \tag{7.3}$$

where F_i is a resistance; μ is fluid viscosity; α is the aerodynamic porosity or permeability of the windbreak; α^{-1} is the viscous resistance coefficient; C_{ir} is the inertial resistance coefficient caused by the windbreak; u_{mag} is the magnitude of the average velocity, and; u_i (i=1, 2, 3, indicating x, y, and z direction) is the mean velocity u in ith direction.

The term $\mu\ u_i / \alpha$ in Eqn (7.3) is Darcy's law for porous medium which calculates the resistance exerted by the windbreak due to fluid viscosity (Bird et al., 2002). The term $C_{ir}\rho u_{mag} u_i / 2$ in Eqn (7.3) computes the inertial loss of the fluid flowing through the windbreak, which varies over the height of the tree depending on its shape (Wang and Takle, 1995; Wilson, 2004; Wilson, 1985). Poplars offer dense foliage at their top compared to conifers which offer more foliage at their base. Accordingly, a valid simulation uses an inertial resistance coefficient which varies over tree height.

For natural windbreaks, the momentum sink is proportional to the leaf area density (Wilson, 1985). Therefore, the inertial resistance C_{ir} can be assumed proportional to the thickness of the windbreak:

$$C_{ir} = \begin{cases} w_1 - \dfrac{w_1 - w_2}{h_1} z & z \le h_1 \\ w_2 - \dfrac{w_2 - w_3}{H - h_1}(z - h_1) & h_1 < z \le H \end{cases} \tag{7.4}$$

where z is height; H is the windbreak height; h_1 is a height between 0 and H, and; w_1, w_2, and w_3 are three constants corresponding to the thickness of the natural

windbreak. During the model calibration, w_1, w_2, and w_3 can be set to allow a specific amount of air flow through the windbreak.

7.3.3. Numerical solver

The RANS models of the Fluent software includes the standard, RNG and realizable k-ε model; the standard and SST k-ω model, and; the RSM model. After testing each one of these, the SST k-ω model was selected because it generated the least cells in which the ratio of turbulence viscosity to molecular viscosity exceeded the physical limit of 10^5.

The SST k-ω model uses two different transport equations to calculate turbulent kinetic energy k and specific dissipation rate ω. The SST k-ω accounts for the principal turbulent shear stress and uses a cross-diffusion term in the ω equation to blend both the k-ω and k-ε models and to ensure that the model equations behave appropriately in both the near-wall and far-field zones. Therefore, the SST k-ω model can outperform the k-ω and k-ε models (Menter et al., 2003).

The Fluent 6.2 steady 3-dimensional segregated solver was used to solve the SST k-ω model. The second and quick orders of discretisation schemes were used to convert the governing equations into algebraic equations for their numerical solution. The second order scheme was used to solve for pressure while the second order upwind scheme was used to solve for odour dispersion. The quick scheme was used to solve for momentum, turbulent kinetic energy, turbulence dissipation rate and energy. The SIMPLE method coupled the velocity and pressure calculations.

Four odour dispersion systems (ODS) were conceived to reproduce the five field tests and calibrate the simulation model (Table 7.2). Simulations 1 and 4 use the same ODS *(Fig. 7.1)* while simulations 2, 3 and 4 used three other ODSs. Each ODS was represented by a rectangular volume encompassing a specific windbreak type located at a given distance from the odour source. The left and right faces of the ODS volume were the wind inlet and outlet, respectively, while

the front, back and top faces had an undisturbed wind velocity and the bottom was the earth's surface.

For all ODSs, the field odour source measured 3 m x 0.376 m x 1.75 m. Odours were blown from the right-up rectangular face (the red zone in *Fig. 7.1*) measuring 0.376 m x 0.376 m, with its centre positioned at 0, 0 and 1.562 m (x, y, z directions respectively). Odour dispersion was presumed to start as soon as generated. The windbreak (green zone in *Fig. 7.1*) was designed as a cube positioned at a specific distance downwind from the source.

Numerical calculations were implemented by meshing the computational volume. For the model calibration, the volume was meshed into 177, 96, and 46 segments in the x, y and z directions, respectively, and the size of the rectangular hexahedral cells gradually increased from the odour generator towards the outward faces of the system. For the odour inlet, 64 rectangles were meshed over an area of 0.376 m x 0.376 m, to effectively transfer the odorous air mass fraction to the other cells.

7.3.4. Fluid properties

Livestock odours consist of at least 168 odorous compounds and six of the ten compounds with the lowest detection threshold contain sulphur (O'Neill and Phillips, 1992). In the present model, hydrogen sulphide (H_2S) was selected as the odorous gas flowing along with clean air. The modelled fluid was defined as a mixture of clean air and H_2S. At the odour source, the H_2S mass fraction was:

$$Y_2 = \frac{OC_g \bullet m_{H_2S}}{\frac{P_a M}{RT} + OC_g \bullet m_{H_2S}} \tag{7.5}$$

where Y_2 is the odour mass fraction at the source; P_a is the atmospheric pressure of 101325 Pa at sea level; T is temperature in K; M is the molecular weight of dry air of 0.028966 kg mol^{-1}; R is the universal gas constant equal to 8.31432J mol^{-1} K^{-1} (Jacobson, 1999); OC_g is the odour concentration at the odour source in OU m^{-3}, and; m_{H_2S} is the mass of H_2S per odour unit and is equal to 7.0×10^{-9} kg OU^{-1} (ASHRAE, 1997).

The clean air and H_2S mixture was presumed to be an incompressible ideal gas, where the density of the fluid mixture varied with T and not with p for a Mach number under 10% (Table 7.1). The specific heat capacity, thermal conductivity and viscosity were calculated using the mass mixing-law and the thermal diffusion coefficient was calculated using the kinetic-theory.

7.3.5. Boundary conditions

The boundary of the computed domain included the clean air and odour inlet, the fluid outlet, the walls of the computational volume and the windbreak. The ODS bottom surface was assumed to have no slip and require as input only temperature and roughness length. The vertical profile of the horizontal wind velocity and temperature were inputs, as well as the turbulence kinetic energy and the specific dissipation.

Odour dispersion around the windbreak was assumed to occur within a homogeneous flat terrain within the surface layer of the atmosphere, and the unidirectional approach wind flow was assumed to satisfy the assumptions of the Monin Obukhov similarity theory (Panofsky and Dutton, 1984). Atmospheric stability was determined by the Monin Obukhov length L_{MO}:

$$L_{MO} = -\frac{u_*^3 \rho C_p T}{k_a g H_F} \tag{7.6}$$

where u_* is the friction velocity; k_a is the von Karman constant ranging from 0.35 to 0.43 where generally $\kappa_a \approx 0.4$; h_{ABL} is the height of the atmospheric boundary layer; T is the earth's surface temperature; C_p is the specific heat of the air; H_F is the vertical heat flux; ρ the air density, and; g is the gravitational acceleration constant (Carruthers and Dyster, 2003; Schnelle and Dey, 2000). When the heat flux is upward, L_{MO} is negative and the air is unstable. When the earth absorbs heat energy, the heat flux is negative, L_{MO} is positive and the air is stable. However, when the heat flux is zero, L_{MO} has a value of infinity and the air is neutral.

The vertical profile of the horizontal wind velocity was defined as:

$$u_{mag}(z)=\begin{cases}\dfrac{u_*}{k_a}\ln\dfrac{z}{z_0} & h_{ABL}/L_{MO}=0 \quad neutral\\ \dfrac{u_*}{k_a}\left(\ln\dfrac{z}{z_0}-\ln\dfrac{(1+x)^2(1+x^2)}{(1+x_0)^2(1+x_0^2)}+2\tan^{-1}(x)-2\tan^{-1}(x_0)\right) & h_{ABL}/L_{MO}<0 \quad unstable\\ \dfrac{u_*}{k_a}\left(\ln\dfrac{z}{z_0}+\dfrac{5(z-z_0)}{L_{MO}}\right) & h_{ABL}/L_{MO}>0 \quad stable\end{cases} \tag{7.7}$$

where

$$x=\left(1-\frac{16z}{L_{MO}}\right)^{\frac{1}{4}} \tag{7.8}$$

$$x_0=\left(1-\frac{16z_0}{L_{MO}}\right)^{\frac{1}{4}} \tag{7.9}$$

where z is height from the surface; z_0 is the roughness length of the surface, and; $u_{mag}(z)$ is the magnitude of the mean horizontal velocity at the height z ($z \geq z_0$) (Blackadar, 1997; Jacobson, 1999; Panofsky and Dutton, 1984).

The vertical temperature profile $T(z)$ assumed that the air temperature was equal to the potential temperature at height z_s (Panofsky and Dutton, 1984):

$$T(z)=\begin{cases}-\gamma_d(z-z_s)+T_s & h_{ABL}/L_{MO}=0 \quad neutral\\ -\gamma_d(z-z_s)+T_s\left(1+\dfrac{u_*^2}{\kappa_a^2 g L_{MO}}\left(\ln\dfrac{z}{z_s}-2\ln\dfrac{1+\sqrt{1-\dfrac{16z}{L_{MO}}}}{1+\sqrt{1-\dfrac{16z_s}{L_{MO}}}}\right)\right) & h_{ABL}/L_{MO}<0 \quad unstable\\ -\gamma_d(z-z_s)+T_s\left(1+\dfrac{u_*^2}{\kappa_a^2 g L_{MO}}\left(\ln\dfrac{z}{z_s}+\dfrac{5(z-z_s)}{L_{MO}}\right)\right) & h_{ABL}/L_{MO}>0 \quad stable\end{cases} \tag{7.10}$$

where $T(z)$ is the air temperature at z ($z \geq z_0$); z_s is a height of 1.35 m above the earth's surface; T_s is the air temperature at z_s; g is the gravitational acceleration constant, and; γ_d is the dry adiabatic lapse rate of 0.01 K m^{-1}.

The vertical turbulence kinetic energy profile of the surface layer was defined as:

$$k(z) = \frac{1}{2}\left(\sigma_u^2 + \sigma_v^2 + \sigma_u^2\right) \tag{7.11}$$

where $k(z)$ is the turbulence kinetic energy (TKE), and; σ_u, σ_v and σ_w are turbulence components of the x, y, z coordinates.

For neutral conditions, $h_{ABL} / L_{MO} = 0$, TKE decreases linearly with height to reach 20% of its ground surface value at the top of the atmospheric boundary layer. Using a value of 0.8 for a_s, σ_u, σ_v and σ_w were calculated as (Carruthers and Dyster, 2003):

$$\sigma_u(z) = 2.5 u_* T_{WN} \tag{7.12}$$

$$\sigma_v(z) = 2.0 u_* T_{WN} \tag{7.13}$$

$$\sigma_w(z) = 1.3 u_* T_{WN} \tag{7.14}$$

where

$$T_{WN} = 1 - a_s \frac{z - z_0}{h_{ABL} - z_0} \tag{7.15}$$

and T_{WN} defines the drop in TKE with height within the atmospheric boundary layer. Substituting for σ_u, σ_v and σ_w in Eqn (7.11) and using the definitions found in Eqns (7.12) to (7.14), TKE for neutral conditions becomes:

$$k(z) = 5.97 u_*^2 T_{WN}^2 \tag{7.16}$$

For unstable conditions, $h_{ABL} / L_{MO} < 0$:

$$\sigma_u(z)^2 = 0.3 w_*^2 + \left(2.5 u_* T_{WN}\right)^2 \tag{7.17}$$

$$\sigma_v(z)^2 = 0.3w_*^2 + \left(2u_*T_{WN}\right)^2 \tag{7.18}$$

$$\sigma_w(z)^2 = 0.4w_*^2T_{WC}^2 + \left(1.3u_*T_{WN}\right)^2 \tag{7.19}$$

where

$$T_{WC} = 2.1\left(\frac{z-z_0}{h_{ABL}-z_0}\right)^{\frac{1}{3}} T_{WN} \tag{7.20}$$

$$w_* = u_*\left(\frac{h_{ABL}-z_0}{k_a|L_{MO}|}\right)^{\frac{1}{3}} \tag{7.21}$$

where w_* is the mixing layer velocity scale.

Therefore, TKE for unstable conditions reduces to:

$$k(z) = 5.97u_*^2T_{WN}^2 + w_*^2\left(0.3+0.2T_{WC}^2\right) \tag{7.22}$$

For the stable conditions ($h_{PBL}/L_{BO} > 0$), TKE is expressed as:

$$\sigma_u(z) = 2.5u_*T_{WN}^{\frac{3}{4}} \tag{7.23}$$

$$\sigma_v(z) = 2.0u_*T_{WN}^{\frac{3}{4}} \tag{7.24}$$

$$\sigma_w(z) = 1.3u_*T_{WN}^{\frac{3}{4}} \tag{7.25}$$

and a_s respects the following function (Carruthers and Dyster, 2003):

$$a_s = \begin{cases} 0.9 & z_0 \le 0.01 \\ 0.9-0.4\left(\dfrac{z_0-0.01}{0.09}\right) & 0.01 < z_0 < 0.1 \\ 0.5 & z_0 \ge 0.1 \end{cases} \tag{7.26}$$

Hence, TKE for stable conditions is:

$$k(z) = 5.97u_*^2T_{WN}^{\frac{3}{2}} \tag{7.27}$$

The vertical turbulence specific dissipation rate $\omega(z)$ was:

$$\omega(z) = \frac{k(z)^{\frac{1}{2}}}{0.09^{\frac{1}{4}} l} \tag{7.28}$$

where l is the turbulence length scale.

For the SST k-ω model, the parameters describing the surface layer conditions (z_0, L_{MO}, h_{ABL}, u_* and T_s) were defined based on the simulation conditions. A surface roughness length of 0.13 m physically described the earth's surface for crop surface roughness heights of 0.095, 0.15, 0.265 and 0.13 m for winter, spring, summer and fall, respectively (WASP, 2006).

The wind velocity and air temperature were measured in the field, and the Pasquill-Gifford stability classes and rural mixing height used for h_{ABL} were obtained from the nearest weather station, namely the Pierre Elliott Trudeau Airport (Montreal, Canada) located 50 km north of the field sites. The Monin Obukhov length L_{MO} was estimated from the Pasquill stability categories for a surface roughness length of 0.13 m: L_{MO} ranges from -11 to -31 m for an air stability category B and from -31 to -151 m for an air stability category C (Golder, 1972). Knowing the wind velocity and air temperature profiles, z_0, L_{MO} and h_{ABL}, u_* and T_s were calculated using Eqns (7.7) and (7.10), respectively (Table 7. 2).

7.3.6. Calibrating the SST k-ω model

The SST k-ω model was initially calibrated for VRR, defined as the ratio of wind speed, at a height of 0.5 H and a downwind distance of 30 H, to that undisturbed at the same height, upwind from the windbreak. The field data collected by Naegeli in 1953 (Eimern *et al.*, 1964) was used for this calibration, where the windbreak was 2.2 m high and offered a permeability of 0.45 to 0.55. The simulation covered a 2-dimensional domain measuring 40 H (-10 H < x < 30 H) in length by 12 H (0 < y < 12 H) in height. The designed windbreak measured 2.2 m in height and width and its right side was positioned at x = 0 m. The mesh size measured 0.2 H and 0.1 H in the x and y directions, respectively. Assuming

neutral air conditions, z_0, h_{ABL}, u_* and T_s were set as 0.1 m, 800.1 m, 0.393 m s^{-1} and 294.063 K, respectively. The coefficients α and C_{ir} were 0.55 and 2.0, respectively.

The five field tests were used to calibrate the SST k-ω model. In the field, an odour generator was positioned at 15 or 30 m upwind from a natural windbreak. The windbreak consisted of a uniform single row of deciduous trees, 7 m in width by 9.2 m in height and 1050 m in length offering optical and aerodynamic porosities of 0.35 and 0.66, respectively (Table 7.2). The five field tests were conducted in September 2003 during the morning under atmospheric stability categories B, C and D and for odour emissions ranging from 744 to 1879 OU s^{-1} (Table 7.2). Three groups of four trained panellists observed the HT of the ambient air at various points downwind from the windbreak. Odour samples were taken at the odour source to determine the odour concentration by olfactometry in compliance with ASTM E679-91 Standard (1997) and CEN prEN13725 Standard (2001) (Lin et al., 2007).

Once calibrated for VRR, the SST k-ω model was calibrated to produce HT contour lines downwind from the windbreak. The SST k-ω model simulated odour mass concentration (SOMC) from the computed mass fraction (OMF) based on H_2S dispersion:

$$SOMC = \frac{OMF}{\frac{Y_2}{OC_g}} m_{H_2S} \times 10^9 \tag{7.29}$$

where SOMC is simulated odour (H_2S) mass concentration in μg m^{-3}; OMF is the odour (H_2S) mass fraction computed by the model for a given point in space, dimensionless; Y_2 and OC_g are odour mass fraction and odour concentration at odour generator defined by Eqn (7.5), dimensionless and OU m^{-3}, respectively, and; m_{H_2S} is the mass of H_2S required to produce 1.0 OU m^{-3} in kg OU^{-1} as expressed in Eqn (7.5).

Then, the exponential relationship between HT and SOMC was obtained by correlating the absolute value of the HT (MAHT) measured in the field with the

SOMC values computed for each 5 field tests (Table 7.2). The resulting regression equations were used to define simulated absolute HT (SAHT) as a function of SOMC. The values of MAHT and SOMC were statistically tested for significance to verify the adequacy of the correlation.

Being able to produce SAHT contours downwind from the windbreak, the SST k-ω model was then modified to also reproduce OC contours. Values of SAHT were converted into OC, by having the trained panellists evaluate for both HT and OC, 65 odour samples collected at the odour source during 17 days of field test. These odour samples were diluted to various levels and randomly presented to the 17 groups of 12 different panellists to produce 5527 pairs of HT and OC values (*Fig. 7.2*). Detected by a panellist at one level of OC, each HT value was significantly related to OC ($P < 0.01$) and the following regression equations were obtained for the average, max and min lines corresponding to the 95 % confidence interval, respectively:

$$OC = 0.92e^{-0.45HT} \tag{7.30}$$

$$OC = 6.73e^{-0.45HT} \tag{7.31}$$

$$OC = 0.13e^{-0.45HT} \tag{7.32}$$

where OC is odour concentration in OU m^{-3}, and; HT is odour hedonic tone from -10 to -1, for OC defined as zero when HT = 0. For HT = -2, the observed OC varied from the 0.3 to 16.6 OU m^{-3}, with a geometric mean of 2.3 OU m^{-3}, implying a panellists rating for HT = -2, of 16.6, 0.3 and 2.3, for the least, most and normal sensitive panellists.

The max line obtained (Eqn 7.32) approaches that measured by Lim et al. (2001) and Nimmermark (2006), while the min and average lines are much lower (*Fig. 7.2*). Although selected using the same standard, the panellists used for this research work were more sensitive to odours than those of Lim et al. (2001) and Nimmermark (2006), perhaps as a result of culture and past experience.

For OC =2 when HT = -1, Eqn (7.30) is replaced by:

$$OC = 1.3e^{-0.45HT} \tag{7.33}$$

Accordingly, when OC is more than 117 OU m^{-3}, HT remains at -10. Eqn 7.33 was used by the SST k-ω model to transform HT contour into OC contours.

The SST k-ω model was presumed to accurately reproduce MAHT values if the correlation between MAHT and SAHT was statistically significant, and the SAHT versus SOMC correlation lines obtained from the 5 simulations were similar in range.

7.3.7. Effect of windbreak tree characteristics

The fully calibrated SST k-ω model was used to verify the impact of different windbreak characteristics using 8 different computations (Table 7.3): 1, 2, and 3 for porosity; 4 and 5 for tree structure; 4 and 6 for tree height, and; 4, 7 and 8 for distance between the windbreak and the odour source. For the 8 computations, the ODS measured 690 m x 184 m x 73.6 m in the x, y and z direction. From the origin, the left and right faces were at 138 and 552 m while the back and front faces were at -92 and 92 m, respectively. The windbreak was 7 m wide and 9.2 m high except for test 6, where it was 4.6 m high. The odour source (*Fig.7.1*) measured 1.5 m in the x direction.

The mesh density was high in the vicinity of the odour source and windbreak, but decreased in the x, y and z directions resulting in 228, 81 and 46 segments, respectively. The neutral atmospheric conditions used for the 8 computations were based on a wind velocity and an air temperature of 3.95m s^{-1} and 294 K, respectively, at a height of 7.62 m. The depth of the atmospheric boundary layer was 1300.13 m to account for the surface roughness length of 0.13 m, as defined from the velocity recovery rate calibration. The wind was blowing from left to right along the positive x direction. The odorous source produced 3293 OU s^{-1} from an air flow rate of 1.653 m^3 s^{-1} and an OC of 1992 OU m^{-3}.

The aerodynamic porosities of 0.2, 0.4 and 0.66 were compared using an inertial resistance coefficient set according to Eqn (7.4). Aerodynamically, tree structure was defined from internal (surface area and volume of leaves, branches, trucks and seeds) and external characteristics (height, width and cross-sectional shape) (Zhou et al., 2002). The tree's internal structure was assumed to be an even

porous medium with a circular cross-section varying with height and tree type. Accordingly, *Fig. 7.3 (a)* illustrates a conifer with a diameter of 0.54 H at the ground level decreasing linearly to 0.39 H at a height of 0.62 H, and then falling faster to zero at 1.0 H:

$$D(z)=\begin{cases} D_1-\dfrac{D_1-D_2}{h_1}z & z\le h_1 \\ D_2-\dfrac{D_2}{H-h_1}(z-h_1) & h_1<z\le H \end{cases} \tag{7.34}$$

where $D(z)$ is the diameter of the conifer as a function of height z; H is tree height; h_1 is the height at which the diameter begins to decrease sharply with height; D_1 is the tree diameter at the ground, and; D_2 is the diameter at h_1.

Fig. 7.3 (b) illustrates the tree structure for a poplar with no leaves at the ground level over height h_1 and then a diameter gradually increasing to a specific value remaining almost constant thereafter up to height 1.0 H:

$$D(z)=\begin{cases} D_1 & 0\le z\le h_2 \\ D_1+\dfrac{D_2-D_1}{h_1}z & h_1<z\le h_2 \\ D_2 & h_2\le z\le h_3 \\ D_2-\dfrac{D_2}{H-h_3}(z-h_3) & h_3<z\le H \end{cases} \tag{7.35}$$

where D_1 is the tree trunk diameter; D_2 is the tree foliage diameter at h_2; h_1 is the height of the lowest branches; h_2 is the height where the tree foliage diameter reaches a maximum, and; h_3 is the height at which the diameter begins to shrink.

For both tree species, the horizontal cross sectional area $S_T(z)$ was:

$$S_T(z)=\frac{\pi}{4}D^2(z) \tag{7.36}$$

The average windbreak thickness was defined as the maximum tree diameter at height z:

$$w_T(z) = \frac{\pi}{4D_{MAX}} D^2(z) \tag{7.37}$$

where $w_T(z)$ is the thickness of the windbreak at height z, and; D_{MAX} is the maximum diameter of the tree.

The windbreak's inertial resistance coefficient C_{ir} is proportional to the tree's average thickness, the number of the trees making up the windbreak and the distribution of the trees in the x and y directions. Therefore, C_{ir} can be interpreted as:

$$C_{ir}(z) = C_{ir0} D^2(z) \tag{7.38}$$

where $C_{ir}(z)$ is the inertial resistance coefficient as a function of height z, and; C_{ir0} is a constant reflecting the factors influencing resistance. In the SST k-ω model, C_{ir0} can be simulated to give a specific aerodynamic porosity.

For conifers, h_1, D_1, and D_2 were equal to 0.64, 0.54 and 0.39 H and for the poplars, h_1, h_2, h_3, D_1, and D_2 were equal to 0.168, 0.31, 0.834, 0.021 and 0.229 H, respectively. For the conifer and poplar windbreaks, C_{ir0} was 0.0829 and 0.5257 m^{-3}, respectively, based on an aerodynamic porosity of 0.4 and a windbreak height of 9.2 m.

The windbreak heights of 9.2 and 4.6 m were compared, assuming a single row of conifers with an aerodynamic porosity of 0.4. The values of 15, 30 and 60 m were used to verify the effect of distance between the windbreak and odour generator.

7.4. Results and discussion

7.4.1. Calibrating the SST k-ω model for velocity recovery rate

For the 2-dimensional calibration, the SST k-ω model required a turbulence length scale l of twice the roughness length of the earth's surface. *Fig. 7.4* shows the simulated and measured wind speed around the windbreak at half height (1.1 m). As compared to the measured values, the simulated VRR values were: 4.5% under

from -10 to 0 *H* and 10 to 30 *H*; 9% under from 2 *H* to 10 *H*, and; equal at 30 *H*. Overall, an R^2 of 0.98 was observed between the measured and simulated velocity.

7.4.2. Calibrating the SST k-ω model for odour dispersion

The five simulations in table 7.2 calibrated the SST k-ω model for odour dispersion. For simulation 1, SOMC versus MAHT is illustrated in *Fig.7.5a*, where SOMC is expressed in μg m^{-3} and plotted against MAHT using an absolute scale of 1 to 10. The regression equation obtained was statistically significant ($P < 0.01$) and was used as transform function of SOMC into simulated absolute hedonic tone (SAHT) in form:

$$SAHT = aSOMC^b \tag{7.39}$$

where SAHT is the simulated absolute hedonic tone; SOMC is the simulated odour mass concentration in μg m^{-3} and; $a = 0.690$ and $b = 0.445$ for simulation 1.

Similarly, the correlations between SAHT and SOMC for the 5 simulations were statistically significant ($P = 0.01$). The value of their parameters *a* and *b* are listed in Table 7.2 (*Fig. 5b)* and are all within close range of each other. Curves 3 and 4 were measured on the same day but with the odour generator located at 15 and 30 m from the windbreak, and under different temperatures. In *Fig. 5b*, slight differences also result from the variability in the human perception of HT and different source of swine manure used for each test day.

Using the 92 pairs of MAHT and SOMC values obtained from the five simulations, the following average transformation function was statistically significant ($P < 0.01$) with an $R^2 = 0.52$:

$$SAHT = 0.57SOMC^{0.46} \tag{7.40}$$

Simulations 1 and 2 produced SAHT lines found in the centre of the MAHT, indication that the model can reproduce measured HT (*Fig. 6a*). Depending on the test, the R^2 value ranged from 0.46 to 0.87 (Table 7.2) and the correlated values were statistically significant ($P < 0.01$). The SOC lines transformed from the SAHT values were also found in the centre of the MOC values and offered R^2 ranging from 0.43 to 0.98.

The statistically significant correlation between the observed and calculated values indicated that the SST k-ω model did accurately predict odour plume HT and OC contours downwind from windbreaks.

7.4.3. Effect of windbreak porosity

The amount of air flowing through the windbreak is determined by the inertial resistance coefficient C_{ir} in Eqn (7.4) for given H, h_1, w_1, w_2, and w_3 values. The value of H and h_1 were 9.2 and 6.9 m for the three simulations, respectively. An aerodynamic porosity of 0.2, 0.4 and 0.66 resulted in w_1, w_2, and w_3 values of: 4.508, 3.864 and 0.644 for $\alpha = 0.2$; 1.204, 1.032 and 0.172 for $\alpha = 0.4$, and; 0.38, 0.2598 and 0.16 for $\alpha = 0.66$, respectively. The odour plume contours for the three aerodynamic porosities are shown in *Fig. 7.7a, b & c,* on the horizontal plane at height $z = 1.5$ m. The odour source was located 30 m upwind from the windbreak (green bar).

The aerodynamic porosity of 0.2 produced an odour plume where 5 OU m^{-3} was reached at 97 m downwind from the source while 3.2 and 2.6 OU m^{-3} were reached at 198 m and 366 m, respectively. The aerodynamic porosity of 0.4 produced an odour plume where 5 OU m^{-3} was reached at 148 m or 51 m further than for an aerodynamic porosity of 0.2; it also took 271 and 475 m to reach 3.2 and 2.6 OU m^{-3}, respectively or 73 and 109 m more. The aerodynamic porosity of 0.66 produced an odour plume where 5 OU m^{-3} was reached at 243 m, or 146 m further than for an aerodynamic porosity of 0.2; it took 422 and over 522 m to reach 3.2 and 2.6 OU m^{-3}, respectively, or 224 m and more than 186 m further, as compared to an aerodynamic porosity of 0.2. Furthermore, the odour plume width (2 OU m^{-3}) for aerodynamic porosities of 0.2, 0.4 and 0.6 were 100, 52 and 42 m, respectively. Thus, the lower aerodynamic porosity produced a wider odour plume, because more odorous air was trapped immediately downwind from the windbreak.

A lower aerodynamic porosity favours a more intensive atmospheric mixing resulting from the creation of a larger zone of low turbulence immediately downwind from the windbreak. Odours trapped in this low turbulence zone have a

longer retention time and are more intensively dispersed when released. The more porous windbreak allows too much odorous air to pass through its foliage without dispersion.

7.4.4. Effect of tree structure and height

Figs. 7.8 (a) & (b) display the odour plume developing on the vertical plane (y = 0 m) for windbreaks consisting of a single row of conifers or poplars, respectively. By contrast, the distance required to reach 2.6 OU m^{-3} is 531 m for the conifers and 494 m or 37 m shorter for the poplars. The 5 OU m^{-3} contour (red zone) reached a distance of 146 m for the conifers and 164 m or 18 m longer for the poplars, but the width of the plume created by the conifers was 48 m or 2 m wider than that of the poplars. Both windbreaks produce the same height of odour plume for 2 OU m^{-3} (Table 7.3).

By creating a different air flow profile, the poplar windbreak had a slightly shorter plume (2 OU m^{-3}) as compared to that of conifers for the same aerodynamic porosity (*Fig. 7.9*). The velocity gradient created by the conifer windbreak gradually increased with height especially above 6.4 m as tree sectional area decreased. For the poplar windbreak, the velocity quickly increased because of the open space close to the ground, but quickly decreased with height because of denser foliage and more air resistance right up to 1.0 *H*.

Although air flow styles through the two windbreaks were quite different, the length of the odour plumes in *Figs. 7.8 (a) & (b)* was similar because the same amount of the air flowed through the two windbreaks. This observation is consistent with the air flow analysis conducted by Wilson (1987).

Fig. 7.10 shows the odour plume forming downwind from two conifer windbreaks with an aerodynamic porosity of 0.4 but a height of 4.6 m and 9.2 m. The taller windbreak formed an odour plume with a 3.2 OU m^{-3} contour at a distance of 295 m, compared to over 525 m for the 4.6m windbreak. For the shorter windbreak, an odour concentration of 5 OU m^{-3} was reached at 252 m, or 106 m further than that of the taller windbreak. The shorter windbreak formed an

odour plume reaching a height of 20 m as compared to the taller windbreak, where the odour plume reached a height of 22 m or 2.0 m more (Table 7.3). Thus, the size of the low turbulence zone was directly related to the height of the windbreak trees.

7.4.5. Effect of the distance between odour source and windbreaks

Figs. 7.11 (a), (b) and (c) show the odour plume developing for a source located 15, 30 and 60 m upwind from the windbreak. For windbreak positioned at 15, 30, and 60 m from odour source, the 3.2 OU m^{-3} contours occurred at a distance of 282, 295, 321 m from the source. When the windbreak is closer to the odour source, a shorter odour plume is produced. However, the 3.2 OU m^{-3} contour occurred 260, 258, and 254 m downwind from the windbreak for the 15, 30, and 60 m distance. Because at height z = 1.5 m and immediately upwind from the windbreak, SOMCs of 1575, 890 and 497 μg m^{-3} were observed for the 15, 30 and 60 m distance, respectively, the odour plume length (3.2 OU m^{-3} contour) measured from the windbreak decreased with increasing distance between the odour source and windbreak.

7.5. Conclusions

The objective of the project was to calibrate and validate the SST k-ω model to simulate odour dispersion around windbreaks and then to use this calibrated model to observe the effect of tree characteristics on odour plume size. The model was calibrated for odour dispersion using field data measured by panellists.

The simulations produced the following conclusions:

1. The SST k-ω model simulated the velocity recovery rate (VRR) observed downwind from a 2-dimensional windbreak with a general error of 4.5%, up to a downwind distance of 30 H, where H is the height of the windbreak;
2. The odour mass concentration calculated by the SST k-ω model was successfully transformed into HT and odour concentration values. Although HT is subjected to the variable sensitivity of panellists, all

curves simulated from 5 different tests fell within a close range of each other;

3. The SST k-ω model was able to accurately reproduce the odour hedonic tone (HT) and odour concentration (OC) measured by the panellists in the field around a windbreak. The correlations between the simulated and measured absolute HT and between the simulated and measured OC were statistically significant ($P < 0.01$);
4. A less porous or denser windbreak (aerodynamic porosity of 0.2 versus 0.4 and 0.66) produced a shorter, wider and more intense odour plume;
5. Assuming that the air flow resistance was proportional to the square of the tree diameter, the trees type had a small effect on the size of the odour plume when they had the same porosity . As opposed to conifers, poplars created a slightly shorter odour plume for the same aerodynamic porosity;
6. A taller windbreak resulted in a shorter odour plume, by creating a taller low turbulence zone downwind from the windbreak, where more odours were trapped and retained for dispersion;
7. When close to odour source, the windbreak produces a shorter odour plume.

7.6. Acknowledgement

The authors wish to acknowledge the financial contribution of Consumaj inc., CDAQ, the Livestock Initiative Program, Agriculture and Agro-Food Canada and the Natural Sciences and Engineering Research Council of Canada.

7.7. References

ASHRAE (1997). ASHRAE fundamentals handbook. American Society of Heating, Refrigeration and Air Conditioning, Atlanta, Georgia, USA, 13.1-13.6

ASTM. 1997. Standard Practice for Determination of Odor and Taste Thresholds By a Forced-Choice Ascending Concentration Series Method of Limits, American Society for the Testing of Materials, Washington, DC, USA.

Bird RB; Stewart W E; Lightfoot E N (2002). Transport phenomena. John Wiley, New York, USA, 895pp

Blackadar A K (1997). Turbulence and diffusion in the atmosphere: lectures in environmental sciences. Springer Berlin publishers, New York, USA, 185pp

Carruthers D J; Dyster S J (2003). Boundary layer structure specification, ADMS 3 P09/01T/03 http://www.cerc.co.uk/software/pubs/3-1techspec.htm visited in April 2006

CEN (2001). Air quality - determination of odour concentration by dynamic olfactometry. prEN13725, European Committee for Standardization, Brussels. http://www.aerox.nl/images/eurstandard.pdf, visited in August 2004

Dirkse M H; van Loon W K P; van der Walle T; Speetjens S L; Bot G P A (2006). A computational fluid dynamics model for designing heat exchangers based on natural convection. Biosystems Engineering, 94(3), 443-452

EPA (2001). Odour impacts and odour emission control measurement for intensive agriculture, <http://www.epa.ie/pubs/docs/Odour%20Impacts%20Final.pdf>, visited in July 2006

Golder D (1972). Relations among stability parameters in the surface layer. Boundary-Layer Meteorology, 3(1), 47

Gorgy T G A (2003). Validation of an air dispersion model for odour impact assessment. Thesis M Eng Thesis, McGill University, Montreal, Canada

Gosman A D (1999). Developments in CFD for industrial and environmental applications in wind engineering. Journal of Wind Engineering and Industrial Aerodynamics, 81(1-3), 21-39

Guo H; Jacobson L D; Schmidt D R; Nicolai R E (2001). Calibrating inpuff-2 model by resident-panellists for long-distance odour dispersion from animal production sites. Transactions of the ASAE, 17(6), 859-86

Hinze J O (1975). Turbulence. McGraw-Hill, New York, 790 pp

Jacobson M Z (1999). Fundamentals of atmospheric modeling. Cambridge University Press, Cambridge, UK, 656 pp

Li Y and Guo H (2006). Comparison of odor dispersion prediction between CFD model and CALPUFF model, Paper # 064102, 2006 ASABE Annual International Meeting. American Socienty of Agricultural and Biological Engineer, Oregon Convention Center, Portland, Oregon. 9 - 12 July 2006.

Lien F-S; Yee E (2005). Numerical modelling of the turbulent flow developing within and over a 3-d building array, part iii: a distributed drag force approach, its implementation and application. Boundary-Layer Meteorology, 114(2), 287 - 313

Lien F-S; Yee E; Wilson JD (2005). Numerical modelling of the turbulent flow developing within and over a 3-d building array, part ii: a mathematical foundation for a distributed drag force approach. Boundary-Layer Meteorology, 114(2), 245-287

Lien F S; Yee E; Cheng Y (2004). Simulation of mean flow and turbulence over a 2D building array using high-resolution CFD and a distributed drag force approach. Journal of Wind Engineering and Industrial Aerodynamics, 92,117-158

Lin X J; Barrington S; Nicell J; Choiniere D; Vezina A (2006). Influence of windbreaks on livestock odour dispersion plume in the field. Agriculture. Ecosystems & Environment, 116 (3-4), 263-272.

Lin X J; Barrington S; Gong G; Choinière D (2007a). Simulation of odour dispersion downwind from natural windbreaks using the CFD standard k-ε model. Transactions of the ASAE presented for publication in January 2007.

Lin X J ; Barrington S; Nicell J; Choinière D (2007b). Effect of natural windbreaks on maximum odour dispersion distance (MODD). Canadian Biosystems Engineering, 49: 6.21 - 6.32.

Menter F R; Kuntz M; Langtry R (2003). Ten years of industrial experience with the SST turbulence model. In: K. Hanjalic, Y. Nagano and M. Tummers (Editors), Turbulence, heat and mass transfer 4. Begell House Inc, Redding, CT, pp. 625-632.

O'Neill D H; Phillips V R (1992). A review of the control of odour nuisance from livestock buildings: Part 3, properties of the odorous substances which have been identified in livestock wastes or in the air around them. Journal of Agricultural Engineering Research, 53, 23-50

Packwood A R (2000). Flow through porous fence in thick boundary layers: comparisons between laboratory and numerical experiments. Journal of Wind Engineering and Industrial Aerodynamics, 88, 75-90

Panofsky H A; Dutton J A (1984). Atmospheric turbulence: models and methods for engineering applications. Wiley, New York, USA, 397 pp

Patton E G; Shaw R H; Judd M J; Raaupach M R (1998). Large-eddy simulation of windbreak flow. Boundary-Layer Meteorology, 87, 275-306

Riddle A; Carruthers D; Sharpe A; McHugh C; Stocker J (2004). Comparisons between FLUENT and ADMS for atmospheric dispersion modelling. Atmospheric Environment, 38 (7), 1029-1038

Saatdjian E B (2000). Transport phenomena: equations and numerical solutions. John Wiley, New York, USA, 414 pp

Schauberger G; Pringer M; Petz E (2000). Diurnal and annual variation of the sensation distance of odor emitted by livestock building calculated by the Austrian odour dispersion model(AODM). Atmospheric Environment, 34, 4839-4851

Schnelle K B; Dey P R (2000). Atmospheric dispersion modeling compliance guidelines. McGraw-Hill Publishers, New York, USA

Schwartz R C; Fryrear D W; Harris B L; Billbro J D; Juo A S R (1995). Mean flow and shear stress distributions as influenced by vegetative windbreak structure. Agricultural and forest meteorology, 75, 1-22

Sheridan B A; Curran T P; Dodd V A (2002). Assessment of the influence of media particle size on the biofiltration of odorous exhaust ventilation air from a piggery facility. Bioresource Technology, 84, 129-143

Sun H; Stowell R R; Keener H M; Michel F C (2002). Comparison of predicted and measured ammonia distribution in a high-riseTM hog building (HRHB) for summer conditions. Transactions of the ASAE, 45 (5), 1559-1568

Ucar T; Hall F R (2001). Review windbreaks as a pesticide drift mitigation strategy: a review. Pest Management Science, 57, 663-675

Wang, H; Takle E S (1995). A numerical simulation of boundary-layer flows near shelterbelts. Boundary-Layer Meteorology, 75(1 - 2), 141-173

Wilson J D (2004). Oblique, stratified winds about a shelter fence. part II: Comparison of measurements with numerical models. Journal of Applied Meteorology, 43 (10), 1392-1409

Wilson J D (1985). Numerical study of flow through a windbreak. Journal of Wind Engineering and Industrial Aerodynamics, 21, 119-154

Wilson J D (1987). On the choice of a windbreak porosity profile. Boundary-Layer Meteorology, 38 (1 - 2), 37

Wilson J D; Yee E (2003). Calculation of winds distribution by an array of fences. Agricultural and forest meteorology, 115, 31-50

Zhou X H; Brandle J R; Takle E S; Mize C W (2002). Estimation of the three-dimensional aerodynamic structure of a green ash shelterbelt. Agricultural and Forest Meteorology, 111(2): 93.

Zhu J; Jacobson L D; Schmidt D R; Nicolai R (2000). Evaluation of inpuff-2 model for predicting downwind odors from animal production facilities. American Society of Agricultural Engineers, 16(2): 159-164.

Nomenclature

AHT is absolute value of odour hedonic tone
a_s is a constant
C_{ir} is the inertial resistance coefficient
C_{ir0} is the constant
D_1 and D_2 are the tree diameters
D_{MAX} is the maximum of the diameters of a tree
$D_{i,m}$ is the diffusion coefficient for species i in the gaseous mixture
$D_{T,i}$ is the thermal diffusion coefficient for species i in the gaseous mixture
H is the total height of the windbreak
HT is odour hedonic tone
H_F is the vertical heat flux
h_1, h_2 and h_3 are the windbreak height at which the porosity changes, with a value between 0 and H
h_{ABL} is the height of the atmospheric boundary layer
J_i is the diffusion flux of species i
k is the turbulence kinetic energy
k_a is the von Karman constant, ranged from 0.35 to 0.43, usually $\kappa_a \approx 0.4$
l is the turbulence length scale
L_{MO} is the Monin Obukhov length
M is the molecular weight of dry air (0.028966kg mol^{-1})
MAHT is measured absolute hedonic tone
MOC is measured odour concentration in OU m^{-3}
m_{H_2S} is the mass of hydrogen sulphide in one odour unit
OC is the odour concentration in OU m^{-3}
OMF is odour mass fraction
p is the static pressure
R is the universal gas constant (8.31432J mol^{-1} K^{-1})
SAHT is simulated absolute hedonic tone
Sc_t is the turbulent Schmidt number generally equal to 0.7
SOC is simulated odour concentration in OU m^{-3}
SOMC is simulated odour mass concentration in μg m^{-3}
$S_T(z)$ is the horizontal section area of an element or tree at height z
T is temperature
T_s is the temperature at the z_s
T_{WC} is a factor to control the convective energy varied with height
T_{WN} is a factor controlling the drop in TKE with height within the atmospheric boundary layer
t is time
$\boldsymbol{u}$ is instantaneous velocity
u and u' are mean and fluctuating component of instantaneous velocity
u_* is the friction velocity

u_i (i=1, 2, 3) is scalar component of the mean velocity in ith direction, indicating in x, y, z direction in Cartesian coordinate system, respectively

u_i' (i=1, 2, 3) is the fluctuating component of the instantaneous velocity in ith direction, indicating in x, y, z direction in Cartesian coordinate system, respectively

u_{mag} is magnitude of mean velocity

w_* is the mixing layer velocity scale

z_0 is roughness length

z_s is a height of 1.35m above surface

w_1, w_2 and w_3 are three constants corresponding to the thickness of the real windbreak

$w_T(z)$ is the thickness of the windbreak at the height z

Y_j is the mass fraction of the species j in a mixture of gases

Y_2 is the odour mass fraction at the odour generator

z is a coordinate in the vertical direction

α is the aerodynamic porosity, or permeability

α^{-1} is the viscous resistance coefficient

μ is viscosity of mixture of the air and odorous gases

μ_t is the turbulence kinetic viscosity

ρ is fluid density

ω is the specific dissipation rate

σ_u, σ_v and σ_w are turbulence components in x, y, z coordinates

γ_d is dry adiabatic lapse rate, 0.01 K m^{-1}

Tables and Figures

Table 7.1
Fluid properties used to simulate odour dispersion

Property	*Mixture*	*Air*	*H_2S*
Density, kg m^{-3}	Impressible-ideal-gas law		
Cp, J kg^{-1} K^{-1}	Mixing law	1005.422[a]	1005.333[a]
Thermal conductivity, W m^{-1} K^{-1}	Mass-weighted-mixing-law	0.0260411[a]	0.0137023[a]
Viscosity, kg m^{-1} s^{-1}	Mass-weighted-mixing-law	1.458E-6 $T^{1.5}$ / (T + 110.1)	-1.4839E-6 + 5.1E-8T -1.26E-11 T^2
Mass diffusivity, m^2 s^{-1}	-1.3497E-5 + 1.05772E-7 T[a]		
Thermal diffusivity coefficient, kg m^{-1} s^{-1}	Kinetic-theory		
Molecular weight, kg kgmol^{-1}		28.966	34.07994

Note: *T* is temperature in K;
[a] temperature range of 283 to 313 K.

Table 7.2
Five simulations for calibration the SST k-ω model

Description	Unit	Simulation				
		1	2	3	4	5
Date		Sep 3	Sep 10	Sep 15	Sep 15	Sep 18
ODS dimensions						
x_L	m	-138	-138	-138	-138	-138
x_R	m	552	552	552	552	552
Y_F	m	-184	-368	-184	-184	-368
Y_B	m	92	46	92	92	92
z_H	m	73.6	73.6	73.6	73.6	73.6
Windbreak height	m	9.2	9.2	9.2	9.2	9.2
Windbreak width	m	7	7	7	7	7
OG	m	30	30	15	30	15
AS	A-F	B	D	D	D	C
L_{MO}	m	-15	Infinite	Infinite	infinite	-90
Z_0	m	0.13	0.13	0.13	0.13	0.13
h_{ABL}	m	1300	1685	1753	1753	990
u_{mag} at 7.62m	ms^{-1}	3.95	2.65	4.93	3.54	1.5
T at 7.62m	°K	294	300	301	297	297
WD	°	0	-50	-23	-6	-49
OE	OU s^{-1}	1373	1096	744	745	1879
Transform function: SAHT = a SOMC ^{b}						
a		0.690	0.237	0.818	0.458	0.358
b		0.445	0.800	0.469	0.543	0.499
n		19	29	13	12	19
R^2 for MAHT and SOMC		0.62	0.50	0.67	0.87	0.47
F-test (P =0.01)		SG	SG	SG	SG	SG
R^2 for MAHT and SAHT		0.59	0.72	0.56	0.87	0.46
F-test (P =0.01)		SG	SG	SG	SG	SG
R^2 for MOC and SOC		0.52	0.98	0.49	0.80	0.43
F-test (P =0.01)		SG	SG	SG	SG	SG

Note: ODS - odour dispersion systems; x_L and x_R are the x-coordinates of left and right faces of the ODS, respectively; y_B and y_F are the y-coordinates for the back and front faces, respectively; and z_H is the height from the bottom to the top faces; OG – odour generator distance downwind from the windbreak; WD - wind direction with respect to the x-axis, 0° being perpendicular to the windbreak; OE – average odour emission during the test; AS – Pasquill-Gifford atmospheric stability conditions where B and C are unstable classes and D is a neutral class; SAHT – simulated absolute hedonic tone; SOMC – simulated odour mass concentration, μg m^{-3}; SG – significant; MAHT – measured absolute hedonic tone; MOC – measured odour concentration; SOC – simulated odour concentration.

Table 7.3
Effect of various windbreak parameters

Description	Unit	Simulation							
		1	2	3	4	5	6	7	8
Factor		Porosity			Conifer	Poplar	Height	Distance	
Windbreak parameters									
α		0.2	0.4	0.66	0.4	0.4	0.4	0.4	0.4
H	m	9.2	9.2	9.2	9.2	9.2	4.6	9.2	9.2
h_1	m	6.9	6.9	6.9					
w_1		4.508	1.204	0.38					
w_2		3.864	1.032	0.2598					
w_3		0.644	0.172	0.16					
C_{ir0}	m^{-1}				0.0829	0.5257	0.0829	0.0829	0.0829
OG	m	30	30	30	30	30	30	15	60
Calculated odour plume									
L2.6	m	366	475	>552	531	494	>552	519	>552
L3.2	m	198	271	422	295	288	525	282	321
L5	m	97	148	243	146	164	252	133	170
Width	m	100	52	42	48	46	41	48	48
Heigth	m	22	22	22	22	22	20	21	19

Note: α – aerodynamic porosity, OG – odour generator distance downwind from the windbreak; L2.6, L3.2 and L5 stand for the odour plume length at the 2.6, 3.2 and 5.0 OU m^{-3} contour.

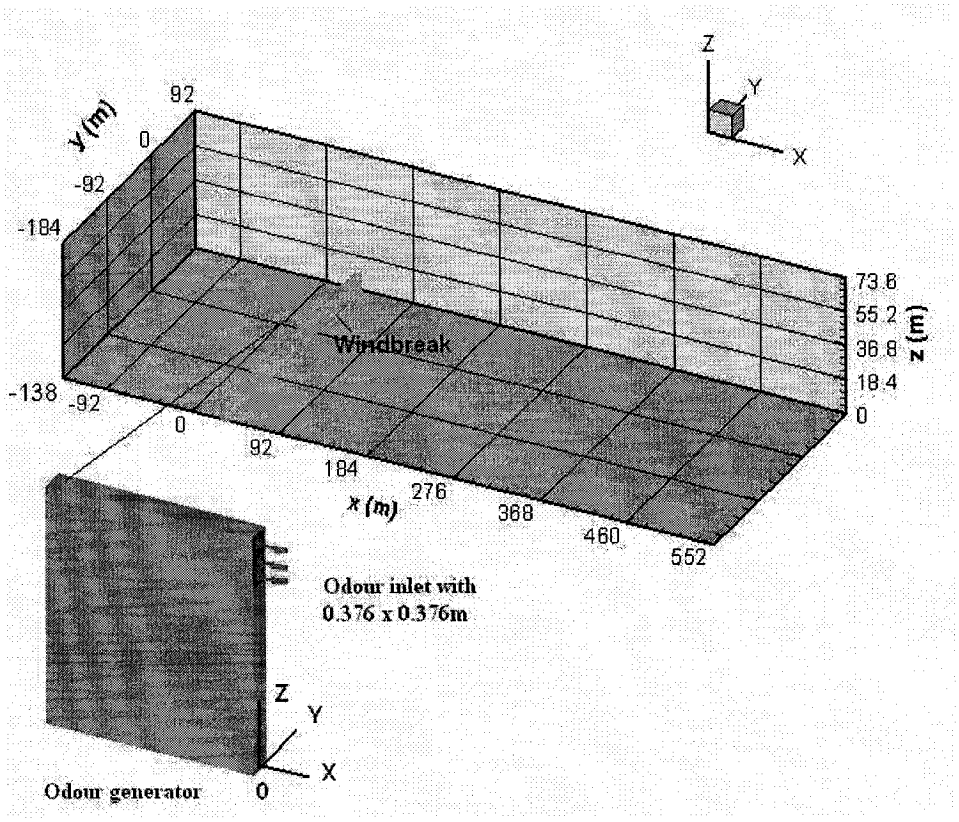

Fig. 7.1. Schematic of the computational volume used to predict odour dispersion. The z coordinate is magnified twice for illustration purposes and the windbreak optical porosity is 0.35. The green bar represents the windbreak. The central position of the generator's odour emission surface stands at x = 0 m, y = 0 m and z = 1.562 m.

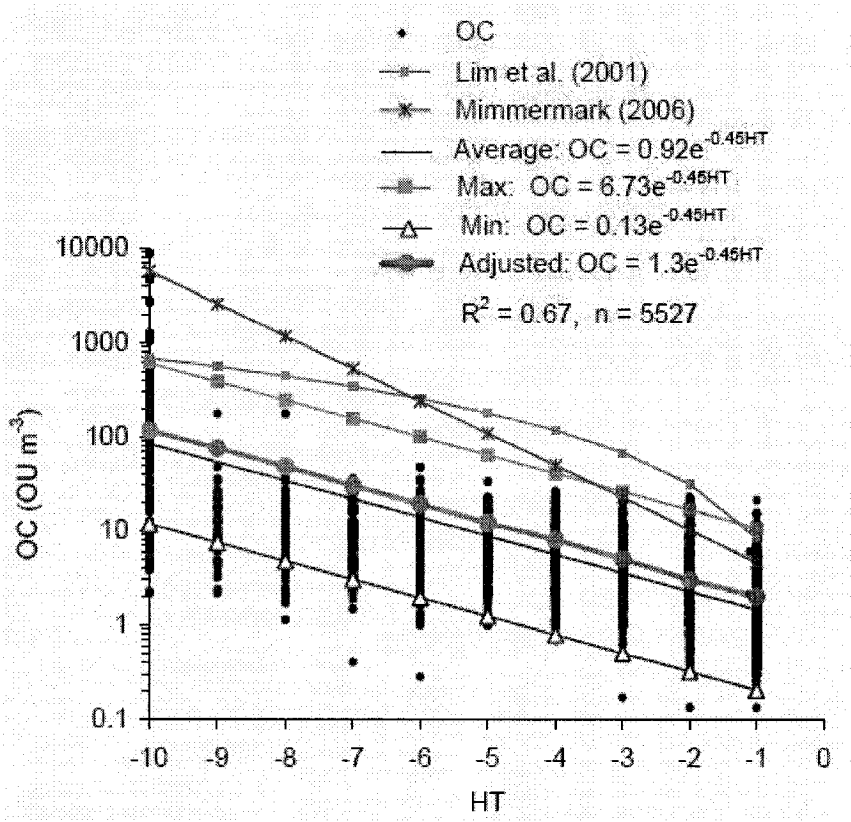

Fig. 7.2. Relationship among 5527 pairs of odour hedonic tone (HT) and odour concentration (OC) observations from the 65 odour samples measured by 17 groups of 12 panellists compared to that of Lim et al. (2001) and Nimmermark (2006). The average represents the exponential regression of all the data, while the maximum and minimum represent the 95 % confidence interval. The Adjusted line is line a little higher than the average with 2 OU m^{-3} at HT is -1. R^2 is the correlation coefficient between the HT and OC and n is total pairs of data.

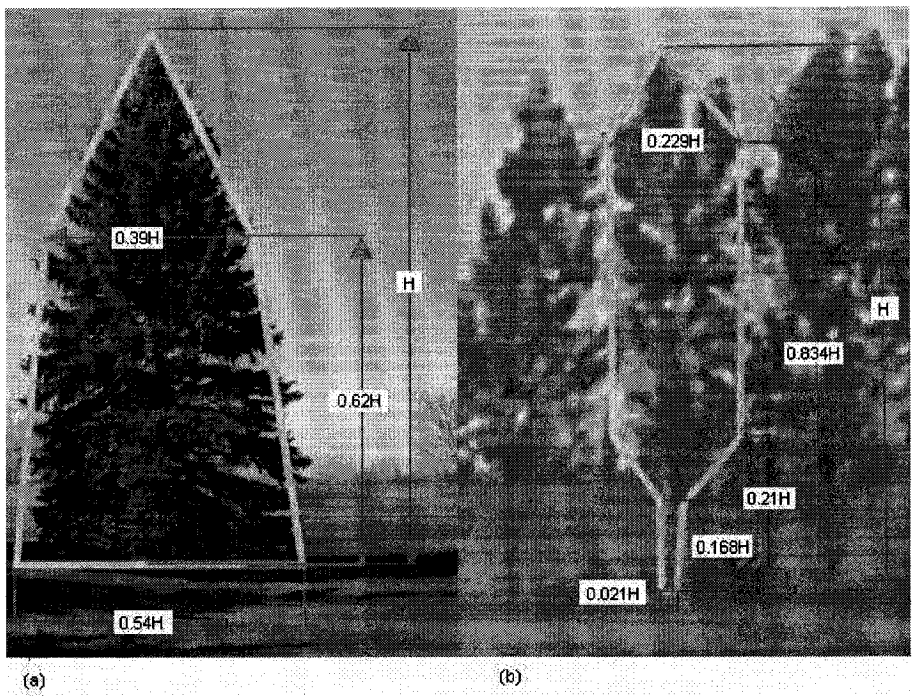

Fig. 7.3. Structure of the trees: (a) conifer, (b) poplar. Note: *H* is the tree height.

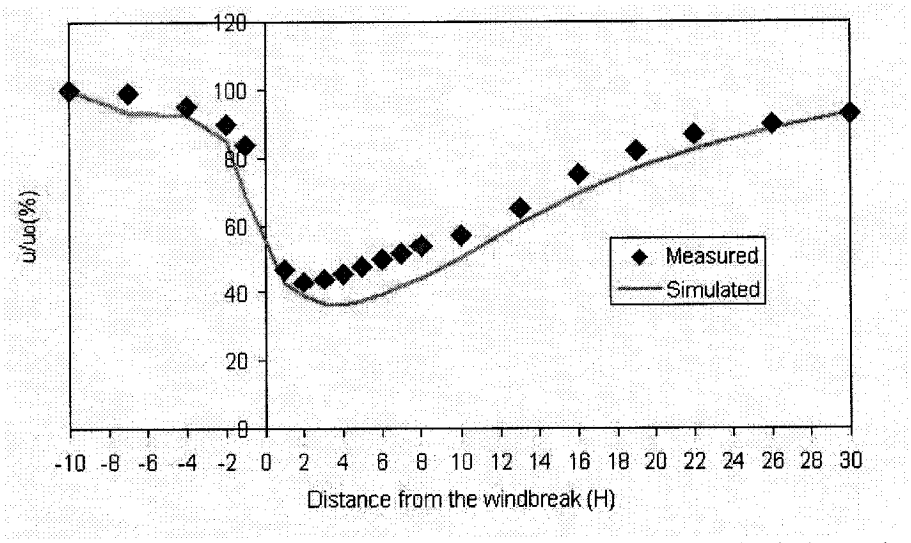

Fig. 7.4. Comparison of the SST k-ω simulated and measured wind speeds at windbreak half height where u is wind speed, u_0 is the undisturbed wind speed, and H is height of the windbreak. The measured wind speed is from Naegeli, 1953 (Eimern *et al.*, 1964).

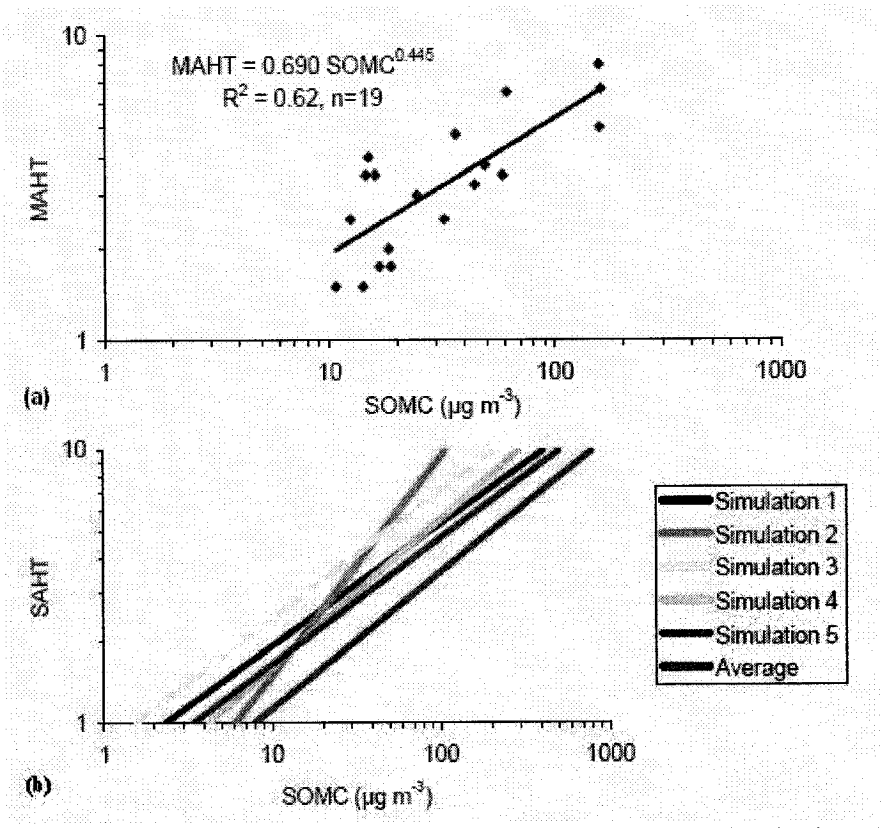

Fig. 7.5. (a) For simulation 1, correlation between the simulated odour (H_2S) mass dispersion (SOMC) and the field measured absolute hedonic tone (MAHT). This correlation produced an equation defining the simulated absolute hedonic tone (SAHT); (b) For the 5 simulated tests, transformation of SOMC into simulated absolute hedonic tone (SAHT).

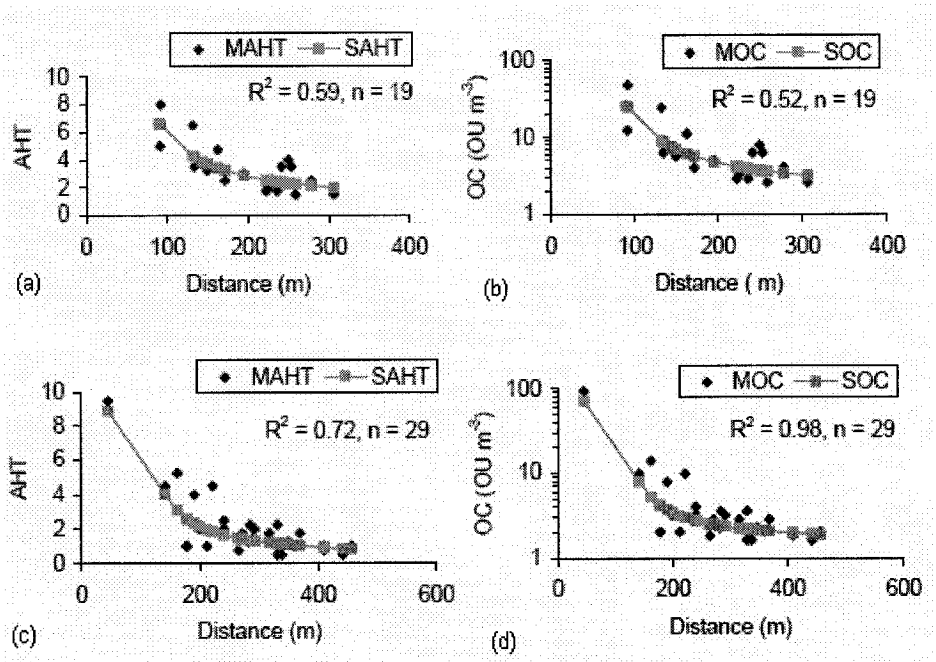

Fig. 7.6. (a) and (c). Measured and simulated absolute hedonic tone for simulations 1 and 2, respectively, where AHT is the absolute hedonic ton, MAHT and SAHT are the measured and simulated hedonic tone, respectively, R^2 is the correlation coefficient between the MAHT and SAHT and n is odour points measured; (b) and (d): Measured and simulated odour concentration for simulations 1 and 2, respectively, where OC is odour concentration, MOC and SOC are respective measured and simulated OC, and R^2 is the correlation coefficient between MOC and SOC. The x axis indicates the distance from the odour source.

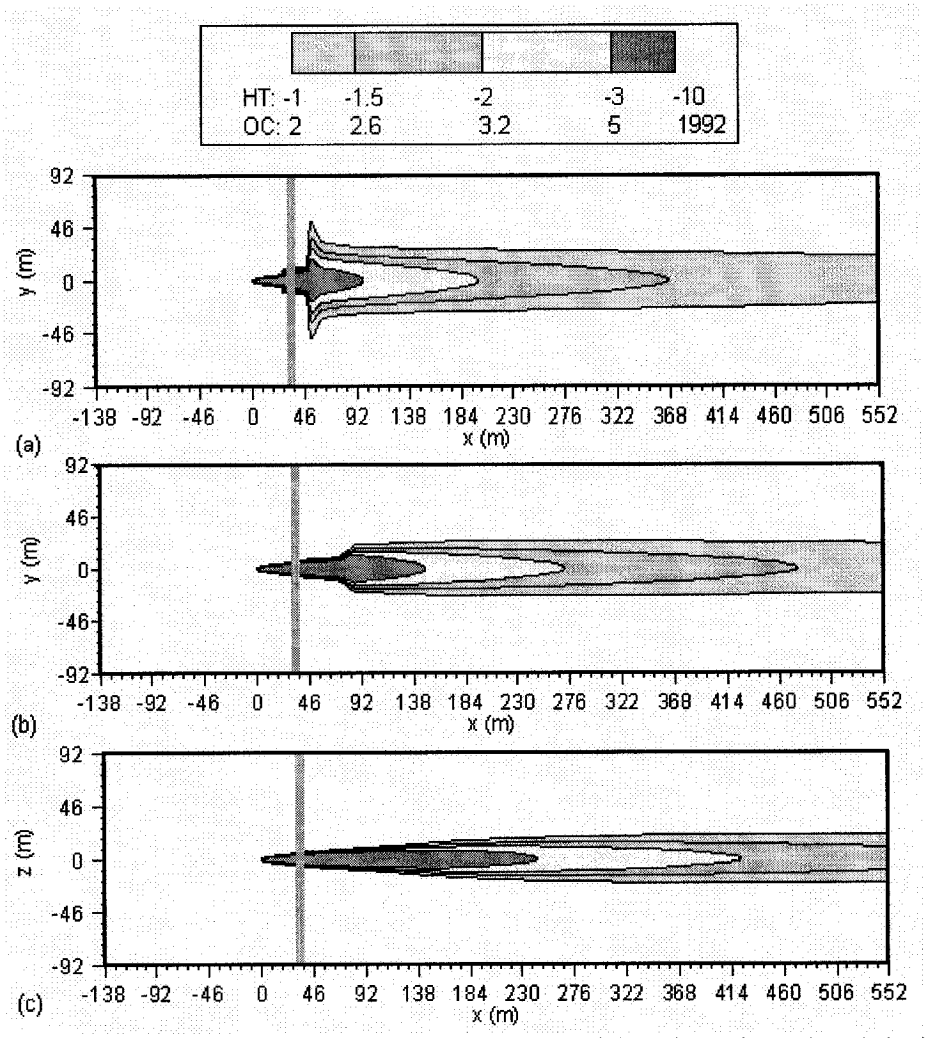

Fig. 7.7. Effect of windbreak porosity. Contours of the odour plume (z = 1.5 m) for an aerodynamic porosity of (a) 0.2 (simulation 1 in Table 7.3), (b) 0.4 (simulation 2) and (c) 0.66 (simulation 3), respectively. The green bar is the windbreak and the unit of the odour concentration is OU m^{-3}.

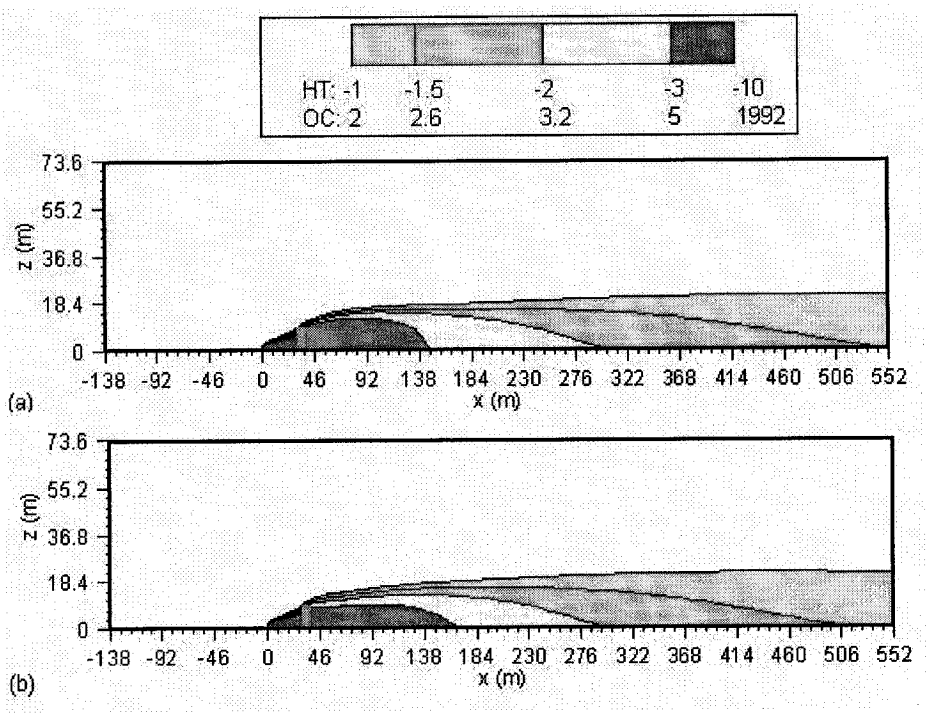

Fig. 7.8. Effect of tree types. Contours of the simulated odour plume (y = 0 m) for the (a) conifer windbreak (simulation 4), (b) poplar windbreak (simulation 5), Note: both windbreaks have an aerodynamic porosity of 0.4 and a height of 9.2 m, and are subjected to neutral atmospheric conditions.

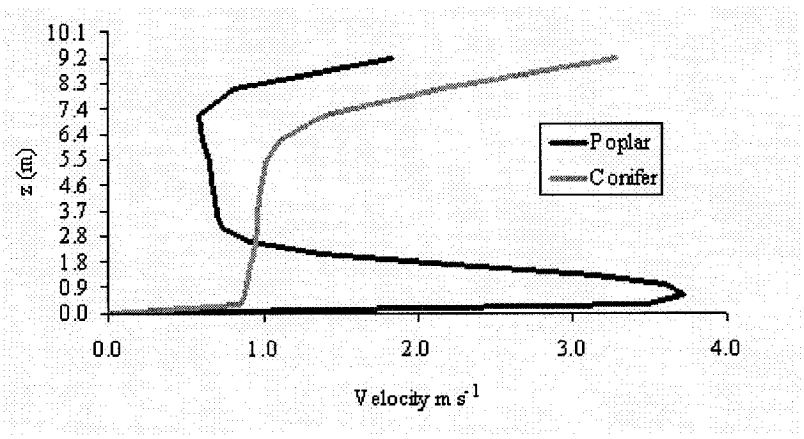

Fig. 7.9. The velocity in the z direction, at x = 37 m, immediately behind the windbreak as a function of height, for the conifer and the poplar windbreaks.

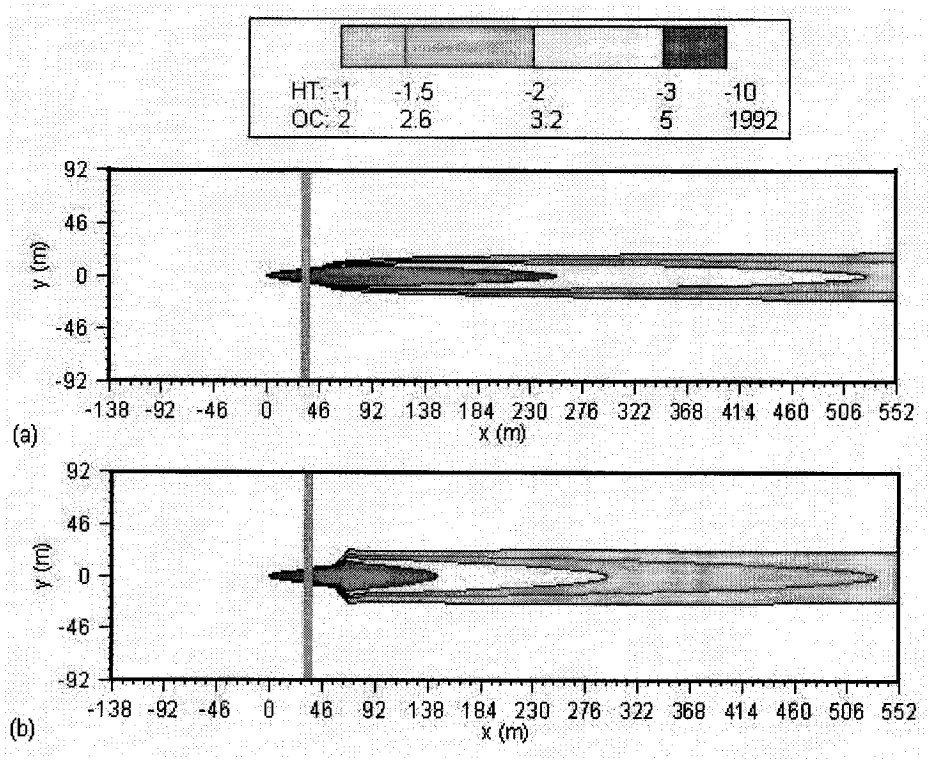

Fig. 7.10. Effect of windbreak height. Contours of the simulated odour plume for conifer windbreaks on horizontal plane (z = 1.5 m) (a) windbreak with height of 4.6 m (simulation 6), (b) windbreak with height of 9.2 m (simulation 4). Note: the aerodynamic porosity of the both windbreaks is 0.4.

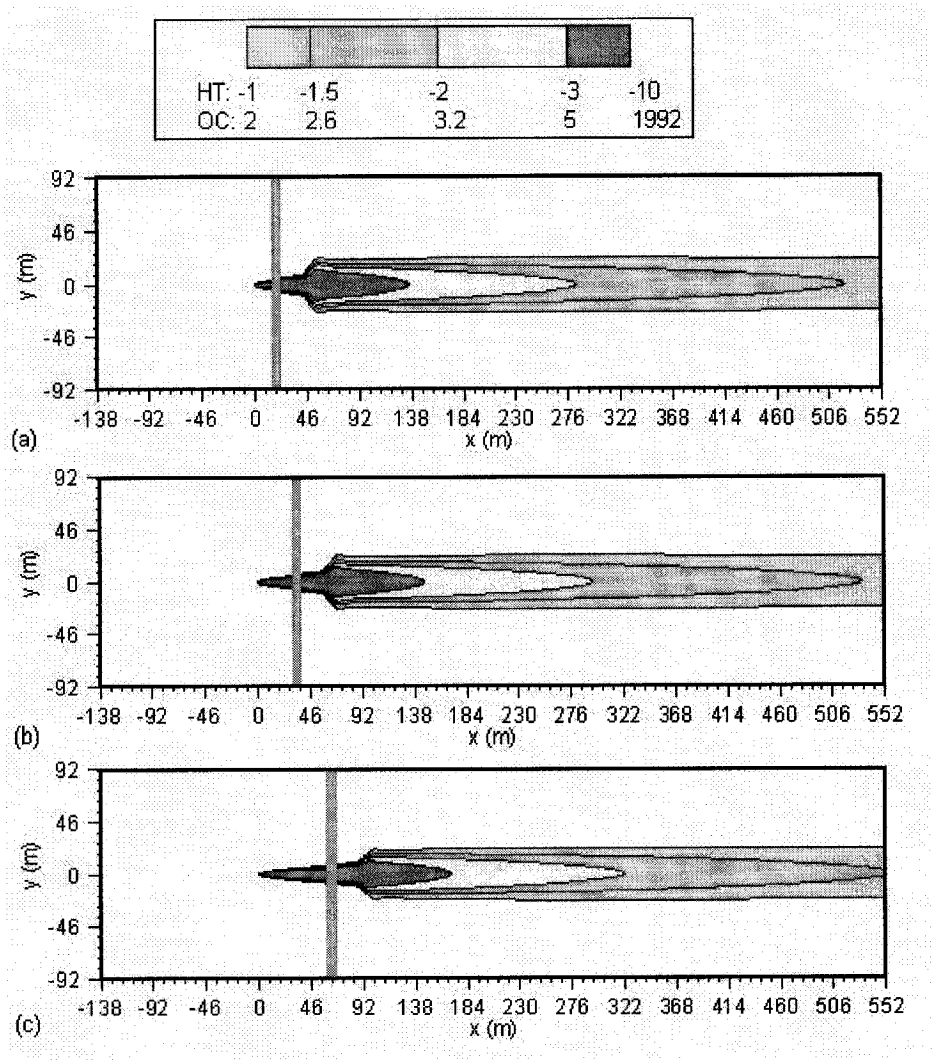

Fig. 7.11. Effect of windbreak position from odour source. Contours of the simulated odour plume on the horizontal plane (z = 1.5 m) for a conifer windbreak separated from the odour source by (a) 15 m (simulation 7), and (b) 30 m (simulation 4), and (c) 60 m (simulation (8). Note: both windbreaks have an aerodynamic porosity of 0.4 and a height of 9.2 m, and are exposed to neutral atmospheric conditions.

Connecting statement

In chapter 7, the SST k-ω was successfully calibrated to simulate the effect of the windbreak characteristics on the odour dispersion. In chapter 8, this model was still used to analyse effects on the odour dispersion around the natural windbreaks, of the weather conditions, such as wind velocity and direction, temperature and atmospheric stability.

This paper was submitted to Journal of Wind Engineering and Industrial Aerodynamics. The contributions of the authors, Lin, X.J., Barrington, S., Choinière, D. and Prasher, S., are i) First author carried out a part of field measurements, the CFD simulation and wrote the manuscript; ii) Second author supervised and helped revise the method of analysis and the content of the paper; iii) Third author organized and managed the collection of the field data, and iv) Last author advised on CFD simulations.

Chapter 8

Simulation of effect of weather conditions on windbreak odour dispersion with the CFD SST k-ω model

8.1. Abstract

Windbreaks are known to enhance the dispersion of livestock odours and thus, improve the environment of rural residents and communities. Although it is a common practice to plant trees and introduce natural windbreaks around livestock shelters, best implementation strategies are still poorly defined. Using computational fluid dynamic modeling, the objective of this paper was to verify the effect of climatic conditions on odour dispersion downwind from natural windbreaks. The Fluent Shear Stress Transport (SST) k-ω model was used to simulate odour dispersion as released by a point source, and as dispersed downwind from a single row coniferous windbreak measuring 9.2 m in height and 7 m in thickness with an aerodynamic porosity 0.4. The 21 simulations demonstrated the effects of wind velocity and direction, and air temperature under unstable, neutral and stable atmospheric conditions. Generally, higher wind velocity produced shorter odour plumes under unstable, neutral and stable atmospheric conditions, but a shorter odour plume was also observed at lower wind velocities under unstable atmospheric stability due to high vertical convection. Wind direction had an impact on the direction and length of the odour dispersion plume, which decreased for wind directions of 0 to 45° (0° being perpendicular to the windbreak), due to the air flowing along and near the leeward side of the windbreak. With neutral atmospheric stability conditions, and at its corresponding mean atmospheric boundary layer height, wind velocity and temperature, odour plume length was shorter than for unstable and stable condition because of higher wind velocities. However, when all conditions were

same, neutral and unstable atmospheric conditions produced slightly longer odour dispersion plumes because of a lower velocity and temperature profile.

Keywords: Fluent SST k-ω model, Simulation, Windbreak, Odour, Dispersion, Wind velocity and direction, Temperature, and Atmospheric stability.

8.2. Introduction

For rural communities and residents, planting natural windbreaks around livestock facilities is an innovative method of reducing the nuisance created by manure odours. Field measurements and model simulations have demonstrated that a windbreak positioned near an odour source can reduce the downwind length of the odour dispersion plume [1]. Nevertheless, weather conditions such as wind velocity and direction relative to the windbreak, and weather stability, solar radiation and mixing height, have an impact on odour dispersion. In the absence of a windbreak and over flat terrain, the INPUFF II model predicted longer odour plumes for slow wind speeds and stable atmospheric conditions [2]. This conclusion does not completely explain all odour events which can often occur under neutral and unstable weather conditions [3]. Hence, odour dispersion under various weather conditions must be investigated.

Computational fluid dynamic (CFD) models, such as the Reynolds Average Navier Stokes (RANS) and the Large-Eddy Simulation (LES), were reported to simulate windbreaks in 2 and 3 dimensions [4, 5, 6, 7, 8, 9, 10, 11, 12, 13]. The RANS models are accurate in predicting mean velocities, but not so accurate in predicting turbulence [12]. Although the models based on physical principles offer well-known weaknesses, the accuracy of their prediction is sufficient for some purposes [14].

CFD models have been successfully used to simulate gas dispersion especially in complex atmospheric situations [15], such as ammonia distribution in barns [16] and the transport of spray droplets [17]. Using field measurements,

the Fluent standard k-ε and SST k-ω models were successful in simulating odour plume length downwind from natural windbreaks. These models therefore were used to research the effect of climatic conditions on the length of odour dispersion plumes [18, 19].

The stability of the atmosphere can be expressed in terms of the Pasquill classes: A through G, where A is strongly unstable, D is neutral and G is strongly stable [20, 21]. Alternatively, the stability can be expressed by the Monin-Obukhov length, denoted by L_{MO}. Atmospheric stability conditions are unstable, neutral and stable, when $1/L_{MO}$ is negative, zero and positive, respectively [22, 23]. Strongly unstable weather occurs during hot, sunny days when rapid vertical mixing occurs. Neutral atmospheric conditions may occur at any time of the day under high wind speed and/or overcast sky. Strongly stable atmospheric conditions occur during calm, clear nights when vertical mixing is nearly non-existent. These conditions strongly influence the dispersion of odours. Unstable conditions facilitate the vertical dispersion of odours while stable conditions help odours travel horizontally [3].

The objective of the present project was therefore to use an already calibrated CFD SST k-ω model to analyse the impact of various weather conditions on the length of the odour dispersion plumes occurring downwind from natural windbreaks.

8.3. Methods and materials

The following steps must be respected before using the SST k-ω model to simulate odour dispersion around windbreaks: firstly, determining the governing equations; secondly, meshing the computational domain; thirdly, selecting the solver capable of defining the properties of the fluid and its components such as the windbreak, and; finally, setting boundary conditions.

8.3.1. Governing equations

For a fixed volume cell through which the odorous air is flowing, the air flow governing equations are those of mass, momentum, energy and species conservation expressed by:

$$\frac{\partial \rho}{\partial t}+\frac{\partial}{\partial x_i}(\rho u_i)=0 \tag{8.1}$$

$$\begin{aligned}\frac{\partial}{\partial t}(\rho u_i)=&-\frac{\partial}{\partial x_j}(\rho u_i u_j)-\frac{\partial p}{\partial x_i}+\frac{\partial}{\partial x_j}\left[\mu\left(\frac{\partial u_i}{\partial x_j}+\frac{\partial u_j}{\partial x_i}-\frac{2}{3}\delta_{ij}\left(\frac{\partial u_1}{\partial x_1}+\frac{\partial u_2}{\partial x_2}+\frac{\partial u_3}{\partial x_3}\right)\right)\right]\\&+\frac{\partial}{\partial x_j}\left(-\rho\overline{u_i' u_j'}\right)+\rho g_i-\frac{\mu}{\alpha}u_i-\frac{1}{2}C_{ir}\rho u_{mag}u_i\end{aligned} \tag{8.2}$$

$$\frac{\partial}{\partial t}(\rho E)+\frac{\partial}{\partial x_j}\left[u_j(\rho E+p)\right]=\frac{\partial}{\partial x_j}\left(k_{eff}\frac{\partial T}{\partial x_j}-\sum_i h_i J_i+u_i(\tau_{ij})_{eff}\right)+S_h \tag{8.3}$$

$$\frac{\partial}{\partial t}(\rho Y_i)+\nabla\bullet(\rho u Y_i)=-\nabla\bullet J_i \tag{8.4}$$

where ρ is fluid density; t is time; u_i (i=1, 2, 3, indicating x, y, and z direction) is the mean velocity u in ith direction; u_i' is the fluctuating component of the instantaneous velocity; μ is fluid viscosity; δ_{ij} is the unit tensor; p is the static pressure; g_i is the gravitational acceleration constant in the ith direction; α is the aerodynamic porosity or permeability of the windbreak; α^{-1} is the viscous resistance coefficient; C_{ir} is the inertial resistance coefficient caused by the windbreak; u_{mag} is the magnitude of the velocity [24, 25]; E is the total energy; k_{eff} is the effective thermal conductivity; S_h represents all volumetric heat sources such as those of chemical reactions; T is temperature, and; $(\tau_{ij})_{eff}$ is the effective deviatoric stress tensor.

The coefficients Y_i, J_i and h_i are the mass fraction, diffusion flux and the sensible enthalpy of the ith atmospheric species [26, 27]. The term $-\rho\overline{u_i' u_j'}$ is called the Reynolds stresses.

In Eq. (8.4), the diffusion flux J_i of the atmospheric species i, arises due to concentration gradients. The diffusion flux for turbulent flow is:

$$J_i=-(\rho D_{i,m}+\frac{\mu_t}{Sc_t})\nabla Y_i-D_{T,i}\frac{\nabla T}{T} \tag{8.5}$$

where Y_i is mass fraction of the species i; $D_{i,m}$ is the diffusion coefficient for species i in the mixture; and $D_{T,i}$ is the thermal diffusion coefficient; Sc_t is the turbulent Schmidt number generally equal to 0.7, and; μ_t is the turbulent viscosity [25, 26].

As a porous medium, the windbreak exerts an air flow resistance considered to be a momentum sink. The term $\mu u_i / \alpha$ in Eq. (8.2) is Darcy's law for porous medium which calculates the resistance exerted by the windbreak due to fluid viscosity [26]. The term $C_{ir}\rho u_{mag} u_i / 2$ in Eq (8.2) computes the inertial loss of fluid energy flowing through the windbreak [10, 12].

For example, the inertial resistance coefficient for a conifer windbreak can be expressed as:

$$C_{ir}(z) = C_{ir0} D^2(z) \tag{8.6}$$

where $C_{ir}(z)$ is the inertial resistance coefficient as a function of height z; C_{ir0} is the constant reflecting all factors that influence the resistance, and; $D(z)$ is the diameter of the tree with height z:

$$D(z) = \begin{cases} D_1 - \dfrac{D_1 - D_2}{h_1} z & z \le h_1 \\ D_2 - \dfrac{D_2}{H - h_1}(z - h_1) & h_1 < z \le H \end{cases} \tag{8.7}$$

where H is the height of the tree; h_1 is the height at which there is a change in rate of tree diameter gradient; D_1 is the diameter of the tree at the bottom, and; D_2 is the diameter of the tree at h_1 [18]. The coefficient C_{ir0} can be obtained from field values or simulated at a specific aerodynamic porosity.

8.3.2. Computational domain

The computational domain was designed as a volume measuring 690 m in length (75 H, H being the height of the windbreak of 9.2 m), 184 m (20 H) in width and 73.6 m (8 H) in height (Fig. 8.1). The left and right faces of the space were the wind inlet and outlet, located 138 and 552 m from the origin, respectively. The

front, back and top faces of the volume were set to have an open or undisturbed wind velocity and were positioned at 92, -92 and 73.6 m from the origin, respectively. The bottom face of the volume was the ground surface.

The odorous air was introduced into this computational volume by a single source opening measuring 1.5 m × 0.376 m × 1.75 m in x, y, z directions with the right face positioned at x = 0 m and the front face at y = -0.188 m. The centre of the odour emission surface was positioned at x = 0 m, y = 0 m and z = 1.562 m. Odours were blown from the right-up rectangular face (the red zone in Fig. 8.1) measuring 0.376 × 0.376 m. The windbreak (green zone in Fig. 8.1) was designed as a porous cubic volume.

For computational purposes, the computational volume was meshed into 228, 81, and 46 segments in the x, y and z coordinates, respectively, and the size of the rectangular cells gradually increased from the odour generator towards the outward faces of the system. For the odour inlet, 64 rectangles were meshed over an area of 0.376 × 0.376 m^2 to effectively transfer the odour mass fraction to other cells.

8.3.3. Numerical solver

The Reynolds stresses in Eq. (8.2) can be computed using the Boussinesq Hypothesis based on the mean velocity gradients:

$$-\rho\overline{u_i'u_j'} = \mu_t\left(\frac{\partial u_i}{\partial x_j}+\frac{\partial u_j}{\partial x_i}\right)-\frac{2}{3}\left(\rho k+\mu_t\frac{\partial u_i}{\partial x_i}\right)\delta_{ij} \tag{8.8}$$

where μ_t is the turbulent viscosity, and; k is the turbulence kinetic energy.

Selected to perform the simulations, the SST k-ω model of the Fluent software uses two different transport equations to express the turbulence kinetic energy k and the specific dissipation rate ω. The SST k-ω accounts for the principal turbulent shear stress and uses a cross-diffusion term in the ω equation to blend both the k-ω and k-ε models and to ensure that the model equations behave appropriately in both the near-wall and far-field zones. Thus, the SST k-ω

model offers a superior simulation performance as compared to the individual k-ω and k-ε models [28].

The Fluent 6.2 steady 3-dimension segregated solver was used to solve the SST k-ω model through second and quick orders of discretisation schemes converting the governing equations into algebraic equations solved numerically while increasing the calculation accuracy. The second order scheme was used to compute the pressure, the second order upwind scheme was used to compute odour dispersion and the quick scheme was used to compute momentum, turbulence kinetic energy, turbulence dissipation rate and energy. The SIMPLE method was applied to the velocity and pressure coupling [29].

8.3.4. Fluid properties

Livestock manures emit over 168 odorous compounds and six of the ten compounds with the lowest detection thresholds contained sulphur [30]. Hydrogen sulphide (H_2S) was selected as odour and presumed to flow along with clean dry air. Therefore, the modelled fluid was defined as clean air and H_2S and its mass fraction at the odour source was:

$$Y_2 = \frac{OC_g \bullet m_{H_2S}}{\frac{P_a M_1}{RT} + OC_g \bullet m_{H_2S}} \tag{8.9}$$

where Y_2 is the odour mass fraction (OMF) at the odour inlet, which is ratio of the odour mass to total mass of air and odour in a cubic meters, dimensionless; P_a is the atmospheric pressure of 101325 Pa at sea level; T is temperature in K; M is the molecular weight of dry air or 0.028966 kg mol^{-1}; R is the universal gas constant or 8.31432J mol^{-1} K^{-1} [31]; OC_g is the odour source concentration, in OU m^{-3}, and; m_{H_2S} is the mass of H_2S required to produce one odour unit, expressed as kg OU^{-1} and $m_{H_2S} = 7.0 \times 10^{-9}$ kg OU^{-1} [32].

The modelled fluid was defined using the physical properties of clean dry air and H_2S, including density, specific heat capacity, thermal conductivity, viscosity, mass and thermal diffusion coefficients for the mixture and individual

species. The modelled fluid was considered incompressible and its density varied with temperature but not with pressure because of a Mach number under 10%. The fluid's specific heat capacity, thermal conductivity and viscosity were calculated using the mass mixing-law and the thermal diffusion coefficient was calculated using the kinetic-theory (Table 8.1).

8.3.5. Boundary conditions

The boundary conditions define the faces of the computational volume and the velocity inlet of the clean air and odorous gas. The bottom face of the odour dispersion system (ODS) was assumed to be no slip requiring as input only temperature and roughness length. As air inlet velocity, the inputs included the vertical profile of the horizontal wind velocity, temperature, turbulence kinetic energy and specific dissipation rate.

Odour dispersion around the windbreak was assumed to occur within a homogeneous flat terrain within the surface layer of the atmosphere, and the unidirectional approach wind flow was assumed to satisfy the assumptions of the Monin Obukhov similarity theory (Panofsky and Dutton, 1984). Atmospheric stability was determined by the Monin Obukhov length L_{MO}:

$$L_{MO} = -\frac{u_*^3 \rho C_p T}{k_a g H_F} \tag{8.10}$$

where u_* is the friction velocity; k_a is the von Karman constant ranging from 0.35 to 0.43 and usually equal to 0.4; T is the surface temperature; C_p is the specific heat of air; H_F is the vertical heat flux; ρ the air density, and; g is the gravitational acceleration constant [21]. When the convective heat flux is upward, L_{MO} is negative and the air is unstable. When the earth absorbs heat energy, the heat flux is negative, L_{MO} is positive and hence the air is stable. However, when the heat flux is zero, L_{MO} is infinite and the air stability conditions are neutral.

The vertical profile of the horizontal mean wind velocity is calculated by:

$$u_{mag}(z)=\begin{cases}\dfrac{u_*}{k_a}\ln\dfrac{z}{z_0} & h_{ABL}/L_{MO}=0 \quad neutral\\ \dfrac{u_*}{k_a}\left(\ln\dfrac{z}{z_0}-\ln\dfrac{(1+x)^2(1+x^2)}{(1+x_0)^2(1+x_0^2)}+2\tan^{-1}(x)-2\tan^{-1}(x_0)\right) & h_{ABL}/L_{MO}<0 \quad unstable\\ \dfrac{u_*}{k_a}\left(\ln\dfrac{z}{z_0}+\dfrac{5(z-z_0)}{L_{MO}}\right) & h_{ABL}/L_{MO}>0 \quad stable\end{cases} \tag{8.11}$$

where

$$x=\left(1-\frac{16z}{L_{MO}}\right)^{\frac{1}{4}} \tag{8.12}$$

$$x_0=\left(1-\frac{16z_0}{L_{MO}}\right)^{\frac{1}{4}} \tag{8.13}$$

where $u_{mag}(z)$ is the magnitude of the horizontal mean wind velocity at height z above the surface ($z \geq z_0$); z_0 is the roughness length of the surface, h_{ABL} is the height of the atmospheric boundary layer; and L_{MO} is the Monin Obukhov length [23, 32, 33].

With assumption that the potential temperature is equal to the temperature as z_s, the vertical temperature profile $T(z)$ can be calculated as [23]:

$$T(z)=\begin{cases}-\gamma_d(z-z_s)+T_s & h_{ABL}/L_{MO}=0 \quad neutral\\ -\gamma_d(z-z_s)+T_s\left(1+\dfrac{u_*^2}{\kappa_a^2 g L_{MO}}\left(\ln\dfrac{z}{z_s}-2\ln\dfrac{1+\sqrt{1-\dfrac{16z}{L_{MO}}}}{1+\sqrt{1-\dfrac{16z_s}{L_{MO}}}}\right)\right) & h_{ABL}/L_{MO}<0 \quad unstable\\ -\gamma_d(z-z_s)+T_s\left(1+\dfrac{u_*^2}{\kappa_a^2 g L_{MO}}\left(\ln\dfrac{z}{z_s}+\dfrac{5(z-z_s)}{L_{MO}}\right)\right) & h_{ABL}/L_{MO}>0 \quad stable\end{cases} \tag{8.14}$$

where z_s is a height of 1.35m above the ground surface; T_s is the temperature at height z_s; g is the gravitational acceleration constant, and; γ_d is the dry adiabatic lapse rate of 0.01 K m^{-1}.

The vertical turbulence kinetic energy profile within the surface atmospheric layer can be defined as:

$$k(z) = \frac{1}{2}\left(\sigma_u^2 + \sigma_v^2 + \sigma_u^2\right) \tag{8.15}$$

where *k(z)* is the turbulence kinetic energy (TKE), and; σ_u, σ_v and σ_w are turbulence components in the x, y, z coordinates.

For neutral conditions, $h_{ABL} / L_{MO} = 0$, TKE linearly decreased with height, and at the top of the atmospheric boundary layer, equals 20% of its value at the ground level [34]. The TKE for neutral condition is:

$$k(z) = 5.97 u_*^2 T_{WN}^2 \tag{8.16}$$

where

$$T_{WN} = 1 - a_s \frac{z - z_0}{h_{ABL} - z_0} \tag{8.17}$$

where $a_s = 0.8$.

For unstable conditions ($h_{ABL} / L_{MO} < 0$), the TKE is:

$$k(z) = 5.97 u_*^2 T_{WN}^2 + w_*^2 \left(0.3 + 0.2 T_{WC}^2\right) \tag{8.18}$$

where

$$T_{WC} = 2.1 \left(\frac{z - z_0}{h_{PBL} - z_0} \right)^{\frac{1}{3}} T_{WN} \tag{8.19}$$

$$w_* = u_* \left(\frac{h_{ABL} - z_0}{k_a |L_{MO}|} \right)^{\frac{1}{3}} \tag{8.20}$$

where w_* is the mixing layer velocity scale.

For stable conditions ($h_{ABL} / L_{BO} > 0$), TKE is expressed as:

$$k(z) = 5.97 u_*^2 T_{WN}^{\frac{3}{2}} \tag{8.21}$$

and a_s =0.5 for roughness length $z_0 \geq 0.1$ m.

The vertical turbulence specific dissipation rate $\omega(z)$ is:

$$\omega(z) = \frac{k(z)^{\frac{1}{2}}}{0.09^{\frac{1}{4}} l} \tag{8.31}$$

where l is the turbulence length scale set as twice the height of the ground surface roughness length ($2z_0$) based on a calibration of the horizontal velocity recovery rate downwind from the windbreak [21, 28].

The parameters defining the surface layer conditions in the SST model, namely z_0, L_{MO}, h_{ABL}, u_* and T_s are determined according to the simulation conditions. Corresponding to the physical conditions of the ground surface, z_0 was 0.13 m [18]. The coefficient L_{MO} was estimated from the Pasquill atmospheric stability categories. When z_0 was 0.13 m, the average L_{MO} was -20 m for the Pasquill stability category B, and was 20 for the stability category F [35]. The coefficient h_{ABL} was designated as the average rural mixing height for each stability category measured at the weather station. Once z_0, L_{MO} and h_{ABL} were determined, u_* and T_s were calculated from the wind velocity and temperature measured at the weather station height of 10 m and using Eqs. (8.11 and 8.14), respectively.

8.3.6. *Simulations of the effect of weather conditions*

The 21 simulations (Table 8.2) were designed to test the effect on odour plume length, of wind velocity (simulations 1 to 9), air temperature (simulations 10 to 12), wind direction (simulations 13 to 19) and atmospheric stability (simulations 20 and 21). The ODS for simulations 1 to 12, 20 and 21 was shown in Fig. 8.1, and an odour concentration was 300 OU m^{-3}, respectively. For simulations 13 to 19, the ODS measured 460 m × 414 m × 73.6 m, and the odour concentration at the source was 550 OU m^{-3}. For all simulations, the surface roughness length was 0.13 m, the odour generator emitted odorous air at a rate of 1.6 m^3 s^{-1} and the natural windbreak consisted of a single row of conifers, measuring 7.0 m in width and 9.2 m in height and offering an aerodynamic porosity of 0.4 with a coefficient C_{ir0} equal to 0.08706. The windbreak was located 30 m downwind from the odour source.

Simulations 1 to 9 tested the effect on odour dispersion of the wind velocity for unstable (category B), neutral (category D) and stable (category F) atmospheric conditions for their average T, L_{MO} and h_{ABL} values. The wind velocity ranges were measured in September 2003 at PE Tudeau airport by Environment Canada for stability category B, D and F. For simulations 1, 2 and 3 under stability category B, the averaged values of T, L_{MO} and h_{ABL} were 293 K, -20 m and 1390 m and the velocities were 1.0, 1.8 and 3.0 m s^{-1}, respectively (Table 8.2). For simulations 4, 5 and 6 under stability category D, the averaged T, L_{MO} and h_{ABL} were 291 K, infinity (∞) and 2090 m, and the velocities were 3.0, 5.4 and 6.4 m s^{-1}, respectively. Finally, for simulations 7, 8 and 9 under stability category F, the averaged T, L_{MO} and h_{ABL} were 287 K, 20 m and 1811 m, and the velocities were set at 1.0, 1.9 and 3.0 m s^{-1}, respectively.

Temperature effects were tested under unstable, neutral and stable atmospheric stability categories, using simulations 10, 11 and 12 with average December 2003 temperatures of 269, 270 and 265 K, and simulations 2, 5 and 8 with average September temperature of 293, 291 and 287 K.

Simulations 13 to 19 tested the effect of the wind direction, measured from the positive x-axis and set at 0, -15, -30, -45, -60, -75 and -90°, respectively. The weather atmospheric stability category D was assumed and T, L_{MO}, h_{ABL} and wind velocity were 291 K, ∞, 2090 m and 5.4 m s^{-1}, respectively.

The effect of the atmospheric stability was tested twice. Simulations 2, 5 and 8 compared average values of wind velocity, atmospheric boundary layer height and temperature. Simulations 4, 20 and 21 were also similar except for their respective stability categories B, D and F. For these three simulations, wind velocity, h_{ABL} and T were set at 3.0 m s^{-1}, 2090 m and 291 K, respectively, which are mean values for the atmospheric stability categories B, D and F.

8.3.7. Output of odour plumes

An odour plume is expressed by a series of odour concentration (OC) contours within a plane. In the field and at various locations, the trained panellists detected the odour hedonic tone (HT) which is the degree of pleasant or unpleasant smells, expressed using a scale 0 to -10, where 0 is neutral and -10 is extremely unpleasant [18]. In the laboratory, the panellists were then asked to detect the HT and OC of 65 odour samples, which produced the following correlation [18]:

$$OC = \begin{cases} 0 & AHT = 0 \\ 1.3e^{0.45\,AHT} & 1 \le AHT \le 10 \end{cases} \tag{8.32}$$

where OC is odour concentration in OU m^{-3}, and; AHT is an absolute value of HT ranging from 0 to 10. From Eq. (8.32), the maximum AHT is 10 and the corresponding OC is 117 OU m^{-3}. Hence, when OC exceeds 117 OU m^{-3}, AHT is still defined as 10, because panellists still feel an extremely unpleasant odour.

To plot the odour plume reflecting HT, the computed dimensionless odour mass fraction (OMF) for all point of the ODS needs to be transformed into a simulated odour mass concentration (SOMC):

$$SOMC = \frac{OMF}{\frac{Y_2}{OC_g}} m_{H_2S} \times 10^9 \tag{8.33}$$

where SOMC is simulated odour (H_2S) mass concentration in μg m^{-3}; OMF is the odour (H_2S) mass fraction computed by the model for a given point in space, dimensionless; Y_2 and OC_g are the odour mass fraction and odour concentration at the odour source as defined by Eq. (8.9), which are respectively dimensionless and in OU m^{-3}, and; m_{H_2S} is the mass of H_2S required to produce 1.0 OU m^{-3} in kg OU^{-1} as described by Eq. (8.9).

Secondly, the SOMC were transformed into SAHT by correlating the 5 field test AHT (absolute HT readings) with SOMC:

$$SAHT = \begin{cases} 0.57 SOMC^{0.46} & SOMC \leq 506.5 \ \mu g\ m^{-3} \\ 10 & SOMC > 506.5 \ \mu g\ m^{-3} \end{cases} \quad (8.34)$$

where SAHT is simulated absolute hedonic tone, and; SOMC is defined by Eq. (8.33). The field test correlation indicated a statistically significance ($P < 0.01$) relationship between AHT and SOMC [18]. In this procedure, the odour mass fraction of 506.5 μg m^{-3} results in AHT of 10 for an OC of 117 OU m^{-3}.

8.4. Results

8.4.1. Effect of wind velocity

Figure 8.2 demonstrates for unstable atmospheric stability conditions (category B), OC contours for simulations 1, 2 and 3 on the vertical plane y = 0 m with wind velocities of 1.0, 1.8 and 3.0 m s^{-1}. The odour plume length for a velocity of 1.0 m s^{-1} (Fig. 8.2 a) was shorter than that for a velocity of 1.8 m s^{-1} (Fig. 8.2 b), but longer than that for a velocity of 3.0 m s^{-1} (Fig. 8.2 c). For the 2 OU contour and a wind velocity of 1.0 m s^{-1}, the odour plume length was 321 m or 85 m shorter than that for a wind velocity 1.8 m s^{-1} , and 53 m longer than that for wind velocity 3.0 m s^{-1} (Table 8.2). At a lower wind velocity (1.0 m s^{-1}), the odour plume was shorter because of the air lifting effect of the unstable conditions. Similarly, the height of the odour plume increased with a drop in wind velocity. At wind velocities of 1.0, 1.8 and 3.0 m s^{-1}, the odour plumes heights were 43, 17 and 15 m, respectively (Table 8.2).

For neutral atmospheric stability conditions (category D) with typical wind velocities of 3.0, 5.4 and 6.4 m s^{-1}, odour plume length decreased with higher wind speeds (Fig. 8.3). A wind velocity of 3.0 m s^{-1} produced an odour plume length (2 OU m^{-3} contour) of 272 m, which exceeded that for wind velocities of 5.4 and 6.4 m s^{-1} by 102 and 121 m, respectively. Wind velocities for neutral atmospheric conditions are higher than those associated with unstable conditions and produce a higher turbulence kinetic energy (TKE) at the windbreak which enhances odour dispersion. This is also reflected in Eq. (8.5) where odour flux is accelerated by the turbulence viscosity μ_t which is proportional to TKE.

For stable atmospheric stability conditions (category F) with typical wind velocities of 1.0, 1.9 to 3.0 m s^{-1}, the length of the odour plume dropped from 552 to 350 and 253 m, respectively (Fig. 8.4). Under stable conditions with limited upwards convection, as compared to unstable conditions, vertical forces are not as strong and less air is projected upwards at the windbreak with the resulting effect that lower wind velocities produce weaker TKE at the windbreak and therefore longer odour plumes.

Therefore, higher wind velocities will generally produce shorter odour plumes except for low wind velocities under unstable atmospheric conditions.

8.4.2. Effect of temperature

In general, air temperature at the ground was found to have very limited effect on odour plume size, when associated with a specific atmospheric condition (Table 8.2). Odour plumes of the same length were obtained at different temperature of 293 and 269 K (simulations 2 and 10, Fig 8.5 a and b) under unstable atmospheric conditions (category B), as well as under neutral and stable conditions (Fig. 8.5 c and d, and Fig. 8.5 e and f).

The phenomenon is explained by Eq. (8.5) where the odour flux is proportional to $(-\frac{\nabla T}{T})$ or the rate of change of T, rather than T. In simulations 5 and 11 for neutral atmospheric conditions, T dropped with height at a rate of 0.01 K m^{-1} but the rate of change of T over height 0 to 20 m was similar for both cases

at 0.069% and 0.074%, respectively and the difference between them was 0.005%. Such differences for simulations 2 and 10, and 8 and 12 were 0.006% and 0.005%, respectively. These very small differences had a little influence on the odour dispersion. Hence, the same odour plumes occurred on the Fig. 8.5 for the different temperature under the same atmospheric stability.

8.4.3. Effect of wind direction

On the horizontal plane z = 1.5 m and for wind directions varying from 0 to -90°, the shape of the odour plume followed wind direction (Figs. 8.6 and 8.7). The length of the odour plume decreased for a wind direction changing from 0 to -45° and then increased from -45 to -90°. For OC contours of 2 OU m^{-3}, the shortest odour plume length measured 178 m with a wind direction of -45°, which is 103 m and 143 m shorter than that for a wind direction of 0° and -75°, respectively (Table 8.2).

The odour plume developed a fin immediately downwind from the windbreak when the wind direction was between -15 and -75° (Fig. 8.6 and Fig. 8.7). This fin was generated when sufficient air flowed parallel to the windbreak and when the windbreak could sufficiently reduce the x-component of the air flow. At a distance of 28 m downwind from the windbreak, the wind streamlines were observed to sharply change direction and become parallel to the windbreak (Fig. 8.8). As a result, the fin reached its maximum length when the wind direction was -45°.

8.4.4. Effect of atmospheric stability

Atmospheric stability condition was found to have a major impact on odour plume length because it determined the wind velocity range and the temperature gradient as well as the strength of the convective air forces. Assuming an average wind velocity, temperature and atmospheric boundary layer height, the odour plume lengths for an OC contour of 2 OU m^{-3}, measured 406, 170 and 350 m for unstable, neutral and stable atmospheric stability conditions (categories B, D and F, simulation 2, 5, 8), respectively (Table 8.2). Hence, the odour plume length

increased from category D, to B and then F, because categories B and F generally exhibit lower wind speeds compared to category D.

For the same atmospheric boundary layer height, wind velocity and air temperature at a height of 10 m, but for stability categories B, D and F, simulations 20, 4 and 21 produced odour plume lengths of 267, 272 and 253 m, respectively, for an OC contour of 2 OU m^{-3} (Fig. 8.9). Only category F produced a shorter odour plume, as compared to B and D. Each stability category is associated with a different profile for wind velocity, temperature and turbulence. The TKE on the upwind side of the windbreak decreased from stability category B, to that of D and then F, but then increased in the opposite order on the downwind side of the windbreak, thus shortening the odour plume.

For stability categories B, D and F (simulations 20, 4 and 21), the vertical wind velocity profile was different for the same value of 3 m s^{-1} at a 10 m height (Fig. 8.10), where the wind velocity and temperature were calculated with Eqs. (8.11 and 8.14), respectively. Stability category B produced a profile value slightly smaller than that of D, but that of B and D were much smaller than that of F.

For a temperature of 291 K at a 10 m height illustrated by simulations 20, 4 and 21, the vertical T profile was quite different for stability categories B, D and F. For stability category D (neutral conditions), T profile decreased with height at a rate 0.01 K m^{-1}, but for that of B (unstable conditions), T dropped much faster over a height of 0 to 10 m and then deceases at a slower rate but still faster than that of stability category D. The T profile for stability category F (stable conditions) increased with height and produced the inverse of stable effects. Because stability category F produced larger profile differences for wind velocity and temperature, between heights of 0 and 73.6 m, compared to D and B, the resulting odour plume was shorter.

Generally, the length of the odour plume for neutral atmospheric conditions (category D) was shorter than that for unstable (category B) and stable conditions (category F), because of the different wind velocity associated with each

condition. However, when all the conditions were the same except for atmospheric stability conditions, category F produced a slightly shorter odour plume compared to that under neutral and unstable conditions.

8.5. Conclusions

To observe the effect of various climatic conditions, this project simulated odour plume length which developed downwind from a conifer windbreak with an optical porosity of 0.4. The simulation comparison indicated that:

1. Generally, higher wind velocities produced shorter plumes under unstable, neutral and stable atmospheric conditions, but the shorter odour plume was also observed under lower wind velocity (1 m s^{-1}) compared to a wind velocity of 1.8 m s^{-1} under unstable atmospheric conditions where convection prevailed.
2. Temperature had little effect on odour dispersion for all three atmospheric stability conditions, namely neutral, unstable and stable;
3. Wind direction determined the odour dispersion direction and length. The shortest plumes were produced with a wind direction of 45°, but this direction produced the longest odour plume fin extending along the downwind side of the windbreak;
4. For a mean atmospheric boundary layer height, wind velocity and temperature corresponding to a specific atmospheric stability condition, odour plume length for neutral atmospheric conditions was shorter than for unstable and stable condition because of a higher wind velocity. However, when all conditions were same, neutral and unstable atmospheric conditions produced slightly longer odour dispersion plumes because of a higher velocity and temperature profile in stable condition.

8.6. Acknowledgement

The authors wish to acknowledge the financial contribution of Consumaj inc., CDAQ, the Livestock Initiative Program, Agriculture and Agro-Food Canada and the Natural Sciences and Engineering Research Council of Canada.

8.7. References

[1] X.J. Lin, S. Barrington, J. Nicell, D. Choiniere, A. Vezina, Influence of windbreaks on livestock odour dispersion plume in the field, Agriculture, Ecosystems & Environment, 116 (3-4) (2006) 263-272.

[2] H. Guo, L.D. Jacobson, D.R. Schmidt, K.A. Janni, Simulation of odor dispersion as impacted by weather conditions, ASAE Publication Number 701P0201 (2001), ASAE, St. Joseph, Mi. USA.

[3] H. Guo, J. Feddes, W. Dehod, C. Laguë, I. Edeogu, Monitoring of odour occurrence in the vicinity of swine farms by resident-observers Part II: Impact of weather conditionson odour occurrence, Canadian Biosystems Enginering 48 (6) (2006) 6.23-6.29.

[4] F. S. Lien, E. Yee, Numerical modelling of the turbulent flow developing within and over a 3-d building array; Part iii: a distributed drag force approach, its implementation and application, Boundary-Layer Meteorology 114 (2) (2005) 287-313.

[5] F.S. Lien, E. Yee, J.D. Wilson, Numerical modelling of the turbulent flow developing within and over a 3-d building array; Part ii: a mathematical foundation for a distributed drag force approach, Boundary-Layer Meteorology 114 (2) (2005) 245- 286.

[6] F.S. Lien, E. Yee, Y. Cheng, Simulation of mean flow and turbulence over a 2D building array using high-resolution CFD and a distributed drag force approach, Journal of Wind Engineering and Industrial Aerodynamics 92 (2004) 117-158.

[7] A.R. Packwood, Flow through porous fence in thick boundary layers: comparisons between laboratory and numerical experiments, Journal of Wind Engineering and Industrial Aerodynamics 88 (2000) 75-90.

[8] E.G. Patton, R.H. Shaw, M.J. Judd, M.R. Raaupach, Large-eddy simulation of windbreak flow, Boundary-Layer Meteorology 87 (1998) 275-306.

[9] R.C. Schwartz, D.W. Fryrear, B.L. Harris, J.D. Billbro, A.S.R. Juo, Mean flow and shear stress distributions as influenced by vegetative windbreak structure, Agricultural and forest meteorology 75 (1995) 1-22.

[10] H. Wang, E.S. Takle, A numerical simulation of boundary-layer flows near shelterbelt, Boundary-Layer Meteorology 75 (1995) 141-173.

[11] J.D. Wilson, Oblique, stratified winds about a shelter fence. Part II: Comparison of measurements with numerical models, Journal of Applied Meteorology 43 (10) (2004) 1392-1409.

[12] J.D. Wilson, Numerical study of flow through a windbreak, Journal of Wind Engineering and Industrial Aerodynamics 21 (1985) 119-154.

[13] J.D. Wilson, E. Yee, Calculation of winds distribution by an array of fences, Agricultural and forest meteorology 115 (2003) 31-50.

[14] A.D. Gosman, Developments in CFD for industrial and environmental applications in wind engineering, Journal of Wind Engineering and Industrial Aerodynamics 81(1-3) (1999) 21-39.

[15] A. Riddle, D. Carruthers, A. Sharpe, C. McHugh, J. Stocker, Comparisons between FLUENT and ADMS for atmospheric dispersion modelling, Atmospheric Environment 38 (7) (2004) 1029-1038.

[16] H. Sun, R.R. Stowell, H.M. Keener, F.C. Michel, Comparison of predicted and measured ammonia distribution in a high-rise^{TM} hog building (HRHB) for summer conditions, Transactions of the ASAE 45 (5) (2002) 1559-1568.

[17] T. Ucar, F.R. Hall, Review windbreaks as a pesticide drift mitigation strategy: a review, Pest Management Science 57 (2001) 663-675.

[18] X.J. Lin, S. Barrington, D. Choinière, S.O. Prasher, Simulation of the effect of windbreaks on odour dispersion using the CFD SST k-ω model, Biosystems Engineering (2007) presented for publication in August 2006.

[19] X.J. Lin, S. Barrington, D. Choinière, Simulation of odour dispersion downwind from natural windbreaks using the CFD standard k-ε model. Transactions of the ASAE (2007) presented for publication in January 14, 2007.

[20] M.R. Beychok, Fundamentals of stack gas dispersion. M.R. Beychok, Irvine, California, USA, 1994.

[21] K.B. Schnelle, P.R. Dey, Atmospheric dispersion modeling compliance guidelines, McGraw-Hill, New York, USA. 2000.

[22] D.J. Carruthers, R.J. Holroyd, J.C.R. Hunt, W.S. Weng, A.G. Robins, D.D. Apsley, D.J. Thompson, F.B. Smith, UK-ADMS: A new approach to modelling dispersion in the earth's atmospheric boundary layer, Journal of Wind Engineering and Industrial Aerodynamics 52 (1994) 139.

[23] H.A. Panofsky, J.A. Dutton, Atmospheric turbulence: models and methods for engineering applications, Wiley, New York, USA, 1984.

[24] J.O. Hinze, Turbulence, McGraw-Hill, New York, USA, 1975.

[25] E.B. Saatdjian, Transport phenomena: equations and numerical solutions, John Wiley, New York, USA, 2000.

[26] R.B. Bird, W.E. Stewart, E.N. Lightfoot, Transport phenomena. John Wiley, New York, USA, 2002.

[27] R.W. Fox, A.T. McDonald, Introduction to fluid mechanics. John Wiley, New York, USA, 1992.

[28] F.R. Menter, M. Kuntz, R. Langtry, Ten years of industrial experience with the SST turbulence model. In: K. Hanjalic, Y. Nagano and M. Tummers (Editors), Turbulence, Heat and Mass Transfer 4. Begell House Inc, Redding, CT, 2003, 625-632.

[29] Fluent inc., Fluent 6.2 user's guide, Fluent Inc., Centerra Resource Park, Lebanon, NH, USA, 2005.

[30] D.H. O'Neill, V.R. Phillips, A review of the control of odour nuisance from livestock buildings: Part 3, properties of the odorous substances which have been identified in livestock wastes or in the air around them, Journal of Agricultural Engineering Research 53 (1992) 23-50.

[31] ASHRAE, Fundamentals handbook. American Society of Heating, Refrigeration and Air Conditioning, Atlanta, Georgia, U.S.A, 1997, 13.1-13.6.

[32] A.K. Blackadar, Turbulence and diffusion in the atmosphere: lectures in environmental sciences. Springer Berlin Publishers, New York, USA, 1997.

[33] M.Z. Jacobson, Fundamentals of atmospheric modeling. Cambridge University Press, Cambridge, UK, 1999.

[34] D.J. Carruthers, S.J. Dyster, Boundary layer structure specification, ADMS 3 P09/01T/03 http://www.cerc.co.uk/software/pubs/3-1techspec.htm visited in April 2006.

[35] D. Golder, Relations among stability parameters in the surface layer. Boundary-Layer Meteorology 3 (1) (1972) 47.

Nomenclature

AHT is absolute hedonic tone
a_s is a factor
C_{ir} is the inertial resistance coefficient
C_{ir0} is the constant
C_p is specific heat of air
D_1 and D_2 are the tree diameters
$D_{i,m}$ is the diffusion coefficient for species i in the gaseous mixture
$D_{T,i}$ is the thermal diffusion coefficient for species i in the gaseous mixture
E is the total energy
g is acceleration of gravity
g_i is the component of the gravitational vector in the ith direction
H is the total height of the windbreak
H_F is the vertical heat flux
h_1 is the height at which the rate of the gradient of the tree diameter with height changed
h_{ABL} is the height of the atmospheric boundary layer
h_j is the sensible enthalpy of jth species
J_i is the diffusion flux of species i
k is the turbulence kinetic energy
k_{eff} is the effective thermal conductivity
l is the turbulence length scale
L_{MO} is the Monin Obukhov length
M is the molecular weight of dry air (0.028966kg mol^{-1})
m_{H_2S} is the mass of hydrogen sulphide in one odour unit
OC is the odour concentration in OU m^{-3}
OC_g is the odour concentration at odour generator in OU m^{-3}
OMF is odour mass fraction, dimensionless
p is the static pressure
P_a is the atmospheric pressure at sea level
R is the universal gas constant (8.31432J mol^{-1} K^{-1})
$SAHT$ is simulated absolute hedonic tone
Sc_t is the turbulent Schmidt number generally equal to 0.7
S_h is the heat of chemical reaction and other volumetric heat sources
SOC is simulated odour concentration in OU m^{-3}
$SOMC$ is odour mass concentration in μg m^{-3}
T is temperature
T_s is the temperature at the z_s
T_{WC} is a factor to control the convective energy varied with height
T_{WN} is a factor controlling the drop in TKE with height within the atmospheric boundary layer
t is time
$\boldsymbol{u}$ is instantaneous velocity
u and u' are mean and fluctuating component of instantaneous velocity

u_* is the friction velocity

u_i (i=1, 2, 3) is scalar component of the mean velocity in ith direction, indicating in x, y, z direction in Cartesian coordinate system, respectively

u_i' (i=1, 2, 3) is the fluctuating component of the instantaneous velocity ith direction, indicating in x, y, z direction in Cartesian coordinate system, respectively

u_{mag} is magnitude of mean velocity

w_* is the mixing layer velocity scale

z_0 is roughness length

z_s is a height of 1.35m above surface

Y_j is the mass fraction of the species j in a mixture of gases

Y_2 is the odour mass fraction at odour inlet

z is a coordinate in the vertical direction

α is the aerodynamic porosity, or permeability

α^{-1} is the viscous resistance coefficient

k_a is the von Karman constant, ranged from 0.35 to 0.43, usually $\kappa_a \approx 0.4$

μ is viscosity of mixture of the air and odorous gases

μ_t is the turbulence kinetic viscosity

ρ is fluid density

ω is the specific dissipation rate

δ_{ij} is the unit tensor

$(\tau_{ij})_{eff}$ is the effective deviatoric stress tensor

σ_u, σ_v and σ_w are turbulence components in x, y, z coordinates

γ_d is dry adiabatic lapse rate, 0.01 K m^{-1}

Tables and Figures

Table 8.1 Clean air and hydrogen sulphide properties

Description	Unit	Mixture	Air	H_2S
Density	kg m^{-3}	Impressible-ideal-gas law		
Cp	J kg^{-1} K^{-1}	Mixing law	1005.422[a]	1005.333[a]
Thermal conductivity	W m^{-1} K^{-1}	Mass-weighted-mixing-law	0.0260411[a]	0.0137023[a]
Viscosity	kg m^{-1} s^{-1}	Mass-weighted-mixing-law	1.458E-6 $T^{1.5}$ / (T + 110.1)	-1.4839E-6 + 5.1E-8T -1.26E-11 T^2
Mass diffusivity	m^2 s^{-1}	-1.3497E-5 + 1.05772E-7T[a]		
Thermal diffusivity coefficient	kg m^{-1} s^{-1}	Kinetic-theory		
Molecular weight	kg $kgmol^{-1}$		28.966	34.07994

Note: T is temperature in K, and [a] is for temperature range from 283 to 313 K.

Table 8.2 Simulation plan to test the effect of weather conditions.

Simu-lation	Weather conditions						Computed results					
	u_{mag} m s^{-1}	T K	Wind °	Atm stability	L_{MO} m	h_{ABL} m	L2 m	L2.6 m	L3.2 m	L5 m	W m	H m
1	1.0	293	0	B	-20	1390	321	243	156	91	40	43
2	1.8	293	0	B	-20	1390	406	186	121	83	35	17
3	3.0	293	0	B	-20	1390	268	135	98	79	30	15
4	3.0	291	0	D	∞	2090	272	137	97	72	37	15
5	5.4	291	0	D	∞	2090	170	100	77	67	25	14
6	6.4	291	0	D	∞	2090	151	92	72	65	22	13
7	1.0	287	0	F	20	1811	552	280	172	99	39	18
8	1.9	287	0	F	20	1811	350	180	121	82	38	15
9	3.0	287	0	F	20	1811	253	139	103	78	31	13
10	1.8	269	0	B	-20	1390	404	186	120	81	33	17
11	5.4	270	0	D	∞	2090	170	100	77	67	25	14
12	1.9	265	0	F	20	1811	351	180	122	83	39	15
13	5.4	291	0	D	∞	2090	281	141	99	71	30	15
14	5.4	291	-15	D	∞	2090	217	111	70	65	57	15
15	5.4	291	-30	D	∞	2090	185	97	71	63	63	15
16	5.4	291	-45	D	∞	2090	178	95	83	70	58	14
17	5.4	291	-60	D	∞	2090	233	128	99	72	38	14
18	5.4	291	-75	D	∞	2090	321	191	156	90	27	15
19	5.4	291	-90	D	∞	2090	>322	>322	207	101	6	11
20	3.0	291	0	B	-20	2090	267	134	97	75	28	15
21	3.0	291	0	F	20	2090	253	139	102	78	29	13

Note: L2, L2.6, L3.2 and L5 are the length of the odour plume to reach 2, 2.6, 3.2 and 5 OU m^{-3}.

: u_{mag} and T are those found at a height of 10 m.

: the value for wind in ° pertains to its direction where 0° is perpendicular to the windbreak.

: Atm stability pertains to the atmospheric stability category, based on the Pasquill classification

:the set of climatic conditions including h_{ABL} data measured at the PE Tudeau airport in 2003 by Environment Canada.

:h_{ABL} is the height of atmospheric boundary layer standing for the rural mixing height.

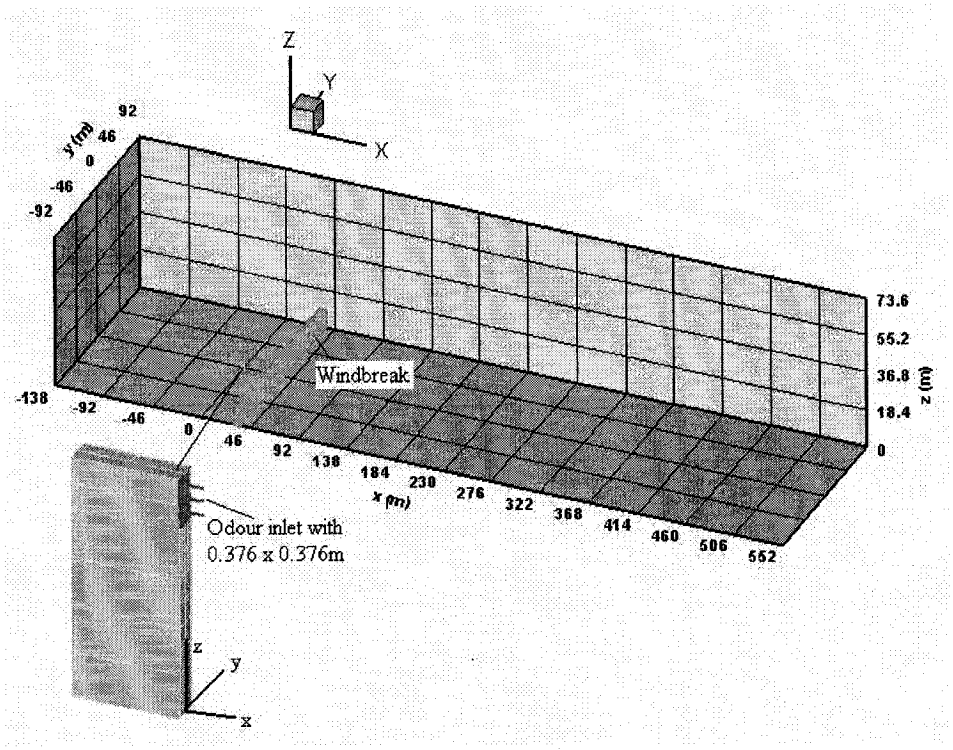

Fig. 8.1. Schematic of the computational volume used to predict odour dispersion. The z coordinate is magnified 2-fold and the windbreak optical porosity is 0.4. The green bar represents the windbreak. The central position of the emission surface for the odour generator stands at x = 0 m, y = 0 m and z = 1.562 m.

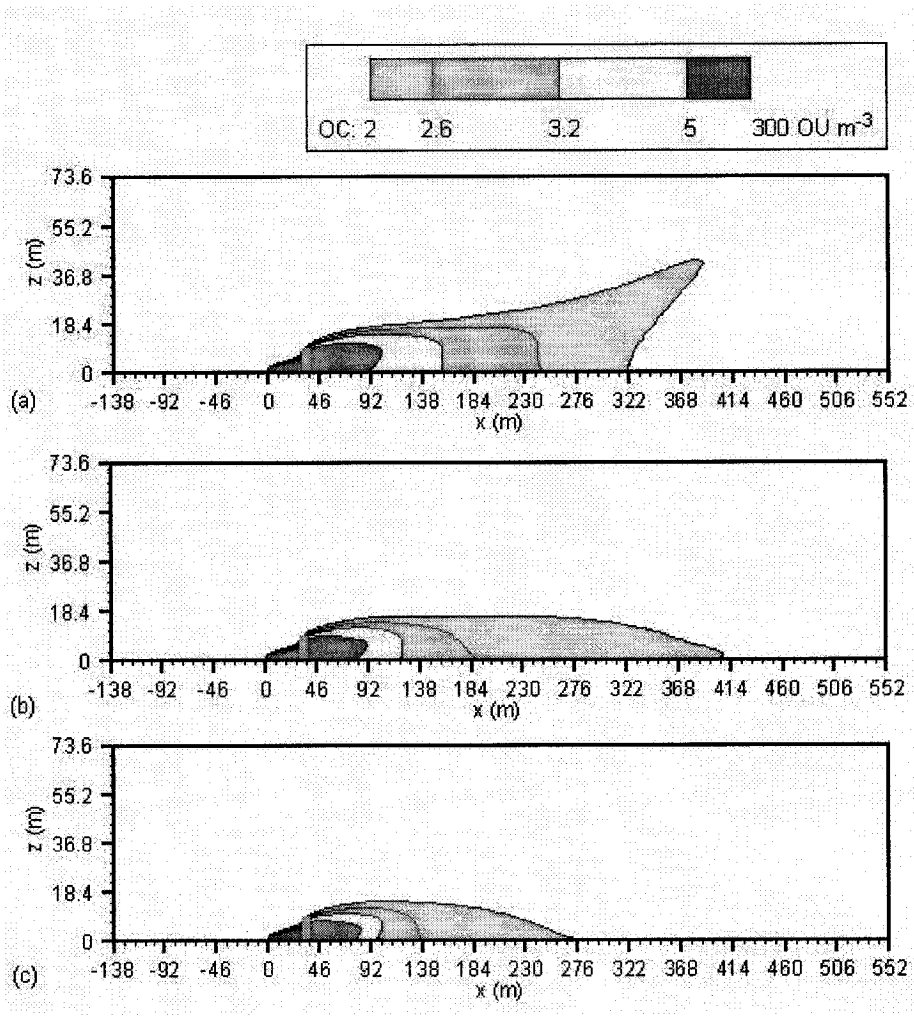

Fig. 8.2. Effect of wind velocity in a unstable atmosphere. Contours of the simulated odour concentrations on the vertical plane y = 0 m under stability class B for velocity (a) 1.0 m s^{-1}; (b) 1.8 m s^{-1} , and (c) 3 m s^{-1} in simulations 1, 2 and 3, respectively. The green bar is the windbreak.

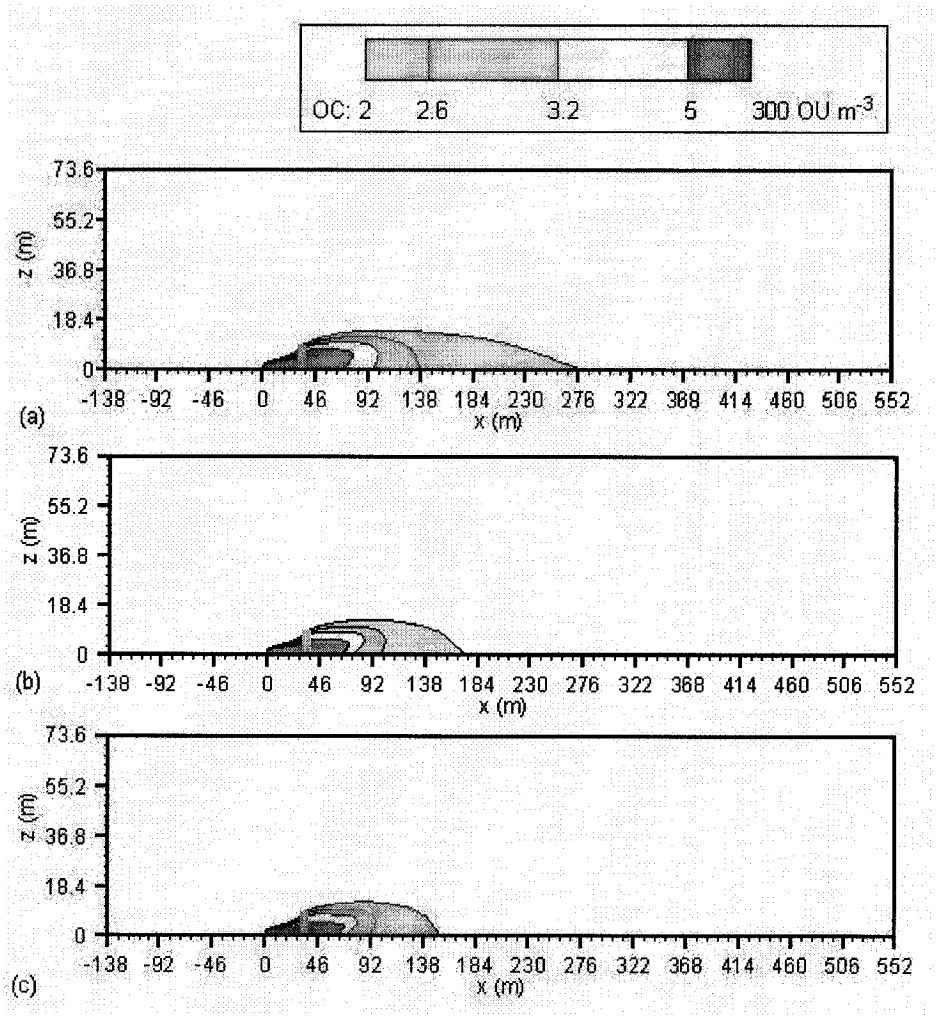

Fig. 8.3. Effect of wind velocity in a neutral atmosphere. Contours of the simulated odour concentrations on the vertical plane y = 0 m under stability class D for velocity (a) 3 m s^{-1}; (b) 5.4 m s^{-1} , and (c) 6.4 m s^{-1} in simulations 4, 5 and 6, respectively. The green bar is the windbreak.

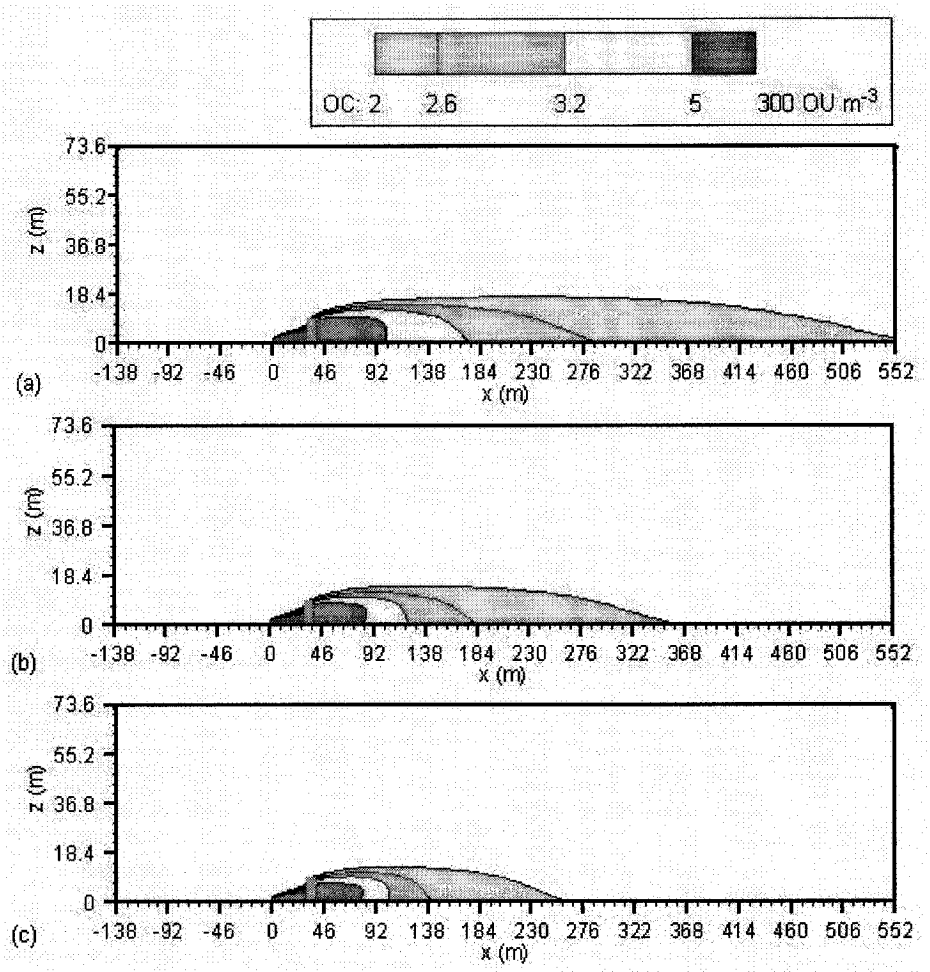

Fig. 8.4. Effect of wind velocity in a stable atmosphere. Contours of the simulated odour concentrations on the vertical plane y = 0 m under atmospheric stability class F for velocity (a) 1 m s^{-1}; (b) 1.9 m s^{-1} , and (c) 3.0 m s^{-1} in simulations 7, 8 and 9, respectively. The green bar is the windbreak.

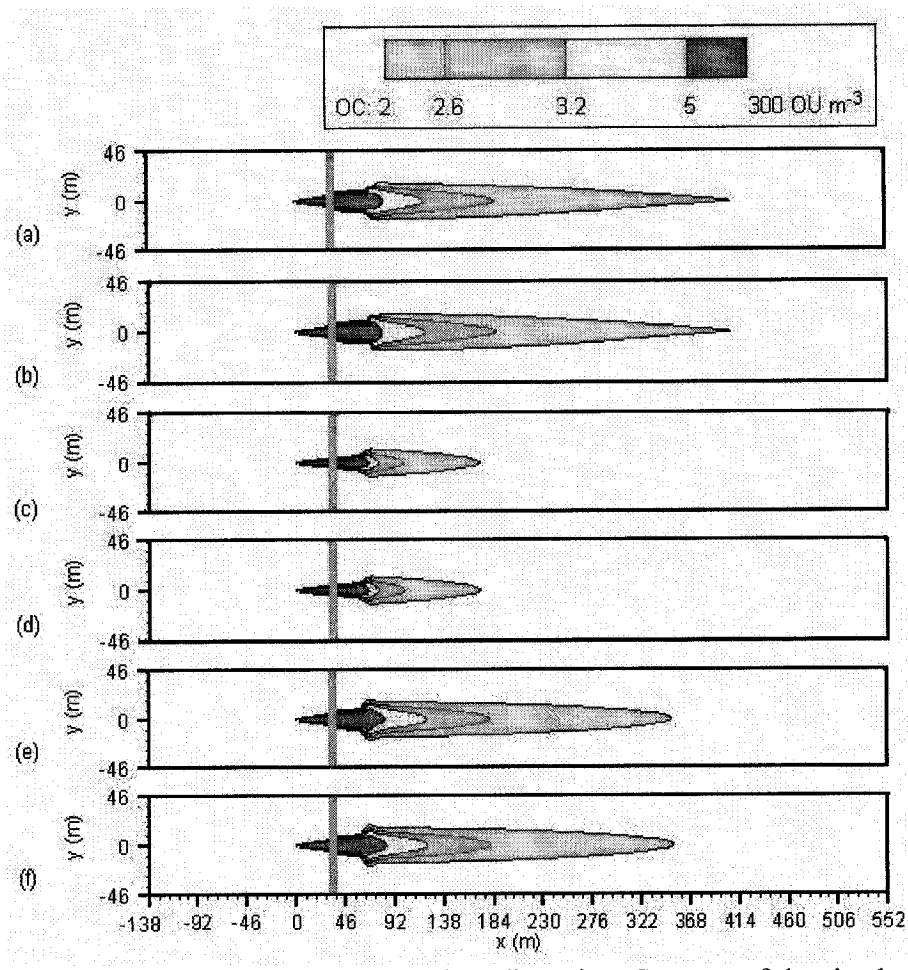

Fig. 8.5. Effect of temperature on odour dispersion. Contours of the simulated odour concentrations on the plane z = 1.5 m for temperature and atmospheric stability classes in simulation (a) 293 K and B in 2; (b) 269 K and B in 10; (c) 291 K and D in 5; (d) 270 K and D in 11; (e) 287 K and F in 8 and (f) 265 K and F in 12, respectively. The green bar is the windbreak. Simulations (a) *vs.* (b) [2 *vs.* 10]; (c) *vs.* (d) [5 *vs.* 11]; (e) *vs.* (f) [8 *vs.* 12], compare the effect of temperature while keeping all other parameters constant.

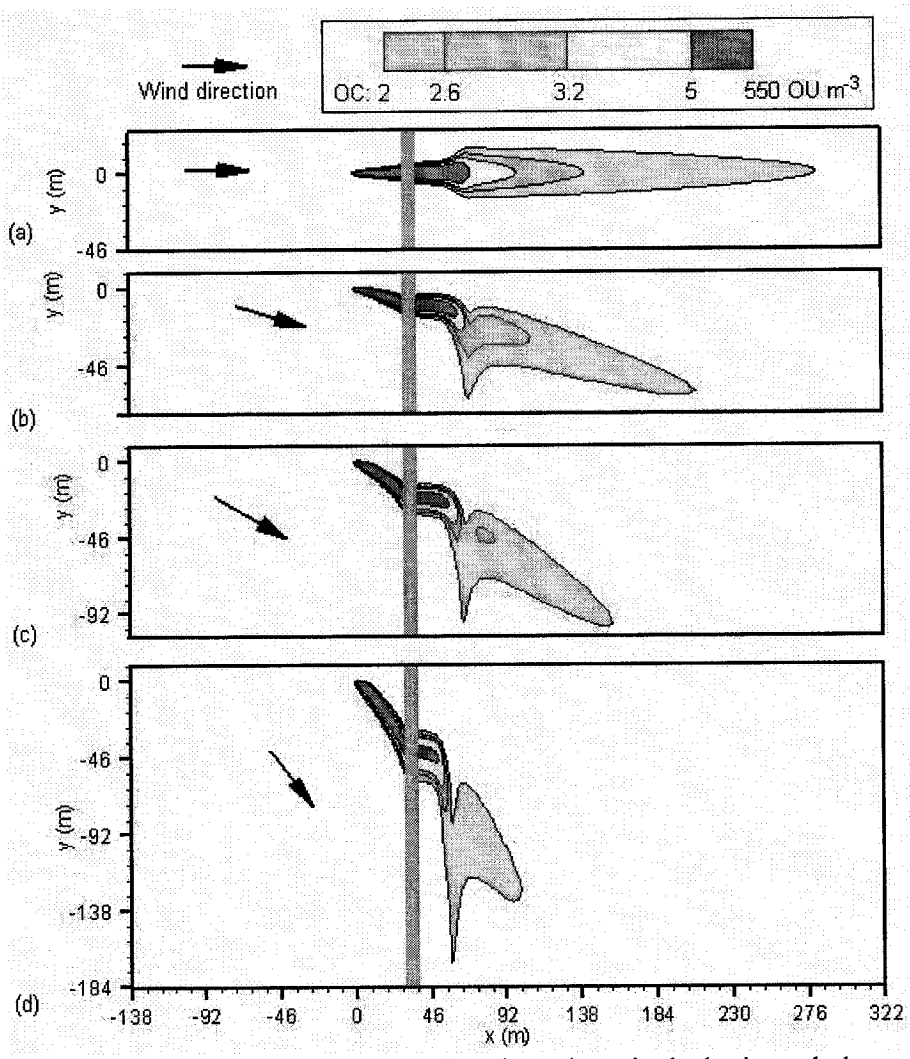

Fig. 8.6. Effect of wind direction on the odour plume in the horizontal plane z = 1.5 m, when the wind direction from the positive x-axis is (a) 0°; (b) -15°; (c) -30°, and; (d) -45° in simulations 13, 14, 15 and 16, respectively. The green bar is the windbreak.

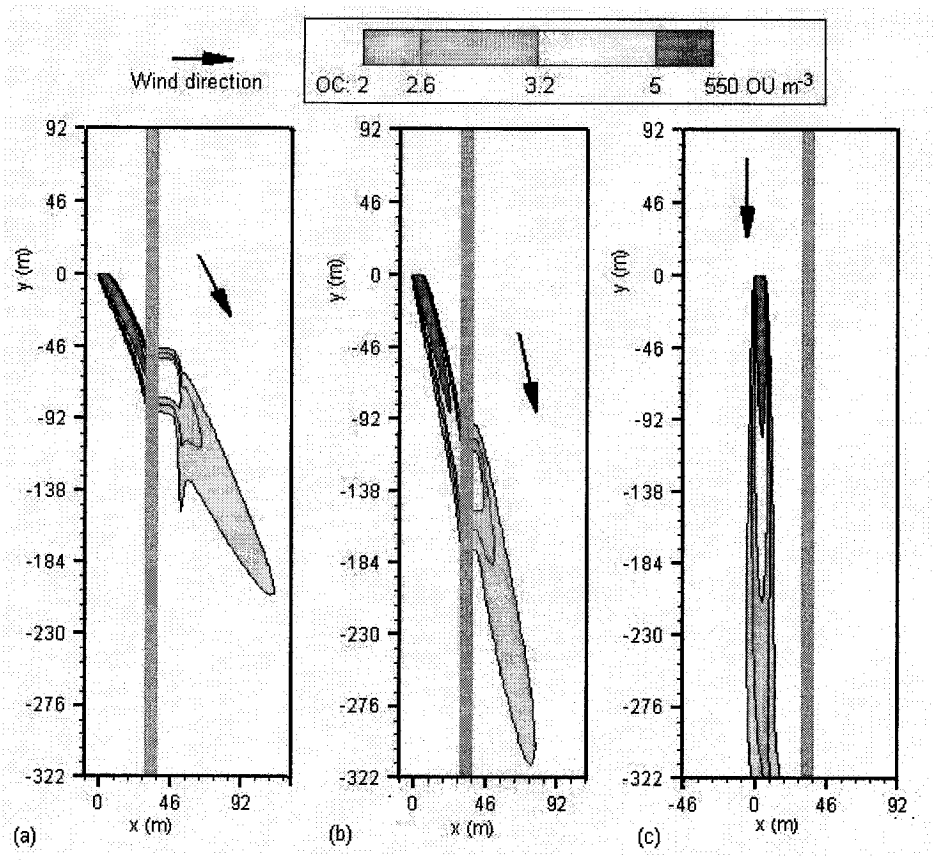

Fig. 8.7. Effect of wind direction on the odour plume on the horizontal plane, with z = 1.5 m, when the wind direction from the positive x-axis is (a) -60°; (b) -75°, and; (c) -90° in simulations 17, 18 and 19, respectively. The green bar is the windbreak.

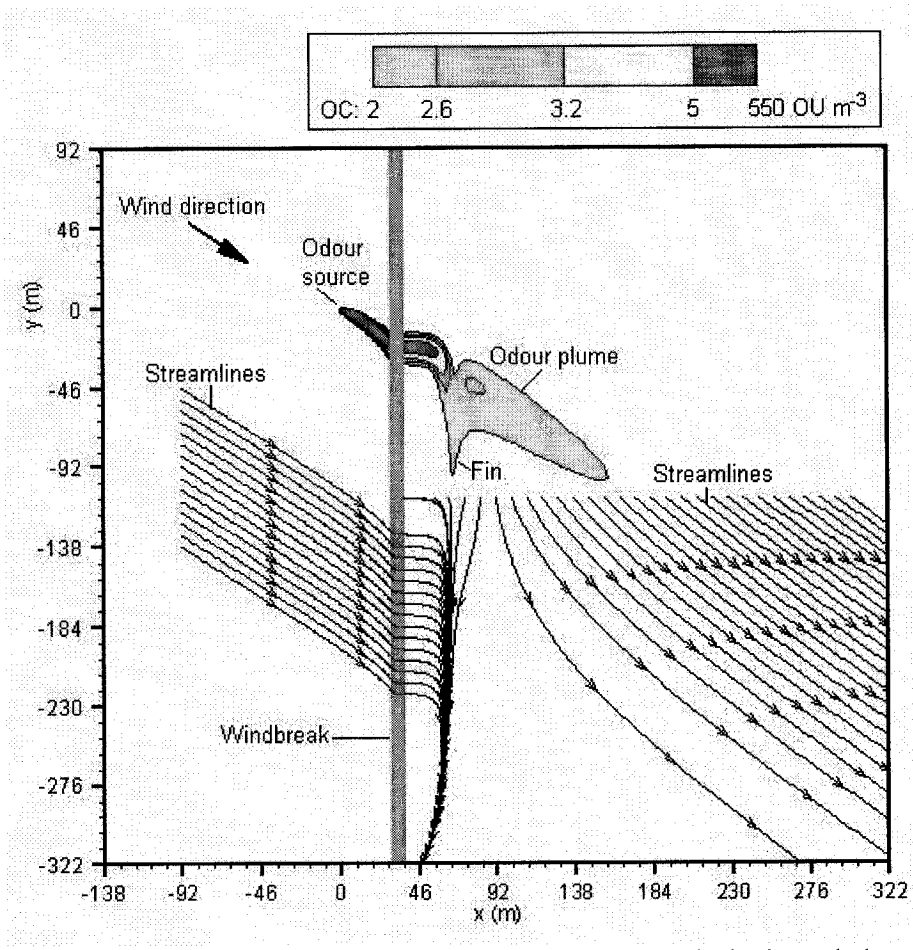

Fig. 8.8. Wind direction of -30° generating odour plume on the horizontal plane z = 1.5 m in simulation 15.

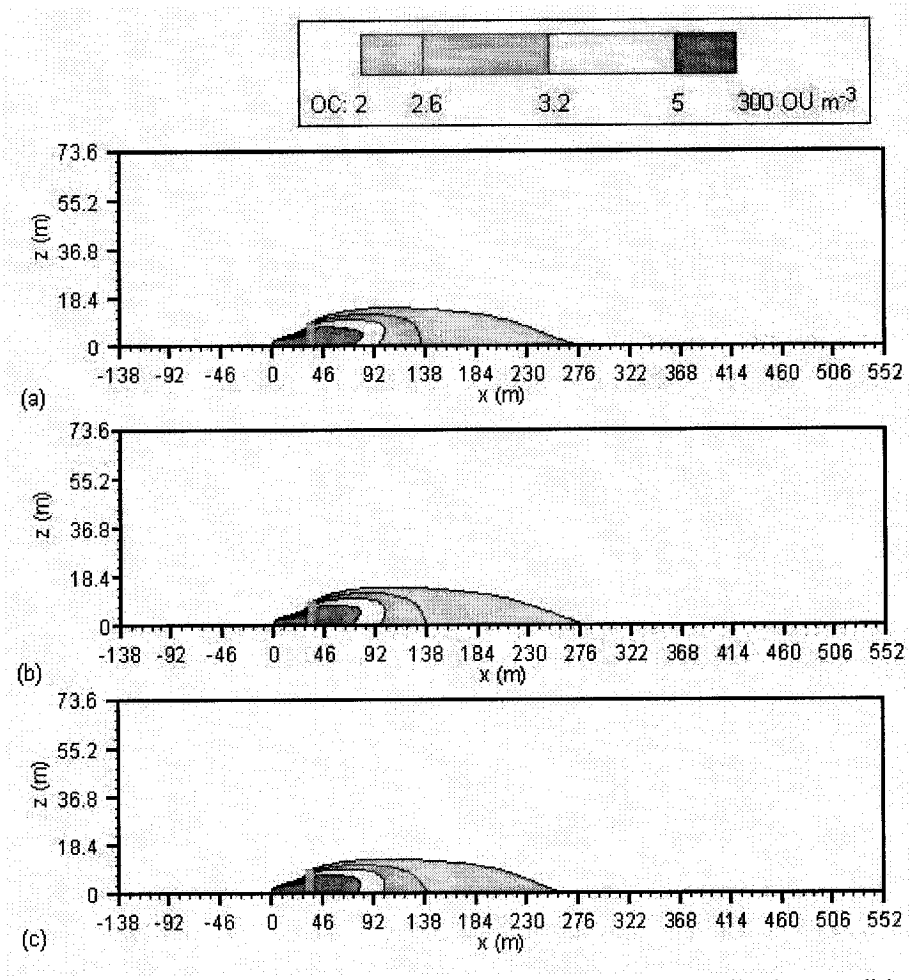

Fig. 8.9. Effect of atmospheric stability on odour plume when all other conditions are the same. Odour concentration contours on vertical plane y = 0 m, for stability class (a) B; (b) D, and; (c) F in simulations 20, 4 and 21, respectively. The green bar is the windbreak.

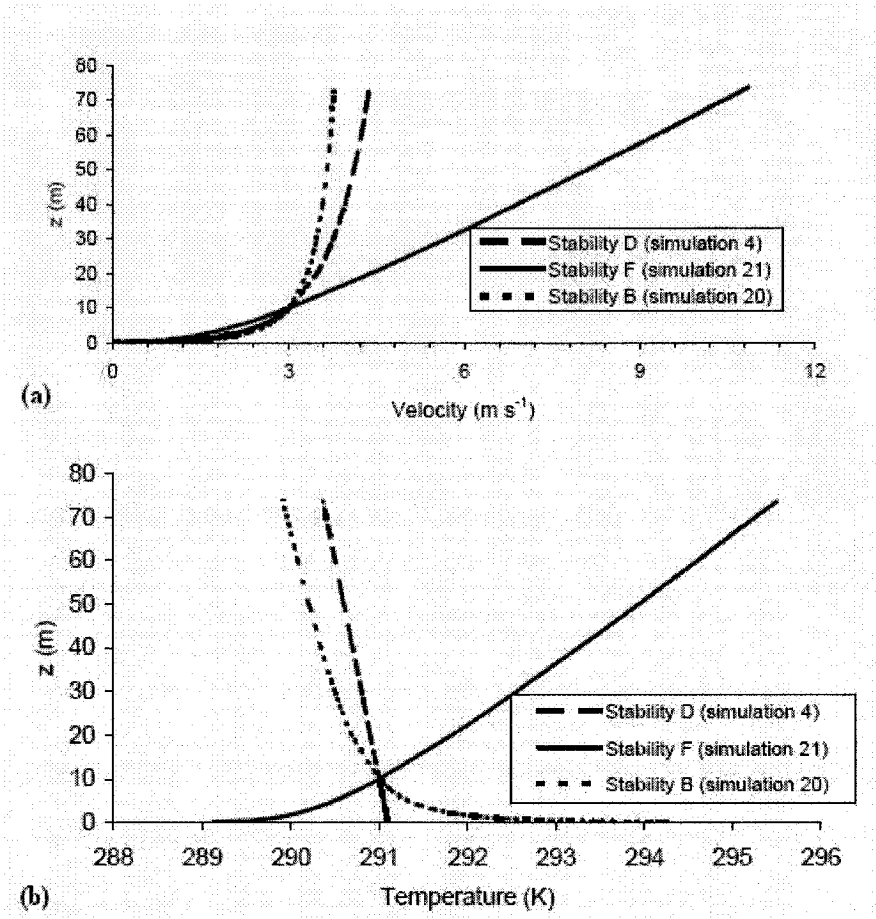

Fig. 8.10. Vertical profiles for (a) velocity, and (b) temperature, under atmospheric stability classes B, D and F, drawn from simulations 20, 4 and 21, respectively.

Chapter 9
Conclusions

9.1. General conclusions

The main objective of this project was to simulate odour dispersions around natural windbreaks. From 39 field measurements conducted by three groups of four trained panellists, the following conclusions were reached:

1. Based on the analysis of odorous air samples collected from the field odour generator, the odour concentration (OC) and the hedonic tone (HT) of the odorous air samples, as perceived by one of 51 groups of four trained panellists, were found to be exponentially related ($P = 0.05$) . When all data was pooled together, the OC was still exponentially related to HT ($P = 0.01$).

2. When OC and wind direction were normalised for all 39 field tests, a visual comparison of the plumes indicated, firstly, that low porosity windbreaks can effectively reduce the size of odour dispersion plumes, when located close (15 m) to the odour source. Secondly, windbreaks can disperse odours and reduce the maximum odour dispersion distance (MODD) by at least 21%; this reduction in MODD was averaged from the performance of a deciduous tree windbreak offering an optical porosity of 0.35, under various climatic conditions and distances from the source, as compared to no windbreak.

3. Without standardisation, the statistical analysis of the field data demonstrated that the presence of a windbreak significantly reduced by 22% the observed length of the odour plume as compared to that of a site without windbreak. When only the windbreaks with an optical porosity of 0.35 were compared to the site without a windbreak, the length of the odour plume was further and significantly reduced by 26.5% ($P < 0.10$). Nevertheless, there was no significant difference observed between the effect of the site without a windbreak and that with a windbreak offering an optical porosity of 0.55.

4. Odour dispersion was optimized with a windbreak of limited optical porosity (35% as compared to 55%); therefore, a porous windbreak designed to reduce wind speed over a long distance on its downwind side, is not designed to disperse odour;

5. Windbreaks will effectively disperse odours when located close to the source; as compared to a distance of 15 m, a distance of 30 and 60 m increased the MODDs by 6 and 12 %, respectively.

From the CFD model calibration, the following conclusions were obtained:

1. The standard k-ε and SST k-ω models can accurately reproduce the field measured HT and OC by transforming the odour mass fraction computed by the models into HT using a power function, and then into OC using an exponential function. The correlations between the simulated and measured absolute HT and between the simulated and measured OC were statistically significant ($P < 0.01$).

2. Describing the windbreak, the inertial resistance parameter was found to be a key factor controlling the amount of the air flowing through the windbreak for both the k-ε and SST k-ω models.

3. By analysing the air flow dynamics, windbreaks were observed to alter the wind velocity magnitude and direction and to create a pressure jump across their width, and hence, produce a strong turbulent field downwind from their position along with a mixing layer with the capability of enhancing odour dispersion.

By simulating the effects of windbreak characteristics, the following conclusions were reached:

1. Less porous or denser windbreak (aerodynamic porosity of 0.2 versus 0.4 and 0.66) produced a shorter, wider and more intense odour plume.

2. The tree structure had an impact on the length and width of the resulting odour plume because of the air flow profile created through the windbreak. The inertial resistance was successfully represented by the square diameter of the tree's horizontal cross section. For the same aerodynamic porosity, the poplar

windbreak allowed more air through its base while the conifer windbreak allowed more air through its foliage. The poplar windbreak created a slightly shorter odour plume as compared to that of the conifer for the same aerodynamic porosity.

3. A taller windbreak resulted in a shorter odour plume, by creating a taller but less turbulence zone downwind from the windbreak, where more odours could be trapped and retained for dispersion;

4. When close to odour source, the windbreak produced a shorter odour plume.

By simulating the effect of atmospheric conditions, the following conclusions were reached:

5. Generally, higher wind velocities produced shorter plumes under unstable, neutral and stable atmospheric conditions, whereas a shorter odour plume was also observed under lower wind velocity (1 m s^{-1}) compared to a wind velocity of 1.8 m s^{-1} for unstable atmospheric conditions where convection prevailed.

6. Temperature has little effect on odour dispersion for neutral, or unstable and stable atmospheric conditions.

7. Wind direction determined the odour dispersion direction. Odour plume length decreased when wind direction increased from the 0 to 45°, due to the air flowing along and near the windbreak leeward side.

8. When the height of the atmospheric boundary layer, wind velocity and temperature were set to represent their statistical mean values associated with each atmospheric stability condition, the odour dispersion distance for neutral conditions was shorter than that for unstable and stable conditions because the wind velocity was slower in both cases. However, when all the other conditions were same, the neutral and unstable atmospheric conditions lead to slightly longer odour dispersion plumes as compared to stable weather conditions; stable weather conditions generally produce higher wind velocities and rates of change of air temperature aloft compared to unstable and neutral conditions.

By summary of the research methods:

1. The methods used in chapters 3, 4, and 5 were visualisation, regression and classification analyses. These three methods were effective methods to analyse the odour dispersion around natural windbreaks. The visualisation method gave an impressive image of odour plumes; the regression methods can calculate an exact maximum odour dispersion distance; and the classification methods can identify the factors which influence the odour dispersion.

2. Compared with the k-ε model, the SST k-ω model better simulated the denser natural windbreaks.

3. The data pertaining to the vertical profiles of the horizontal wind velocity, temperature and turbulence energy were obtained by site measurements as used in chapter 6, or by the Monin Obukhov similarity theory as used in chapters 7 and 8.

4. For the SST k-ω model, simulated odour mass concentration (SOMC) was transformed into simulated absolute hedonic tone (SAHT) with equation (8.34), and simulated absolute hedonic tone was transformed into odour concentration (OC) with equation (8.32):

$$SAHT = \begin{cases} 0.57 SOMC^{0.46} & SOMC \le 506.5 \ \mu g\ m^{-3} \\ 10 & SOMC > 506.5 \ \mu g\ m^{-3} \end{cases} \tag{8.34}$$

$$OC = \begin{cases} 0 & AHT = 0 \\ 1.3e^{0.45 AHT} & 1 \le AHT \le 10 \end{cases} \tag{8.32}$$

9.2. Contributions to knowledge

Accordingly, this project has the following contributions to knowledge:

1. This project is the first to report odour dispersion measurements in the field, observed downwind from different natural windbreaks;

2. This project is the first to measure the impact of windbreaks on the dispersion of odours in the field; as compared to a site without a windbreak, a site with a windbreak offering an optical porosity of 0.35 and a height of 9.2 m, and located 15 m downwind from the a single odour source, was able to reduce on the average, the length of the odour plume by 26.5%, whether constituted of poplars or conifers;

3. This project is the first to identify best management practices associated with the implementation of natural windbreak for maximum odour dispersion: to optimize odour dispersion, a windbreak should offer an optical porosity of 0.35 over a tall height of at least 10 m, and be located close to the source (15 m). A windbreak with an optical density of 0.55 had no effect on the length of the odour plume, as compared to a site without a windbreak; therefore, odour dispersion requires from a windbreak, a low porosity, when most guidelines presently recommend a high porosity, being based on principles of wind speed attenuations;

4. This project is the first to calibrate CFD models for the simulation of odour dispersion, using field data, around windbreaks. The standard Fluent 6.2 k-ε model was calibrated for such simulations and demonstrated the effects of the mixing and quiet zones on the leeward side of the windbreak. This project also compared the performance of both the standard k-ε and SST k-ω models in simulating odour dispersion around the windbreak. The SST k-ω model was found to be superior because it was better designed to deal with the high wind turbulence needed to disperse odours;

5. This project is also the first to demonstrate the effect of windbreak tree characteristics on odour dispersion around windbreaks, using the SST k-ω model;

6. Combined with the Monin-Obukhov similarity theory, this project is first to show by means of SST k-ω model simulation, the effect on odour dispersion around windbreaks of wind velocity and direction, temperature and atmospheric stability conditions;

7. This project also demonstrated that the inertial resistance parameter is a key factor controlling the amount of air flowing through the windbreak. The

inertial resistance was found to be proportional to the square diameter of the tree's horizontal cross section.

9.3. Recommended future works for windbreak odour dispersion

1. Field measurements should be repeated to correlate wind velocity distribution and odour concentration downwind from the windbreak;

2. Windbreak odour dispersion system should be implemented to represent real livestock facilities with buildings and manure storage facilities. The design of the system can be simulated using the SST k-ω model.

3. The Large Eddy Simulation (LES) model should be tested to simulate odour dispersion.

4. Artificial neural network (ANN) systems should be tested to predict odour dispersion around natural windbreaks.

Chapter 10
References

Agriculture and Agro-Food Canada, 1998. Research strategy for hog manure management in Canada. Supply & Services Canada, No. A42-77/1998F, Ottawa, Canada.

Aiken, J.D., 2001. Manure matters archive files Nebraska livestock nuisance law. http://manure.unl.edu/adobe/v7n7_01.pdf, visited 200607.

ASHRAE, 1997. ASHRAE fundamentals handbook. American Society of Heating, Refrigeration and Air Conditioning, Atlanta, Georgia, U.S.A, 13.1-13.6 pp.

ASHRAE, 2001. ASHRAE fundamentals handbook. American Society of Heating, Refrigeration and Air Conditioning, Atlanta, Georgia, U.S.A., 13.1-13.8 pp.

ASHRAE, 2003. Handbook of fundamentals. American Society of Heating Refrigeration and Air Conditioning Engineering. Atlanta, USA. Chapter 12.

ASTM, 1990. Standard method for defining and calculating sensory thresholds from intermediate size. AWMA E 18.04.25. American Society for the Testing of Materials, Washington, DC, USA.

ASTM, 1997. Standard Practice for Determination of Odor and Taste Thresholds By a Forced-Choice Ascending Concentration Series Method of Limits, American Society for the Testing of Materials, Washington, DC, USA.

ASTM, 1998. Standard Practices for referencing supra-threshold odour intensity. American Society for the Testing of Materials, Washington, DC, USA.

Beychok, M.R., 1994. Fundamentals of stack gas dispersion. Beychok, Milton R., Irvine, California, USA, 193 pp.

Bird, R.B., Stewart, W.E. and Lightfoot, E.N., 2002. Transport phenomena. J. Wiley, New York, 895 pp.

Blackadar, A.K., 1997. Turbulence and diffusion in the atmosphere: lectures in environmental sciences. Springer, Berlin; New York, 185 pp.

Boldes, U., Colman, J. and Leo, J.M.D., 2001. Field study of the flow behind single and double row herbaceous windbreaks. Journal of Wind Engineering and Industrial Aerodynamics, 89: 665-687.

Bottcher, R.W., Munilla, R.D., Baughman, G.R. and Keener, K.M., 2000. Designs for windbreak walls for mitigating dust and odor emissions from tunnel ventilated swine buildings. pp. 174-181 in: Swine Housing, Proc. of the 1st International Conference, Oct. 9-11, 2000, Des Moines, Iowa. American Society of Agricultural Engineers, 2950 Niles road, St. Joseph, Mi. USA.

Bottcher, R.W., Munilla, R.D., Keener, K.M. and Gates, R.S., 2001. Dispersion of livestock building ventilation using windbreaks and ducts. 2001 ASAE Annual International Meeting.: Paper No. 01-4071. 2950 Niles road, St. Joseph, Mi. USA.

Brant, R.C. and Elliott, H.A., 2002. Pennsylvania odor management manual, Pennsylvania State University, University Park, PA. USA.

Carruthers, D.J. and Dyster, S.J., 2003. Boundary layer structure specification, ADMS 3 P09/01T/03 http://www.cerc.co.uk/software/pubs/3-1techspec.htm visited at 2006.

Carruthers, D.J., Holroyd, R.J., Hunt, J.C.R., Weng, W.S., Robins, A.G., Apsley, D.D., Thompson, D.J. and Smith, F.B., 1994. UK-ADMS: A new approach to modelling dispersion in the earth's atmospheric boundary layer. Journal of Wind Engineering and Industrial Aerodynamics, 52: 139.

CEN, 1995a. Document 064/e, Odour concentration measurement by dynamic olfactometry. CEN TC 264/WG2. Comité Européen de Normalisation. Dusseldorf, Germany.

CEN, 1995b. Odour Standards. CEN/TC 264N 134. Comité Européen de Normalisation, Dusseldorf, Germany.

CEN, 2001. Air quality - determination of odor concentration by dynamic olfactometry. prEN13725, European Committee for Standardization, 36 rue de Stassart, B-1050 Brussels. <http://www.aerox.nl/images/eurstandard.pdf>, visited August, 2004.

Chapin, A., Boulind, C. and Moore, A., 1998.Controlling odor and gaseous emission problems from Industrial swine facilities. Yale Environmental Protection Clinic Handbook. <http://www.kerrcenter.com/publications/Controlling_Odor.pdf#search='Controlling%20Odor%20and%20Gaseous%20Emission%20Problems%20from'>.

Choinière, D., 2003. Validation of a dispersion model for agricultural odors in Quebec, The CSAE Odor dispersion annd regulation workshop, The Canadian society for engineering in agricultural, food and biological systems, Saskatoon, Canada.

Choinière, D., 2004. L'influence des haies brise-vent naturelles sur les odeur, Division Environnement Consumajing, Saint-Hyacinthe (Québec).

Choinière, D. and Barrington, S., 1998. The conception of an automated dynamic olfactometer, CSAE/SCGR Paper No. 98-208. The Canadian society for engineering in agricultural, food and biological systems, Saskatoon, Canada.

Cleugh, H.A., 1998. Effects of windbreaks on airflow, microclimates and crop yields. Agroforestry Systems, 41: 5-84.

Cue, R.I., 2006. Statistical methods AEMA-610. http://animsci.agrenv.mcgill.ca/servers/anbreed/statisticsII/stats2e.pdf (visited 200606).

Das, K.C., Kastner, J.R. and Hassan, S.M., 2004. Potential of particulate matter as a pathway for odor dispersion. ASAE paper number 04-4125. American Society of Agricultural Engineering, St Joseph, Michigan, USA.

Dierickx, W., Cornelis, W.M. and Gabriels, D., 2003. Wind tunnel study on rough and smooth surface turbulent approach flow and on inclined windscreens. Biosystems Engineering, 86(2): 151-166.

Dierickx, W., Gabriels, D. and Cornelis, W.M., 2002. Wind tunnel study on oblique windscreens. Biosystems Engineering, 82(1): 87-95.

Dirkse, M.H., van Loon, W.K.P., van der Walle, T., Speetjens, S.L. and Bot, G.P.A., 2006. A Computational Fluid Dynamics Model for Designing Heat Exchangers based on Natural Convection. Biosystems Engineering, 94(3): 443.

Edeogn, I., Feddes, J.J.R., Qu, G., Coleman, R. and Leonard, J., 2001. Odour measurement and emissions from pig manure treatment/storage systems. Final report to Canada Pork Council. Project Number CPC-01. University of Alberta, Edmonton, AB. http://www.cpc-ccp.com/HEMS/CPC-01_Feddes.PDF (2007/01/17).

Eimern, J.v., Karschon, R., Razumova, L.A. and Robertson, G.W., 1964. Windbreaks and shelterbelts. Report of a working group of the Commission for Agricultural Meteorology, World Meteorological Organization, Technical Note No. 59. Secretariat of the World Meteorological Organization, Geneva, 188 pp.

EPA, 2001. Odor impacts and odor emission control measurement for intensive agriculture, <http://www.epa.ie/pubs/docs/Odour%20Impacts%20Final.pdf>,visited on July, 2006.

Fang, F.M. and Wang, D.Y., 1997. On the flow around a vertical porous fence. Journal of Wind Engineering and Industrial Aerodynamics, 67 & 68: 415-424.

Fluent inc., 2005. Fluent 6.2 user's guide, Fluent Inc., Centerra Resource Park, 10 Cavendish Court, Lebanon, NH 03766, USA.

Fox, R.W. and McDonald, A.T., 1992. Introduction to fluid mechanics. J. Wiley, New York, USA, 829 pp.

Gan, G. and Riffat, S.B., 1997. Pressure loss characteristics of orifice and perforated plates. Experimental Thermal and Fluid Science, 14: 160-165.

Geiger, R., Aron, R.H. and Todhunter, P., 2003. The climate near the ground. Rowman & Littlefield, Lanham, Md., 584 pp.

Golder, D., 1972. Relations among stability parameters in the surface layer. Boundary-Layer Meteorology, 3(1): 47.

Gorgy, T.G.A., 2003. Validation of an air dispersion model for odour impact assessment. M Eng, McGill Unversity, Montreal, Canada. Thesis, 69 [50] leaves pp.

Gosman, A.D., 1999. Developments in CFD for industrial and environmental applications in wind engineering. Journal of Wind Engineering and Industrial Aerodynamics, 81(1-3): 21-39.

Guan, D., Zhang, Y. and Zhu, T., 2003. A wind-tunnel study of windbreak drag. Agri. Ecosystem & Environment, 118: 75-84.

Guo, H., Feddes, J., Dehod, W., Laguë, C. and Edeogu, I., 2006. Monitoring of odour occurrence in the vicinity of swine farms by resident-observers Part II: Impact of weather conditionson odour occurrence. Canadian Biosystems Engineering, 48: 6.23-6.29.

Guo, H., Jacobson, L.D., Schmidt, D.R. and Janni, K.A., 2001a. Simulation of odor dispersion as impacted by weather conditions. ASAE Publication Number 701P0201, 2950 Niles road, St. Joseph, Mi. USA.

Guo, H., Jacobson, L.d., SChmidt, D.R. and Nicodai, R.E., 2003. Evaluation of influence of atmospheric condition on odor dispersion from animal

production sites. American Society of Agricultural Engineers, 46(2): 461-466.

Guo, H., Jacobson, L.D., Schmidt, D.R. and Nicolai, R.E., 2001b. Calibrating inpuff-2 model by resident-panelists for long-distance odor dispersion from animal production sites. American Society of Agricultural Engineers, 17(6): 859-868.

Guo, H., Jacobson, L.D., Schmidt, D.R., Nicolai, R.E., Zhu, J. and Janni, K.A., 2005. Development of the OFFSET model for determination of odor-annoyance-free setback distances from animal production sites: part II. model development and evaluations. Transaction of the ASAE, 48(6): 2269-2276.

Guo, H., Jacobson, L.D., Schmidt, D.R., Nicollai, R.E. and Janni, K.A., 2001c. Comparison of five models for setback distance determination. ASAE Meeting Presentation Paper Number 01-4045, ST Joseph, Michigan, USA.

Heisler, G.M. and Dewalle, D.R., 1988. Effects of windbreak structure on wind flow. Agriculture, Ecosystems and Environment, 22-23: 41-69.

Hinze, J.O., 1975. Turbulence. McGraw-Hill, New York; USA, 790 pp.

Hipsey, M.R., Sivapalan, M. and Clement, T.P., 2004. A numerical and field investigation of surface heat fluxes from small wind-sheltered waterbodies in semi-arid western austrilia. Environmental Fluid mechanics, 4: 79-106.

Ierardi, J.A., 2000. Air property calculator. http://users.wpi.edu/~ierardi/FireTools/air_prop.html.

Jacobson, L.D., Guo, H., Schmidt, D.R., Nicolai, R.E., Zhu, J. and Janni, K.A., 2005. Development of the OFFSET model for determination of odor-annoyance-free setback distances from animal production sites: part I. review and experiment. Transaction of the ASAE, 48(6): 2259-2268.

Jacobson, M.Z., 1999. Fundamentals of atmospheric modeling. Cambridge University Press, Cambridge, UK, 656 pp.

Kempen, T.v. and Heugten, E.v., 2003. Impact of diet on odor. http://mark.asci.ncsu.edu/SwineReports/2003/vankempen2.htm.

Lakes Environmental Software, 2002. ISCST3 tech guide. <http://www.weblakes.com/ISCVOL2/Contents.htm>, Waterloo, Ontario, Canada.

Lammers, P., S., Wallenfang, O. and Boeker, P., 2001. Computer modelling for assessing means to reduce odour emissions. Paper number 01-4042. American Society of Agricultural Engineering, St Joseph, Michigan, USA.

Lee, S.-J. and Kim, H.-B., 1999. Laboratory measurements of velocity and turbulence field behind porous fences. Journal of Wind Engineering and Industrial Aerodynamics, 80: 311-326.

Lee, S. and Lim, H., 2001. A numerical study on flow around a triangular prism located behind a porous fence. FLUID DYNAMICS RESEARCH, 28(3): 209-221.

Leuty, T., 2003. Using shelterbelt to reduce odors associated with livestock production barns. Ministry of Agriculture and Food, Ontario, http://www.gov.on.ca/OMAFRA/english/crops/facts/info_odours.htm, visited in 2004.

Leuty, T., 2004. Wind management can reduce offensive farm odours. Ministry of Agriculture and food, Ontario, http://www.omafra.gov.on.ca/english/crops/facts/info_odours.htm (2007/01/24).

Li, Y. and Guo, H., 2006. Comparison of odor dispersion prediction between CFD model and CALPUFF model, Paper # 064102, 2006 ASABE Annual International Meeting. American Socienty of Agricultural and Biological Engineer, Oregon Convention Center, Portland, Oregon. 9 - 12 July 2006.

Lien, F.-s. and Yee, E., 2005. Numerical modelling of the turbulent flow developing within and over a 3-d building array, part iii: a distributed drag

force approach, its implementation and application. Boundary-Layer Meteorology, 114(2): 287-313.

Lien, F.-s., Yee, E. and Wilson, J.D., 2005. Numerical modelling of the turbulent flow developing within and over a 3-d building array, part ii: a mathematical foundation for a distributed drag force approach. Boundary-Layer Meteorology, 114(2): 245.

Lien, F.S., Yee, E. and Cheng, Y., 2004. Simulation of mean flow and turbulence over a 2D building array using high-resolution CFD and a distributed drag force approach. Journal of Wind Engineering and Industrial Aerodynamics, 92: 117-158.

Lim, T.T., Heber, A.J., Ni, J.Q., Sutton, A.L. and Kelly, D.T., 2001. Characteristics and Emission Rates of Odor from Commercial Swine Nurseries. Trnsaction of the ASAE, 44(5)(0001-2351): 1275-1282.

Lin, X.J., Barrington, S., Choinière, D. and Prasher, S.O., 2006a. Simulation of the effect of windbreaks on odour dispersion using the CFD SST k-ω model. Biosystems Engineering, Presented for publication on August 20, 2006, submission number be 06 199.

Lin, X.J., Barrington, S., Gong, G. and Choinière, D., 2007a. Simulation of odour dispersion downwind from natural windbreaks using the CFD standard k-ε model. Transactions of the ASAE presented for publication in January 2007.

Lin, X.J., Barrington, S., Nicell, J. and Choinière, D., 2007b. Effect of natural windbreaks on maximum odour dispersion distance (MODD). Canadian Biosystems Engineering, 49: 6.21 - 6.32.

Lin, X.J., Barrington, S., Nicell, J., Choiniere, D. and Vezina, A., 2006. Influence of windbreaks on livestock odour dispersion plume in the field. Agriculture, Ecosystems & Environment, 116(3-4): 263-272.

Lyman, W.J., Reehl, W.F. and Rosenblatt, D.H., 1990. Handbook of chemical property estimation methods: environmental behavior of organic compounds. American Chemical Society, Washington, DC, USA, 1000 pp.

McNaughton, K.G., 1988. Effects of windbreaks on turbulent transport and microclimate. Agri. Ecosystem & Environment, 22-23: 17-39.

Menter, F.R., Kuntz, M. and Langtry, R., 2003. Ten years of industrial experience with the SST turbulence model. In: K. Hanjalic, Y. Nagano and M. Tummers (Editors), Turbulence, heat and mass transfer 4. Begell House Inc, Redding, Connecticut, USA, pp. 625-632.

Miner, J.R., 1997. Nuisance concerns and odor control. J Dairy Sci, 80: 2667-2672.

Mussio, P., Gnyp, A.W. and Henshaw, P.F., 2001. A Fluctuating plume dispersion model for the prediction of odor-impact frequencies from continuous stationary sources. Atmospheric Environment, 35: 2955-2962.

Nimmermark, S., 2006. Characterization of odor from livestock and poultry operation by the hedonic tone. Paper number 064157. In: ASABE (Editor), 2006 American Society of Agricultural and Biological Engineering Annual International Meeting, Oregon Convention Center, Portland, Oregon, 9 - 12 July 2006.

O'Neill, D.H. and Phillips, V.R., 1992. A review of the control of odour nuisance from livestock buildings: Part 3, properties of the odorous substances which have been identified in livestock wastes or in the air around them. Journal of Agricultural Engineering Research, 53: 23-50.

Packwood, A.R., 2000. Flow through porous fence in thick boundary layers: comparisons between laboratory and numerical experiments. Journal of Wind Engineering and Industrial Aerodynamics, 88: 75-90.

Panofsky, H.A. and Dutton, J.A., 1984. Atmospheric turbulence: models and methods for engineering applications. Wiley, New York, 397 pp.

Parker, D.B., Rhoades, M.B., Schuster, G.L., Koziel, I.A. and Perschbacher-Buser, Z.L., 2005. Odor characterization at open-lot beef cattle feedyards using triangular forced-choice olfactometry. Transactions of the ASAE, 48(4): 1527-1535.

Patton, E.G., Shaw, R.H., Judd, M.J. and Raaupach, M.R., 1998. Large-eddy simulation of windbreak flow. Boundary-Layer Meteorology, 87: 275-306.

Plate, E.J., 1971. The aerodynamics of shelter belts. Agric. Meteorol, 8, 203.

Quebec Regulation, 2006. Guidelines for determining minimum distance to ensure odour management in rural areas, R.Q. c. P-41.1, r.1.1. Quebec Ministry of Environment, Quebec, Canada. http://www.canlii.org/qc/laws/regu/p-41.1r.1.1/20060614/whole.html.

Riddle, A., Carruthers, D., Sharpe, A., McHugh, C. and Stocker, J., 2004. Comparisons between FLUENT and ADMS for atmospheric dispersion modelling. Atmospheric Environment, 38(7): 1029-1038.

Saatdjian, E.b., 2000. Transport phenomena: equations and numerical solutions. John Wiley, New York, USA, 414 pp.

SAS Institute Inc., 2001. SAS (r) Proprietary Software Release 8.2, Cary, NC, USA.

Schauberger, G., Piringer, M. and Petz, E., 2002. Calculating direction-dependent separation distance by a dispersion model to avoid livestock odor annoyance. Biosystems Engineering, 82(1): 25-37.

Schauberger, G., Pringer, M. and Petz, E., 2000. Diurnal and annual variation of the sensation distance of odor emitted by livestock building calculated by the Austrian odor dispersion model(AODM). Atmospheric Environment, 34: 4839-4851.

Schnelle, K.B. and Dey, P.R., 2000. Atmospheric dispersion modeling compliance guide. McGraw-Hill, New York, USA.

Schwartz, R.C., Fryrear, D.W., Harris, B.L., Billbro, J.D. and Juo, A.S.R., 1995. Mean flow and shear stress distributions as influenced by vegetative windbreak structure. Agricultural and forest meteorology, 75: 1-22.

Sheridan, B.A., Curran, T.P. and Dodd, V.A., 2002. Assessment of the influence of media particle size on the biofiltration of odorous exhaust ventilation air from a piggery facility. Bioresource Technology, 84: 129-143.

Sheridan, B.A., Hayes, E.T., Curran, T.P. and Dodd, V.A., 2003. A dispersion modeling approach to determining the odor impact of intensive pig production units and Ireland. Bioresource Technology, 91: 145-152.

Sun, H., Keener, H., Stowell, R.R. and Michel, F.C., 2001. Three-dimensional numerical simulation of mechanical ventilation in a high-riseTM hog building (HRHB), 2001 ASAE International Meeting, Sacramento, CA, pp. Paper No. 014040.

Sun, H., Keener, H., Stowell, R.R. and Michel, F.C., 2002a. Two-dimensional computational fluid dynamics (CFD) modeling of air velocity and ammonia distribution in a high-riseTM hog building, 2002 ASAE Annual International Meeting/CIGR International Congress. ASAE, Chicago, USA, pp. Paper No. 024117.

Sun, H., Stowell, R.R., Keener, H.M. and Michel, F.C., 2002b. Comparison of predicted and measured ammonia distribution in a high-riseTM hog building (HRHB) for summer conditions. Transactions of the ASAE, Vol. 45(5): 1559-1568.

Telega, L., 2003. Legal primer for farms and their neighbors. http://www.dairybusiness.com/northeast/June03/F2%20p22,23%20Legal%20primer.pdf.

Thé, J.L., Thé, C.L. and Johnson, M.A., 2002. ISC-AERMOD View User's Guide. Lakes Environmental Software. Lakes Environmental Software, 419 Phillip Street, Unit 3, Waterloo, Ontario N2L 3X2.

Tyndall, J. and Collettii, J., 2000. Air quality and shelterbelts: Odour mitigation and livestock production - A literature review. Final project report to USDA National Agroforestry Center, Lincoln, NB. Project Number 4124-4521-48-3209. Forestry Department, Iowa State University, Ames, IA. http://www.forestry.iastate.edu/res/Shelterbelts_and_Odor_Final_Report.pdf (2007/01/17).

Ucar, T. and Hall, F.R., 2001. Review windbreaks as a pesticide drift mitigation strategy: a review. Pest Management Science, 57: 663-675.

VanDevender, K., 2000. Arkansas swine odor survey. http://www.uaex.edu/Other_Areas/publications/PDF/FSA-1030.pdfodorsurvey.pdf, visited 200408.

Vigiak, O., Sterk, G., Warren, A. and Hagen, L.J., 2003. Spatial modeling of wind speed around windbreaks. Catena, 52: 273-288.

Wang, H. and Takle, E.S., 1995. A numerical simulation of boundary-layer flows near shelterbelts. Boundary-Layer Meteorology, 75(1 - 2): 141-173.

Wang, H. and Takle, E.S., 1997. Momentum budget and shelter mechanism of boundary-layer flow near a shelterbelt. Boundary-Layer Meteorology, 82: 417-435.

WASP, 2006. Table of roughness lengths. http://www.risoe.dk/vea/projects/nimo/WAsPHelp/TableofRoughnessLengths.htm.

Wilson, J., 2004. Oblique, stratified winds about a shelter fence. part II: Comparison of measurements with numerical models. Journal of Applied Meteorology, 43(10): 1392-1409.

Wilson, J.D., 1985. Numerical study of flow through a windbreak. Journal of Wind Engineering and Industrial Aerodynamics, 21: 119-154.

Wilson, J.D., 1987. On the choice of a windbreak porosity profile. Boundary-Layer Meteorology, 38(1 - 2): 37.

Wilson, J.D. and Yee, E., 2003. Calculation of winds distribution by an array of fences. Agricultural and forest meteorology, 115: 31-50.

Yaws, C.L., 2001. Chemical properties handbook -physical, thermodynamic, environmental, transport, safety, and health related properties for organic and inorganic chemicals. McGraw-Hill, New York. USA.

Zhang, Q., Feddes, J., Edeogu, I., Nyachoti, M., House, J., Small, D., Liu, C., Mann, D. and Clark, G., 2002. Odor production, evaluation and control. http://www.manure.mb.ca/projects/completed/pdf/02-hers-03.pdf, visited August, 2004., Manitoba Livestock manure Management Initiative Inc.

Zhang, Q., Feddes, J.J.R., Edeogu, I.K. and Zhou, X.J., 2003. Correlation between odor intensity assessed by human assessors and odor concentration measured with olfactometers. CANADIAN BIOSYSTEMS ENGINEERING, 44 (6): 27-32.

Zhou, X.H., Brandle, J.R., Takle, E.S. and Mize, C.W., 2002. Estimation of the three-dimensional aerodynamic structure of a green ash shelterbelt. Agricultural and Forest Meteorology, 111(2): 93.

Zhu, J., Jacobson, L.D., Schmidt, D.R. and Nicolai, R., 2000. Evaluation of inpuff-2 model for predicting downwind odors from animal production facilities. American Society of Agricultural Engineers, 16(2): 159-164.